Substituent-controlled, Mild Oxidative Fluorination of Iodoarenes: Synthesis and Structural Study of Aryl I(III)- and I(V)-Fluorides

Joel Häfliger,† Cody Ross Pitts,† Dustin Bornemann, Roland Käser, Nico Santschi, Julie Charpentier, Elisabeth Otth, Nils Trapp, René Verel, Hans Peter Lüthi, and Antonio Togni*

Department of Chemistry and Applied Biosciences, ETH Zürich, Vladimir-Prelog-Weg 2, 8093 Zürich, Switzerland

Contents

General Information

Unless otherwise stated, all reactions were carried out under strictly anhydrous conditions and Ar or N_2 atmosphere. All solvents were dried and distilled using standard methods (i.e. MeCN and CH_2Cl_2 were dried and distilled over CaH_2 and stored over molecular sieves prior to use). Trichloroisocyanuric acid was used without prior drying or purification. Spray-dried (or otherwise rigorously dried) KF was always weighed out under N_2 atmosphere in a glove box. All ^1H and ^{13}C NMR spectra were acquired on either a 300, 400, or 500 MHz spectrometer. All ^{19}F NMR spectra were acquired on either a 300, 400, or 500 MHz spectrometer. For ^{19}F NMR yield determination, either trifluorotoluene or fluorobenzene was introduced after each reaction as an internal standard, and the d1 relaxation delay was increased to 10 s during data collection. The ^1H, ^{13}C, and ^{19}F NMR chemical shifts are given in parts per million (δ) and calibrated to either residual solvent signal (^1H and ^{13}C),[1] α,α,α-trifluorotoluene (^{19}F, δ = –63.10 in CD_3CN),[2] fluorobenzene (^{19}F, δ = –114.81 in CD_3CN),[2] or $CFCl_3$ (^{19}F, δ = 0.65 in $CDCl_3$).[2] NMR data are reported in the following format: chemical shift (integration, multiplicity (s = singlet, d = doublet, t = triplet, q = quartet, quint = quintet, m = multiplet, br = broad), coupling constants (Hz)). IR data were collected on a Thermo Fischer Scientific Nicolet 6700 FT-IR equipped with a PIKE technologies GladiATR or a Perkin-Elmer BX II using ATR FT-IR technology and absorption maxima are reported in cm^{-1}. GC/MS was performed on a Thermo Fischer Trace GC 2000 equipped with a flame ionization detector, using a ZB-5 column with guardian (L: 30 m, i.d.: 0.25 mm, DF = 0.25 μm) and helium as the carrier gas with a constant flow of 1.1 mL min^{-1} and a Shimadzu-QP 2010 Ultra using HP-5 column with a parallel MS and FID detection. HRMS data were collected by MoBiAS - the MS-service of the "Laboratorium für Organische Chemie der ETH Zürich." Compounds **35** and **36** were synthesized according to literature procedure.[3]

General Procedure for Synthesis of Difluoro(aryl)-λ^3-iodanes

Trichloroisocyanuric acid (0.350 g, 1.5 mmol, 4.0 equiv.) was added to an oven-dried microwave vial equipped with a stir bar; the vessel was then transported inside a glove box under N_2 atmosphere. Spray-dried (or crushed and rigorously dried) potassium fluoride (0.131 g, 2.3 mmol, 6.0 equiv.) was added to the reaction vessel, which was then sealed with a cap with septum using a crimper. The closed vial was removed from the glove box. Under Ar atmosphere, a solution of the aryl iodide substrate (0.38 mmol, 1.0 equiv.) in 4.0 mL MeCN was added to the vial. The reaction mixture was stirred vigorously at 40 °C for ca. 24 h. *Note that substrates with limited solubility in MeCN were introduced to the reaction mixture as solids in the glove box.* Upon reaction completion, an aliquot of the reaction mixture was passed through a PTFE syringe filter, and an NMR sample was prepared with 0.4 mL of the filtered aliquot + 0.1 mL internal standard solution (made immediately prior to use with x g of either trifluorotoluene or fluorobenzene in y mL CD_3CN) for ^{19}F NMR yield determination. In order to obtain NMR characterization data, reactions were run in CD_3CN and filtered prior to measurement to remove KF and most of the TCICA (note that we were unable to extract the aryl-IF_2 compounds from TCICA completely, so the residual TCICA signal is labelled in the $^{13}C\{^1H\}$ NMR spectra).

General Procedure for Synthesis of Tetrafluoro(aryl)-λ^5-iodanes

Trichloroisocyanuric acid (0.350 g, 1.5 mmol, 4.0 equiv.) was added to an oven-dried microwave vial equipped with a stir bar; the vessel was then transported inside a glove box under N_2 atmosphere. Spray-dried (or crushed and rigorously dried) potassium fluoride (0.131 g, 2.3 mmol, 6.0 equiv.) was added to the reaction vessel, which was then sealed with a cap with septum using a crimper. The closed vial was removed from the glove box. Under Ar atmosphere, a solution of the aryl iodide substrate (0.38 mmol, 1.0 equiv.) in 4.0 mL MeCN was added to the vial. The reaction mixture was stirred vigorously at 40 °C for ca. 48 h. *Note that substrates with limited solubility in MeCN were introduced to the reaction mixture as solids in the glove box.* Upon reaction completion, an aliquot of the reaction mixture was passed

[1] G. R. Fulmer, A. J. M. Miller, N. H. Sherden, H. E. Gottlieb, A. Nudelman, B. M. Stolz, J. E. Bercaw, and K. I. Goldberg, *Organometallics*, 2010, **29**, 2176.
[2] C. P. Rosenau, B. J. Jelier, A. D. Gossert, and A. Togni, *Angew. Chem. Int. Ed.*, 2018, **57**, 9528.
[3] V. Matoušek, E. Pietrasiak, R. Schwenk, and A. Togni, *J. Org. Chem.*, 2013, **78**, 6763.

through a PTFE syringe filter, and an NMR sample was prepared with 0.4 mL of the filtered aliquot + 0.1 mL internal standard solution (made immediately prior to use with x g of either trifluorotoluene or fluorobenzene in y mL CD_3CN) for ^{19}F NMR yield determination.

In order to remove KF and TCICA (and its byproducts), the reaction vessel atmosphere and solvent was purged with Ar and transported into the glove box. Subsequently, the crude reaction mixture was filtered into a PFA vessel, washed with dry MeCN, and then concentrated in vacuo. Then, the crude reaction mixture was diluted with n-hexane, filtered into a PFA vessel, and concentrated in vacuo. (*Note that repeating dilution and filtration multiple times will provide better results due to limited solubility of aryl-IF_4 compounds.*)

Procedures and Characterization Data for Starting Materials

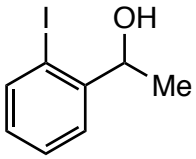

***1-(2-Iodophenyl)ethan-1-ol*:** A solution of 2-iodoacetophenone (1.0 g, 4.1 mmol, 1.0 eq.) in methanol (20 mL) was cooled to 0 ˚C. $NaBH_4$ (0.16 g, 4.1 mmol, 1.0 eq.) was added as a solid. The reaction was warmed to room temperature and stirred for 1 h. The reaction was quenched by adding saturated aqueous NH_4Cl to the reaction mixture. The aqueous layer was extracted three times with Et_2O. The combined organic layers were washed with brine and dried over $MgSO_4$. The solvent was removed at reduced pressure. The product was obtained as a yellow oil in 98% yield (0.99 g, 4.0 mmol), which was used without further purification. ^1H NMR (300 MHz, $CDCl_3$): δ = 7.80 (1H, dd, *J* = 7.9, 1.2 Hz), 7.56 (1H, dd, *J* = 7.8, 1.7 Hz), 7.38 (1H, td, *J* = 7.6, 1.2 Hz), 6.96 (1H, td, *J* = 7.6, 1.7 Hz), 5.06 (1H, qd, *J* = 6.3, 3.1 Hz), 2.08 (1H, d, *J* = 3.2 Hz), 1.46 (3H, d, *J* = 6.3 Hz); $^{13}C\{^1H\}$ NMR (75 MHz, $CDCl_3$): δ = 147.6, 139.5, 129.3, 128.9, 126.5, 97.4, 73.9, 23.9. ν_{max} (ATR-IR): 3315 (br) cm^{-1}. HRMS (ESI-TOF): calc'd for C_8H_9INaO $[M+Na]^+$: 270.9590, found: 270.9590.[4]

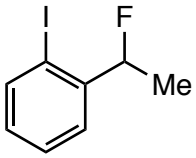

1-*(1-Fluoroethyl)-2-iodobenzene*: 1-(2-Iodophenyl)ethanol (0.25 g, 1.0 mmol, 1.0 eq.) was dissolved in dry DCM (6.0 mL) under an Ar atmosphere and stirred. The solution was cooled to −78 ˚C using an acetone/dry ice bath. Subsequently, DAST (0.16 mL, 1.2 mmol, 1.2 eq.) was added carefully to the reaction mixture. After a few minutes, the cooling bath was removed, and the mixture was allowed to warm gradually to room temperature. After one hour, full conversion was indicated by TLC analysis, and the reaction was quenched with saturated aqueous K_2CO_3. The organic layer was separated, and the aqueous phase was extracted with DCM three times. The combined organic layers were washed with

[4] Procedure adapted from: J. R. Wolstenhulme, J. Rosenqvist, O. Lozano, J. Ilupeju, N. Wurz, K. M. Engle, G. W. Pidgeon, P. R. Moore, G. Sandford and V. Gouverneur, *Angew. Chem. Int. Ed.* 2013, **52**, 9796.

brine and dried over $MgSO_4$. The crude material was purified by flash column chromatography using hexanes as an eluent. The product was obtained in 55% yield (0.14 g, 0.55 mmol) as a colorless liquid. ^{1}H NMR (300 MHz, $CDCl_3$): δ = 7.81 (1H, d, *J* = 7.9 Hz), 7.50 (1H, dd, *J* = 7.8, 1.8 Hz), 7.41 (1H, t, *J* = 7.5 Hz), 7.02 (1H, td, *J* = 7.6, 1.8 Hz), 5.76 (1H, dq, *J* = 46.4, 6.3 Hz), 1.62 (3H, dd, *J* = 24.0, 6.3 Hz); ^{13}C{^{1}H} NMR (75 MHz, $CDCl_3$): δ = 144.1 (d, *J* = 20.8 Hz), 139.4, 129.9 (d, *J* = 1.8 Hz), 128.8, 126.2 (d, *J* = 10.0 Hz), 95.4 (d, *J* = 5.8 Hz), 94.3 (d, *J* = 170.6 Hz), 22.4. (d, *J* = 25.7 Hz); ^{19}F NMR (282 MHz, $CDCl_3$): δ = −170.94 (1F, dq, *J* = 47.6, 23.8 Hz). HRMS (EI): calc'd for C_8H_8FI $[M]^+$: 249.3649, found: 249.3646.[5]

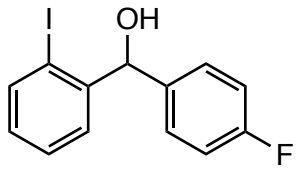

(*4-Fluorophenyl)(2-iodophenyl)methanol*: 1,2-Diiodobenzene (0.66 g, 2.0 mmol, 1.0 eq.) was dissolved in dry THF (10 mL), and the mixture was cooled to −40 ˚C using an acetonitrile/dry ice bath. After stirring for a few minutes at −40 ˚C, a 2 M solution of *i*-PrMgCl in THF (1.1 mL, 2.2 mmol, 1.1 eq.) was added to the reaction mixture. The mixture was warmed to −20 ˚C and stirred for 30 min. In the next step, a solution of 4-fluorobenzaldehyde (0.25 g, 2.0 mmol, 1.0 eq.) in dry THF (1.0 mL) was added drop wise to the reaction mixture. After complete addition, the reaction mixture was warmed to room temperature and stirred overnight. The reaction was quenched with saturated aqueous NH_4Cl. Then, Et_2O was added, and the organic layer was separated. The aqueous layer was extracted three times with Et_2O. The combined organic layers were dried over $MgSO_4$, filtered and the solvent was removed under reduced pressure. The crude material was purified by gradient column chromatography on silica gel eluting with hexanes and ethyl acetate. The product was obtained in 78% yield (0.51 g, 1.6 mmol) as a white solid; m.p. 95.8-97.7 ˚C. ^{1}H NMR (300 MHz, $CDCl_3$): δ = 7.83 (1H, dd, *J* = 7.9, 1.2 Hz), 7.50 (1H, dd, *J* = 7.8, 1.7 Hz), 7.42 – 7.30 (3H, m), 7.07 – 6.95 (3H, m), 5.99 (1H, d, *J* = 3.6 Hz), 2.77 (1H, d, *J* = 3.7 Hz); ^{13}C{^{1}H} NMR (101 MHz, $CDCl_3$): δ = 162.3 (d, *J* = 246.4 Hz), 145.3, 139.7, 137.9 (d, *J* = 3.3 Hz), 129.7, 129.1 (d, *J* = 8.2 Hz), 128.8, 128.3, 115.4 (d, *J* = 21.4 Hz), 98.6, 78.5; ^{19}F NMR (282 MHz, $CDCl_3$): δ = −114.36 (1F, tt, *J* = 8.7, 5.3 Hz). ν_{max} (ATR-IR): 3271 (br) cm^{-1}. HRMS (ESI-TOF): calc'd for $C_{13}H_{10}FINaO$ $[M+Na]^+$: 350.9653, found: 350.9651.[6]

[5] Procedure adapted from: A. L. Johnsen, *J. Org. Chem.* 1982, **47**, 5220.
[6] Procedure adapted from: M. Wang, Q. Fan and X. Jiang, *Org. Lett.* 2018, **20**, 216.

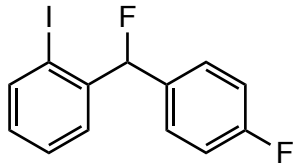

(*4-Fluorophenyl)(2-iodophenyl)methanol*: (4-Fluorophenyl)(2-iodophenyl)methanol (0.33 g, 1.0 mmol, 1.0 eq.) was dissolved in dry DCM (6 mL) under an argon atmosphere. The solution was cooled to −78 ˚C using an acetone/dry ice bath and stirred. In the next step, DAST (0.16 mL, 1.2 mmol, 1.2 eq.) was added carefully to the reaction mixture. After 15 min at −78 ˚C, the cooling bath was removed, and the mixture was allowed to warm to room temperature. After full conversion (determined by TLC), the reaction was quenched with saturated aqueous K_2CO_3. The organic layer was separated, and the aqueous phase was extracted with DCM three times. The combined organic layers were washed with brine and dried over $MgSO_4$. The crude material was purified by flash column chromatography using hexanes as an eluent. The product was obtained in 27% yield (88 mg, 0.27 mmol) as a white solid; m.p. 44.0-45.6 ˚C. ^{1}H NMR (300 MHz, $CDCl_3$): δ = 7.86 (1H, d, *J* = 7.9 Hz), 7.59 – 7.40 (2H, m), 7.40 – 6.30 (2H, m), 7.14 – 6.97 (3H, m), 6.61 (1H, d, *J* = 46.6 Hz); ^{13}C{^{1}H} NMR (75 MHz, $CDCl_3$): δ = 163.0 (d, *J* =248.0 Hz), 141.7 (d, *J* = 22.7 Hz), 139.8, 134.2 (dd, *J* = 22.3, 3.3 Hz), 130.3 (d, *J* = 1.6 Hz) 129.8 (dd, *J* = 8.5, 5.2 Hz), 128.7, 127.9 (d, *J* = 9.5 Hz), 115.7 (d, *J* = 21.9 Hz), 97.0 (d, *J* = 5.1 Hz), 96.5 (d, *J* = 174.1 Hz); ^{19}F NMR (282 MHz, $CDCl_3$): δ = −112.49 – −112.72 (1F, m), −161.85 (1F, dd, *J* = 46.9 Hz). HRMS (EI): calc'd for $C_8H_8F_2I$ $[M]^+$: 329.9712, found: 329.9709.[5]

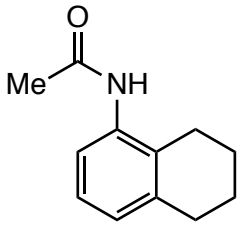

***N-(5,6,7,8-Tetrahydronaphthalen-1-yl)acetamide*:** Acetic anhydride (6.3 g, 61 mmol, 2.1 eq.) was dissolved in EtOH (100 mL), and the mixture was cooled to 0 ˚C. Then, a solution of 5,6,7,8-tetrahydronaphthalenamine (4.3 g, 29 mmol, 1.0 eq.) in EtOH (18 mL) was added slowly. After complete addition, the reaction was stirred for five minutes at 0 ˚C before the reaction mixture was warmed to room temperature. After stirring the reaction mixture for an additional 18 h at room temperature, the solvent was evaporated. The remaining solid was dried at 50 ˚C under reduced pressure (8 mbar). The product was obtained in 97% yield (5.3 g, 28 mmol) as a light brown solid; m.p. 158.9-160.7 ˚C. It was used without further purification. ^{1}H NMR (300 MHz, $CDCl_3$): δ = 7.59 (1H, d, *J* = 8.0 Hz), 7.12 (1H, t, *J* = 7.7 Hz), 6.92 (1H, d, *J* = 7.7 Hz), 6.88 (1H, s), 2.78 (2H, t, *J* = 6.2 Hz), 2.59 (2H, t, *J* = 6.3 Hz), 2.20 (3H, s), 1.89 – 1.71 (4H, m); ^{13}C{^{1}H} NMR (75 MHz, $CDCl_3$): δ = 168.5, 138.2,

135.4, 128.8, 126.6, 125.9, 121.1, 29.9, 24.7, 24.4, 23.0, 22.7. ν_{max} (ATR-IR): 3287, 1653, 1537 cm^{-1}. HRMS (ESI-TOF): calc'd for $C_{12}H_{15}NNaO$ $[M+Na]^+$: 212.1046, found: 212.1050.[7]

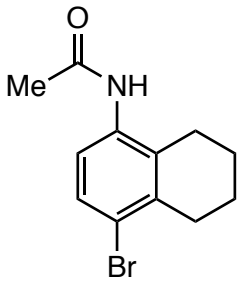

***N-(4-Bromo-5,6,7,8-tetrahydronaphthalen-1-yl)acetamide*:** *N*-(5,6,7,8-Tetrahydronaphthalen-1-yl)-acetamide (5.3 g, 28 mmol, 1.0 eq.) was dissolved in AcOH (40 mL), and the mixture was cooled to 10 ˚C using a cold water bath. Then, a solution of Br_2 (1.4 mL, 28 mmol, 1.0 eq.) in AcOH (3.0 mL) was added drop wise using a drop funnel. After complete addition, the drop funnel was washed with an additional AcOH (2.0 mL). The reaction mixture was warmed to room temperature and stirred for 4 h. The yellow slurry obtained was poured into ice water (100 mL). The suspension was filtered, and the solid was washed with cold water. The remaining solid was dissolved in DCM, and the organic phase was washed with water. The aqueous phase was extracted three times with DCM. The organic phase was dried over $MgSO_4$, filtered and then the solvent was removed under reduced pressure. The product was obtained in 91% yield (6.8 g, 26 mmol) as a white solid; m.p. 178.9-181.4 ˚C. It was used without further purification. ^{1}H NMR (300 MHz, $CDCl_3$): δ = 7.47 (1H, d, *J* = 8.7 Hz), 7.38 (1H, d, *J* = 8.5 Hz), 6.92 (1H, s) 2.79 – 2.69 (2H, m), 2.59 (2H, m), 2.18 (3H, s), 1.83 – 1.72 (4H, m); $^{13}C\{^1H\}$ NMR (75 MHz, $CDCl_3$): δ = 168.4, 137.3, 134.7, 131.5, 130.1, 122.5, 122.4, 30.9, 25.5, 24.4, 22.7, 22.4. ppm. ν_{max} (ATR-IR): 3272, 1651 cm^{-1}. HRMS (ESI-TOF): calc'd for $C_{12}H_{15}BrNO$ $[M+H]^+$: 268.0332, found: 268.0334.[7]

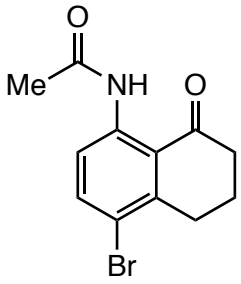

***N-(4-Bromo-8-oxo-5,6,7,8-tetrahydronaphthalen-1-yl)acetamide*:** *N*-(4-Bromo-5,6,7,8-tetrahydro-naphthalen-1-yl)acetamide (6.8 g, 26 mmol, 1.0 eq.) was dissolved in acetone (180 mL), then a solution of 15% $MgSO_4$ in H_2O (4.4 g of $MgSO_4$ in 25 mL H_2O) was added to the solution. $KMnO_4$ (13 g, 80 mmol, 3.1 eq.) was added portion-wise over 30 min as a solid. After stirring for 14 h at room temperature, the reaction mixture was filtered through a pad of Celite. The remaining solid was washed

[7] Procedure adapted from: W. C. Cronk, O. A. Mukhina and A. G. Kutateladze, *J. Org. Chem.* 2014, **79**, 1235.

with H_2O (200 mL) and $CHCl_3$ (200 mL). The aqueous phase was separated and washed three times with $CHCl_3$, and the organic phase was washed two times with brine. After drying the organic phase over $MgSO_4$, the organic phase was filtered, and the solvent was evaporated under reduced pressure. The crude product was purified by gradient column chromatography on silica gel eluting with hexanes and ethyl acetate. The product was obtained in 44% yield (3.2 g, 11 mmol) as a white solid; m.p. 174.3-175.8 ˚C. ^{1}H NMR (300 MHz, $CDCl_3$): δ = 12.12 (1H, s), 8.55 (1H, d, *J* = 9.1 Hz), 7.69 (1H, d, *J* = 9.1 Hz), 3.03 (2H, t, *J* = 6.2 Hz), 2.69 (2H, t, *J* = 6.6 Hz), 2.22 (3H, s), 2.11 (2H, p, *J* = 6.6 Hz); ^{13}C{^{1}H} NMR (75 MHz, $CDCl_3$): δ = 203.0, 169.6, 144.1, 142.5, 138.9, 119.9, 119.7, 117.5, 40.2, 31.4, 25.7, 21.8. ν_{max} (ATR-IR): 3167 (br), 1652 cm^{-1}. HRMS (ESI-TOF): calc'd for $C_{12}H_{13}BrNO_2$ $[M+H]^+$: 282.0124, found: 282.0124.[7]

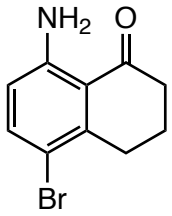

***8-Amino-5-bromo-3,4-dihydronaphthalen-1(2H)-one*:** *N*-(4-Bromo-8-oxo-5,6,7,8-tetrahydro-naphthalen-1-yl)acetamide (0.59 g, 2.1 mmol, 1.0 eq.) was suspended in 6 M HCl (9.7 mL). The mixture was stirred for 8 h at 90 ˚C. After cooling to room temperature, ice was added to the reaction mixture followed by solid $NaHCO_3$ in order to quench the reaction. The pH was adjusted to 8 using 2 M NaOH. The aqueous layer was extracted four times with EtOAc, and the organic layer was washed with brine and dried over $MgSO_4$. The solvent was removed under reduced pressure, and the product was obtained in 99% yield (0.50 g, 2.1 mmol) as a brown solid; m.p. 94.5-97.8 ˚C. It was used without further purification. ^{1}H NMR (300 MHz, $CDCl_3$): δ = 7.35 (1H, d, *J* = 8.9 Hz), 6.53 (2H, s), 6.40 (1H, d, *J* = 8.9 Hz), 2.92 (2H, t, *J* = 6.2 Hz), 2.61 (2H, t, *J* = 6.6 Hz), 2.04 (2H, p, *J* = 6.4 Hz); ^{13}C{^{1}H} NMR (75 MHz, $CDCl_3$): δ = 200.9, 150.6, 143.9, 138.1, 116.7, 116.4, 109.2, 39.8, .31.3, 22.1. ν_{max} (ATR-IR): 3442, 3328, 1638, 1599 cm^{-1}. HRMS (ESI-TOF): calc'd for $C_{10}H_{11}BrNO$ $[M+H]^+$: 240.0019, found: 240.0019.[7]

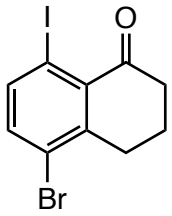

***5-Bromo-8-iodo-3,4-dihydronaphthalen-1(2H)-one*:** 8-Amino-5-bromo-3,4-dihydronaphthalen-1(2H)-one (0.43 g, 1.8 mmol, 1.0 eq) was dissolved in a mixture of H_2O (2.2 mL), AcOH (2.2 mL) and concentrated HCl (0.6 mL). After cooling to 0 ˚C, a solution of $NaNO_2$ (0.14 g, 2.0 mmol, 1.1 eq.) in H_2O (0.6 mL) was added drop wise. The mixture was stirred at 0 ˚C for 15 min, followed by drop wise

addition of a solution of KI (0.32 g, 1.9 mmol, 1.1 eq.) in H_2O (0.6 mL). After stirring at 0 ˚C for 10 min, the reaction mixture was heated to 60 ˚C and stirred for an additional 1 h. After cooling to room temperature, the reaction was quenched using 40% aqueous $NaHSO_3$. DCM was added, and the organic layer was separated. The aqueous phase was extracted with DCM three times. The combined organic layers were washed with saturated aqueous $NaHCO_3$, brine and saturated aqueous $Na_2S_2O_3$. The organic layer was dried over $MgSO_4$, and, after filtration, the solvent was removed under reduced pressure. The crude material was purified by gradient column chromatography on silica gel eluting with hexanes and ethyl acetate. In order to obtain an analytically pure sample, the product was subjected to preparative HPLC eluting with hexanes and ethyl acetate. The product was obtained in 45% yield (0.28 g, 0.81 mmol) as a light yellow solid; m.p. 77.2-79.0 ˚C.^{1}H NMR (300 MHz, $CDCl_3$): δ = 7.81 (1H, d, *J* = 8.4 Hz), 7.32 (1H, d, *J* = 8.4 Hz), 3.04 (2H, t, *J* = 6.2 Hz), 2.71 (2H, t, *J* = 6.6 Hz), 2.14 (2H, p, *J* = 6.4 Hz); $^{13}C\{^1H\}$ NMR (75 MHz, $CDCl_3$): δ = 196.3, 145.2, 142.1, 137.0, 134.6, 125.6, 91.7, 38.6, .31.4, 21.7. ν_{max} (ATR-IR): 1683 cm^{-1}. HRMS (ESI-TOF): calc'd for $C_{10}H_9BrIO$ $[M+H]^+$: 350.8876, found: 350.8878.[8]

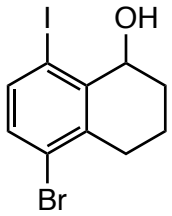

***5-Bromo-8-iodo-1,2,3,4-tetrahydronaphthalen-1-ol*:** $NaBH_4$ (14 mg, 0.40 mmol, 1.1 eq.) was added as a solid to a stirred solution of *5-Bromo-8-iodo-3,4-dihydronaphthalen-1(2H)-one* (0.13 g, 0.37 mmol, 1.0 eq.) in methanol (3 mL) at 0 ˚C. After full conversion was determined by TLC, the reaction was quenched with saturated aqueous NH_4Cl. Et_2O was added, and the organic layer was separated. The aqueous phase was extracted with Et_2O three times. The combined organic layers were washed with brine. The organic layer was dried over $MgSO_4$, and, after filtration, the solvent was removed under reduced pressure. The crude product was purified by gradient column chromatography on silica gel eluting with hexanes and ethyl acetate. The product was obtained in 87% yield (0.11 g, 0.81 mmol) as a pale brown solid; m.p. 64.0-65.8 ˚C. ^{1}H NMR (300 MHz, $CDCl_3$): δ = 7.58 (1H, d, *J* = 8.4 Hz), 7.22 (1H, d, *J* = 8.4 Hz), 4.83 (1H, q, *J* = 3.5 Hz), 2.95 (1H, dd, *J* = 18.0, 5.6 Hz), 2.62 – 2.43 (1H, m), 2.37 (1H, dd, *J* = 4.1, 1.2 Hz), 2.19 (1H, dm, *J* = 13.6 Hz), 2.11 – 1.95 (1H, m), 1.92 – 1.79 (1H, m), 1.71 (1H, tm, *J* = 13.9 Hz); $^{13}C\{^1H\}$ NMR (126 MHz, $CDCl_3$): δ = 142.1, 139.7, 138.3, 133.6, 126.8, 101.4, 70.6, 31.2, 30.6, 17.4. ν_{max} (ATR-IR): 3202 (br) cm^{-1}. HRMS (ESI-TOF): calc'd for $C_{10}H_{10}BrINaO$ $[M+Na]^+$: 374.8852, found: 374.8859.[4]

[8] Procedure adapted from: P. Nguyen, E. Corpuz, T. M. Heidelbaugh, K. Chow and M. E. Garst, *J. Org. Chem.* 2003, **68**, 10195.

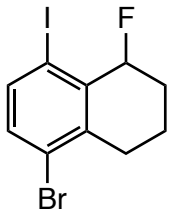

***5-Bromo-1-fluoro-8-iodo-1,2,3,4-tetrahydronaphthalene*:** 5-Bromo-8-iodo-1,2,3,4-tetrahydro-naphthalen-1-ol (0.11 g, 0.32 mmol, 1.0 eq.) was dissolved in dry DCM (2.0 mL) under an argon atmosphere and stirred. The solution was cooled to −78 ˚C using an acetone/dry ice bath. In the next step, DAST (0.05 mL, 0.40 mmol, 1.25 eq.) was added carefully to the reaction mixture. After a few minutes, the cooling bath was removed, and the mixture was allowed to warm gradually to room temperature. After 15 min, full conversion was indicated by TLC, and the reaction was quenched with saturated aqueous K_2CO_3. The organic layer was separated, and the aqueous phase was extracted with DCM for three times. The combined organic layers were washed with brine and dried over $MgSO_4$. The crude product was purified by flash column chromatography using hexanes as an eluent. The product was obtained in 69% yield (77 mg, 0.22 mmol) as a colorless liquid. ^{1}H NMR (500 MHz, $CDCl_3$): δ = 7.63 (1H, d, *J* = 8.3 Hz), 7.27 (1H, dd, *J* = 8.3, 2.3 Hz), 5.61 (1H, dt, *J* = 48.5, 2.9 Hz), 3.02 – 2.94 (1H, m), 2.57 – 2.46 (1H, m), 2.45 – 2.34 (1H, m), 2.01 – 1.85 (2H, m), 1.83 – 1.64 (1H, m); ^{13}C{^{1}H} NMR (126 MHz, $CDCl_3$): δ = 140.5 (d, *J* = 3.8 Hz), 138.7 (d, *J* = 2.9 Hz), 137.5 (d, *J* = 16.8 Hz), 134.7 (d, *J* = 3.8 Hz), 126.4 (d, *J* = 2.7 Hz), 102.2 (d, *J* = 3.3 Hz), 90.4 (d, *J* = 169.7 Hz), 30.9 (d, *J* = 1.6 Hz), 29.5. (d, *J* = 22.3 Hz), 17.4; ^{19}F NMR (471 MHz, $CDCl_3$): δ = −160.59 – −161.11 (1F, m). HRMS (ESI-TOF): calc'd for $C_{10}H_9BrFINa$ $[M+Na]^+$: 376.8809, found: 376.8815.[5]

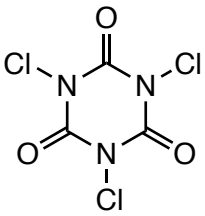

***Trichloroisocyanuric acid*:** ^{13}C{^{1}H} NMR (75 MHz, CD_3CN): δ = 144.9.

Route for Synthesis of Probe Molecule 21

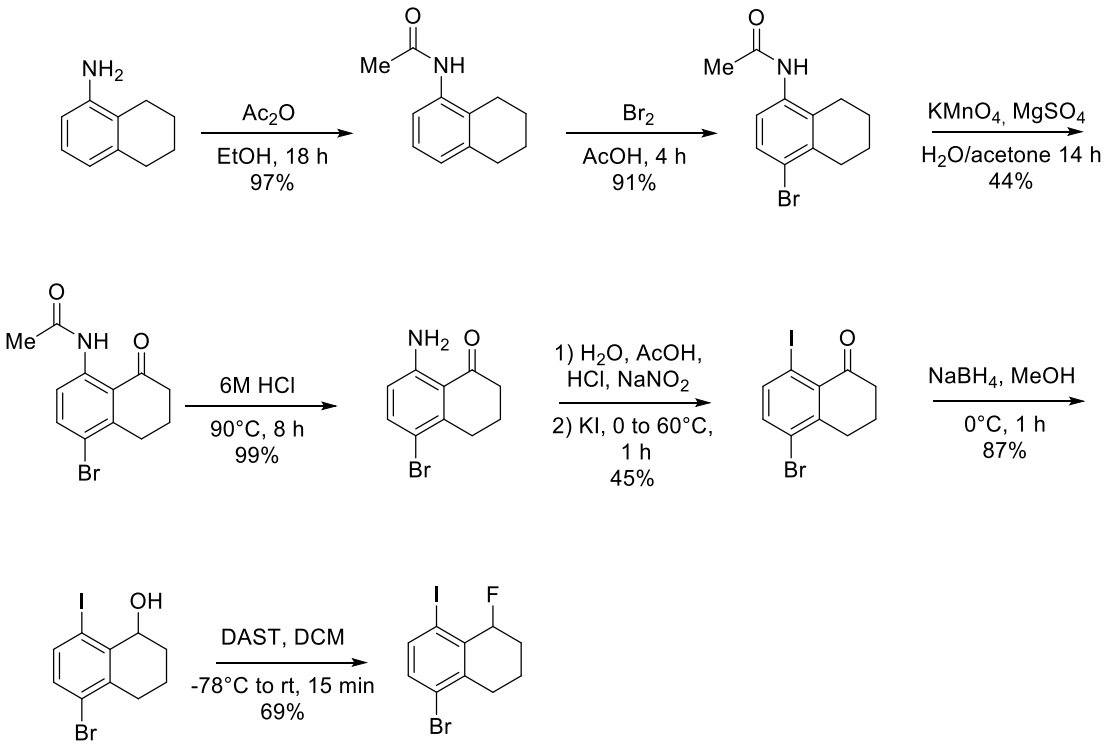

Procedure for Synthesis of 21 with XeF_2

5-Bromo-1-fluoro-8-iodo-1,2,3,4-tetrahydronaphthalene (21 mg, 0.06 mmol, 1.0 equiv.) was added to an oven-dried 5 mL PFA vessel equipped with a stir bar under glove box (N_2) atmosphere, and then diluted with DCM (1.0 mL). In one portion, XeF_2 (8.9 mg, 0.05 mmol, 0.9 equiv.) was added. The PFA vessel was sealed (to prevent solvent evaporation), and the reaction mixture was stirred for 24 h. An aliquot was taken for ^{19}F NMR analysis; approximately 85% conversion of the starting material to **21** was observed. Subsequently, the reaction mixture was diluted with n-hexane, and single crystals suitable for X-ray analysis were obtained by slow solvent evaporation of the DCM/n-hexane mixture under inert atmosphere.

Procedure for Synthesis of 37 with XeF_2

A dry NMR tube with a screw cap (J Young NMR tube) was charged with **36** (19 mg, 0.05 mmol, 1.0 equiv.) and MeCN (0.5 mL) under glove box (N_2) atmosphere. XeF_2 (14 mg, 0.08 mmol, 1.6 equiv.) was then added (in the dark). The NMR tube was sealed with the screw cap, and its contents were mixed. The tube was transported outside of the glovebox, where it was connected to a Schlenk line and kept under argon atmosphere for several minutes to ensure pressure equalization. (Note that the sample was protected from light with aluminum foil.) The solution turned yellow about 1 h after starting the reaction, and the reaction was monitored by ^{19}F NMR. After several hours, the reaction had gone to completion, and **37** was obtained by removal of the solvent. Single crystals suitable for X-ray analysis were obtained by sublimation; they were maintained under inert atmosphere.

Characterization Data for Difluoro(aryl)-λ^3-iodanes and Tetrafluoro(aryl)-λ^5-iodanes

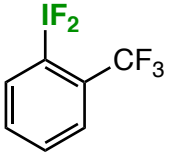

Difluoro(2-(trifluoromethyl)phenyl)-λ^3-iodane **(Compound 2):** The reaction was run according to the general procedure in CD_3CN, and the product was characterized directly from the reaction mixture. ^{1}H NMR (400 MHz, CD_3CN): δ = 8.72 (1H, d, *J* = 7.8 Hz), 8.06 (1H, d, *J* = 7.7 Hz), 7.93 (1H, t, *J* = 7.8 Hz), 7.85 (1H, t, *J* = 7.8 Hz); ^{13}C{^{1}H} NMR (101 MHz, CD_3CN): δ = 140.3, 136.6 – 136.5 (m), 134.6 (t, *J* = 1.8 Hz), 129.8 (q, *J* = 32.6 Hz), 129.00 (q, *J* = 5.4 Hz), 125.2 (q, *J* = 273.7 Hz), 124.3 (tq, *J* = 14.3, 1.7 Hz); ^{19}F NMR (376 MHz, CD_3CN): δ = −60.36 (3F, s), −161.65 (2F, s).

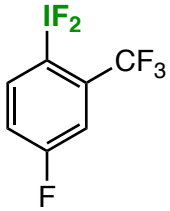

(4-Fluoro-2-(trifluoromethyl)phenyl)difluoro-λ^3-iodane **(Compound 3):** The reaction was run according to the general procedure in CD_3CN, and the product was characterized directly from the reaction mixture. ^{1}H NMR (400 MHz, CD_3CN): δ = 8.75 (1H, br dd, *J* = 8.7, 5.1 Hz), 7.80 (1H, br d, *J* = 8.7 Hz), 7.56 (1H, br t, *J* = 7.3 Hz); ^{13}C{^{1}H} NMR (101 MHz, CD_3CN): δ = 165.1 (d, *J* = 256.2 Hz), 143.5 (d, *J* = 9.4 Hz), 133.1 (qd, *J* = 33.7, 8.9 Hz), 123.5 (d, *J* = 22.1 Hz), 123.0 (qd, *J* = 273.9, 2.3 Hz), 119.7 – 119.1 (m), 117.7 (dq, *J* = 27.0, 5.5 Hz); ^{19}F NMR (376 MHz, CD_3CN): δ = −60.82 (3F, s), −103.17 (1F, s), −159.84 (2F, s).

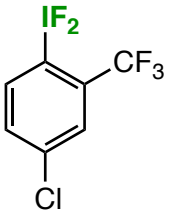

(4-Chloro-2-(trifluoromethyl)phenyl)difluoro-λ^3-iodane **(Compound 4):** The reaction was run according to the general procedure in CD_3CN, and the product was characterized directly from the reaction mixture. ^{1}H NMR (500 MHz, CD_3CN): δ = 8.67 (1H, d, *J* = 8.5 Hz), 8.05 (1H, s), 7.84 (1H, d, *J* = 8.5 Hz); ^{13}C{^{1}H} NMR (126 MHz, CD_3CN): δ = 141.9, 140.6, 136.5, 131.8 (q, *J* = 33.2 Hz), 129.6 (q, *J* = 5.4 Hz),123.2 (q, *J* = 274.2 Hz), 122.2 (tm, *J* = 14.7 Hz); ^{19}F NMR (471 MHz, CD_3CN): δ = −60.77 (3F, s), −160.27 (2F, s).

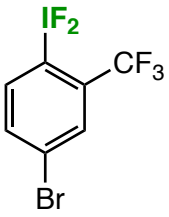

(4-Bromo-2-(trifluoromethyl)phenyl)difluoro-λ³-iodane **(Compound 5):** The reaction was run according to the general procedure in CD_3CN, and the product was characterized directly from the reaction mixture. ^1H NMR (500 MHz, CD_3CN): δ = 8.58 (1H, d, *J* = 8.4 Hz), 8.20 (1H, s), 8.00 (1H, d, *J* = 8.5 Hz); $^{13}C\{^1H\}$ NMR (126 MHz, CD_3CN): δ = 141.7, 139.5, 132.3 (q, *J* = 5.3 Hz), 131.6 (q, *J* = 33.1 Hz), 128.7 (t, *J* = 2.1 Hz), 123.0 (q, *J* = 274.3 Hz), 122.9 – 122.6 (m); ^{19}F NMR (471 MHz, CD_3CN): δ = −60.70 (3F, s), −160.35 (2F, s).

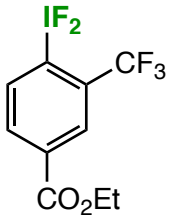

Ethyl 4-(difluoro-λ³-iodanyl)-3-(trifluoromethyl)benzoate **(Compound 6):** The reaction was run according to the general procedure in CD_3CN, and the product was characterized directly from the reaction mixture. ^1H NMR (400 MHz, CD_3CN): δ = 8.80 (1H, d, *J* = 8.2 Hz), 8.53 (1H, s), 8.37 (1H, d, *J* = 8.2 Hz), 4.42 (2H, q, *J* = 7.0 Hz), 1.39 (3H, t, *J* = 7.1 Hz); $^{13}C\{^1H\}$ NMR (101 MHz, CD_3CN): δ = 164.6, 140.7, 136.9, 136.0, 130.4 (q, *J* = 33.2 Hz), 129.4 (q, *J* = 5.3 Hz), 127.4 (t, *J* = 13.9 Hz), 123.5 (q, *J* = 273.8 Hz), 63.2, 14.4; ^{19}F NMR (376 MHz, CD_3CN): δ = −60.62 (3F, s), −161.25 (2F, s).

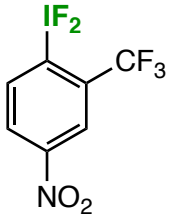

Difluoro(4-nitro-2-(trifluoromethyl)phenyl)-λ³-iodane **(Compound 7):** The reaction was run according to the general procedure in CD_3CN, and the product was characterized directly from the reaction mixture. ^1H NMR (500 MHz, CD_3CN): δ = 8.93 (1H, br d, *J* = 8.6 Hz), 8.73 (1H, br s), 8.59 (1H, br d, *J* = 8.5 Hz); $^{13}C\{^1H\}$ NMR (126 MHz, CD_3CN): δ = 150.8, 141.9, 131.7 (q, *J* = 34.1 Hz), 131.3, 128.3 (t, *J* = 14.4 Hz), 124.5 (q, *J* = 5.5 Hz), 122.9 (q, *J* = 274.3 Hz); ^{19}F NMR (471 MHz, CD_3CN): δ = −60.88 (3F, s), −160.30 (2F, s).

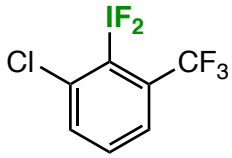

(2-Chloro-6-(trifluoromethyl)phenyl)difluoro-λ³-iodane **(Compound 8):** The reaction was run according to the general procedure in CD_3CN, and the product was characterized directly from the reaction mixture. ^1H NMR (500 MHz, CD_3CN): δ = 8.16 (1H, d, *J* = 8.2 Hz), 7.95 (1H, d, *J* = 7.8 Hz), 7.87 (1H, t, *J* = 8.2 Hz); $^{13}C\{^1H\}$ NMR (126 MHz, CD_3CN): δ = 139.7, 136.5, 134.6, 133.0 (q, *J* = 32.3 Hz), 130.2 (t, *J* = 14.3 Hz), 127.5 (q, *J* = 5.7 Hz), 123.6 (q, *J* = 274.3 Hz); ^{19}F NMR (471 MHz, CD_3CN): δ = −60.10 (3F, s), −163.36 (2F, s).

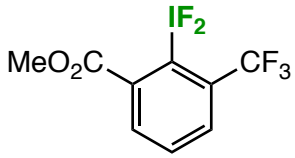

Methyl 2-(difluoro-λ³-iodanyl)-3-(trifluoromethyl)benzoate **(Compound 9):** The reaction was run according to the general procedure in CD_3CN, and the product was characterized directly from the reaction mixture. ^1H NMR (500 MHz, CD_3CN): δ = 8.33 (1H, d, *J* = 7.8 Hz), 8.22 (1H, d, *J* = 7.9 Hz), 8.00 (1H, t, *J* = 7.9 Hz), 4.03 (3H, s); $^{13}C\{^1H\}$ NMR (126 MHz, CD_3CN): δ = 166.6, 135.5, 135.2, 134.8, 132.2 (q, *J* = 5.6 Hz), 131.9 (q, *J* = 32.0 Hz), 124.1 (q, *J* = 274.3 Hz), 123.4 (q, *J* = 14.0 Hz), 54.4; ^{19}F NMR (471 MHz, CD_3CN): δ = −59.23 (3F, s), −159.98 (2F, s).

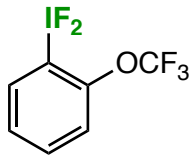

Difluoro(2-(trifluoromethoxy)phenyl)-λ³-iodane **(Compound 10):** The reaction was run according to the general procedure in CD_3CN, and the product was characterized directly from the reaction mixture. ^1H NMR (500 MHz, CD_3CN): δ = 8.46 (1H, dd, *J* = 8.0, 1.8 Hz), 7.82 (1H, t, *J* = 8.0 Hz), 7.72 (1H, d, *J* = 8.5 Hz), 7.56 (1H, t, *J* = 7.8 Hz); $^{13}C\{^1H\}$ NMR (126 MHz, CD_3CN): δ = 146.4 (q, *J* = 1.8 Hz), 137.9, 136.6, 130.5, 123.2 (t, *J* = 13.8 Hz), 121.41 (q, *J* = 259.8 Hz), 121.40 (q, *J* = 1.9 Hz); ^{19}F NMR (471 MHz, CD_3CN): δ = −57.60 (3F, s), −166.40 (2F, s).

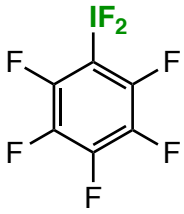

Difluoro(perfluorophenyl)-λ³-iodane **(Compound 11):** The reaction was run according to the general procedure in CD_3CN, and the product was characterized directly from the reaction mixture. ^{19}F NMR (282 MHz, CD_3CN): δ = −124.10 to −124.65 (2F, m), −145.92 (1F, tt, *J* = 19.9, 5.1 Hz), −158.21 to −158.66 (2F, m), −162.08 (2F, s).

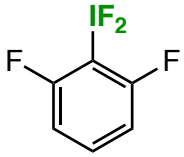

(*2,6-Difluorophenyl)difluoro-λ³-iodane* **(Compound 12):** The reaction was run according to the general procedure in CD_3CN, and the product was characterized directly from the reaction mixture. ^1H NMR (500 MHz, CD_3CN): δ = 7.80 (1H, t, *J* = 7.7 Hz), 7.37 (2H, br s); $^{13}C\{^1H\}$ NMR (126 MHz, CD_3CN): δ = 160.0 (dd, *J* = 253.9, 4.6 Hz), 138.7 (dd, *J* = 11.2, 8.9 Hz), 113.5 – 113.2 (m), 108.4 – 107.6 (m); ^{19}F NMR (471 MHz, CD_3CN): δ = −97.43 (2F, br. s), −165.78 (2F, s).

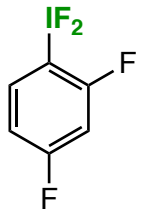

(2,4-Difluorophenyl)difluoro-λ³-iodane **(Compound 13):** The reaction was run according to the general procedure in CD_3CN, and the product was characterized directly from the reaction mixture. ^1H NMR (500 MHz, CD_3CN): δ = 8.37 (1H, dt, *J* = 9.0, 4.6 Hz), 7.34 (1H, td, *J* = 8.9, 2.8 Hz), 7.20 (1H, td, *J* = 8.6, 2.7 Hz); $^1H\{^{19}F\}$ NMR (500 MHz, CD_3CN): δ = 8.37 (1H, d, *J* = 8.9 Hz), 7.34 (1H, d, *J* = 2.8 Hz), 7.20 (1H, td, *J* = 9.0, 2.8 Hz); $^{13}C\{^1H\}$ NMR (126 MHz, CD_3CN): δ = 167.0 (ddt, *J* = 256.1, 12.0, 1.9 Hz), 160.4 (dd, *J* = 253.9, 13.3 Hz), 115.5 (dd, *J* = 23.0, 3.4 Hz), 112.2 (dtd, *J* = 23.3, 15.2, 4.5 Hz), 106.3 (t, *J* = 26.8 Hz); ^{19}F NMR (471 MHz, CD_3CN): δ = −94.80 (1F, d, *J* = 11.4 Hz), −101.28 (1F, dt, *J* = 11.1, 4.3 Hz), −165.09 (2F, s).

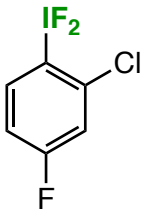

(2-Chloro-4-fluorophenyl)difluoro-λ³-iodane **(Compound 14):** The reaction was run according to the general procedure in CD_3CN, and the product was characterized directly from the reaction mixture. ^1H NMR (400 MHz, CD_3CN): δ = 8.47 (1H, dd, *J* = 8.9, 5.6 Hz), 7.64 (1H, dd, *J* = 8.6, 2.8 Hz), 7.28 (1H, td, *J* = 8.5, 2.8 Hz); $^{13}C\{^1H\}$ NMR (101 MHz, CD_3CN): δ = 160.0 (dt, *J* = 256.6, 1.7 Hz), 140.7 (d, *J* = 10.0 Hz), 138.6 (d, *J* = 11.5 Hz), 127.6 (td, *J* = 14.6, 4.0 Hz), 118.8 (t, *J* = 26.7 Hz), 118.3 (t, *J* = 22.7 Hz); ^{19}F NMR (376 MHz, CD_3CN): δ = −103.50 (1F, tq, *J* = 9.3, 4.8 Hz), −164.37 (2F, d, *J* = 4.2 Hz); $^{19}F\{^1H\}$ NMR (376 MHz, CD_3CN): δ = −103.50 (1F, t, *J* = 4.5 Hz), −164.37 (2F, d, *J* = 3.7 Hz).

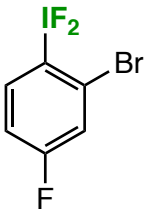

(2-Bromo-4-fluorophenyl)difluoro-λ³-iodane **(Compound 15):** The reaction was run according to the general procedure in CD_3CN, and the product was characterized directly from the reaction mixture. ^1H NMR (400 MHz, CD_3CN): δ = 8.47 (1H, dd, *J* = 8.9, 5.5 Hz), 7.78 (1H, dd, *J* = 8.8, 2.7 Hz), 7.36 – 7.25 (1H, m); $^{13}C\{^1H\}$ NMR (101 MHz, CD_3CN): δ = 165.5 (dt, *J* = 257.4, 1.7 Hz), 141.1 (d, *J* = 9.6 Hz), 130.7 (td, *J* = 14.7, 4.0 Hz), 128.5 (d, *J* = 10.4 Hz), 122.0 (t, *J* = 26.3 Hz), 118.7 (t, *J* = 22.7 Hz); ^{19}F NMR (376 MHz, CD_3CN): δ = −103.74 (1F, br s), −163.35 (2F, br s).

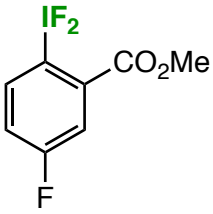

Methyl 2-(difluoro-λ³-iodaneyl)-5-fluorobenzoate **(Compound 16):** The reaction was run according to the general procedure in CD_3CN, and the product was characterized directly from the reaction mixture. ^1H NMR (500 MHz, CD_3CN): δ = 8.47 (1H, dd, *J* = 8.8, 5.1 Hz), 7.88 (1H, dd, *J* = 9.0, 3.1 Hz), 7.52 (1H, td, *J* = 8.4, 3.1 Hz), 3.98 (3H, s); $^{13}C\{^1H\}$ NMR (126 MHz, CD_3CN): δ = 165.2 (d, *J* = 253.8 Hz), 164.7 (d, *J* = 2.7 Hz), 140.5 (d, *J* = 9.0 Hz), 133.15 (d, *J* = 8.2 Hz), 122.6 (d, *J* = 22.7 Hz), 121.8 (td, *J* = 13.6, 3.6 Hz), 119.9 (d, *J* = 25.4 Hz), 54.0; ^{19}F NMR (471 MHz, CD_3CN): δ = -106.14 to -106.21 (1F, m), -165.51 (2F, br s).

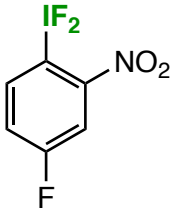

Difluoro(4-fluoro-2-nitrophenyl)-λ³-iodane **(Compound 17):** The reaction was run according to the general procedure in CD_3CN, and the product was characterized directly from the reaction mixture. ^1H NMR (400 MHz, CD_3CN): δ = 8.51 (1H, dd, *J* = 8.9, 5.2 Hz), 8.06 (1H, dd, *J* = 8.3, 2.8 Hz), 7.69-7.64 (1H, m); $^{13}C\{^1H\}$ NMR (101 MHz, CD_3CN): δ = 165.3 (d, *J* = 256.9 Hz), 148.7 (br d, *J* = 8.4 Hz), 140.3 (d, *J* = 8.9 Hz), 123.7 (d, *J* = 22.5 Hz), 115.7 (d, *J* = 28.4 Hz), 114.5 (td, *J* = 14.8, 4.4 Hz); ^{19}F NMR (376 MHz, CD_3CN): δ = -103.45 to -103.57 (1F, m), -164.72 (2F, br s).

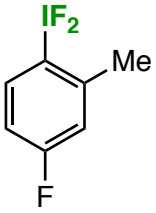

Difluoro(4-fluoro-2-methylphenyl)-λ³-iodane **(Compound 18):** The reaction was run according to the general procedure in CD_3CN, and the product was characterized directly from the reaction mixture. ^1H NMR (400 MHz, CD_3CN): δ = 8.32 (1H, dd, *J* = 8.9, 5.5 Hz), 7.34 (1H, dd, *J* = 9.8, 3.0 Hz), 7.12 (1H, td, *J* = 8.6, 3.1 Hz), 2.74 (3H, s); $^{13}C\{^1H\}$ NMR (101 MHz, CD_3CN): δ = 165.7 (dt, *J* = 252.4, 1.9 Hz), 144.4 (d, *J* = 9.5 Hz), 139.6 (d, *J* = 9.5 Hz), 128.5 (td, *J* = 13.6, 3.0 Hz), 118.9 (t, *J* = 23.1 Hz), 116.8 (t, *J* = 22.8 Hz), 25.1; ^{19}F NMR (376 MHz, CD_3CN): δ = −106.86 (1F, tt, *J* = 9.9, 4.8 Hz), −168.31 (2F, d, *J* = 3.7 Hz); $^{19}F\{^1H\}$ NMR (376 MHz, CD_3CN): δ = −106.86 (1F, t, *J* = 4.7 Hz), −168.32 (2F, d, *J* = 4.2 Hz).

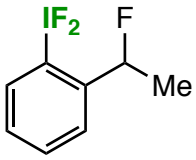

Difluoro(2-(1-fluoroethyl)phenyl)-λ³-iodane **(Compound 19):** The reaction was run according to the general procedure in CD_3CN, and the product was characterized directly from the reaction mixture. ^1H NMR (500 MHz, CD_3CN): δ = 8.39 (1H, d, *J* = 8.0 Hz), 7.85 – 7.77 (2H, m), 7.57 (1H, d, *J* = 7.6 Hz), 6.07 (1H, dd, *J* = 46.1, 6.4 Hz), 1.72 (3H, dd, *J* = 24.1, 6.4 Hz); $^{13}C\{^1H\}$ NMR (126 MHz, CD_3CN): 141.8 (d, *J* = 20.9 Hz), 137.3, 134.7, 132.4, 129.4 (td, *J* = 13.2, 4.3 Hz), 128.5 (d, *J* = 7.7 Hz), 93.8 (d, *J* = 129.7 Hz), 23.5 (d, *J* = 25.2 Hz); ^{19}F NMR (471 MHz, CD_3CN): δ = −165.35 (2F, s), −165.58 (1F, dq, *J* = 47.8, 24.2 Hz).

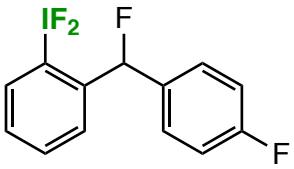

Difluoro(2-(fluoro(4-fluorophenyl)methyl)phenyl)-λ³-iodane **(Compound 20):** The reaction was run according to the general procedure in CD_3CN, and the product was characterized directly from the reaction mixture. ^1H NMR (500 MHz, CD_3CN): δ = 8.42 (1H, d, *J* = 8.0 Hz), 7.85 – 7.77 (2H, m), 7.61 (1H, br t, *J* = 7.5 Hz), 7.45 (2H, br t, *J* = 6.9 Hz), 7.17 (2H, br t, *J* = 8.5 Hz), 7.02 (1H, d, *J* = 46.1 Hz); $^{13}C\{^1H\}$ NMR (126 MHz, CD_3CN): δ = 163.6 (dd, *J* = 246.6, 2.8 Hz), 139.6 (d, *J* = 23.1 Hz), 138.1 (d, *J* = 28.4 Hz), 137.6, 134.9 (dd, *J* = 22.2, 3.2 Hz), 134.6, 132.8 (d, *J* = 1.8 Hz), 130.6 (dd, *J* = 8.7, 5.8 Hz), 129.7 (d, *J* = 8.6 Hz), 116.6 (d, *J* = 21.9 Hz), 95.4 (d, *J* = 174.0 Hz); ^{19}F NMR (471 MHz, CD_3CN): δ = −113.59 (1F, br. s), −161.74 (1F, d, *J* = 46.2 Hz), −165.69 (2F, br. s).

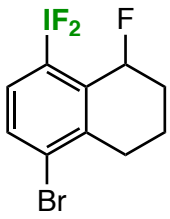

(4-Bromo-8-fluoro-5,6,7,8-tetrahydronaphthalen-1-yl)difluoro-λ³-iodane **(Compound 21):** The reaction was run according to the general procedure in CD_3CN, and the product was characterized directly from the reaction mixture. ^1H NMR (500 MHz, CD_2Cl_2): δ = 8.16 (1H, d, *J* = 8.4 Hz), 7.79 (1H, dd, *J* = 8.4, 2.1 Hz), 5.97 (1H, dt, *J* = 49.3, 3.2 Hz), 3.12 – 3.05 (1H, m), 2.67 – 2.54 (1H, m), 2.50 – 2.41 (1H, m), 2.02 – 1.95 (2H, m), 1.92 – 1.82 (1H, m); $^{13}C\{^1H\}$ NMR (126 MHz, CD_2Cl_2): δ = 142.1, 136.4 (d, *J* = 44.2 Hz), 135.3 (d, *J* = 17.6 Hz), 132.0, 117.0, 88.4 (d, *J* = 170.1 Hz), 31.4, 29.2 (d, *J* = 21.5 Hz), 17.4, 2.1; ^{19}F NMR (471 MHz, CD_3CN): δ = −156.94 to −157.21 (1F, m), −165.33 (2F, s).

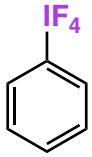

Tetrafluoro(phenyl)-λ⁵-iodane **(Compound 25):** The reaction was run according to the general procedure, and the product was characterized by the diagnostic IF_4 signal in the ^{19}F NMR spectrum. ^{19}F NMR (282 MHz, CD_3CN): δ = -27.95 (4F, br s).

Tetrafluoro(4-fluorophenyl)-λ^5-iodane **(Compound 26):** The reaction was run according to the general procedure, and the product was isolated via extraction with n-hexane as an air-sensitive white solid. ^{1}H NMR (500 MHz, CD_3CN): δ = 8.16 (2H, dd, *J* = 9.2, 4.7 Hz), 7.51 (2H, t, *J* = 8.7 Hz); ^{1}H{^{19}F} NMR (500 MHz, CD_3CN): δ = 8.16 (2H, d, *J* = 9.2 Hz), 7.51 (2H, t, *J* = 8.7 Hz); ^{13}C{^{1}H} NMR (126 MHz, CD_3CN): δ = 166.2 (d, *J* = 254.9 Hz), 155.76 (br s), 131.05 (d, *J* = 10.1 Hz), 118.5 (d, *J* = 23.8 Hz); ^{19}F NMR (471 MHz, CD_3CN): δ = −25.84 (4F, br s), −104.32 (1F, m). Additionally, single crystals suitable for X-ray analysis were obtained by cooling a concentrated solution of **26** in n-hexane at approximately -20 °C in a PFA vessel inside a glovebox freezer.

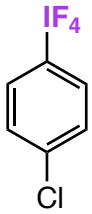

Tetrafluoro(4-chlorophenyl)-λ^5-iodane **(Compound 27):** The reaction was run according to the general procedure, and the product was characterized by the diagnostic IF_4 signal in the ^{19}F NMR spectrum. ^{19}F NMR (282 MHz, CD_3CN): δ = -26.46 (4F, br s).

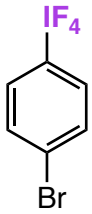

Tetrafluoro(4-bromophenyl)-λ^5-iodane **(Compound 28):** The reaction was run according to the general procedure, and the product was characterized by the diagnostic IF_4 signal in the ^{19}F NMR spectrum. ^{19}F NMR (282 MHz, CD_3CN): δ = -26.62 (4F, br s).

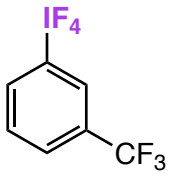

Tetrafluoro(3-(trifluoromethyl)phenyl)-λ^5-iodane **(Compound 29):** The reaction was run according to the general procedure, and the product was characterized by the diagnostic IF_4 signal in the ^{19}F NMR spectrum. ^{19}F NMR (282 MHz, CD_3CN): δ = -26.03 (4F, br s), -63.33 (3F, s).

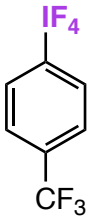

Tetrafluoro(4-(trifluoromethyl)phenyl)-λ^5-iodane **(Compound 30):** The reaction was run according to the general procedure, and the product was characterized by the diagnostic IF_4 signal in the ^{19}F NMR spectrum. ^{19}F NMR (282 MHz, CD_3CN): δ = -26.64 (4F, br s), -63.86 (3F, s).

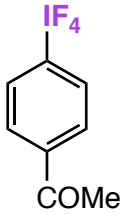

1-(4-(Tetrafluoro-λ^5-iodanyl)phenyl)ethan-1-one **(Compound 31):** The reaction was run according to the general procedure, and the product was characterized by the diagnostic IF_4 signal in the ^{19}F NMR spectrum. ^{19}F NMR (282 MHz, CD_3CN): δ = -27.26 (4F, br s).

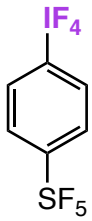

Pentafluoro(4-(tetrafluoro-λ^5-iodanyl)phenyl)-λ^6-sulfane **(Compound 32):** The reaction was run according to the general procedure, and the product was characterized by the diagnostic IF_4 signal in the ^{19}F NMR spectrum. ^{19}F NMR (282 MHz, CD_3CN): δ = +80.76 (1F, quint, *J* = 149.0 Hz), +61.79 (4F, d, *J* = 149.0 Hz), -26.05 (4F, br s).

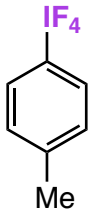

Tetrafluoro(p-tolyl)-λ^5-iodane **(Compound 33):** The reaction was run according to the general procedure, and the product was characterized by the diagnostic IF_4 signal in the ^{19}F NMR spectrum. ^{19}F NMR (282 MHz, CD_3CN): δ = -27.68 (4F, br s).

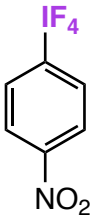

Tetrafluoro(4-nitrophenyl)-λ^5-iodane **(Compound 34):** The reaction was run according to the general procedure, and the product was characterized by the diagnostic IF_4 signal in the ^{19}F NMR spectrum. ^{19}F NMR (282 MHz, CD_3CN): δ = -25.74 (4F, br s).

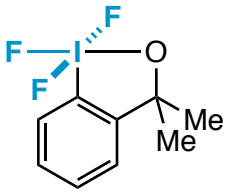

1,1,1-Trifluoro-3,3-dimethyl-1,3-dihydro-1λ^5-benzo[d][1,2]iodaoxole **(Compound 37):** The reaction was run according to the general procedure for the synthesis of tetrafluoro(aryl)-λ^5-iodanes using either compound **35** or **36** as the starting material, and the product was characterized by the diagnostic ^{19}F NMR signals (consistent with literature).[9] ^{19}F NMR (282 MHz, CD_3CN): δ = -20.02 (2F, d, *J* = 107.6 Hz), -33.79 (1F, t, *J* = 107.6 Hz).

[9] (a) R. L. Amey and J. C. Martin, *J. Am. Chem. Soc.*, 1979, **101**, 5294; (b) J. Charpentier, PhD Thesis, ETH Zürich, 2016.

Temperature Calibration of the NMR Spectrometer

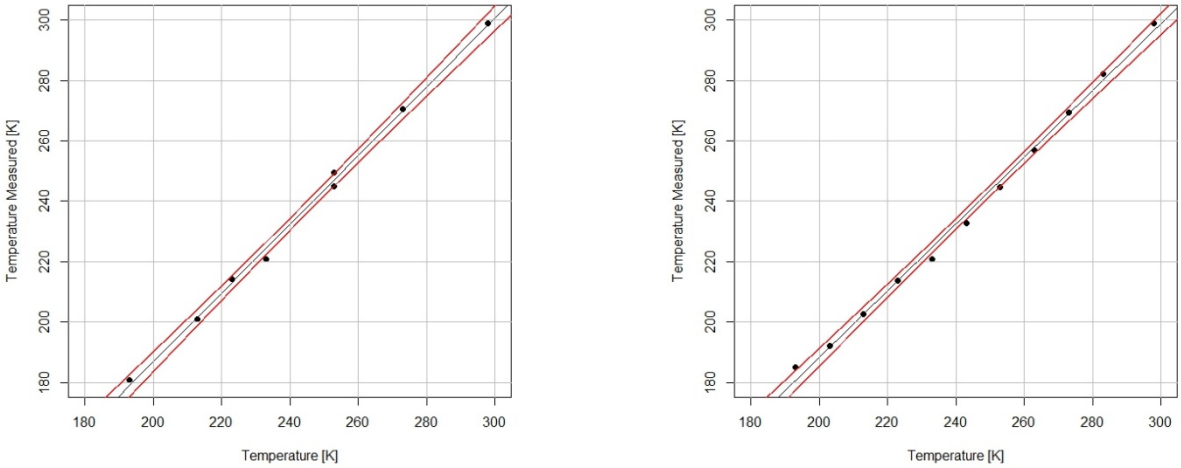

Figure S 1. Temperature calibration curves for VT-NMR measurements. **Left:** High concentration experiment. **Right:** Low concentration experiment.

The temperature calibration was performed using the statistical computing software R. The temperature displayed in the TopSpin software was plotted against the real temperature obtained. The real temperatures were determined using a calibration sample (4% MeOH in MeOD-d_4). The difference in chemical shifts between the two MeOH signals were measured at different temperatures. Dependencies of the chemical shift difference between the two MeOH signals from the temperature were published by van Geet.[10] Using the linear regression shown above, the real temperatures for VT-NMR measurements were calculated. The linear equations describing the dependency of the real temperature from the temperature indicated was found to be $y = -41(6) + 1.14(3)x$ for both, low and high concentration experiment. Y is the real temperature in the sample and x is the temperature displayed. Values and the corresponding confidence intervals are listed in the following tables.

[10] A. L. Van Geet, *Anal. Chem.*, 1970, **42**, 679.

Table S 1. Temperature calibration data for the high concentration experiment

Temperature [K]	Temperature Measured [K]	Confidence Interval [K][a]
183	168	± 4
193	179	± 4
203	190	± 3
213	202	± 3
223	213	± 2
233	224	± 2
234	226	± 2
235	227	± 2
236	228	± 2
237	229	± 2
238	230	± 2
243	236	± 2
253	247	± 2
263	259	± 2
273	270	± 3
283	281	± 3
298	298	± 4

Table S 2. Temperature calibration data for the low concentration experiment.

Temperature [K]	Temperature Measured [K]	Confidence Interval [K][a]
183	170	± 4
193	181	± 3
203	192	± 3
213	203	± 2
223	214	± 2
232	224	± 2
233	225	± 2
234	226	± 2
235	227	± 2
236	228	± 2
238	230	± 2
243	236	± 2
253	247	± 2
263	258	± 2
273	269	± 2
283	280	± 3
298	296	± 3

Determination of Line Widths and Peak Separation for Line Shape Analysis

Line-shape analysis was performed at different temperatures in order to calculate rate constants (k). Therefore, three different temperature regimes were considered: $T < T_C$, $T = T_C$ and $T > T_C$. Additionally, depending on the regime, there are different relationships between the line widths, the differences in chemical shifts and the rate constant. In order to perform the analysis, line widths for the IF_2 signals were determined using Bruker TopSpin 4.0.2. The data are listed in **Table S 3** and **Table S 4** . The values for Δ_{FWHM} are the only values needed for the calculation of k in the low temperature regime. For the determination of k at coalescence or above, one needs the maximum observed chemical shift difference $|(\nu_A - \nu_B)|$ between the two distinct IF_2 fluorine signals below coalescence.

Table S 3. Values for the full width at half maximum (Δ_{FWHM}) obtained during the high concentration experiment for the IF_2 signal of probe molecule at different temperatures.

Temperature [K]	Δ_{FWHM} [Hz]	Temperature [K]	Δ_{FWHM} [Hz]
168 ± 4	31.5	236 ± 2	-
179 ± 4	32.5	247 ± 2	153.4
190 ± 3	57.7	259 ± 2	68.4
202 ± 3	206.5	270 ± 3	34.0
213 ± 2	-	281 ± 3	18.7
224 ± 2	-	298 ± 4	12.3
228 ± 2	coalescence		

Table S 4. Values for the full width at half maximum (Δ_{FWHM}) obtained during the low concentration experiment for the IF_2 signal of probe molecule at different temperatures.

Temperature [K]	Δ_{FWHM} [Hz]	Temperature [K]	Δ_{FWHM} [Hz]
170 ± 4	24.5	236 ± 2	-
181 ± 3	28.5	247 ± 2	137.2
192 ± 3	53.2	258 ± 2	71.6
203 ± 2	202.7	269 ± 2	33.9
214 ± 2	-	280 ± 3	19.0
224 ± 2	-	296 ± 3	11.6
226 ± 2	coalescence		

It was found that the two signals reach a maximum in separation at 202 ± 3 K and 203 ± 2 K, respectively. Upon further cooling to 168 ± 4 K (170 ± 4 K), the signals seem to converge. One explanation for this observation is a different temperature dependence of the ^{19}F chemical shifts assigned to the two distinct IF_2 signals. This observation complicates the elucidation of a clear value for $|(\nu_A - \nu_B)|$, which further affects the values calculated for the rate constants k at and above coalescence. In order to handle this problem, the data was analyzed using different assumptions for the chemical shift difference $|(\nu_A - \nu_B)|$. First, the rate constants k were calculated using the values for $|(\nu_A - \nu_B)|$ at maximal (202 ± 3 K and 203 ± 2 K) and minimal observed peak separation (168 ± 4 K and 170 ± 4 K).

Table S 5. Chemical shift differences $|(\nu_A - \nu_B)|$ calculated under different assumptions for the high concentration measurement..

Temperature [K]	$\lvert(\nu_A - \nu_B)\rvert$ [Hz]	Assumption
168 ± 4	989	(1) Lowest peak separation observed
202 ± 3	1152	(2) Largest peak separation observed

Table S 6. Chemical shift differences $|(\nu_A - \nu_B)|$ calculated under different assumptions for the low concentration measurement..

Temperature [K]	$\lvert(\nu_A - \nu_B)\rvert$ [Hz]	Assumption
170 ± 4	987	(1) Lowest peak separation observed
203 ± 2	1095	(2) Largest peak separation observed

With the values for $|(\nu_A - \nu_B)|$ and Δ_{FWHM} in hand, it was possible to calculate the rate constants k under the different assumptions given above.

Calculation of Rate Constants

With the values for $|(\nu_A - \nu_B)|$ and Δ_{FWHM} in hand, it was possible to calculate the rate constants k under the different assumptions given above.

Table S 7. Rate constants determined for the rotation around the C-I-bond in the probe molecule under the different assumptions given in the tables above. The subscript at the k-values denote the assumption made for the calculation. Coalescence is shaded grey.

High Concentration			**Low Concentration**		
Temperature [K]	$k_{(1)}$ [s^{-1}]	$k_{(2)}$ [s^{-1}]	Temperature [K]	$k_{(1)}$ [s^{-1}]	$k_{(2)}$ [s^{-1}]
168 ± 4	99	99	170 ± 4	77	77
179 ± 4	102	102	181 ± 3	90	90
190 ± 3	181	181	192 ± 3	167	167
202 ± 3	649	649	203 ± 2	637	637
228 ± 2	2197	2559	226 ± 2	2193	2432
247 ± 2	10016	13589	247 ± 2	11153	13728
259 ± 2	22462	30477	258 ± 2	21372	26305
270 ± 3	45189	61312	269 ± 2	45139	55558
281 ± 3	82162	111476	280 ± 3	80538	99128
298 ± 4	123913	169480	296 ± 3	131916	162364

As seen above, the influence of the chosen chemical shift differences $|(\nu_A - \nu_B)|$ on the rate constants k is significant over a range of temperatures. The activation energies were determined using the linearized Arrhenius equation (see equation (4)). The corresponding Arrhenius plots are shown below (Figure S 2) and the slopes and intercepts obtained from the regression lines are listed in Table S 8. Note that the data points corresponding to the rate constants determined at extremely low temperatures as well as the ones determined at 298 ± 4 K (or 296 ± 3 K, depending on concentration), deviate from the linear behavior, and thus were not included in the linear regression. The reason for the deviation is potentially the increasing contribution of the natural line width (T_2 relaxation) to Δ_{FWHM}, which is not in agreement with the assumptions made for the calculation of the rate constants. The activation energies E_A were calculated using the two assumptions shown in Table S 5 and Table S 6 and are listed in Table S 8. The activation energies E_A were computed in kcal using the slopes obtained from the Arrhenius plots and the ideal gas constant R ($1.99 \cdot 10^{-3}$ kcal/mol K).

Table S 8. Results obtained from the Arrhenius plots assuming different values for $|(\nu_A - \nu_B)|$ at different concentrations of the probe molecule (HC: high concentration, LC, low concentration).

Assumption[a]	Slope[b]	Intercept[b]	E_A [kcal/mol][b]
(1) HC	–3500 ± 470	23.5 ± 2.0	7.0 ± 0.9
(2) HC	–3720 ± 450	24.7 ± 2.0	7.4 ± 0.9
(1) LC	–3670 ± 360	24.3 ± 1.6	7.3 ± 0.7
(2) LC	–3830 ± 330	25.1 ± 1.5	7.6 ± 0.7

[a] The assumptions are based on different values used for $|(\nu_A - \nu_B)|$ as shown in Table S 5 and Table S 6. [b] Since the uncertainties for the temperature values were extremely small, they were neglected when calculating the values for E_A.

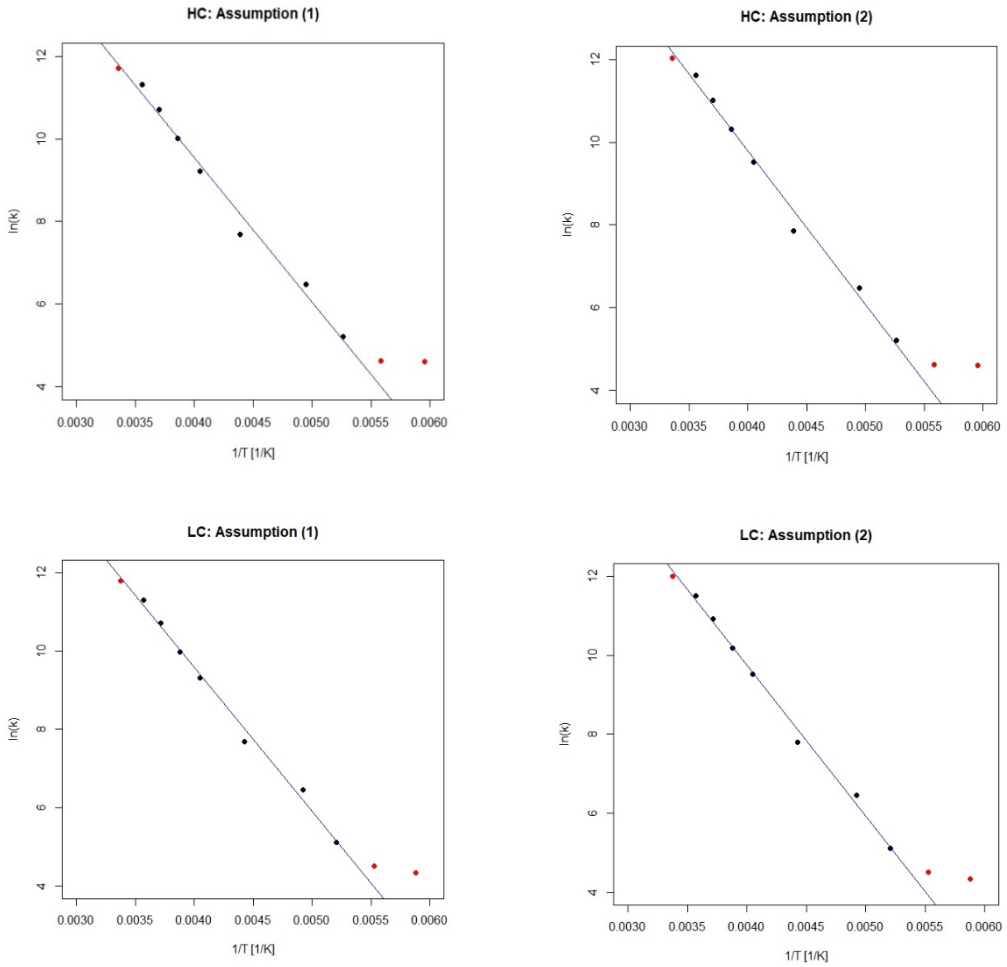

Figure S 2. Arrhenius plots obtained for the rate constants k using the different assumptions shown in Table S 5 and Table **S 6** and different concentrations (HC: high concentration, LC: low concentration). The red dots were not taken into account, since they deviate from the expected linearity. For the red dots, the line shape is dominated by the natural line width.

Subsequently, other thermodynamic quantities such as enthalpy of activation ($\Delta^{\ddagger}H^{\ominus}$) and entropy of activation ($\Delta^{\ddagger}S^{\ominus}$) were determined using the linearized form of the Eyring equation (see equation (5)). Based on this equation, 1/T was plotted against ln(k/T) (Eyring plots). A linear regression model was chosen to fit the data points. Similar to the activation energy, it is

possible to calculate $\Delta^{\ddagger}H^{\Theta}$ directly from the slope of the regression line. The values for $\Delta^{\ddagger}S^{\Theta}$ were derived from the intercept of the regression line (see Table S 9).

Table S 9. Regression line data and values for $\Delta^{\ddagger}H^{\Theta}$ and $\Delta^{\ddagger}S^{\Theta}$ computed for the rotation around the C-I bond in the probe molecule. The values are listed for two different concentrations of the probe molecule (HC: high concentration, LC, low concentration).

Assumption[a]	Slope[b]	Intercept[b]	$\Delta^{\ddagger}H^{\Theta}$ [kcal/mol][b]	$\Delta^{\ddagger}S^{\Theta}$ [cal/(mol K)][b]
(1) HC	–3270 ± 460	17.1 ± 2.0	6.5 ± 0.9	–13 ± 4
(2) HC	–3490 ± 440	18.2 ± 1.8	6.9 ± 0.9	–11 ± 4
(1) LC	–3420 ± 280	17.7 ± 1.1	6.8 ± 0.6	–12 ± 3
(2) LC	–3560 ± 260	18.4 ± 1.1	7.2 ± 0.6	–10 ± 3

[a] The assumptions are based on different values used for $|(\nu_A - \nu_B)|$ as shown in Table S 5 and Table S 6. [b] Since the uncertainties for the temperature values were extremely small, they were neglected when calculating the values for $\Delta^{\ddagger}H^{\Theta}$ and $\Delta^{\ddagger}S^{\Theta}$.

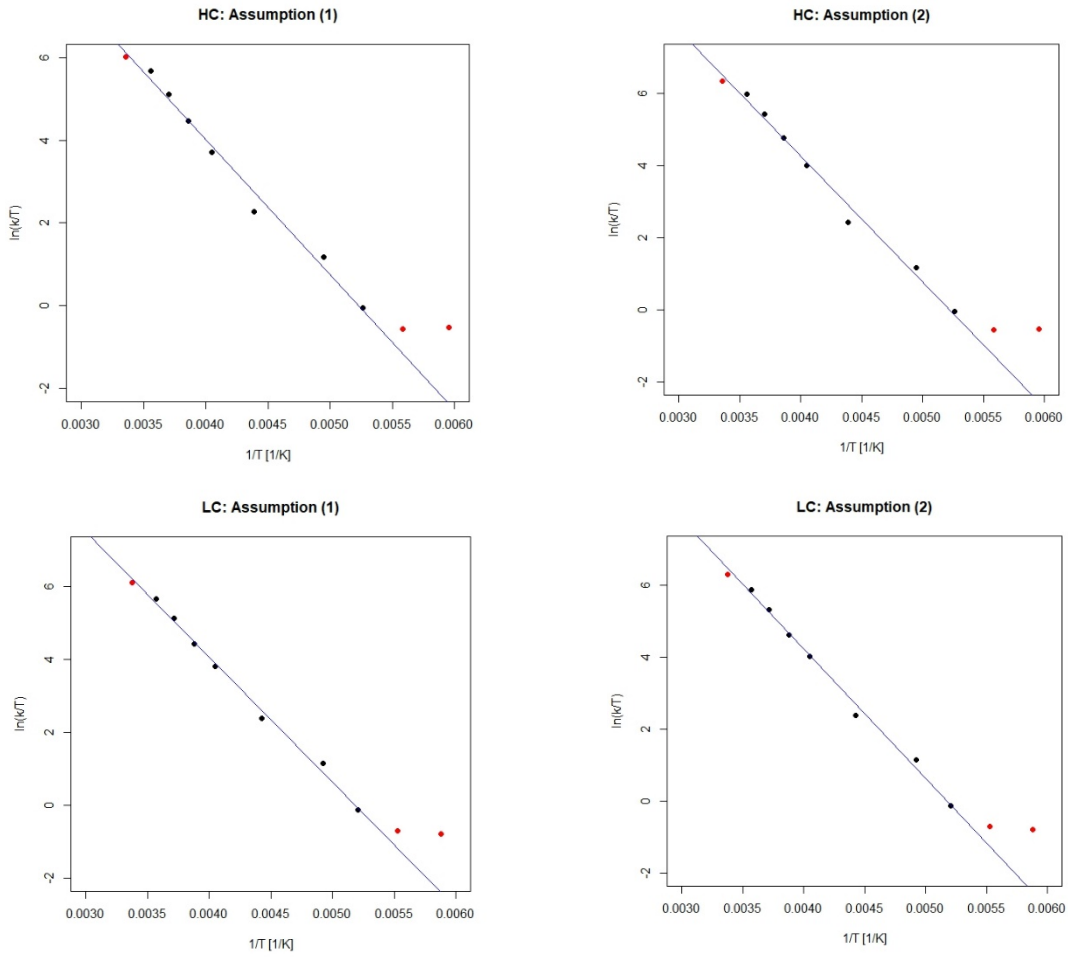

Figure S 3. Eyring plots obtained for the rate constants k using the different assumptions shown in Table S 5 and Table **S 6** and different concentrations (HC: high concentration, LC: low concentration). The red dots were not taken into account, since they deviate from the expected linearity. For the red dots, the line shape is dominated by the natural line width.

Important Equations for Dynamic NMR Analyses

Formula	Comment	Number
$k \cong \pi\Delta_{FWHM}$	$T < T_C$	(1)
$k = \frac{\pi\Delta\nu}{\sqrt{2}} = \frac{\pi(v_A - v_B)}{\sqrt{2}}$	$T = T_C$	(2)
$k = \frac{\pi\Delta(v_A - v_B)^2}{2\Delta_{FWHM}}$	$T > T_C$	(3)
$\ln k = \frac{-E_A}{RT} + \ln A$	Linearized Arrhenius Equation	(4)
$\ln\left(\frac{k}{T}\right) = \frac{-\Delta^{\ddagger}\mathrm{H}}{RT} + \ln\frac{k_B}{h} + \frac{\Delta^{\ddagger}\mathrm{S}}{R}$	Linearized Eyring Equation	(5)

NMR Spectra

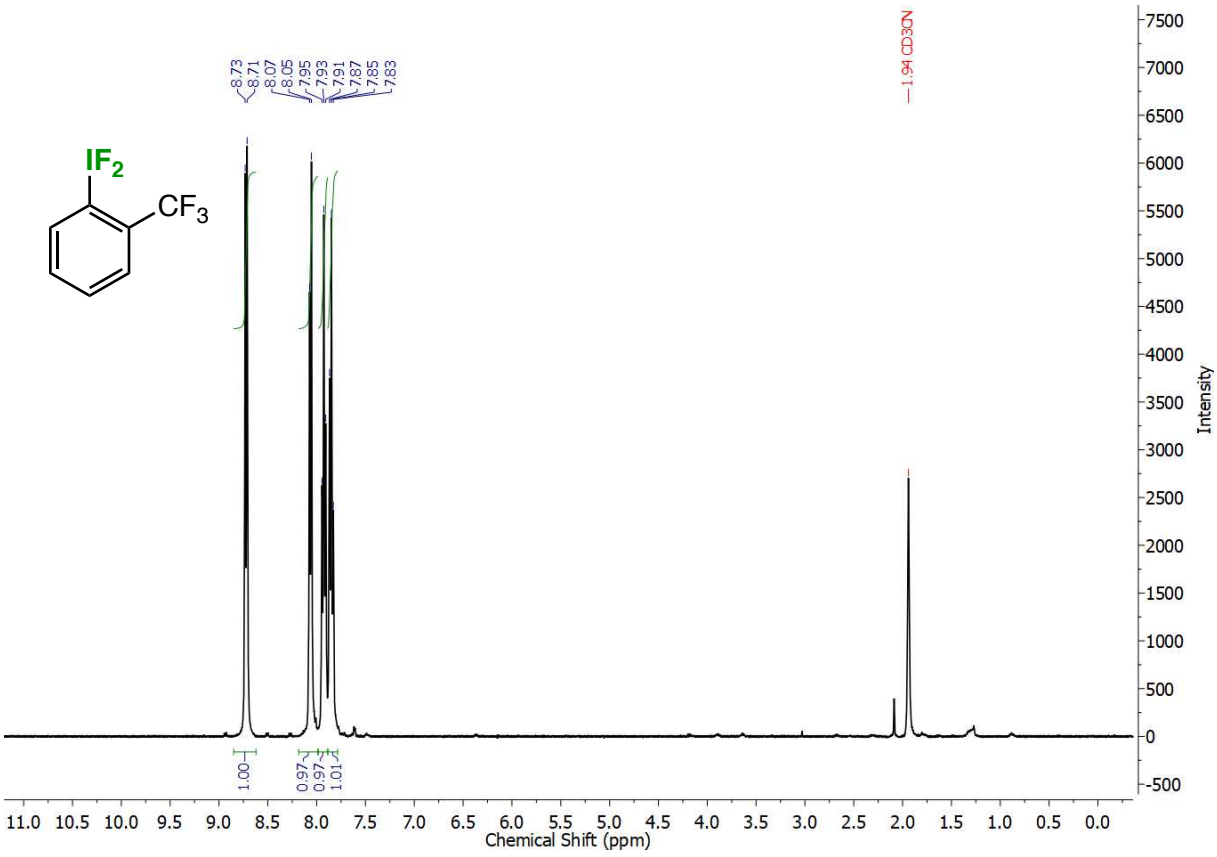

Figure S 4. ^{1}H NMR spectrum of difluoro(2-(trifluoromethyl)phenyl)-λ^3-iodane (compound **2**).

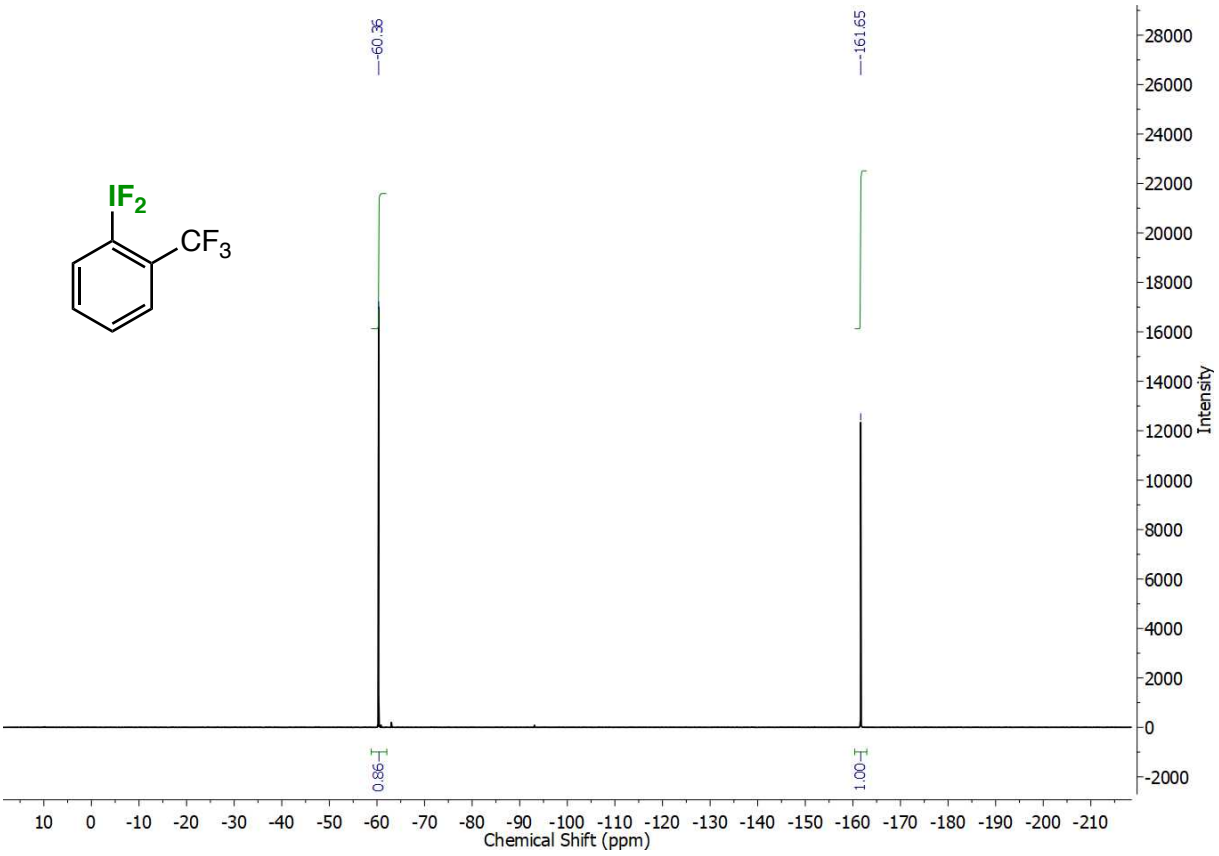

Figure S 5. ^{19}F NMR spectrum of difluoro(2-(trifluoromethyl)phenyl)-λ^3-iodane (compound **2**).

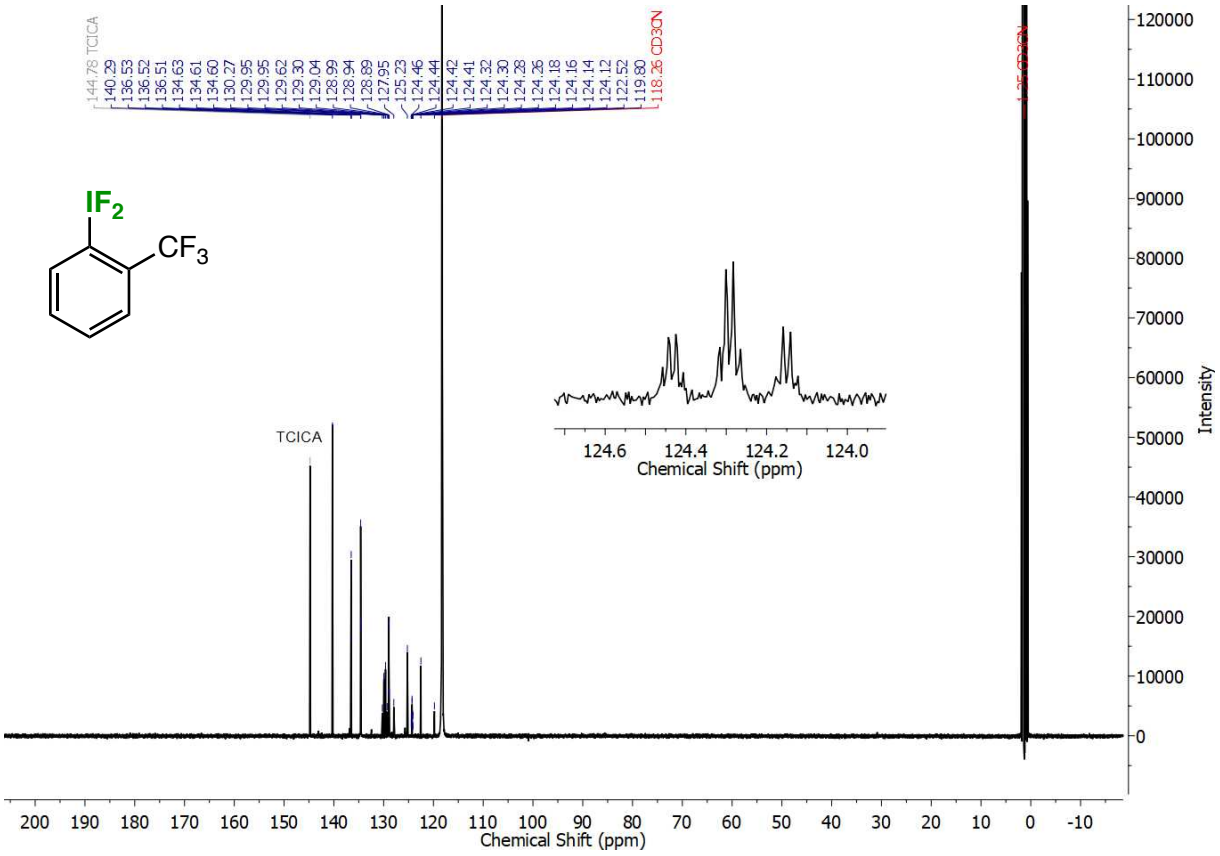

Figure S 6. $^{13}C\{^{1}H\}$ NMR spectrum of difluoro(2-(trifluoromethyl)phenyl)-λ^3-iodane (compound **2**).

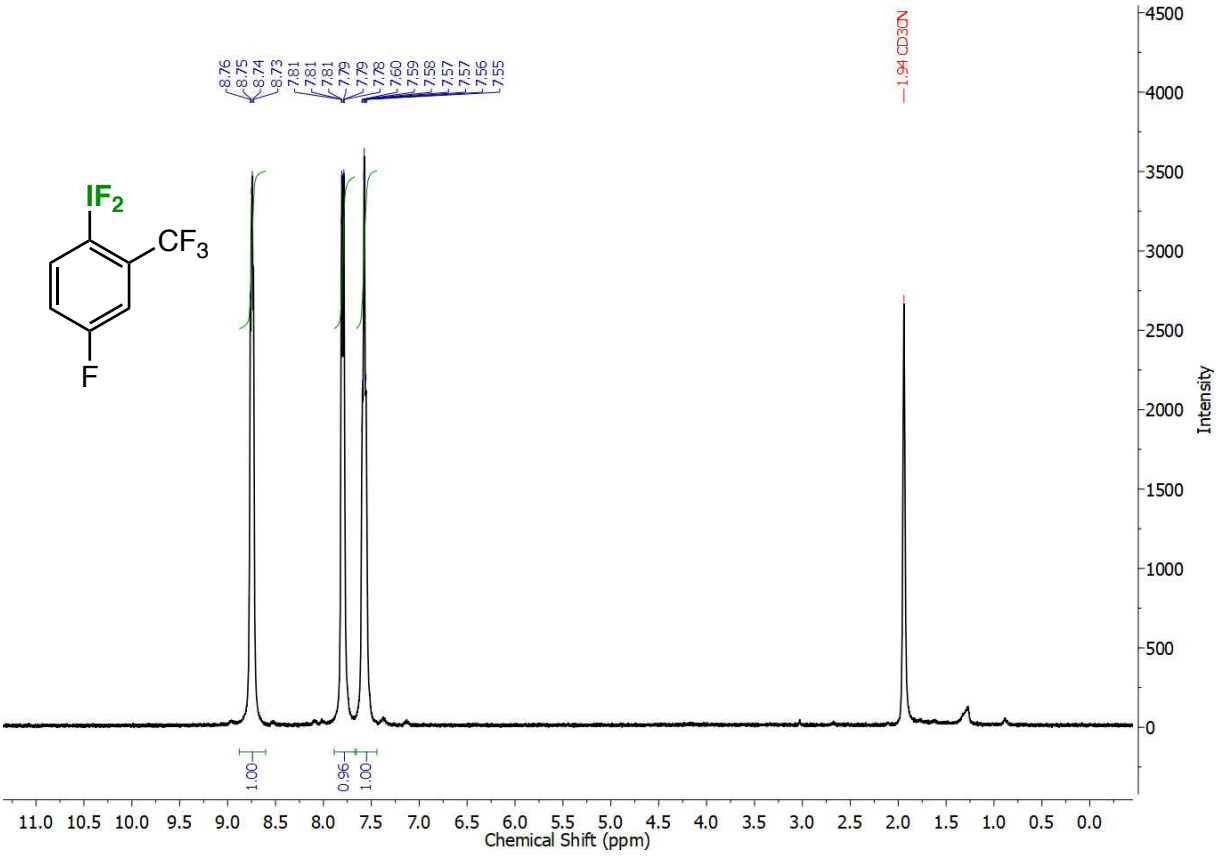

Figure S 7. ^{1}H NMR spectrum of (4-fluoro-2-(trifluoromethyl)phenyl)difluoro-λ^{3}-iodane (compound **3**).

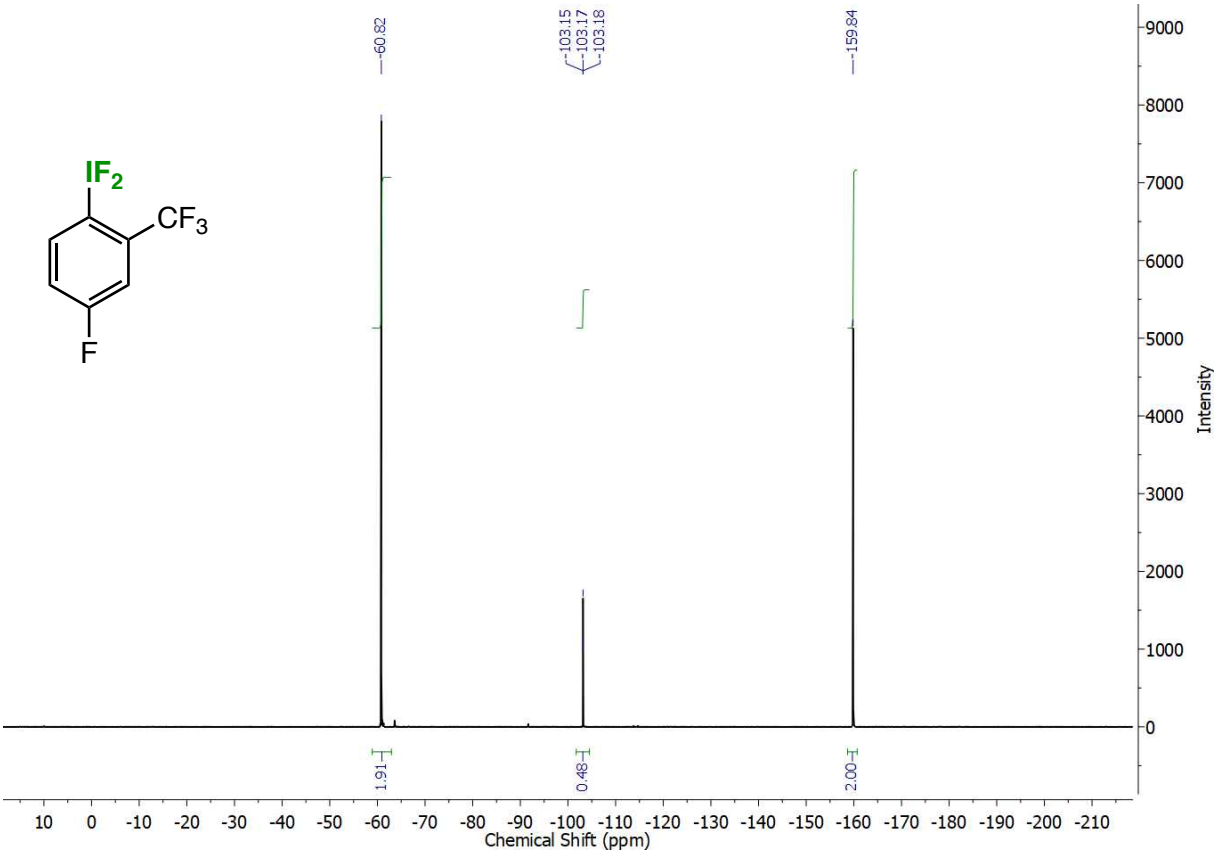

Figure S 8. ^{19}F NMR spectrum of (4-fluoro-2-(trifluoromethyl)phenyl)difluoro-λ^3-iodane (compound **3**).

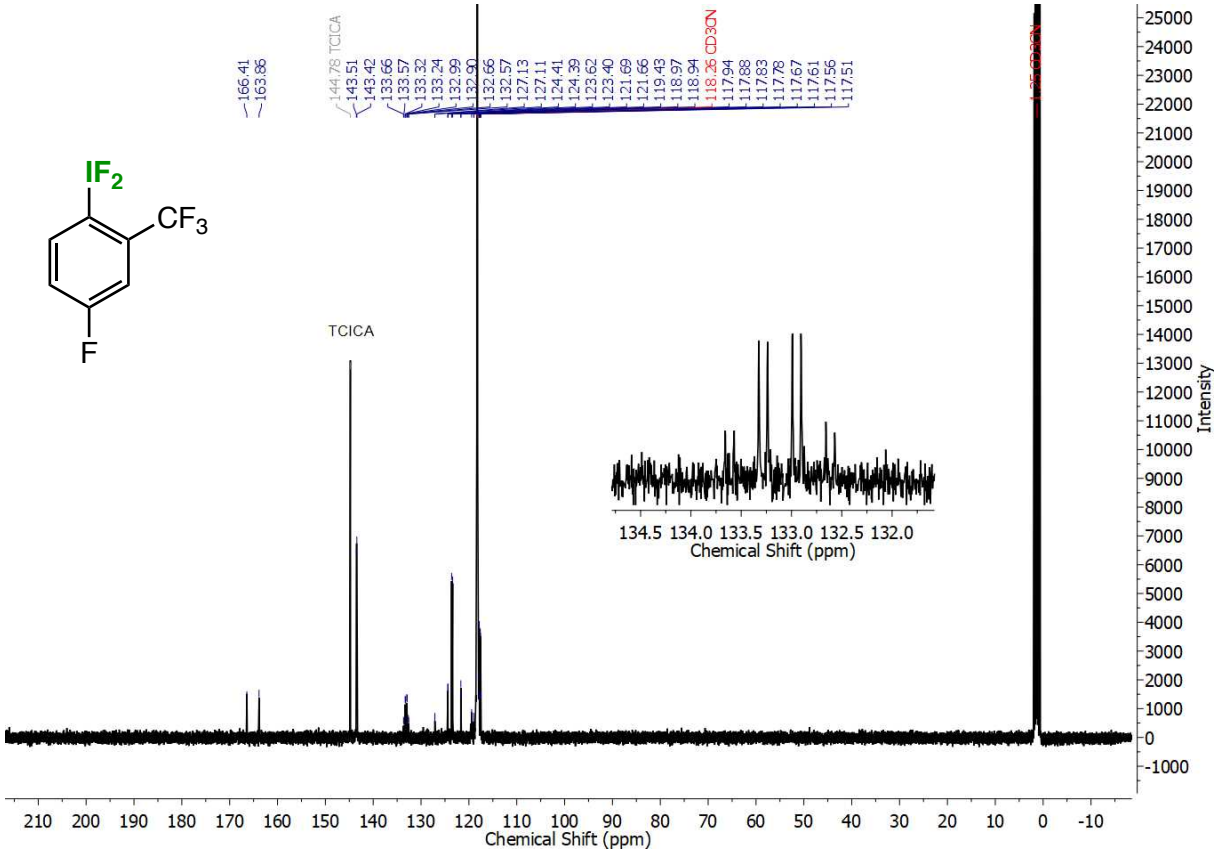

Figure S 9. $^{13}C\{^{1}H\}$ NMR spectrum of (4-fluoro-2-(trifluoromethyl)phenyl)difluoro-λ^3-iodane (compound **3**).

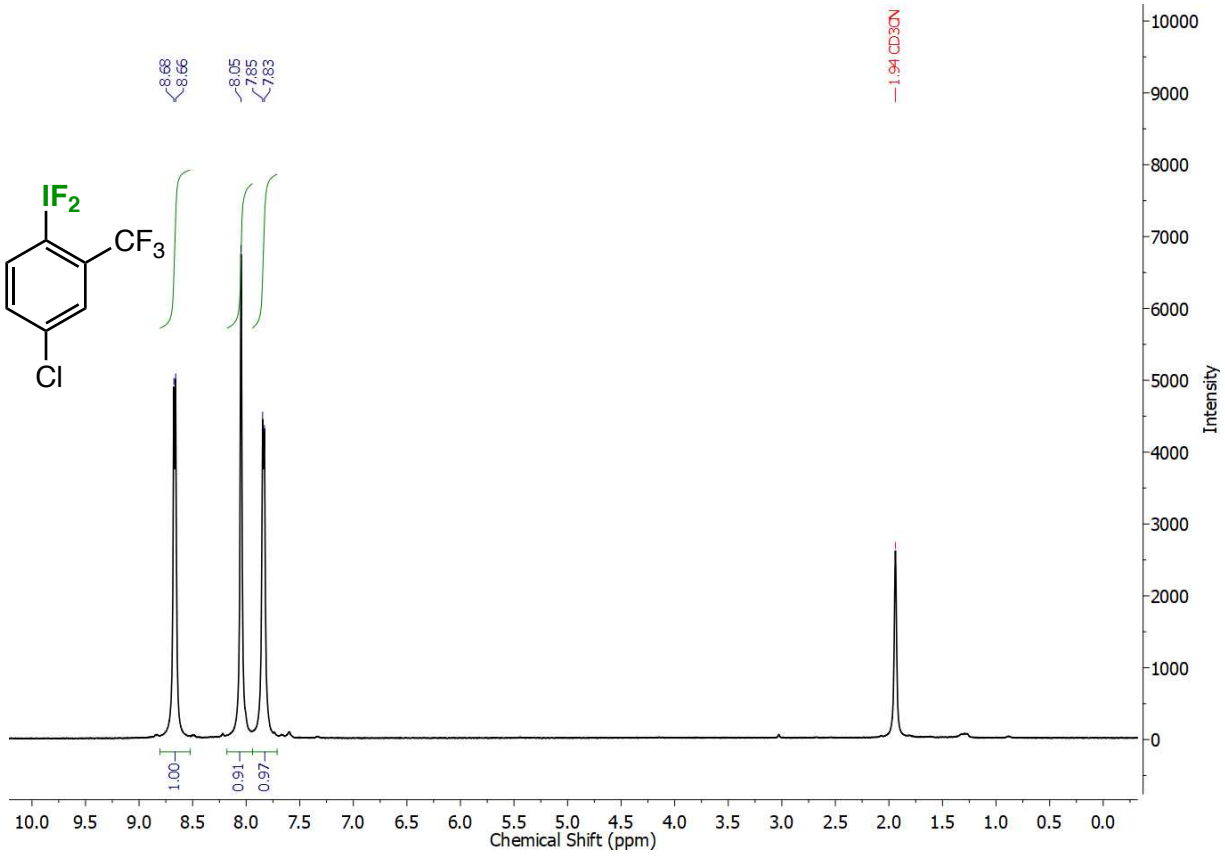

Figure S 10. ^{1}H NMR spectrum of (4-chloro-2-(trifluoromethyl)phenyl)difluoro-λ^{3}-iodane (compound **4**).

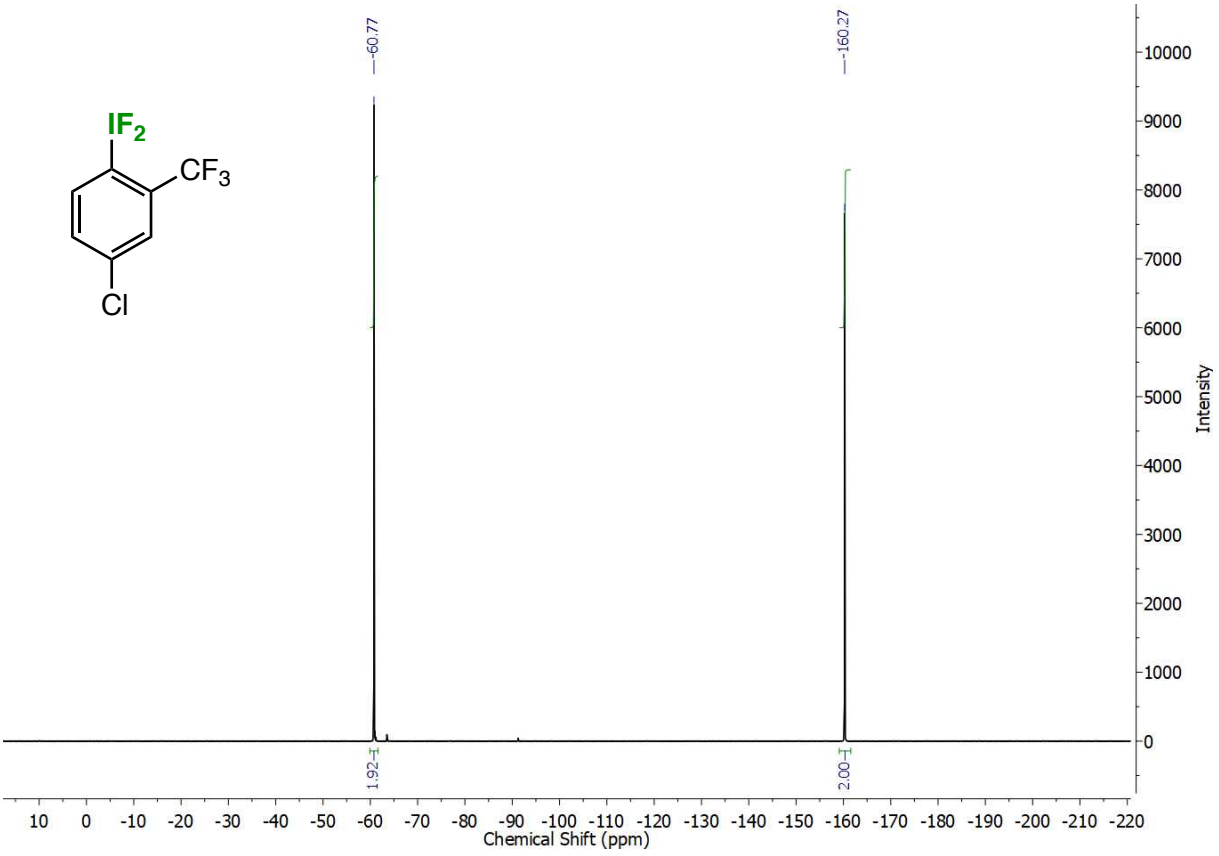

Figure S 11. ^{19}F NMR spectrum of (4-chloro-2-(trifluoromethyl)phenyl)difluoro-λ^3-iodane (compound **4**).

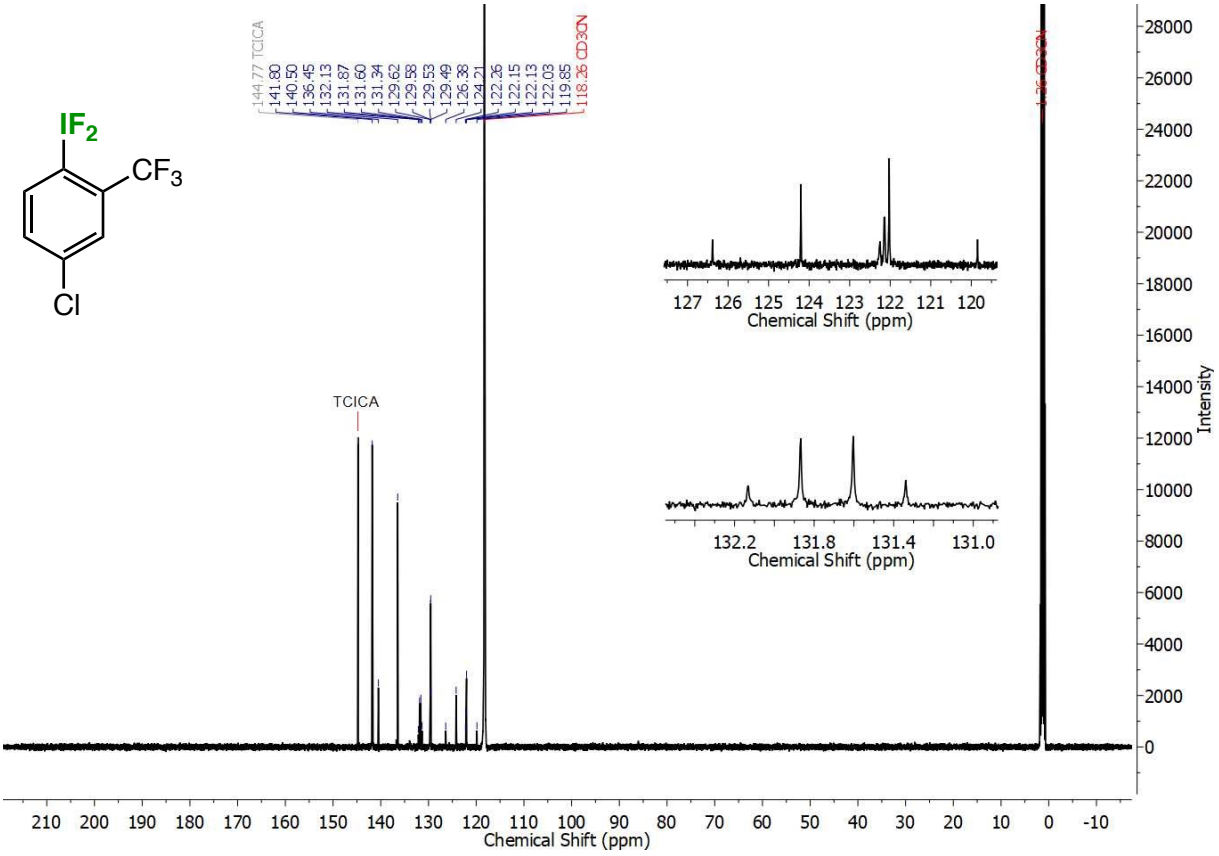

Figure S 12. $^{13}C\{^{1}H\}$ NMR spectrum of (4-chloro-2-(trifluoromethyl)phenyl)difluoro-λ^3-iodane (compound **4**).

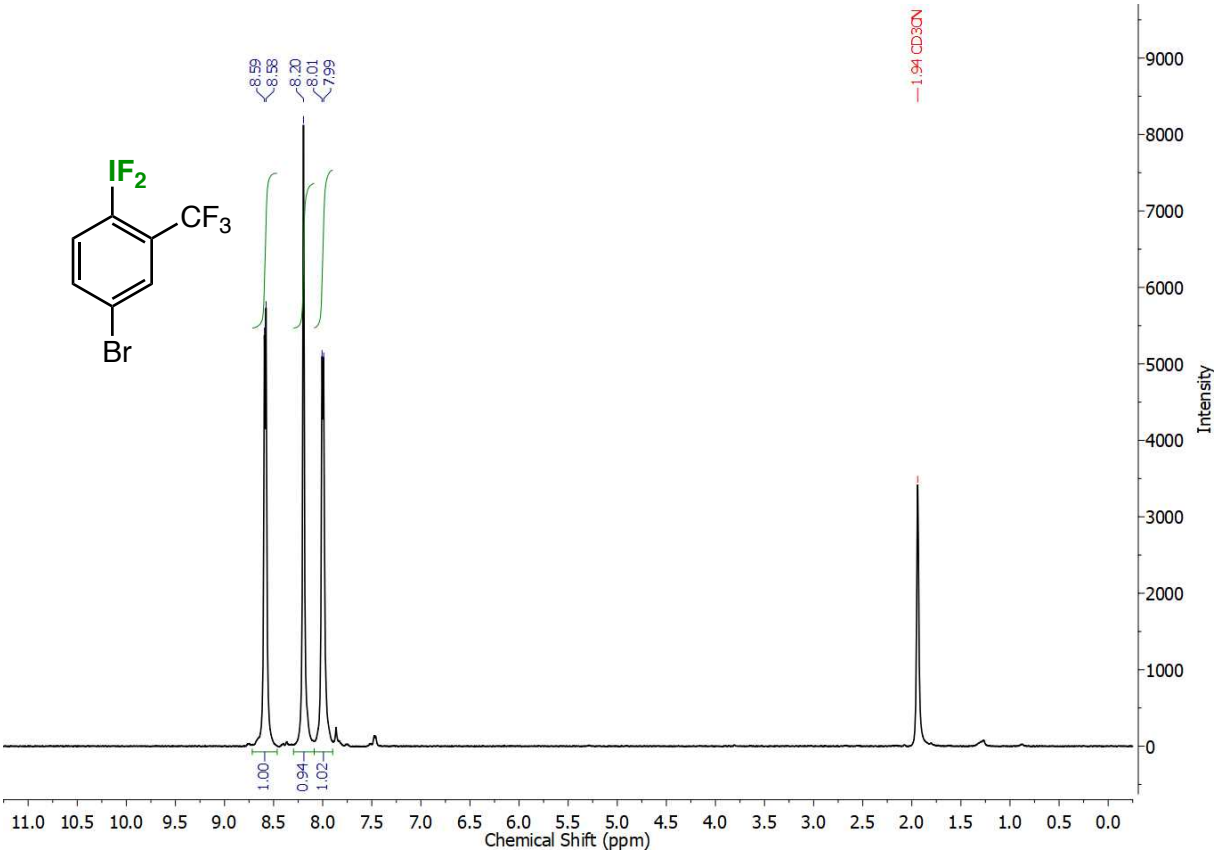

Figure S 13. ^{1}H NMR spectrum of (4-bromo-2-(trifluoromethyl)phenyl)difluoro-λ^{3}-iodane (compound **5**).

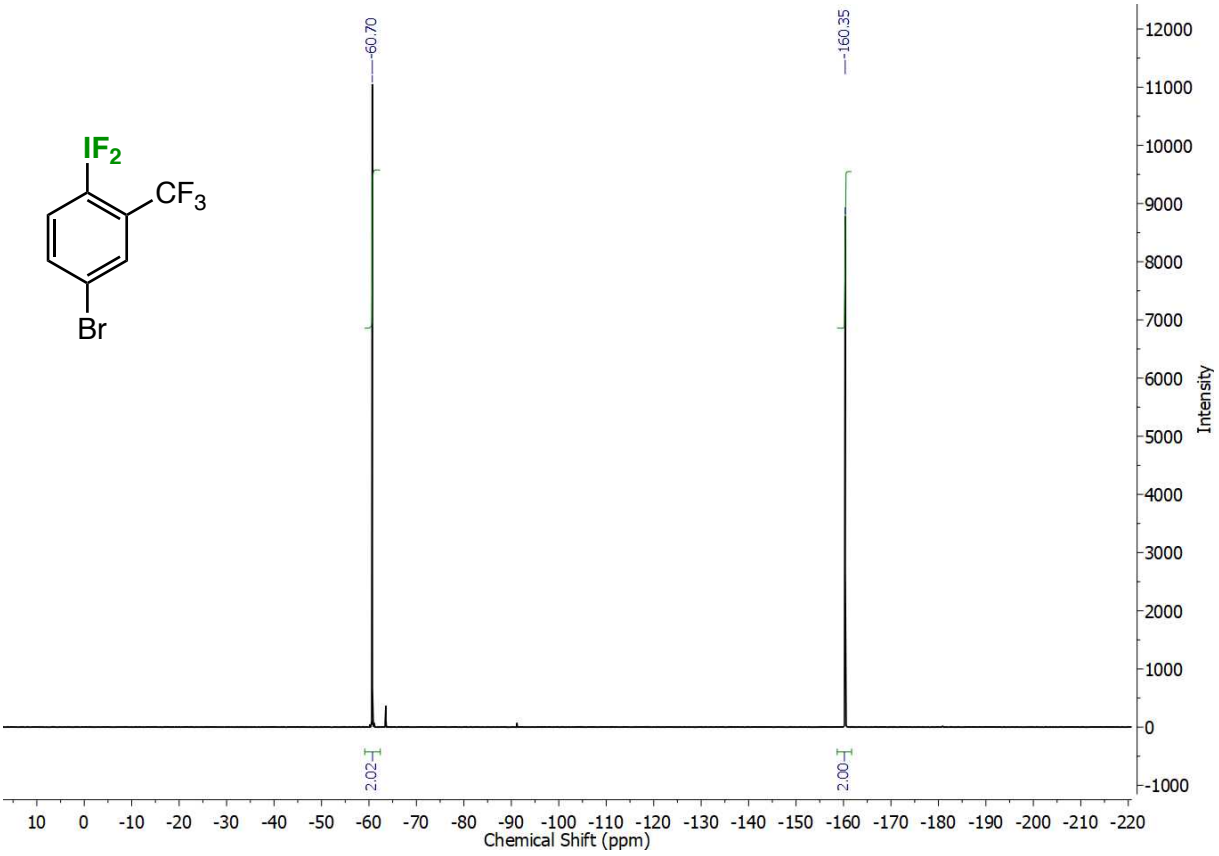

Figure S 14. ^{19}F NMR spectrum of (4-bromo-2-(trifluoromethyl)phenyl)difluoro-λ^3-iodane (compound **5**).

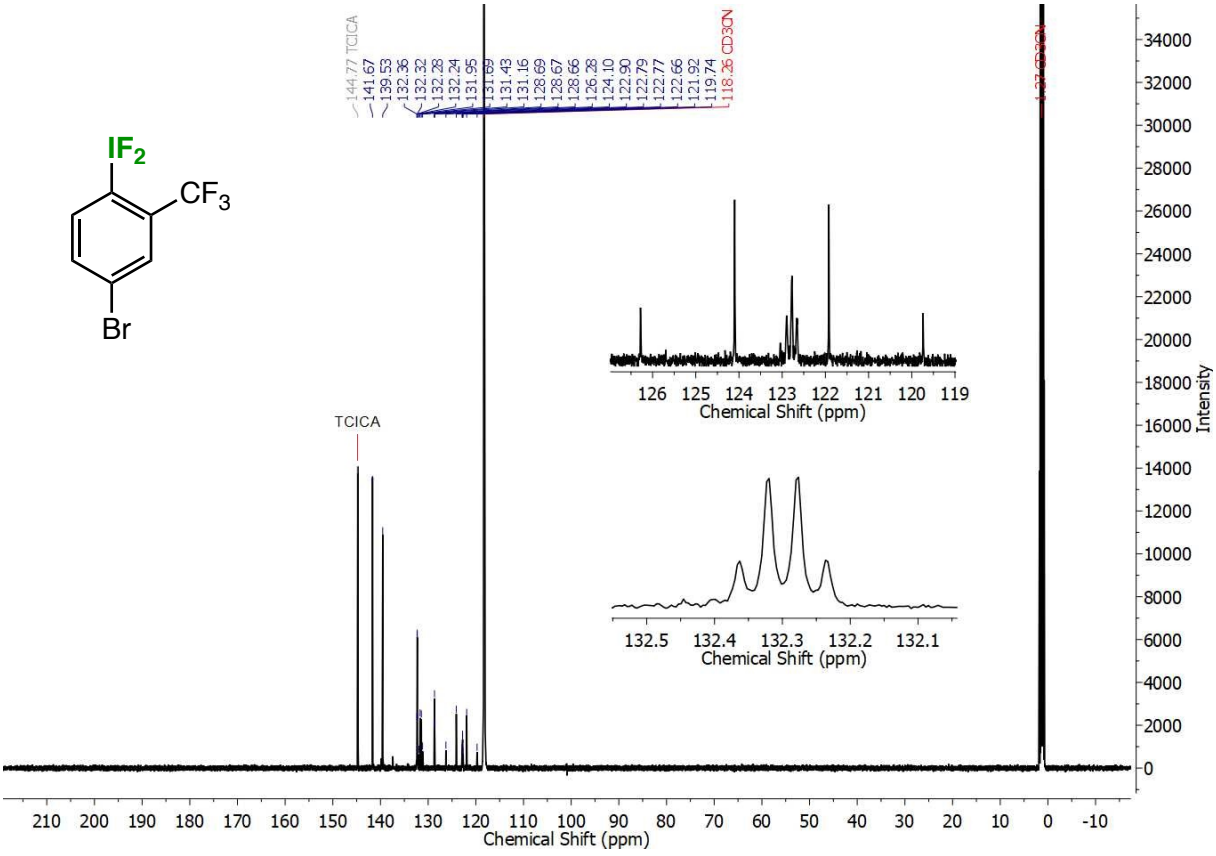

Figure S 15. $^{13}C\{^{1}H\}$ NMR spectrum of (4-bromo-2-(trifluoromethyl)phenyl)difluoro-λ^3-iodane (compound **5**).

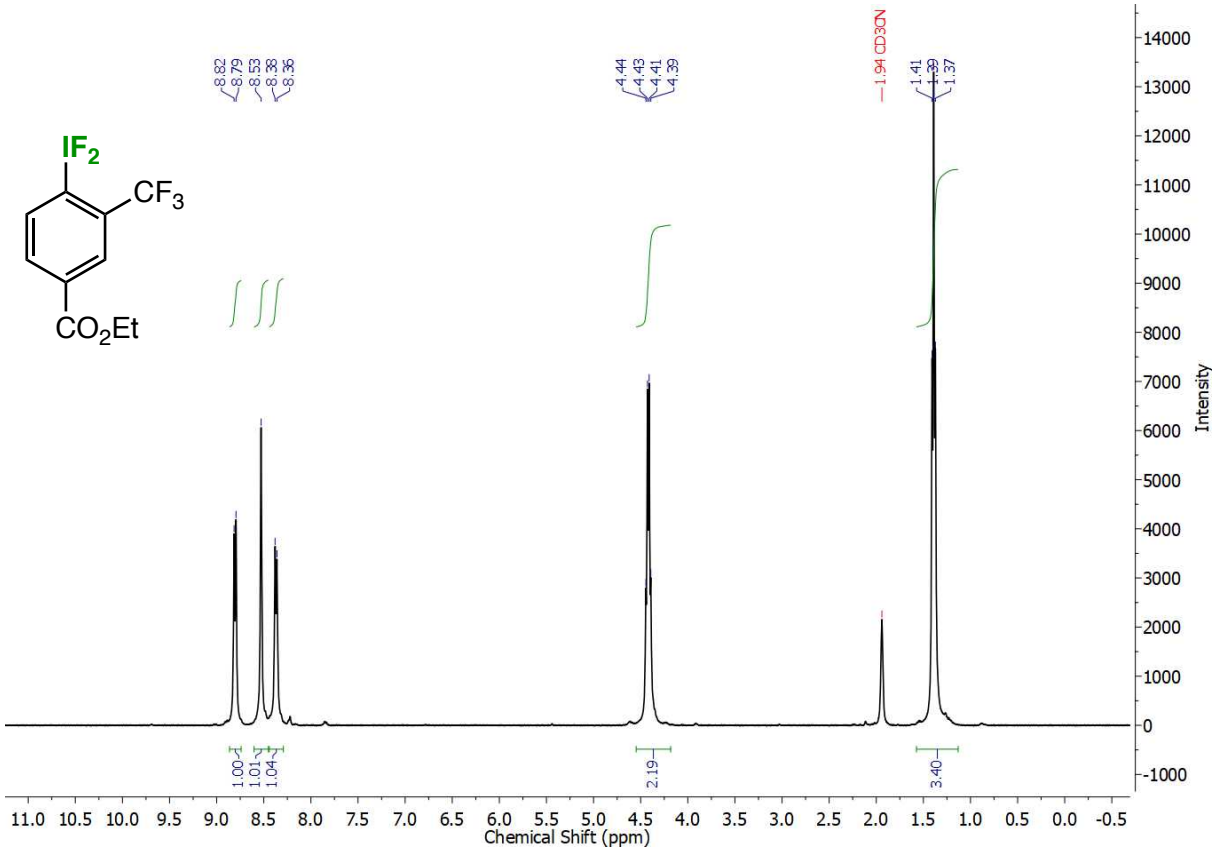

Figure S 16. ^{1}H NMR spectrum of ethyl 4-(difluoro-λ^3-iodanyl)-3-(trifluoromethyl)benzoate (compound **6**).

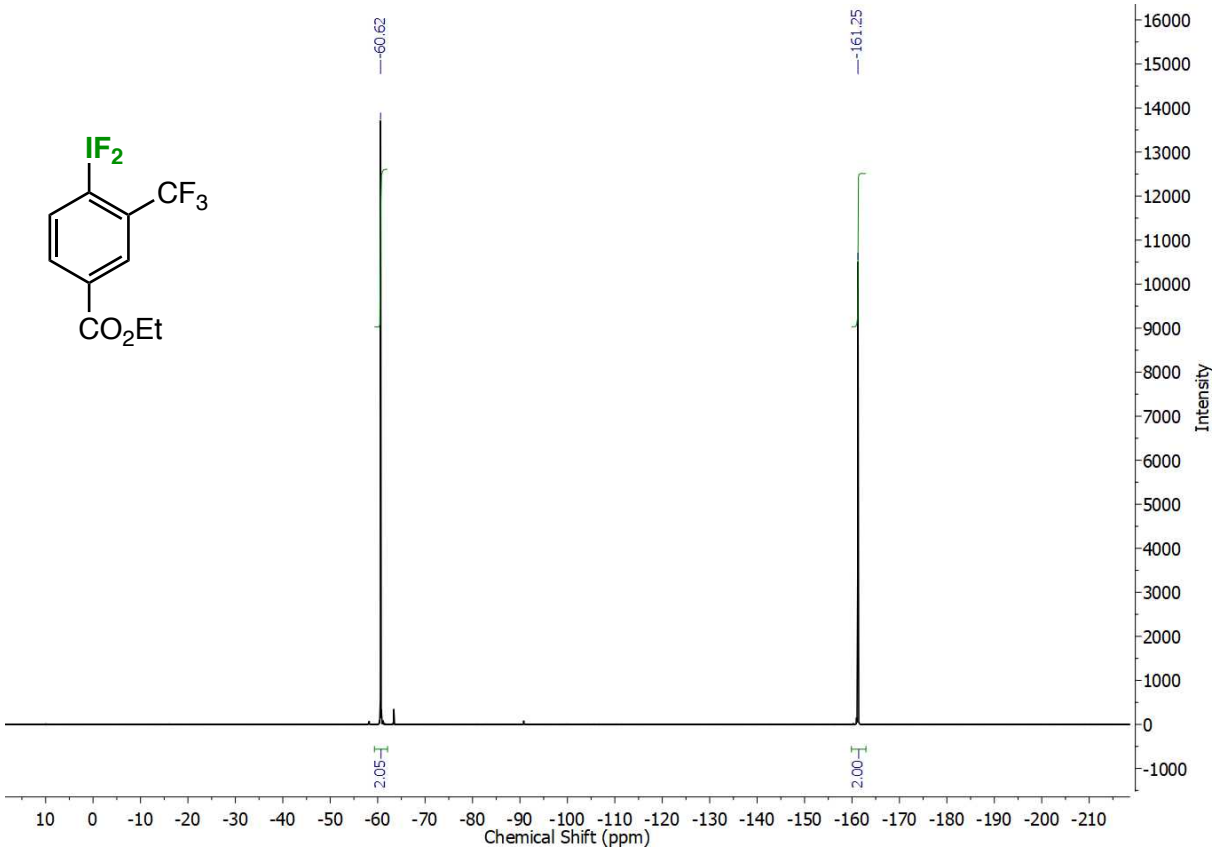

Figure S 17. ^{19}F NMR spectrum of ethyl 4-(difluoro-λ^3-iodanyl)-3-(trifluoromethyl)benzoate (compound **6**).

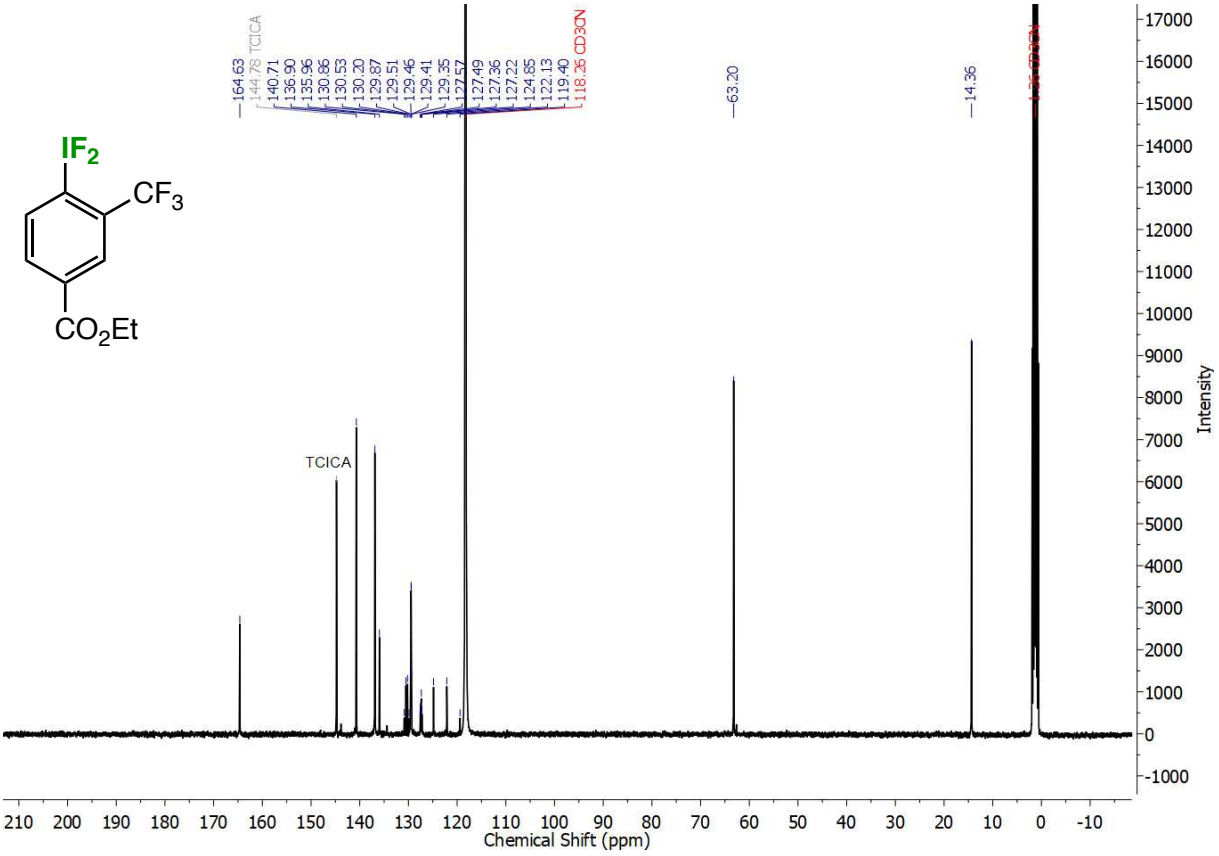

Figure S 18. $^{13}C\{^{1}H\}$ NMR spectrum of ethyl 4-(difluoro-λ^3-iodanyl)-3-(trifluoromethyl)benzoate (compound **6**).

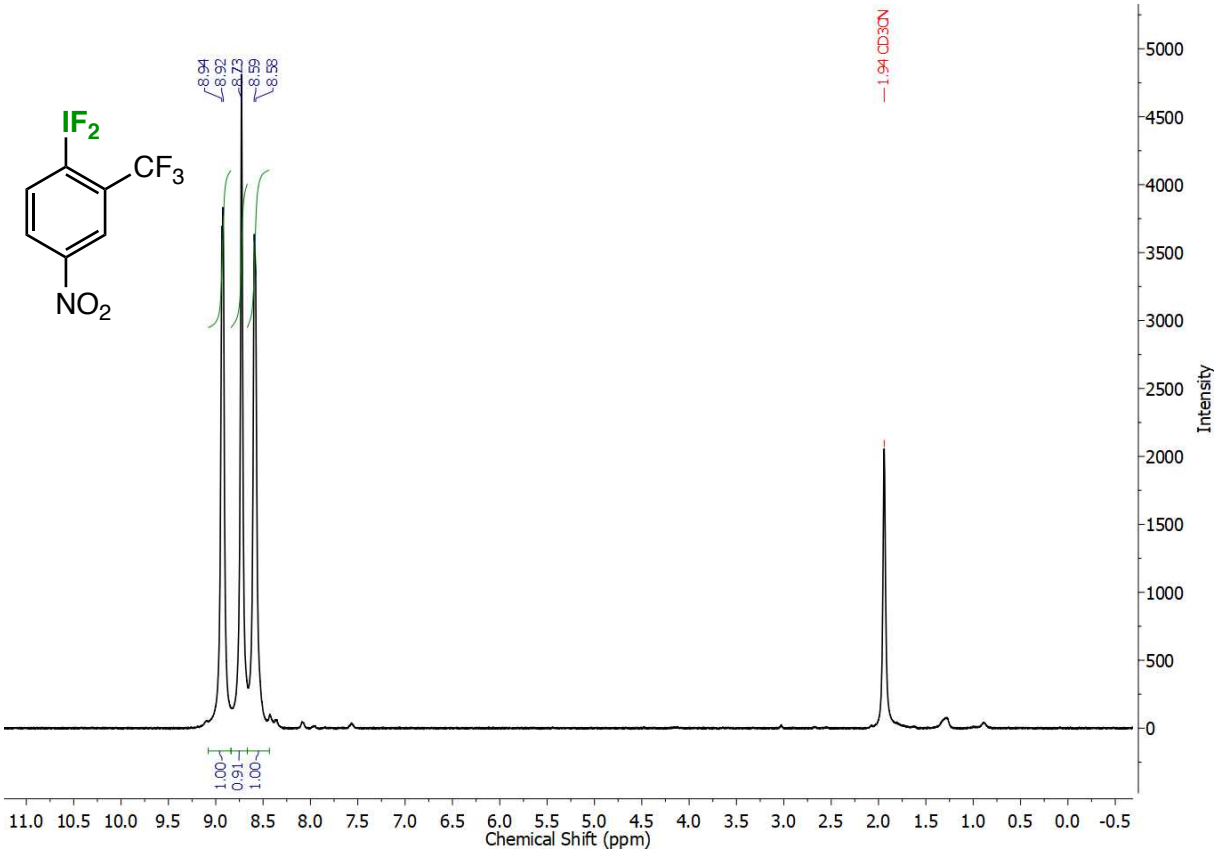

Figure S 19. ^{1}H NMR spectrum of difluoro(4-nitro-2-(trifluoromethyl)phenyl)-λ^{3}-iodane (compound **7**).

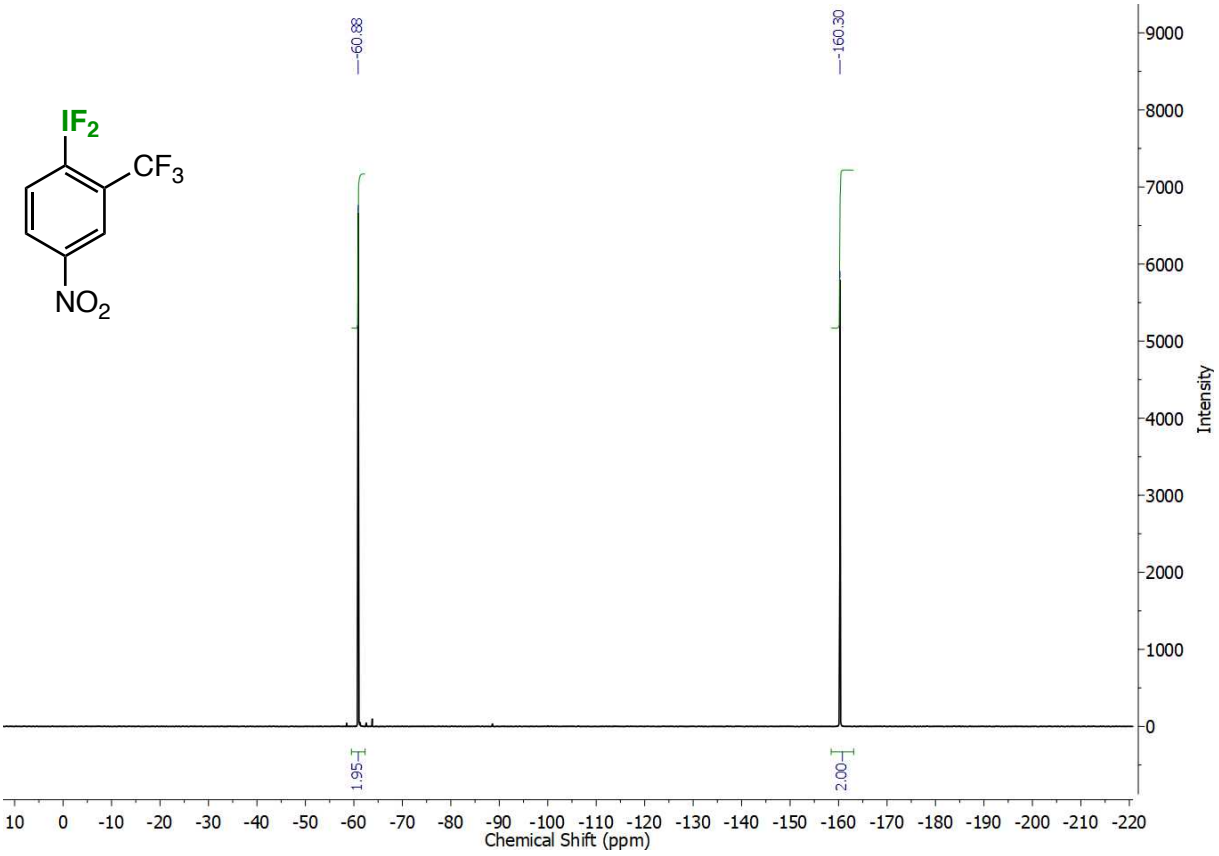

Figure S 20. ^{19}F NMR spectrum of difluoro(4-nitro-2-(trifluoromethyl)phenyl)-λ^3-iodane (compound **7**).

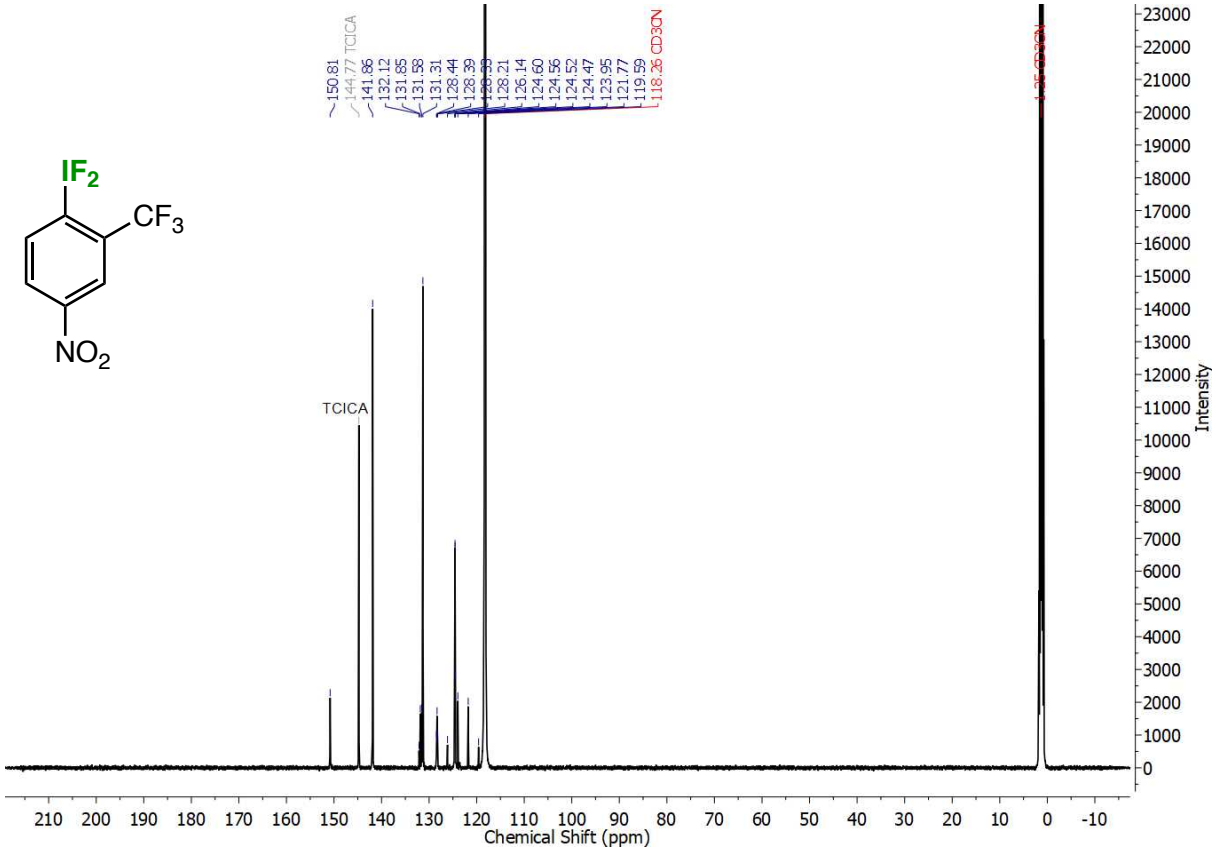

Figure S 21. $^{13}C\{^{1}H\}$ NMR spectrum of difluoro(4-nitro-2-(trifluoromethyl)phenyl)-λ^3-iodane (compound **7**).

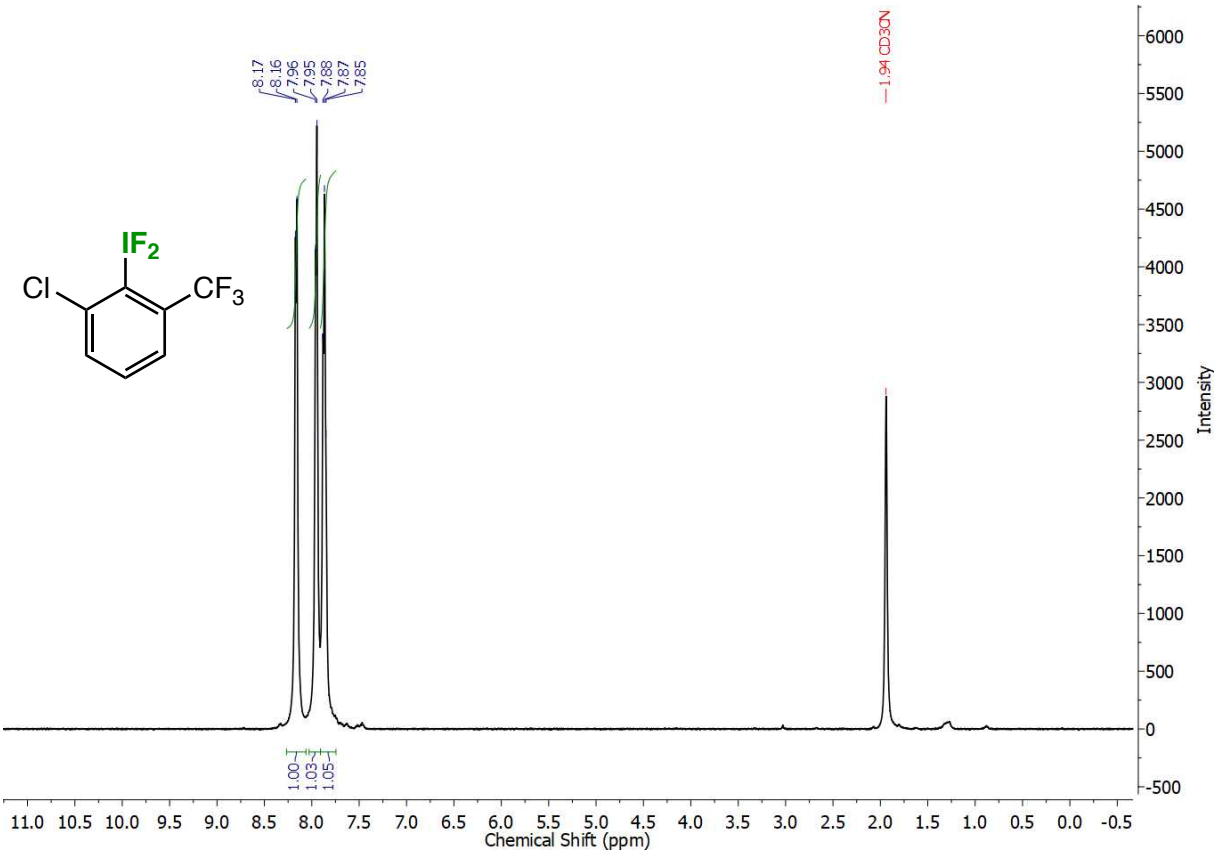

Figure S 22. ^{1}H NMR spectrum of (2-chloro-6-(trifluoromethyl)phenyl)difluoro-λ^3-iodane (compound **8**).

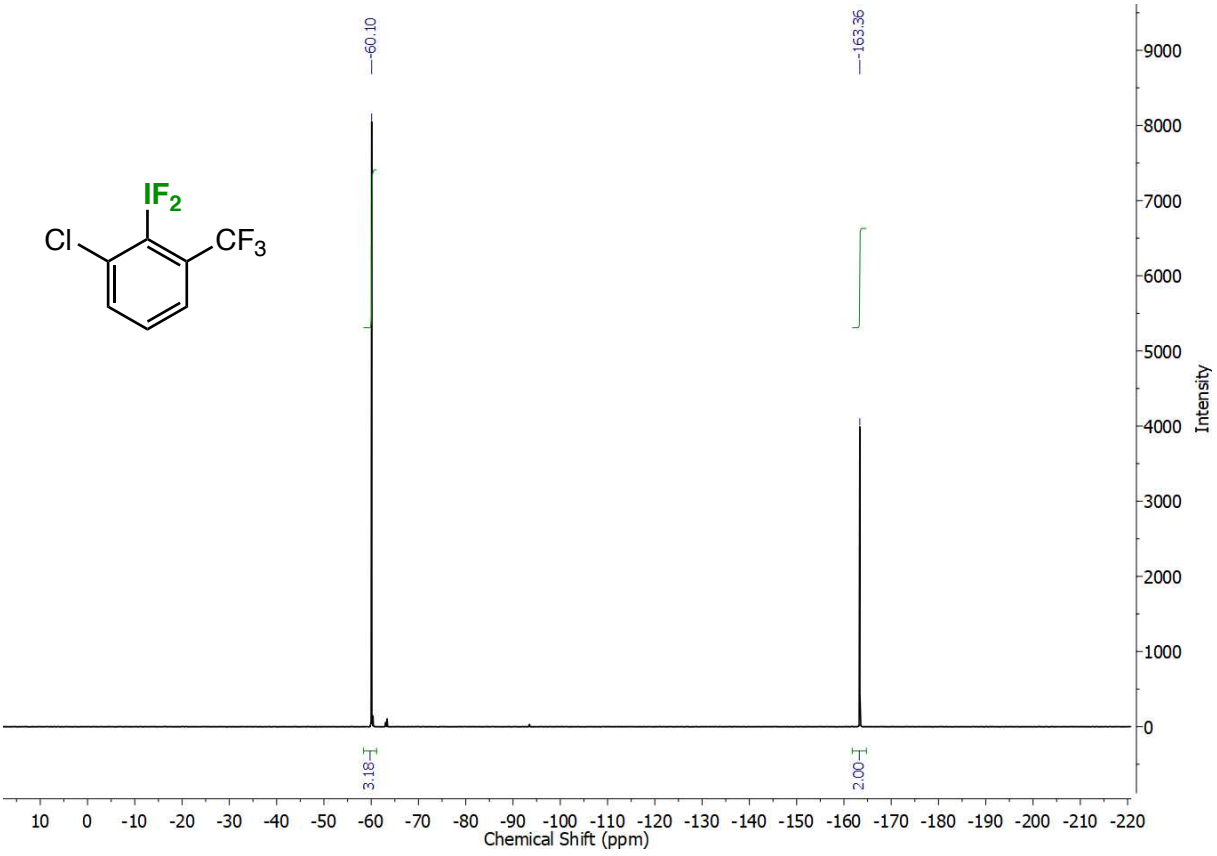

Figure S 23. ^{19}F NMR spectrum of (2-chloro-6-(trifluoromethyl)phenyl)difluoro-λ^3-iodane (compound **8**).

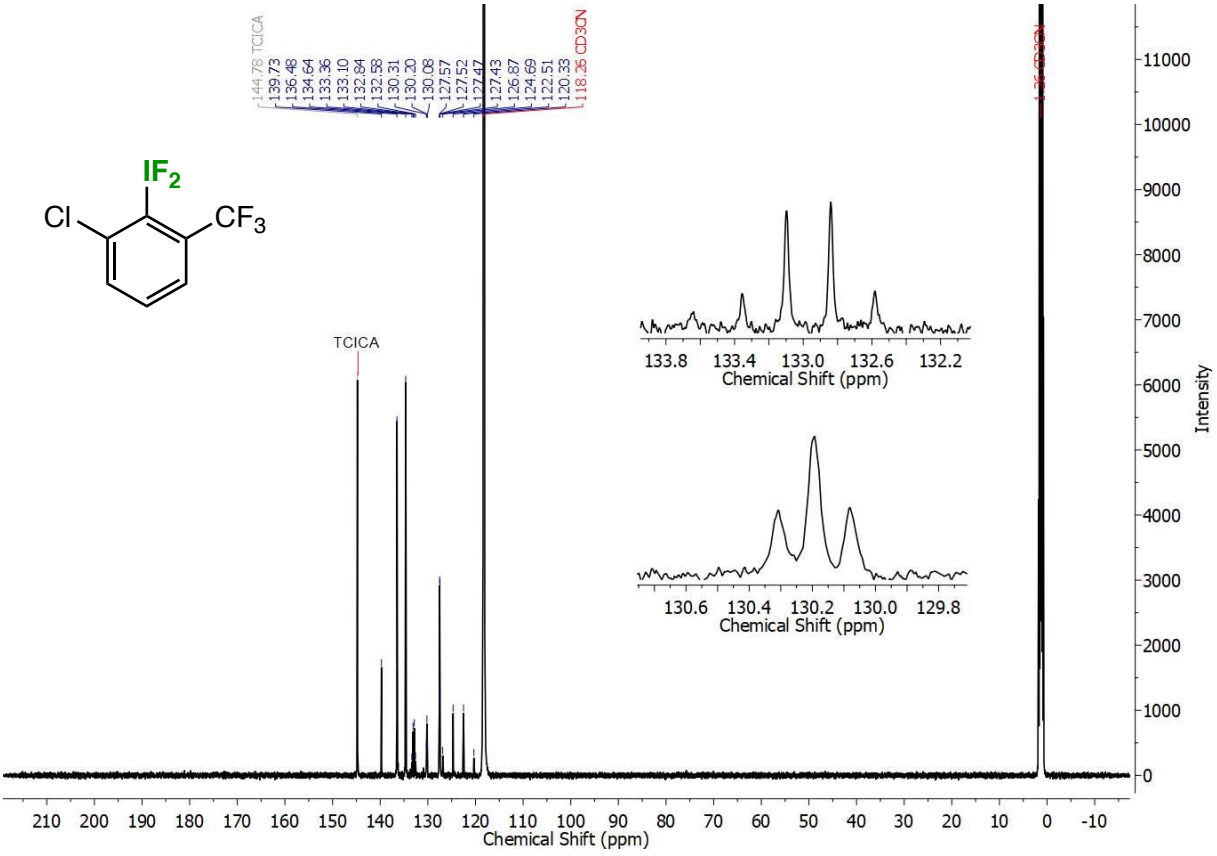

Figure S 24. $^{13}C\{^{1}H\}$ NMR spectrum of (2-chloro-6-(trifluoromethyl)phenyl)difluoro-λ^3-iodane (compound **8**).

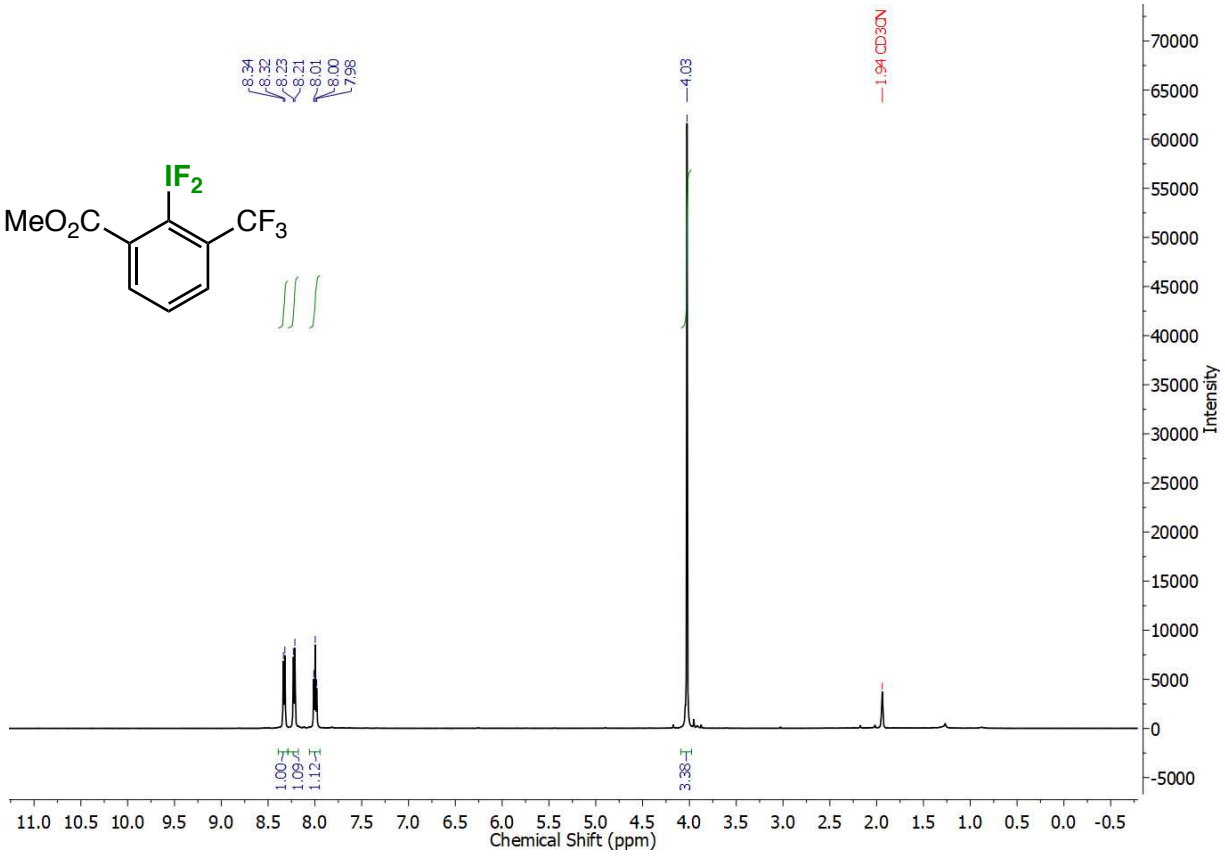

Figure S 25. ^{1}H NMR spectrum of methyl 2-(difluoro-λ^{3}-iodanyl)-3-(trifluoromethyl)benzoate (compound **9**).

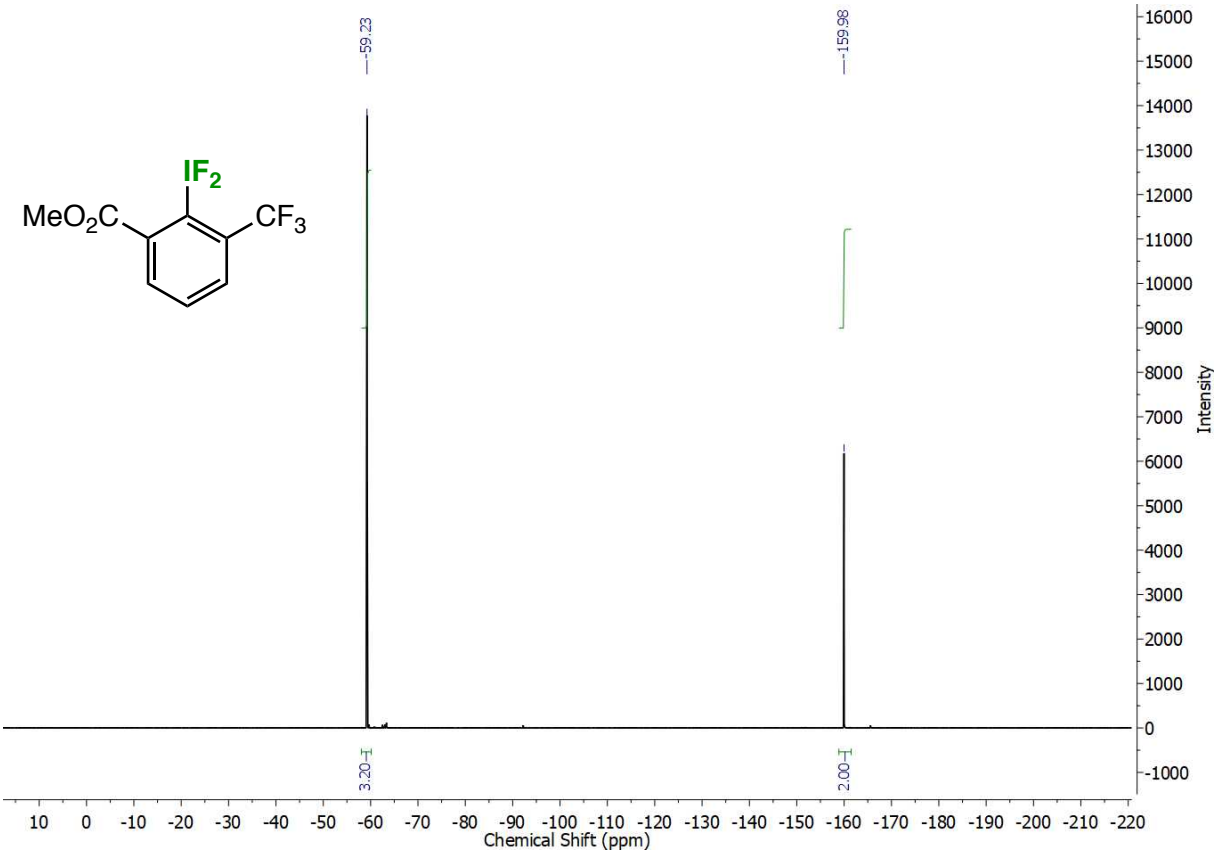

Figure S 26. ^{19}F NMR spectrum of methyl 2-(difluoro-λ^3-iodanyl)-3-(trifluoromethyl)benzoate (compound **9**).

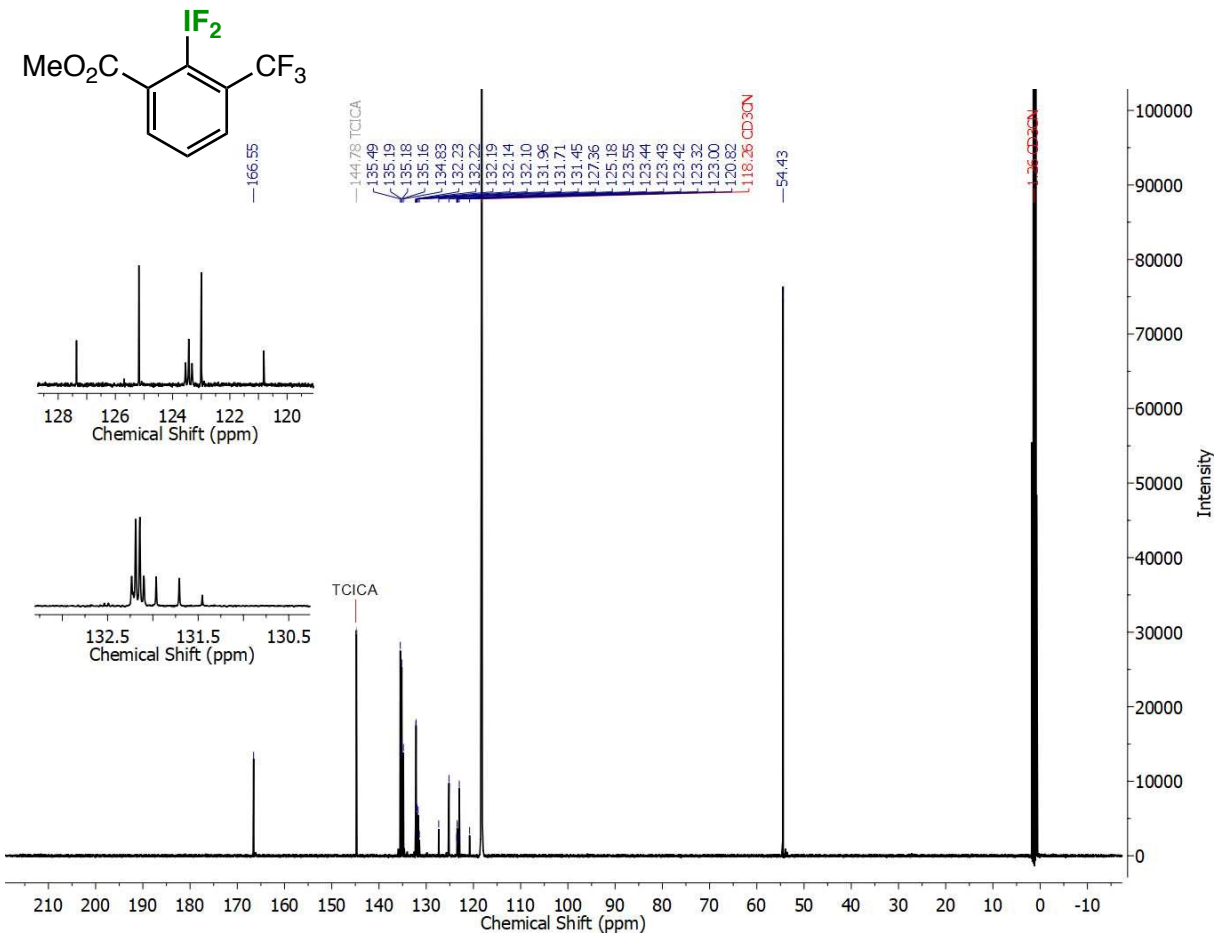

Figure S 27. $^{13}C\{^{1}H\}$ NMR spectrum of methyl 2-(difluoro-λ^3-iodanyl)-3-(trifluoromethyl)benzoate (compound **9**).

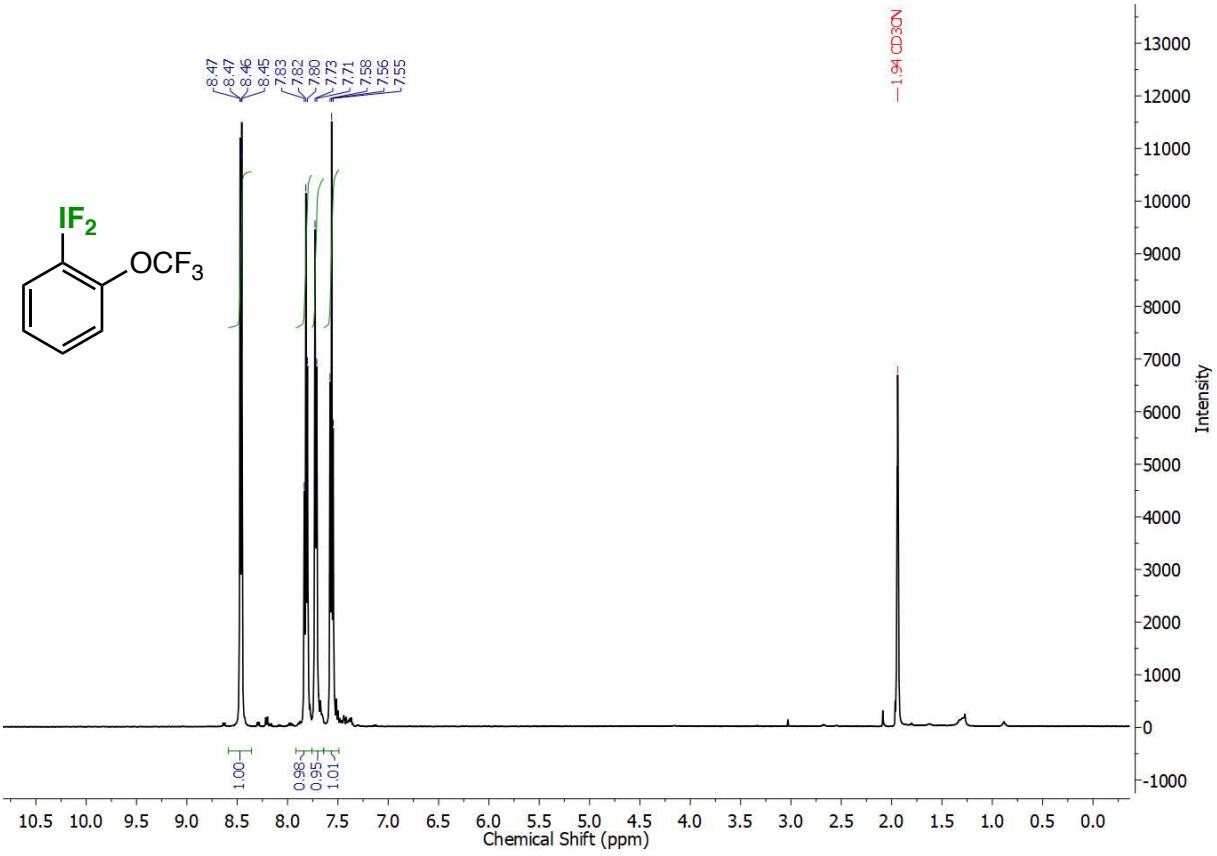

Figure S 28. ^{1}H NMR spectrum of difluoro(2-(trifluoromethoxy)phenyl)-λ^{3}-iodane (compound **10**).

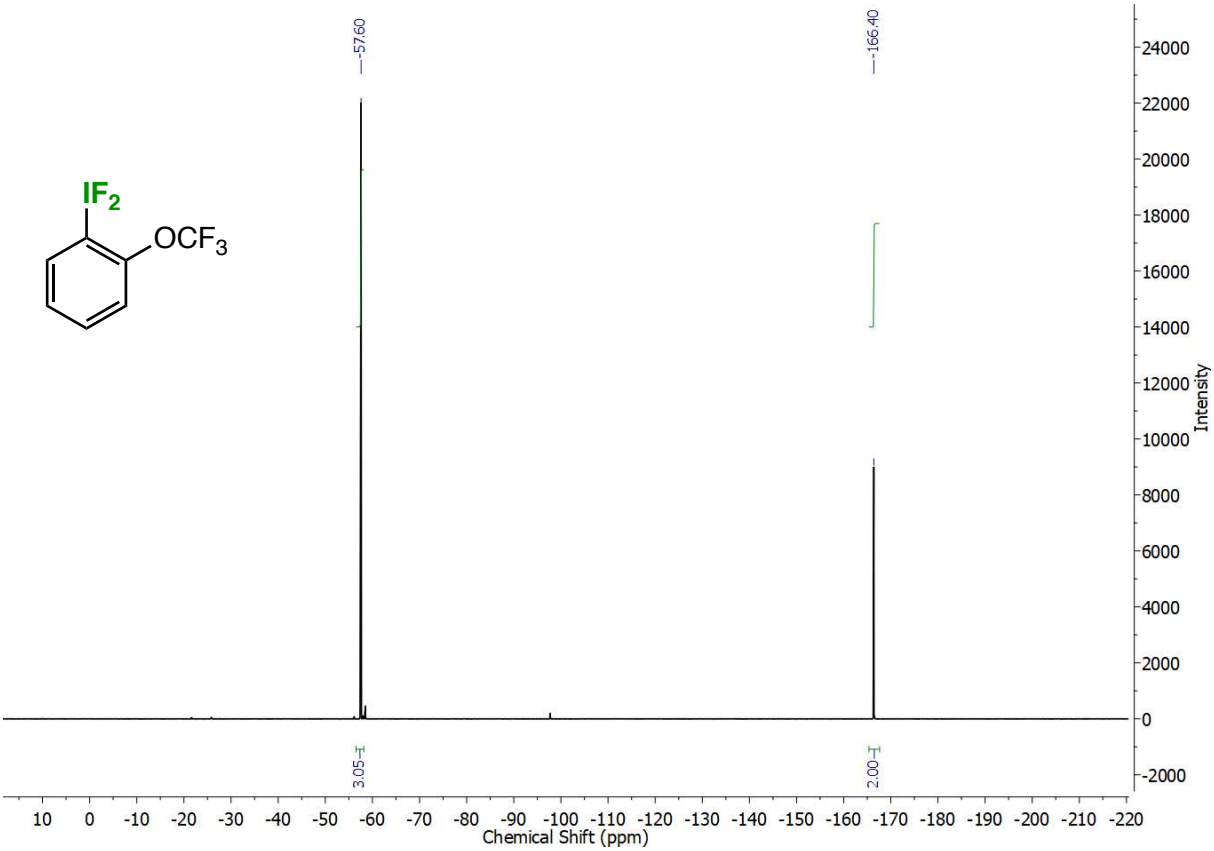

Figure S 29. ^{19}F NMR spectrum of difluoro(2-(trifluoromethoxy)phenyl)-λ^3-iodane (compound **10**).

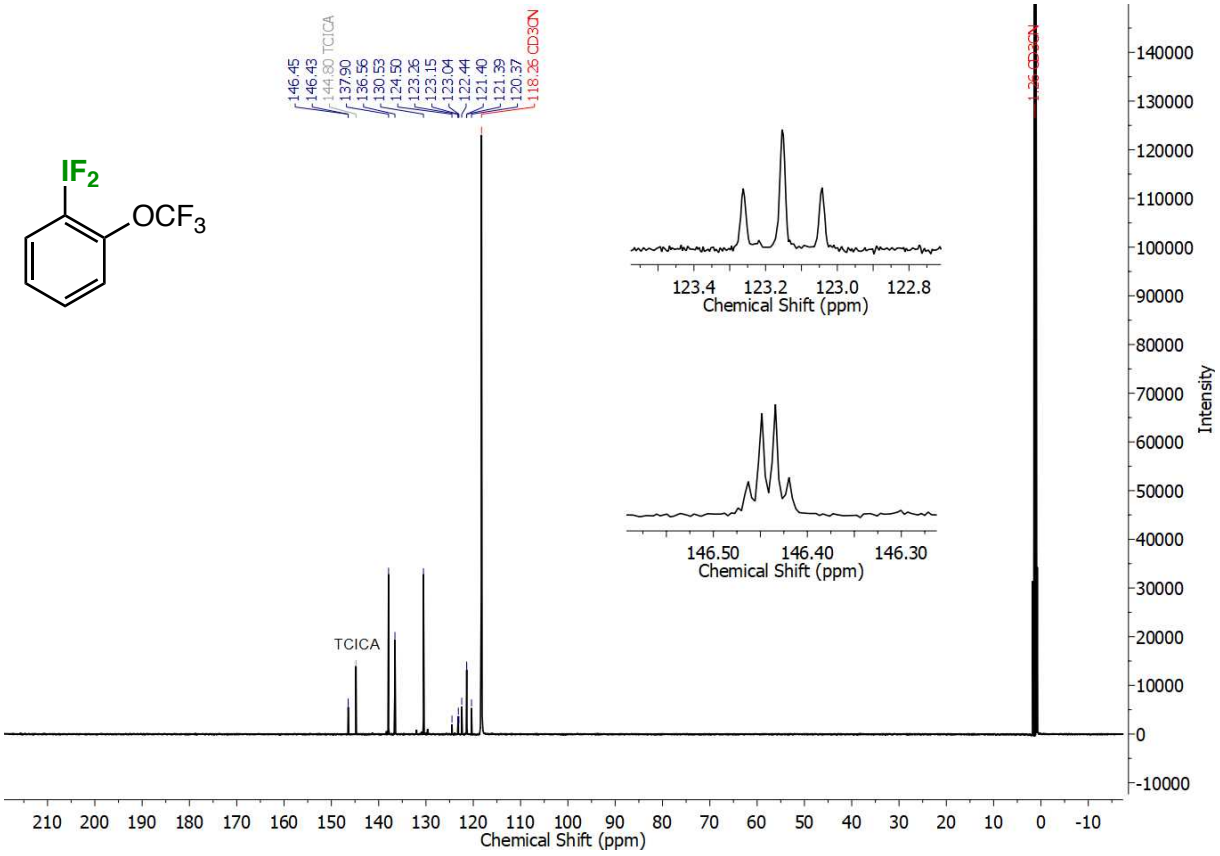

Figure S 30. $^{13}C\{^{1}H\}$ NMR spectrum of difluoro(2-(trifluoromethoxy)phenyl)-λ^3-iodane (compound **10**).

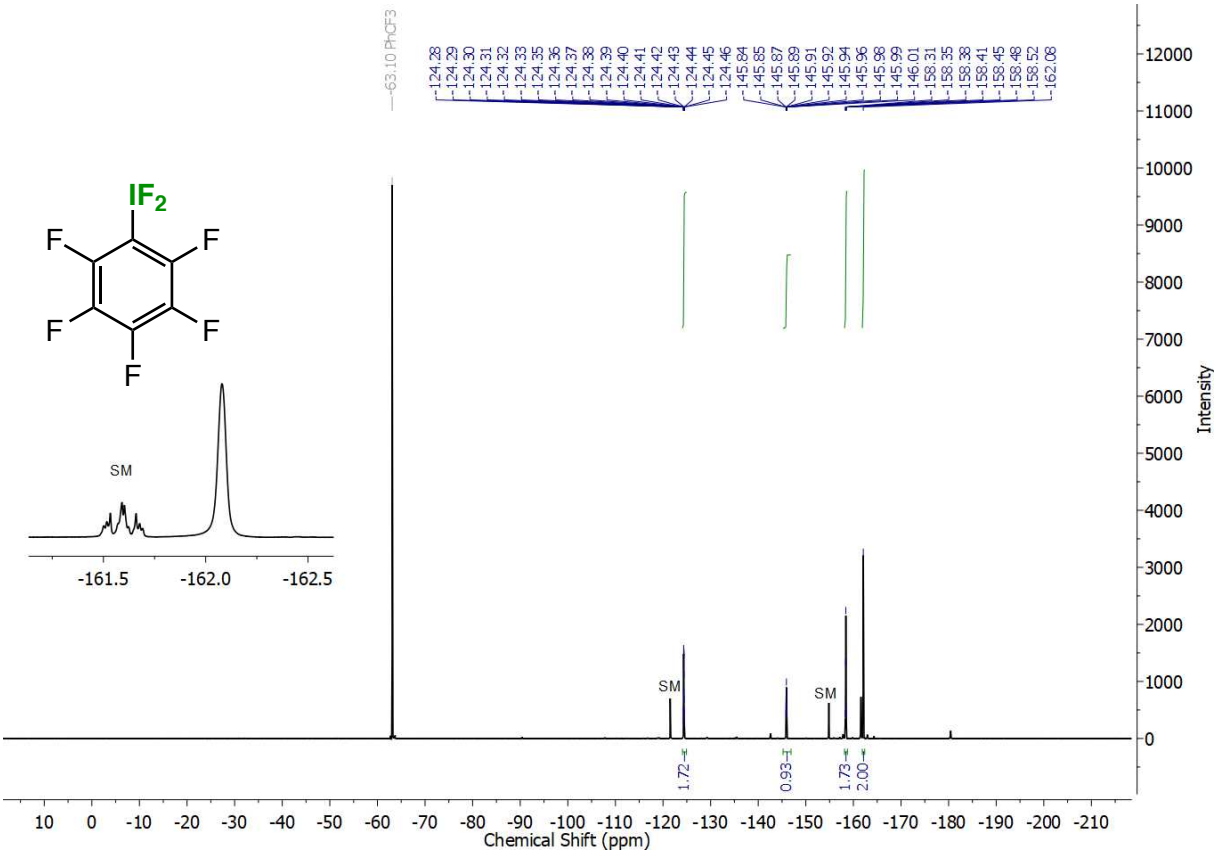

Figure S 31. ^{19}F NMR spectrum of difluoro(perfluorophenyl)-λ^3-iodane (compound **11**) with $PhCF_3$ as an internal standard. SM denotes the starting material perfluoroiodobenzene.

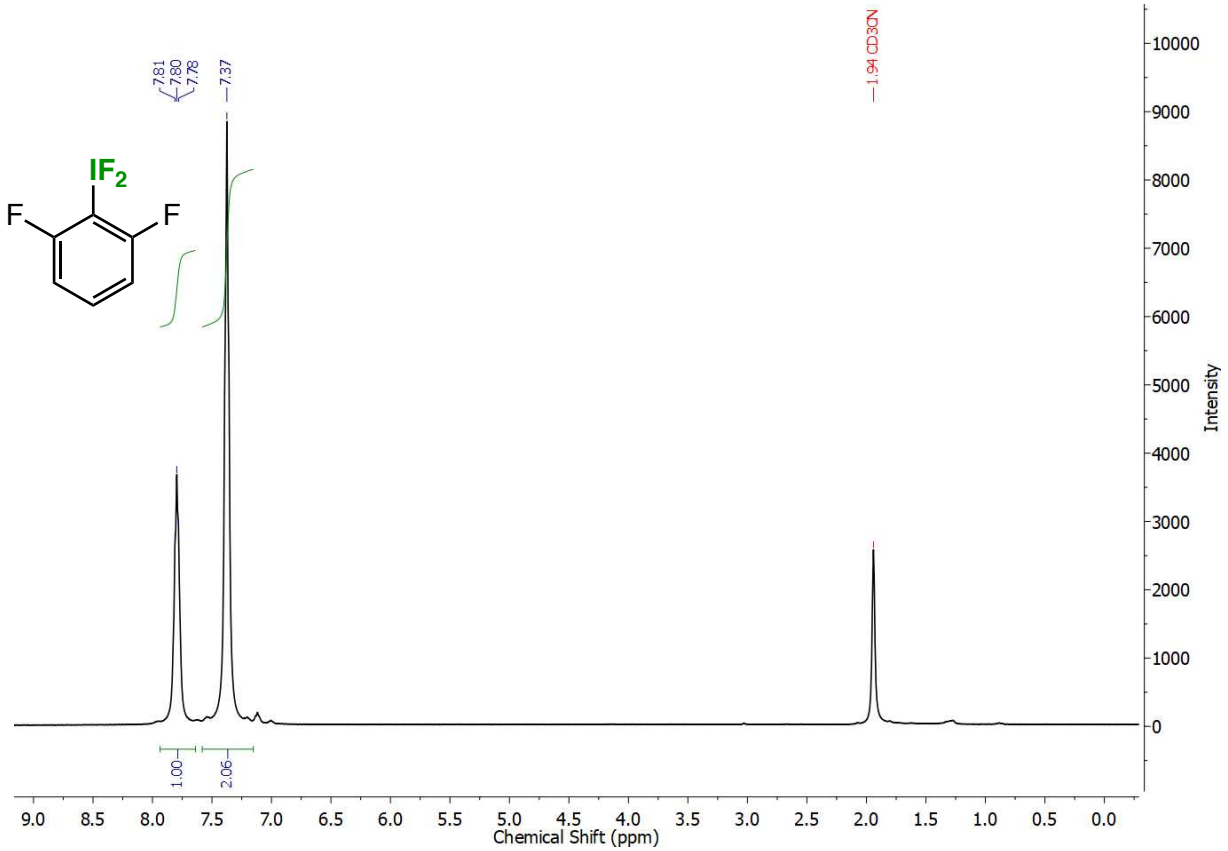

Figure S 32. ^{1}H NMR spectrum of (2,6-difluorophenyl)difluoro-λ^3-iodane (compound **12**).

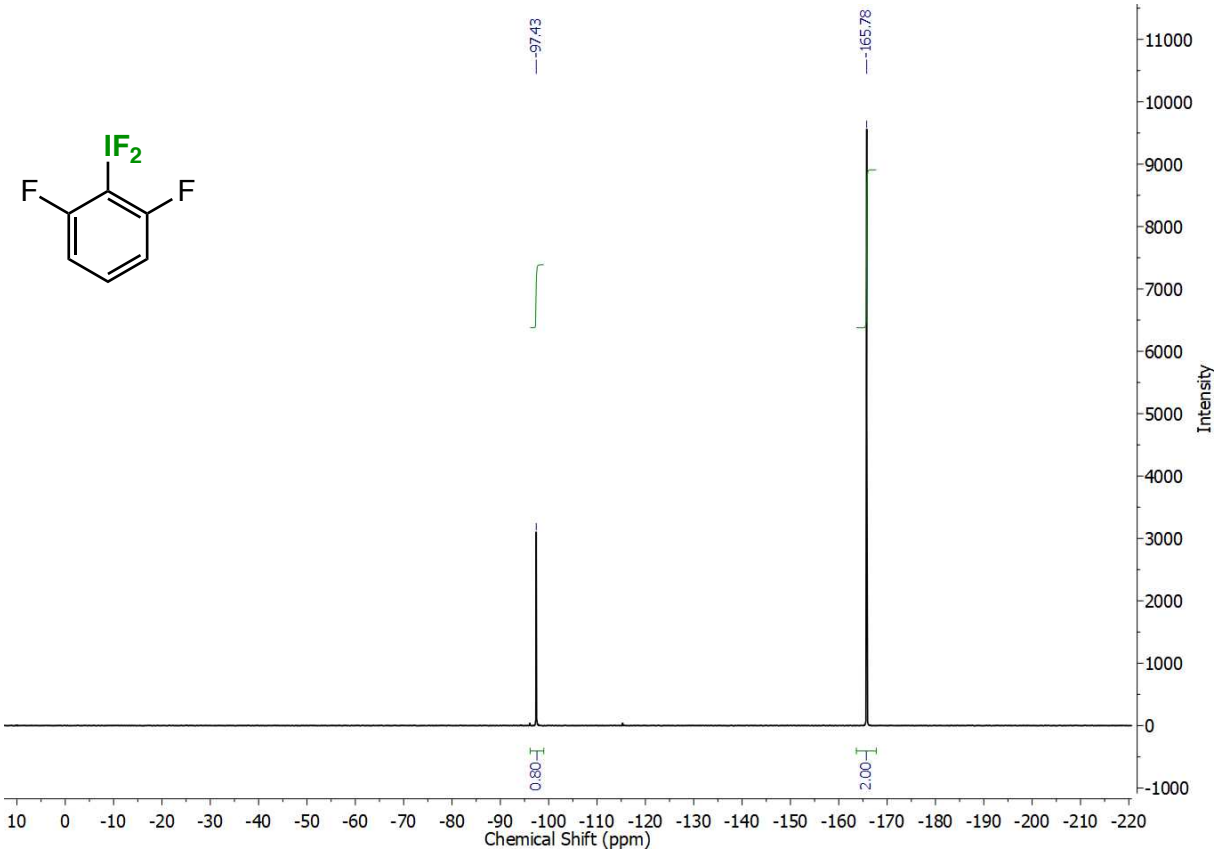

Figure S 33. ^{19}F NMR spectrum of (2,6-difluorophenyl)difluoro-λ^3-iodane (compound **12**).

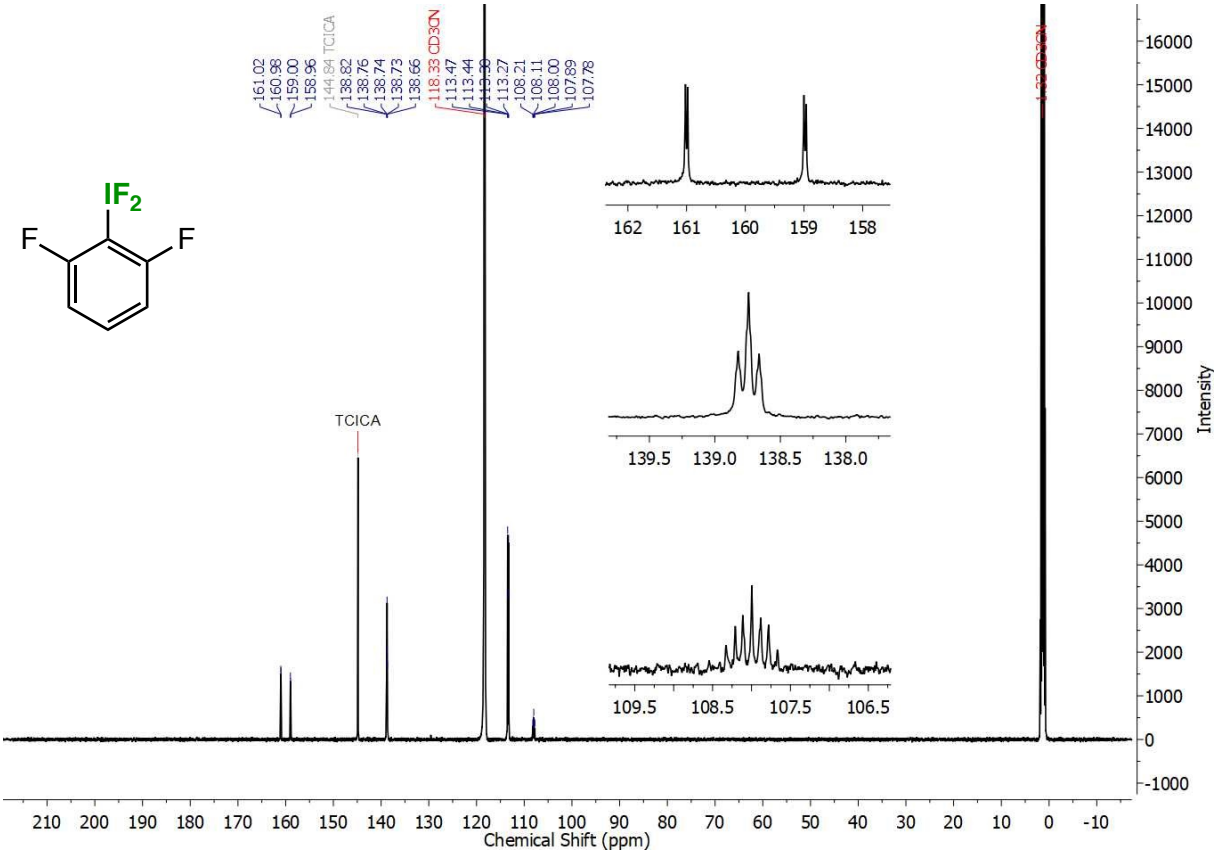

Figure S 34. $^{13}C\{^{1}H\}$ NMR spectrum of (2,6-difluorophenyl)difluoro-λ^3-iodane (compound **12**).

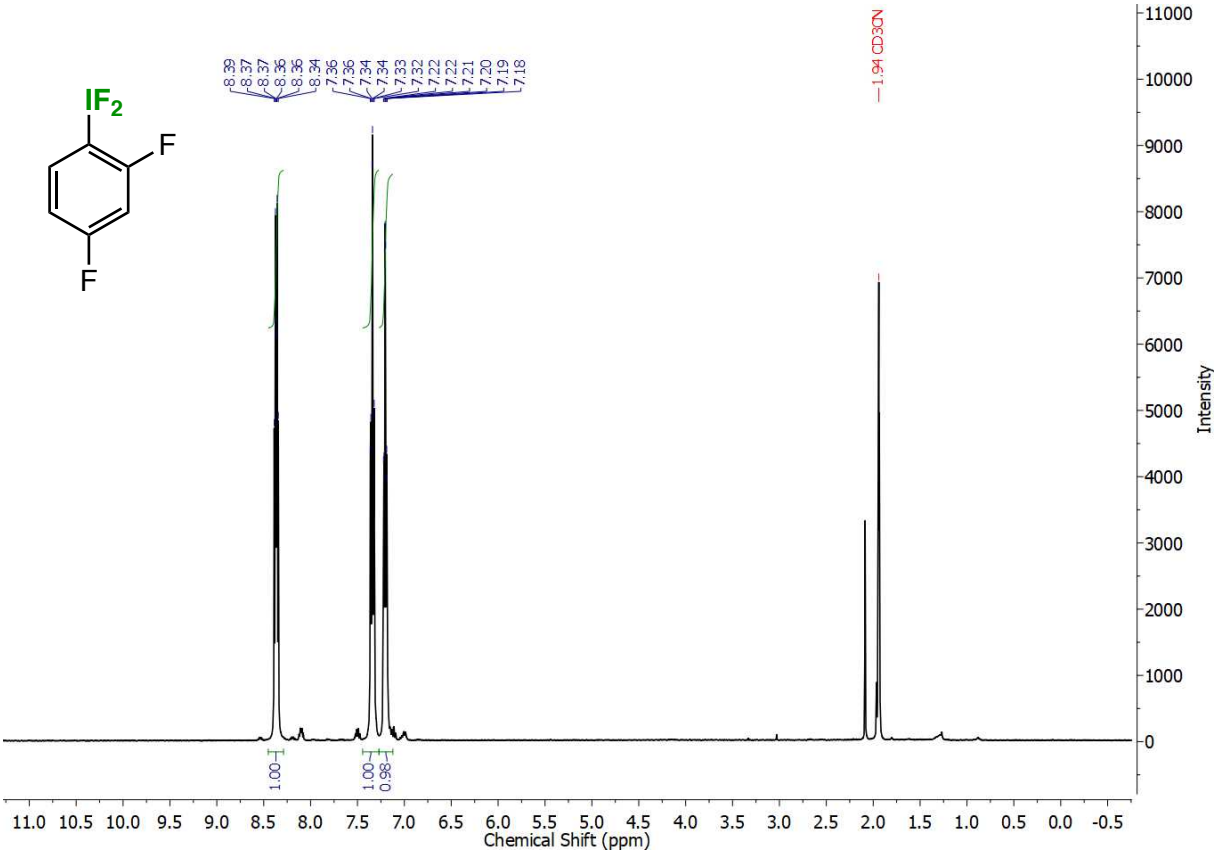

Figure S 35. ^{1}H NMR spectrum of (2,4-difluorophenyl)difluoro-λ^{3}-iodane (compound **13**).

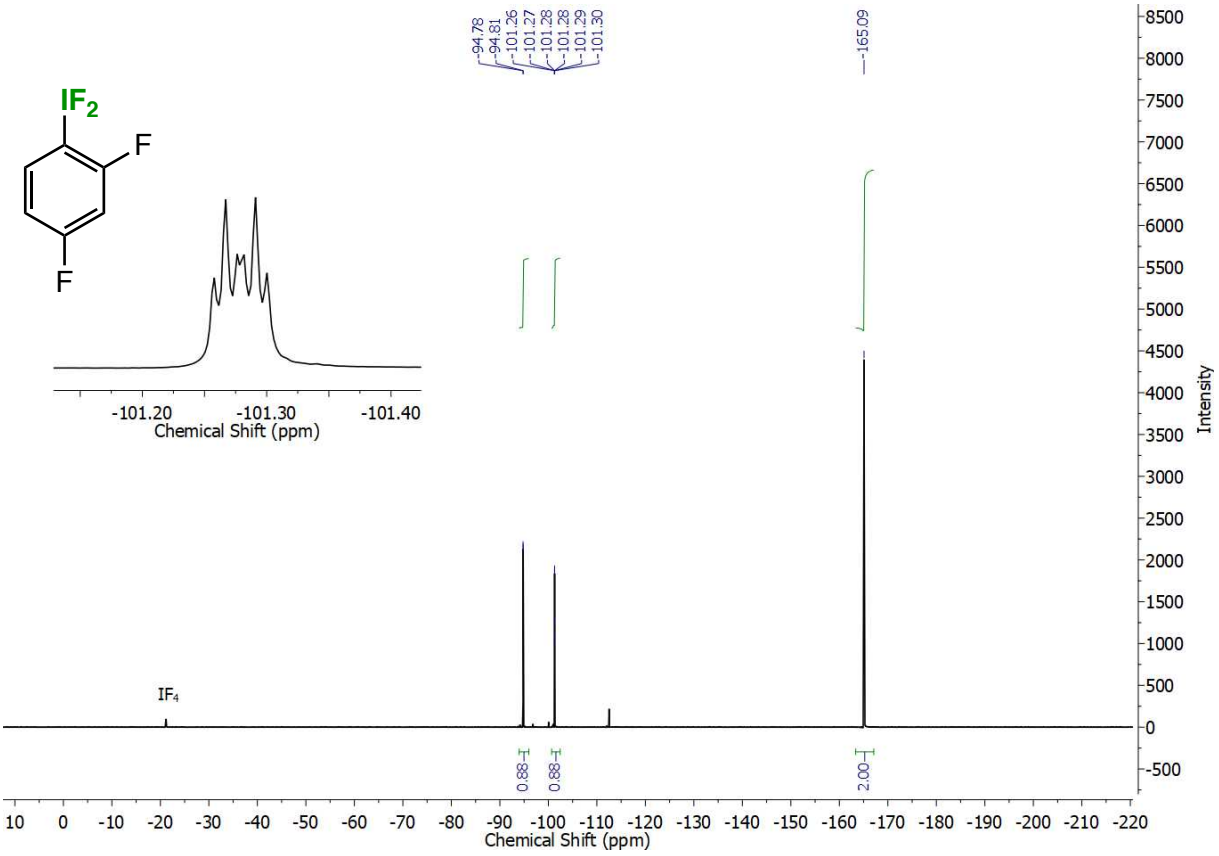

Figure S 36. ^{19}F NMR spectrum of (2,4-difluorophenyl)difluoro-λ^3-iodane (compound **13**).

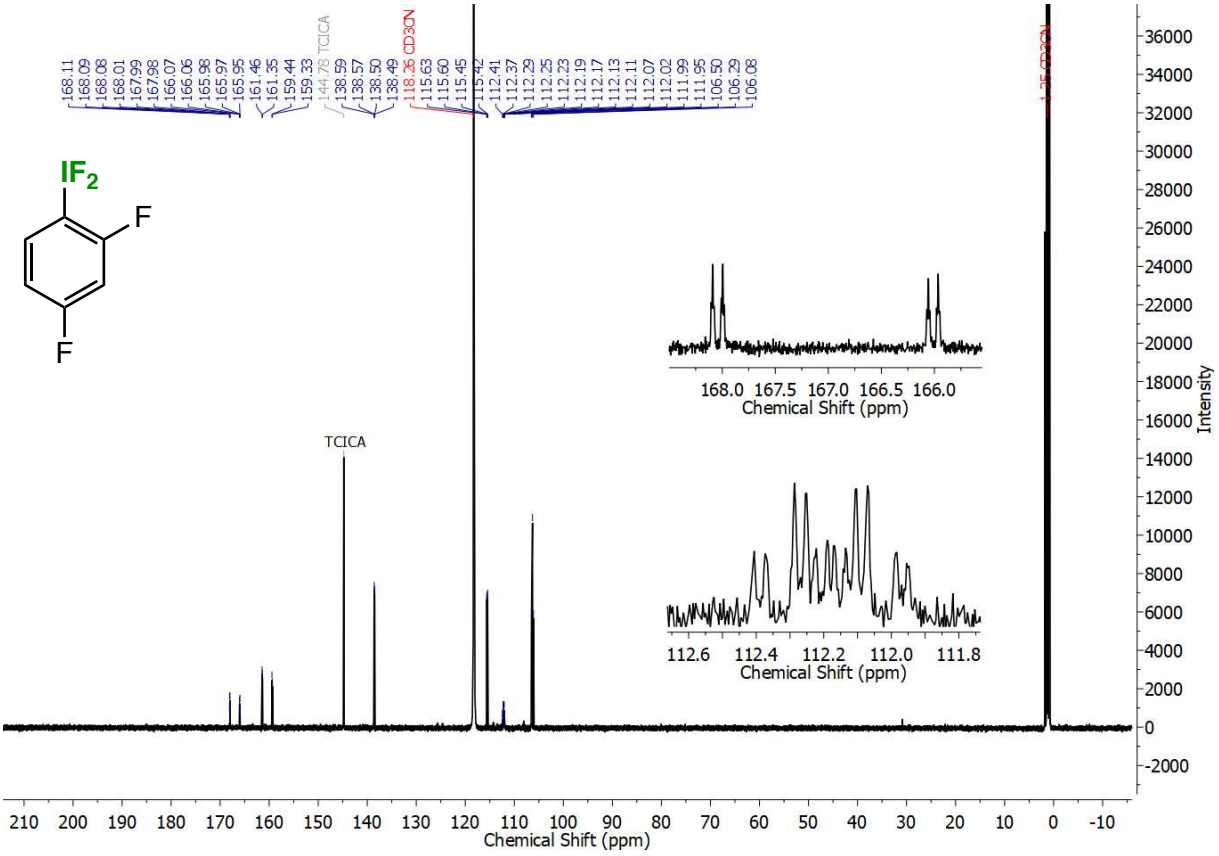

Figure S 37. $^{13}C\{^{1}H\}$ NMR spectrum of (2,4-difluorophenyl)difluoro-λ^3-iodane (compound **13**).

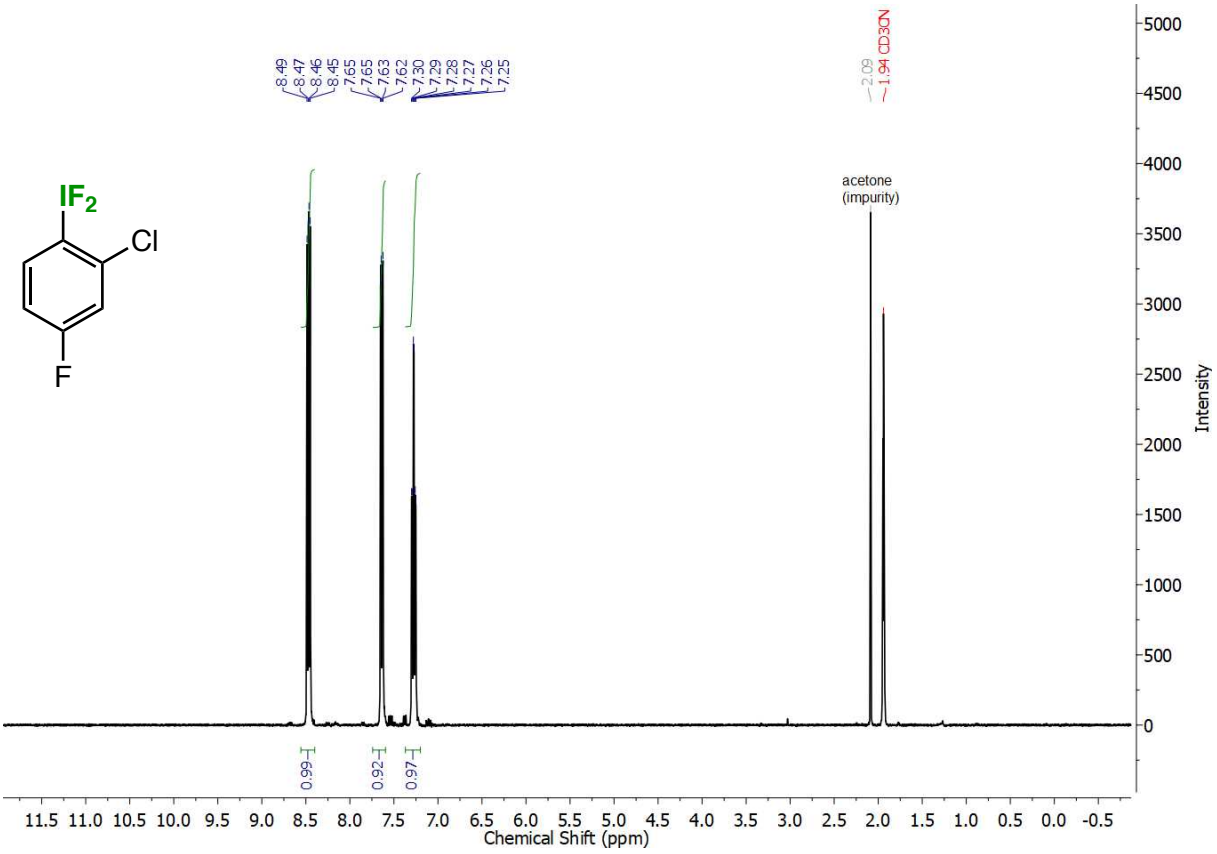

Figure S 38. ^{1}H NMR spectrum of (2-chloro-4-fluorophenyl)difluoro-λ^{3}-iodane (compound **14**).

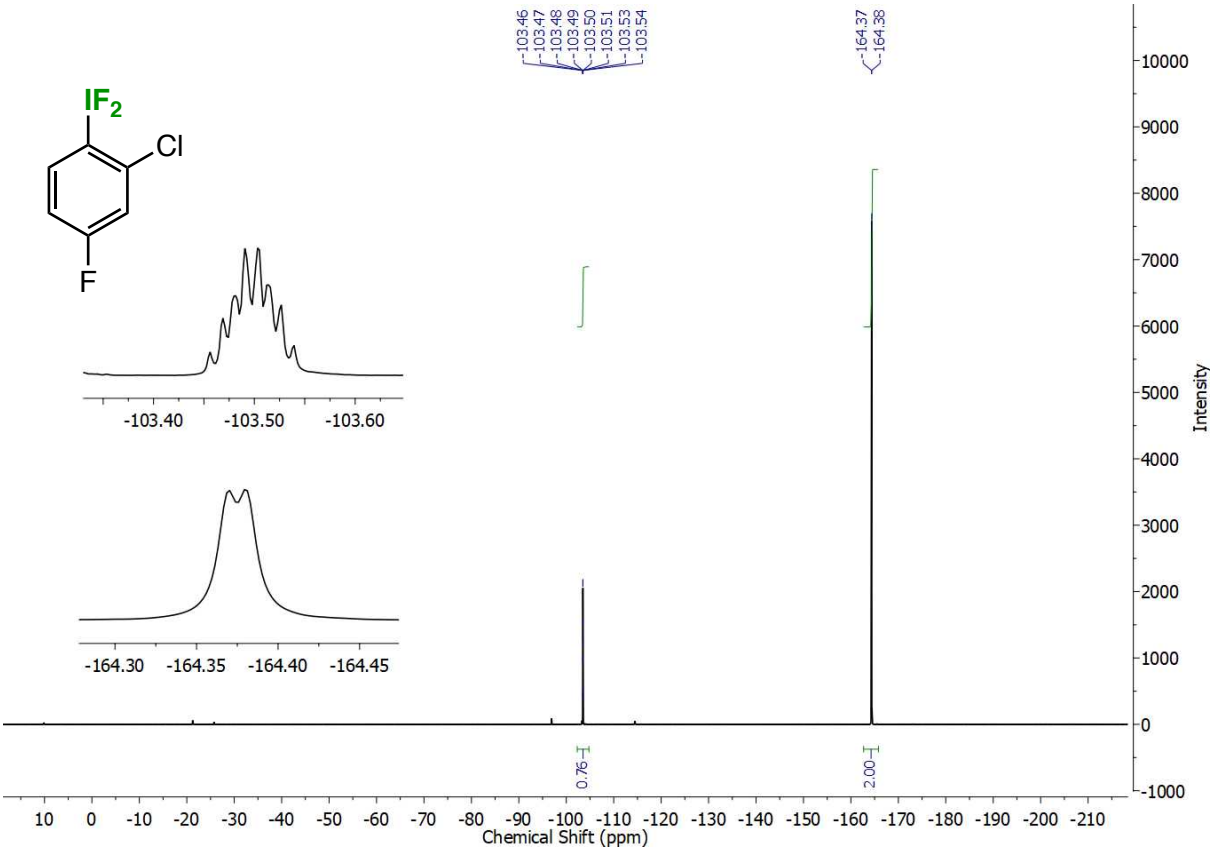

Figure S 39. ^{19}F NMR spectrum of (2-chloro-4-fluorophenyl)difluoro-λ^3-iodane (compound **14**).

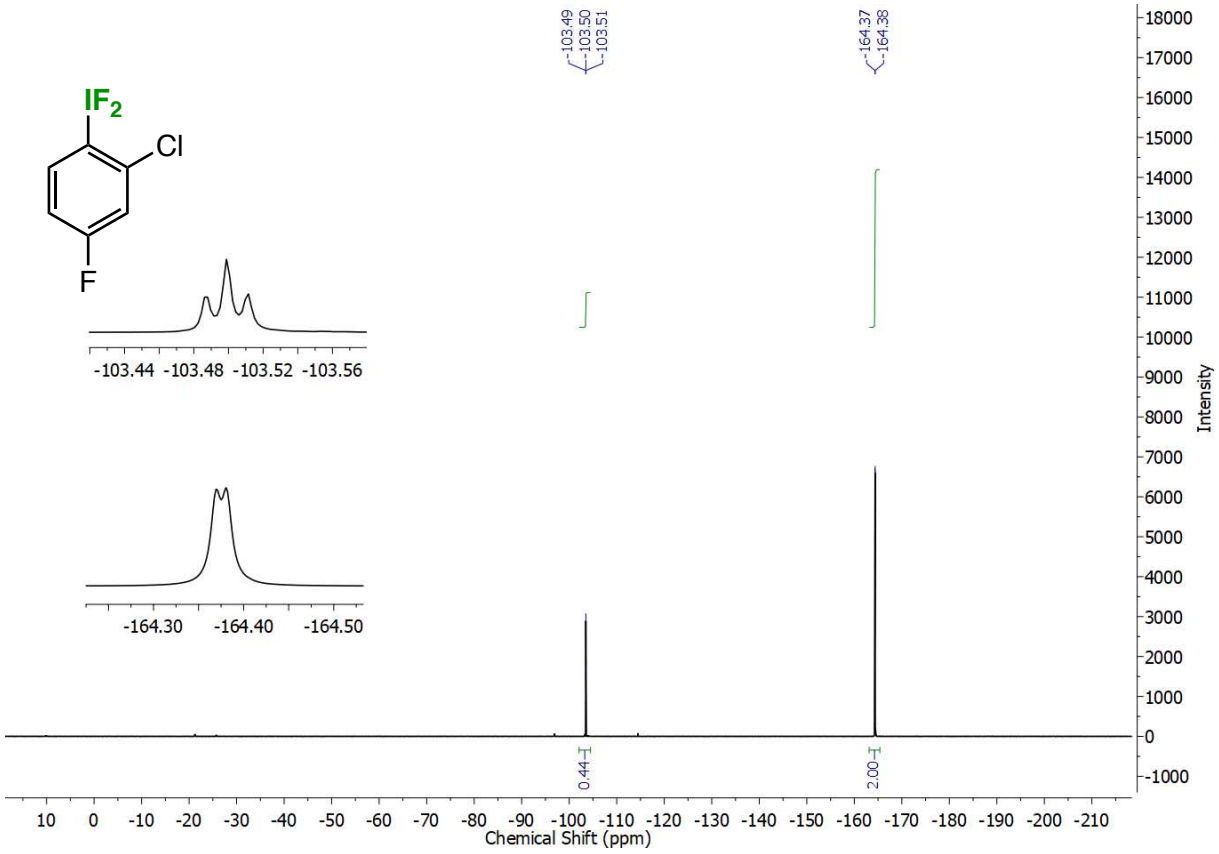

Figure S 40. $^{19}F\{^{1}H\}$ NMR spectrum of (2-chloro-4-fluorophenyl)difluoro-λ^3-iodane (compound **14**).

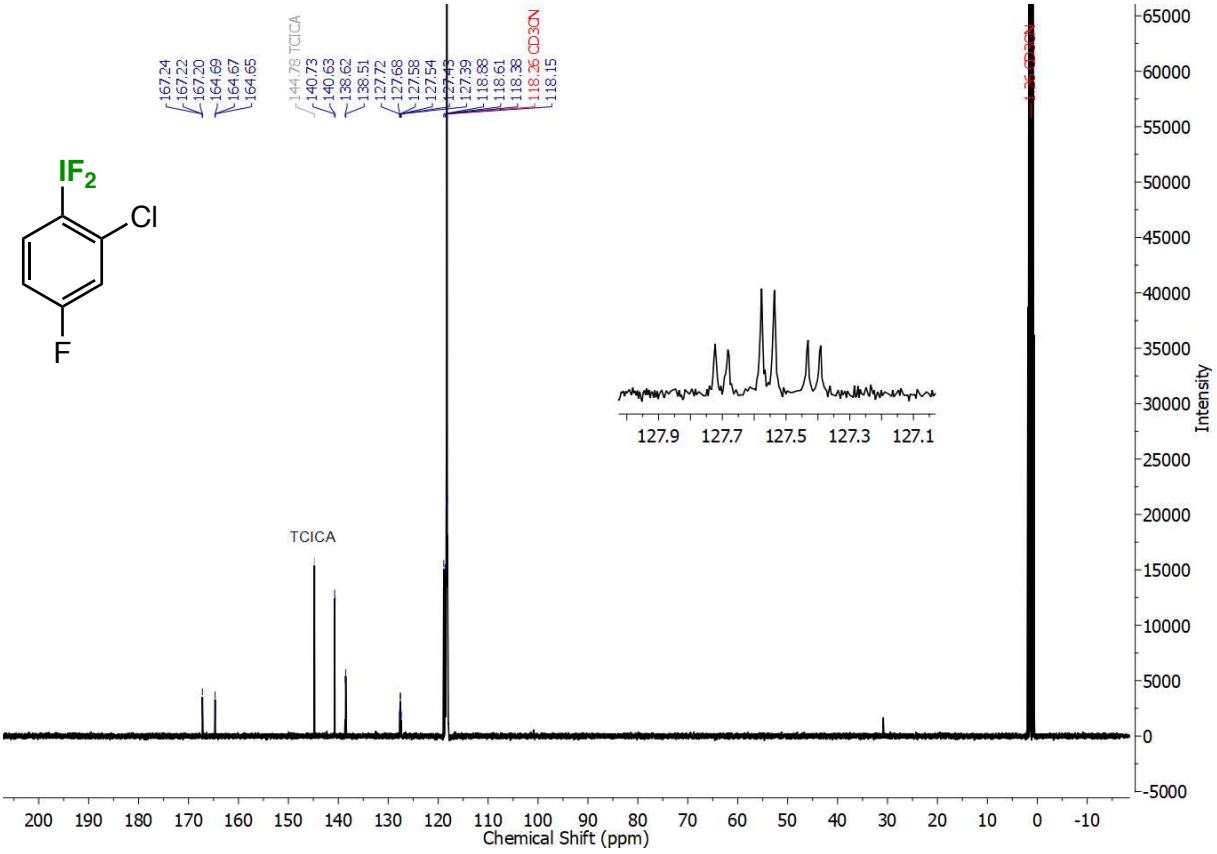

Figure S 41. $^{13}C\{^{1}H\}$ NMR spectrum of (2-chloro-4-fluorophenyl)difluoro-λ^3-iodane (compound **14**).

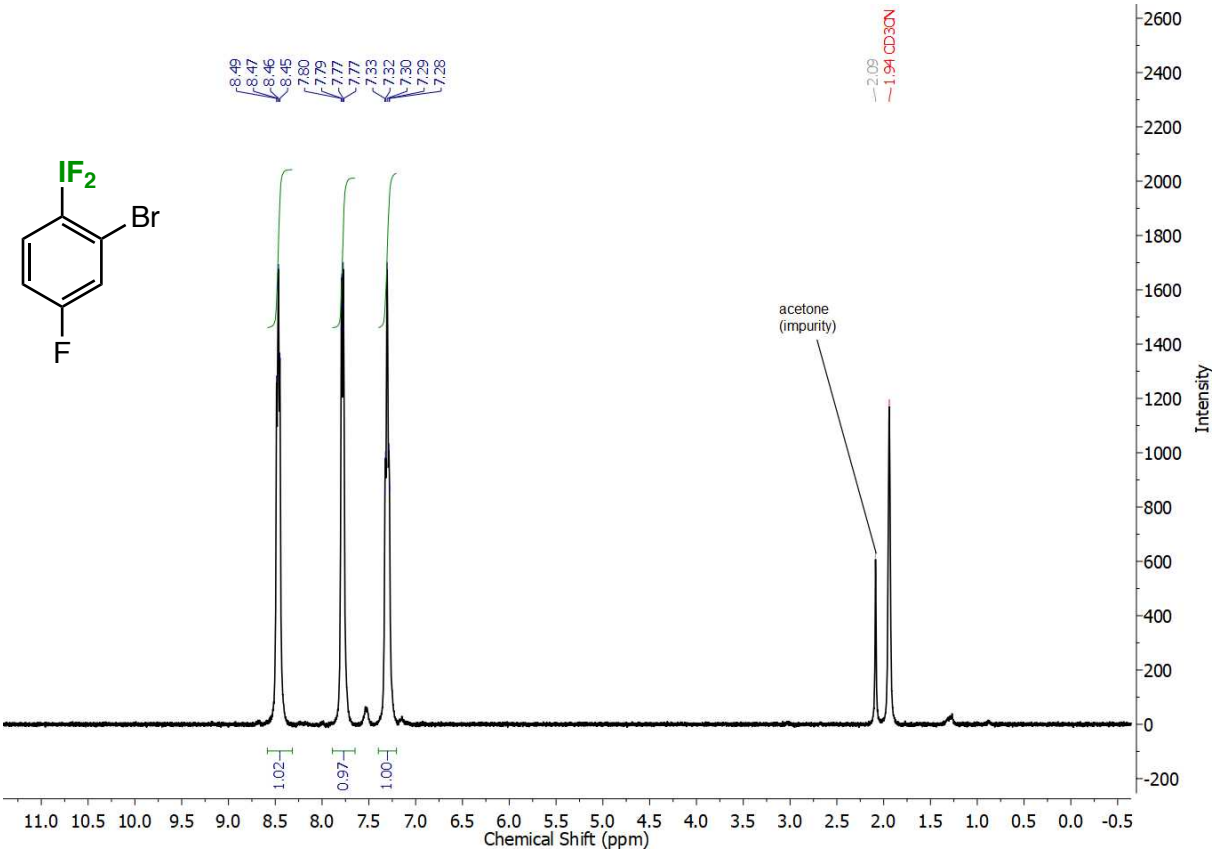

Figure S 42. ^{1}H NMR spectrum of (2-bromo-4-fluorophenyl)difluoro-λ^3-iodane (compound **15**).

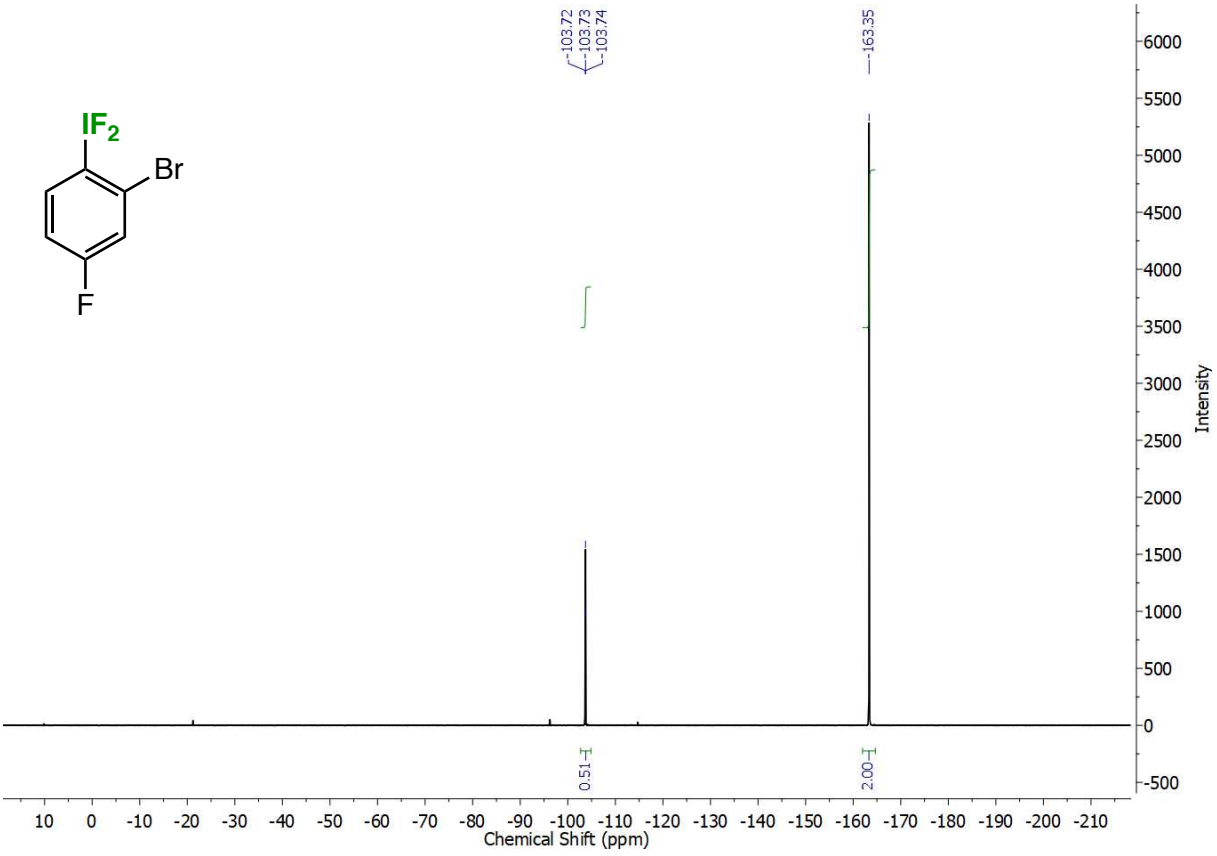

Figure S 43. ^{19}F NMR spectrum of (2-bromo-4-fluorophenyl)difluoro-λ^3-iodane (compound **15**).

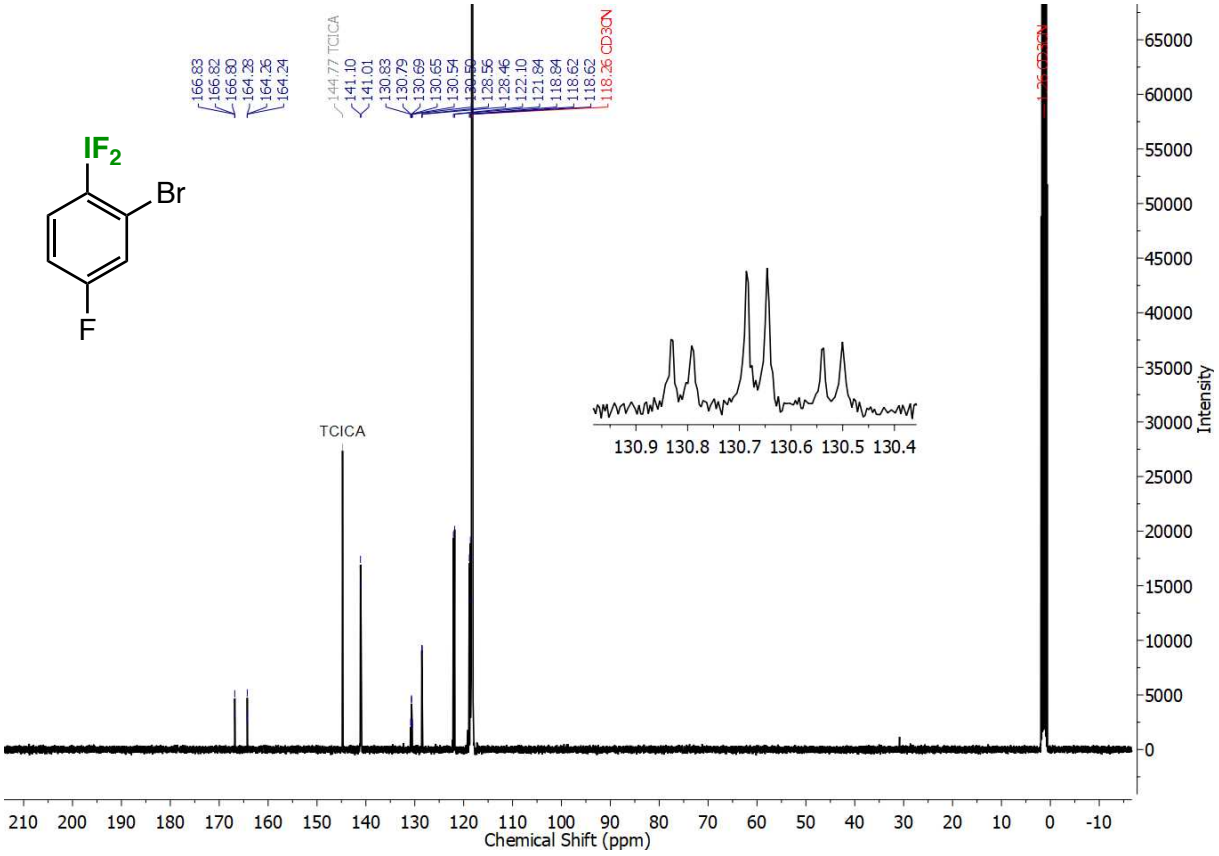

Figure S 44. $^{13}C\{^{1}H\}$ NMR spectrum of (2-bromo-4-fluorophenyl)difluoro-λ^3-iodane (compound **15**).

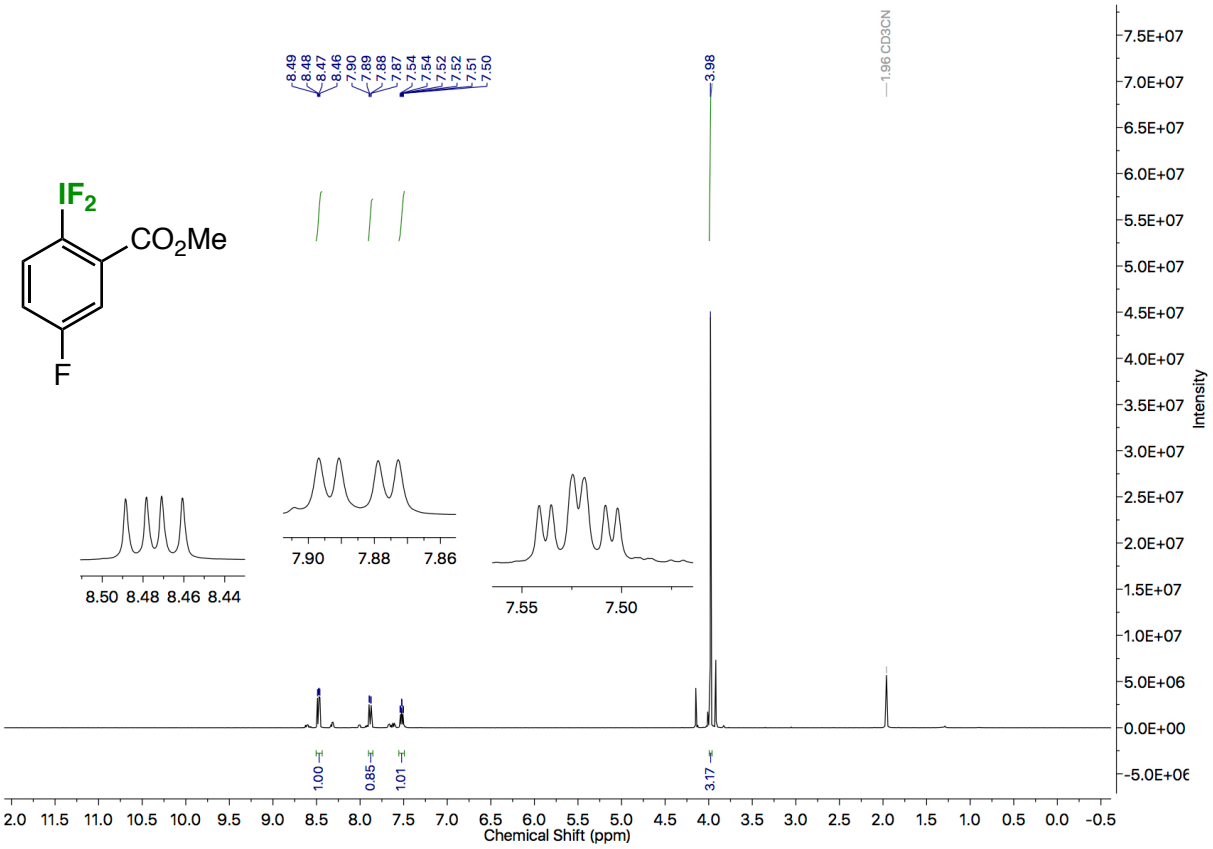

Figure S 45. ^{1}H NMR spectrum of methyl 2-(difluoro-λ^3-iodaneyl)-5-fluorobenzoate (compound **16**).

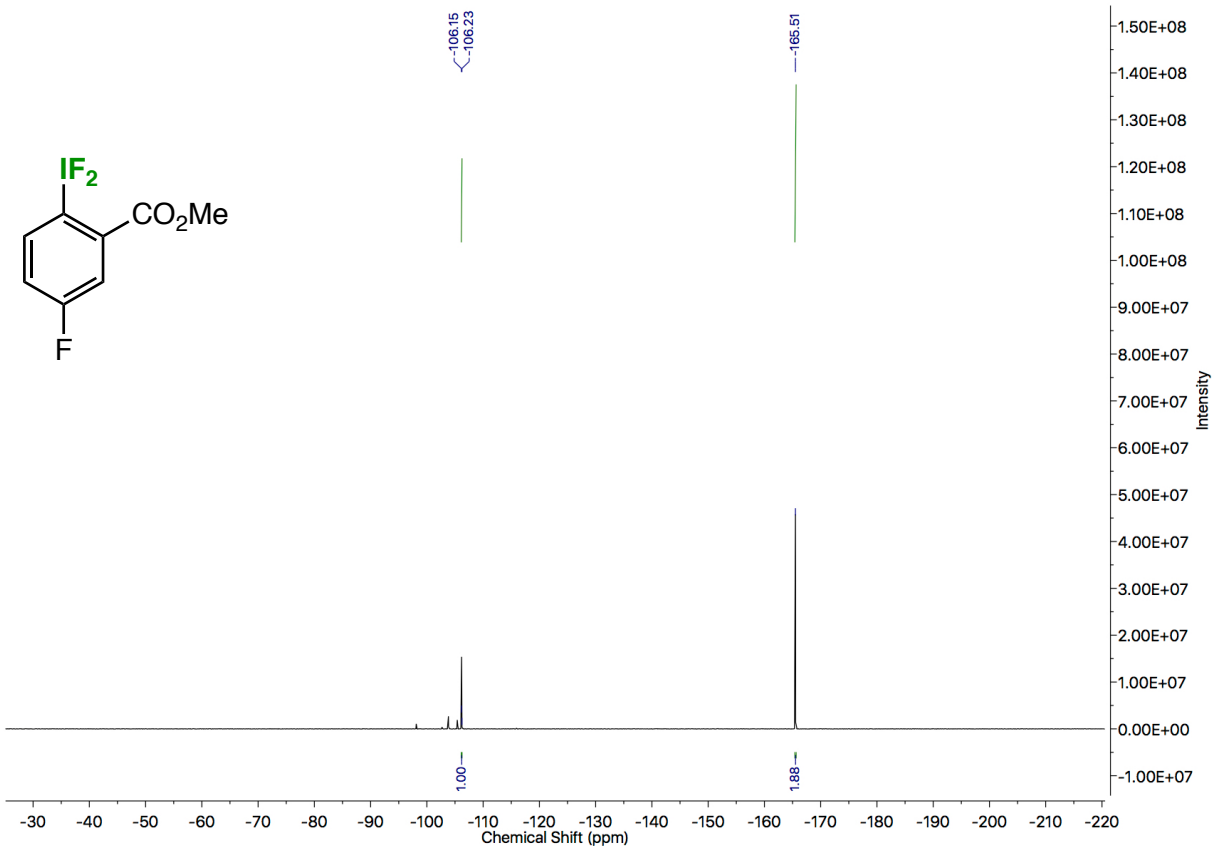

Figure S 46. ^{19}F NMR spectrum of methyl 2-(difluoro-λ^3-iodaneyl)-5-fluorobenzoate (compound **16**).

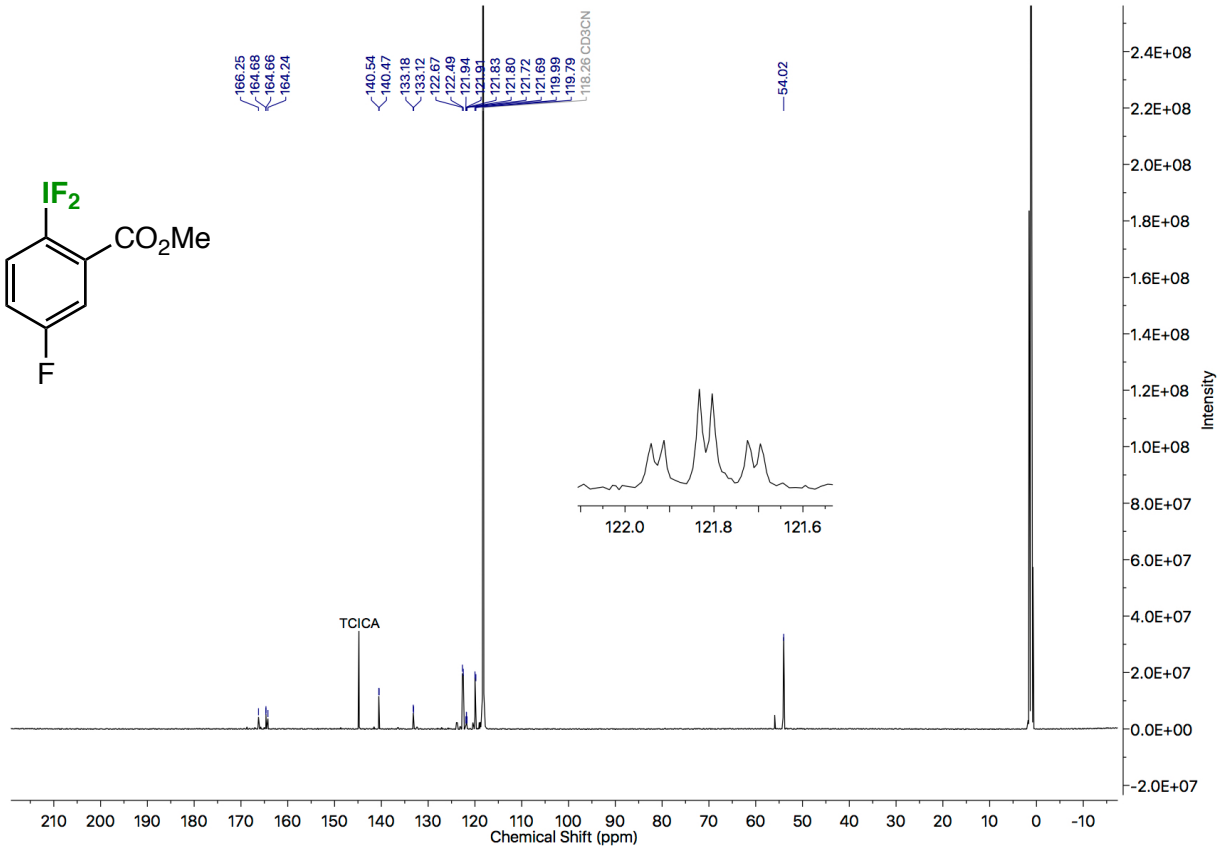

Figure S 47. $^{13}C\{^{1}H\}$ NMR spectrum of methyl 2-(difluoro-λ^3-iodaneyl)-5-fluorobenzoate (compound **16**).

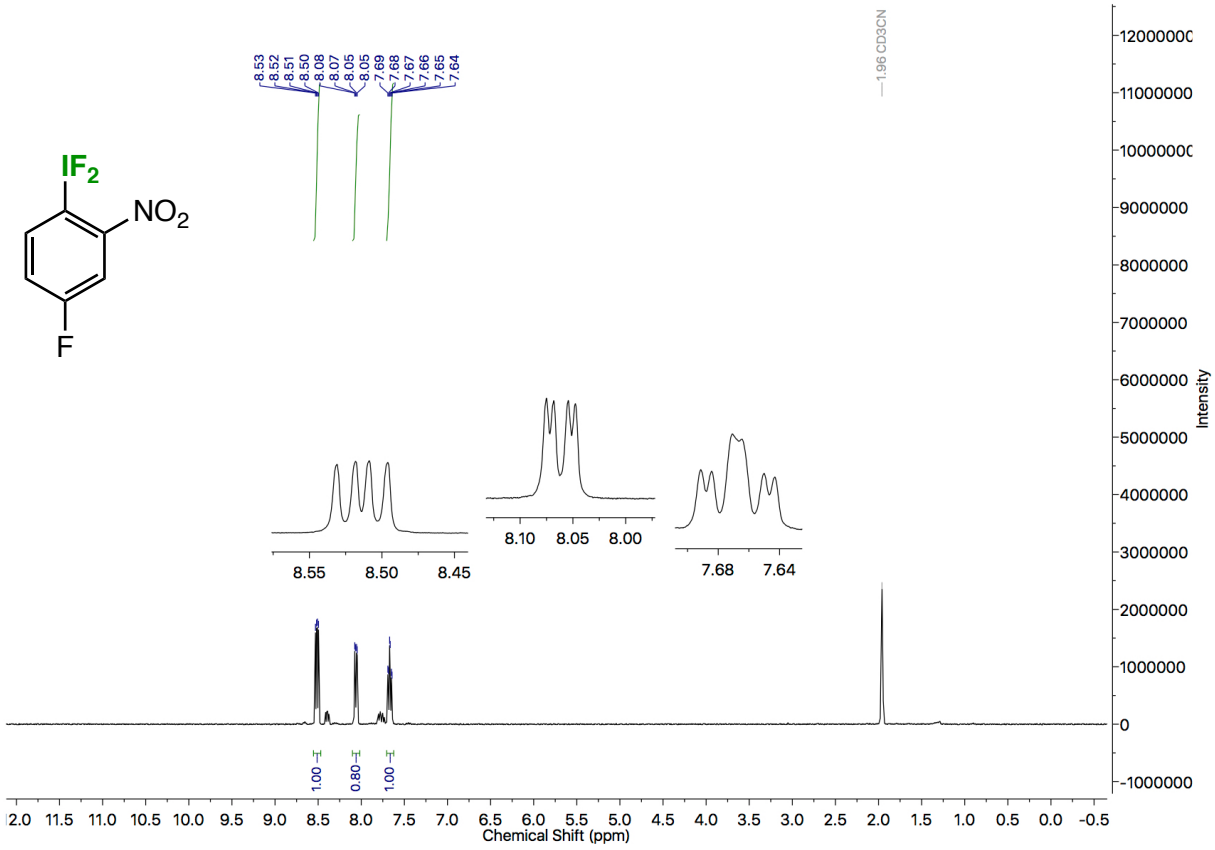

Figure S 48. ^{1}H NMR spectrum of difluoro(4-fluoro-2-nitrophenyl)-λ^3-iodane (compound **17**).

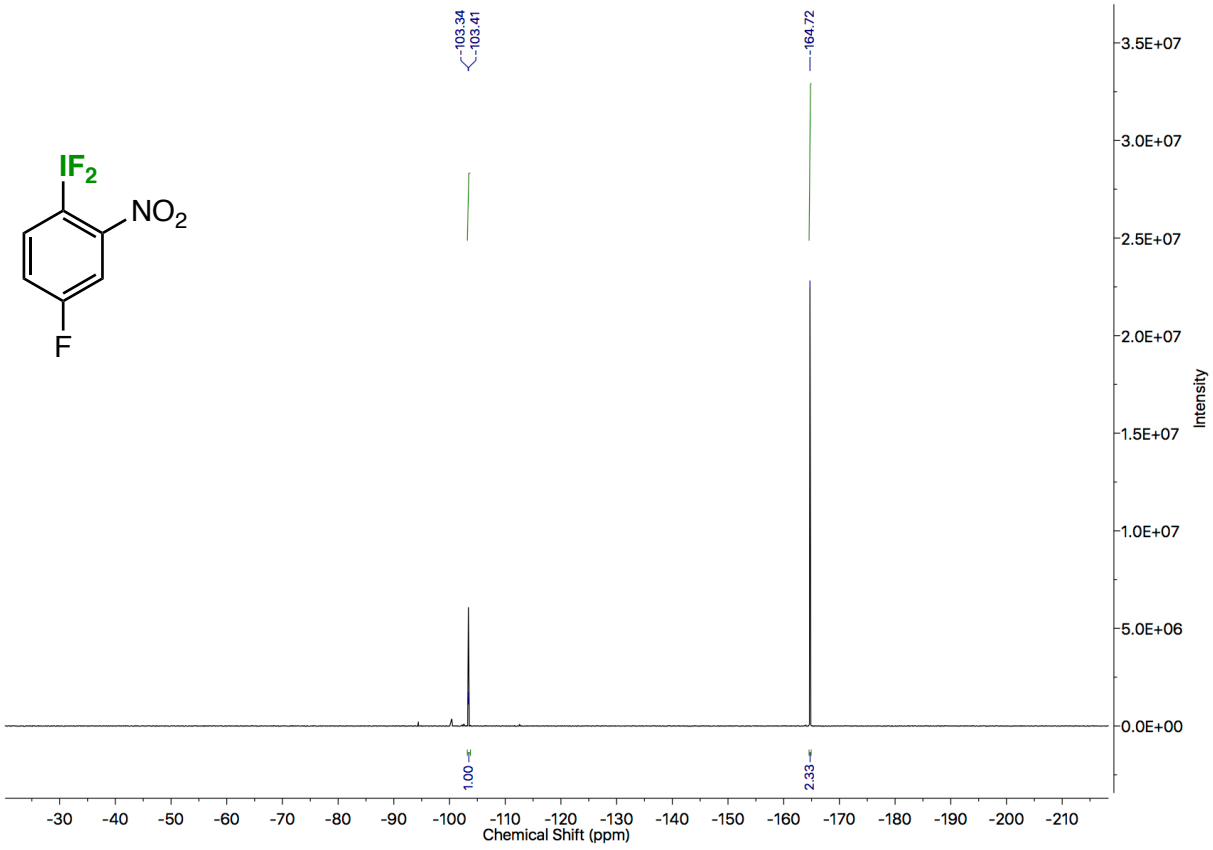

Figure S 49. ^{19}F NMR spectrum of difluoro(4-fluoro-2-nitrophenyl)-λ^3-iodane (compound **17**).

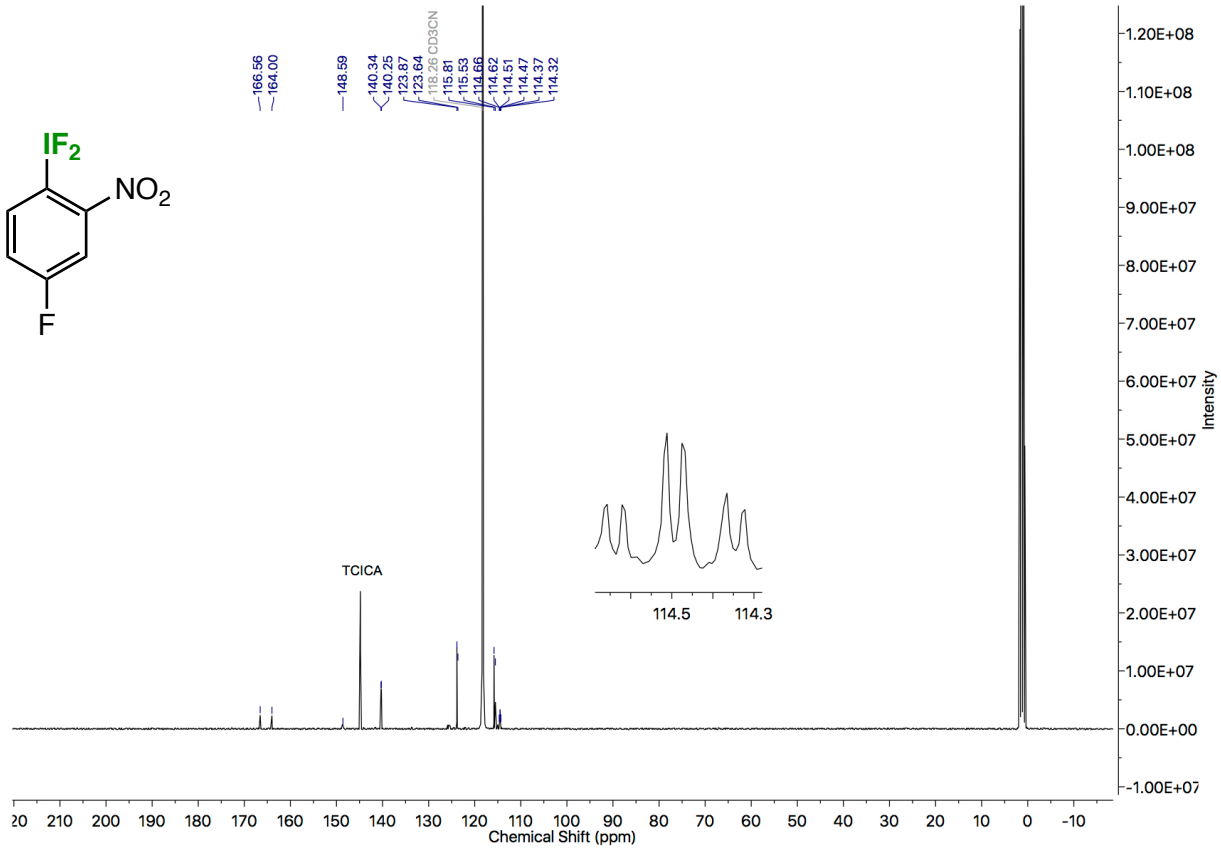

Figure S 50. $^{13}C\{^{1}H\}$ NMR spectrum of difluoro(4-fluoro-2-nitrophenyl)-λ^3-iodane (compound **17**).

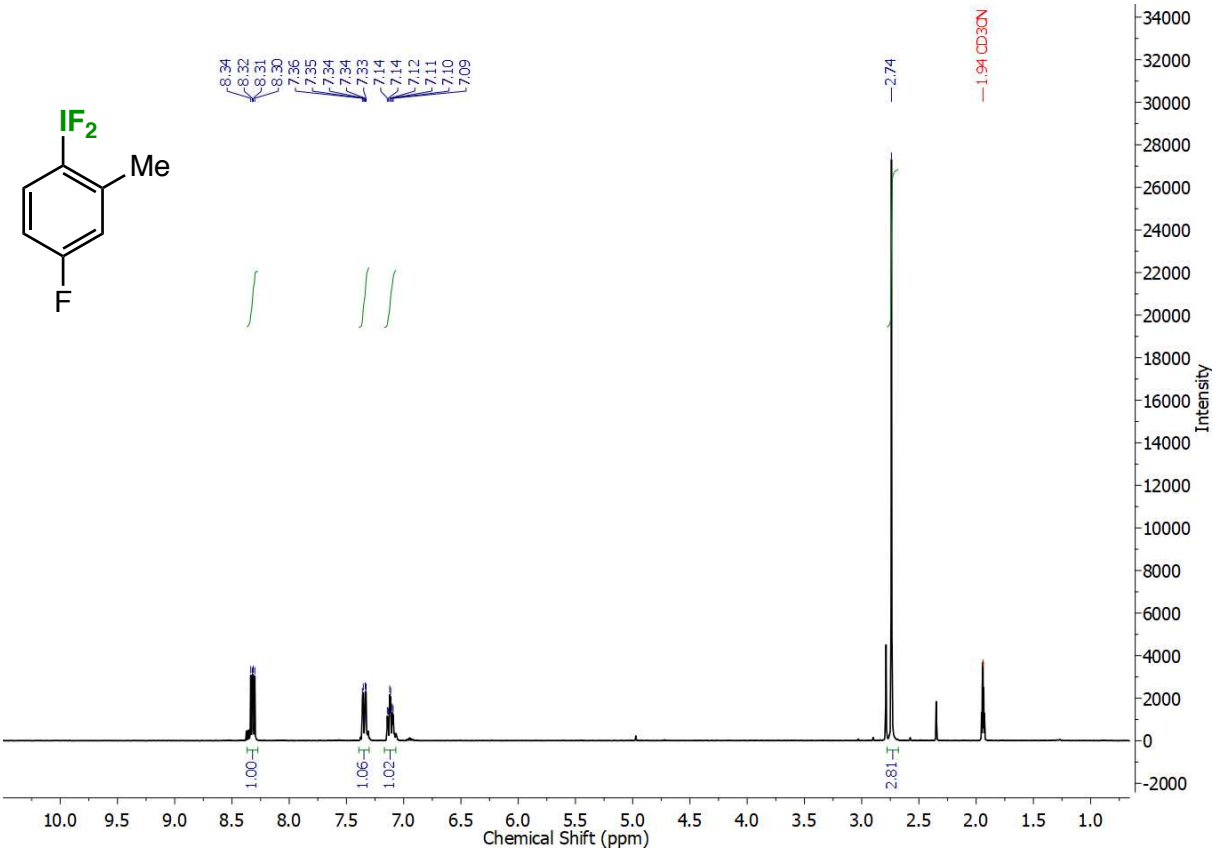

Figure S 51. ^{1}H NMR spectrum of (4-fluoro-2-methylphenyl)difluoro-λ^{3}-iodane (compound **18**).

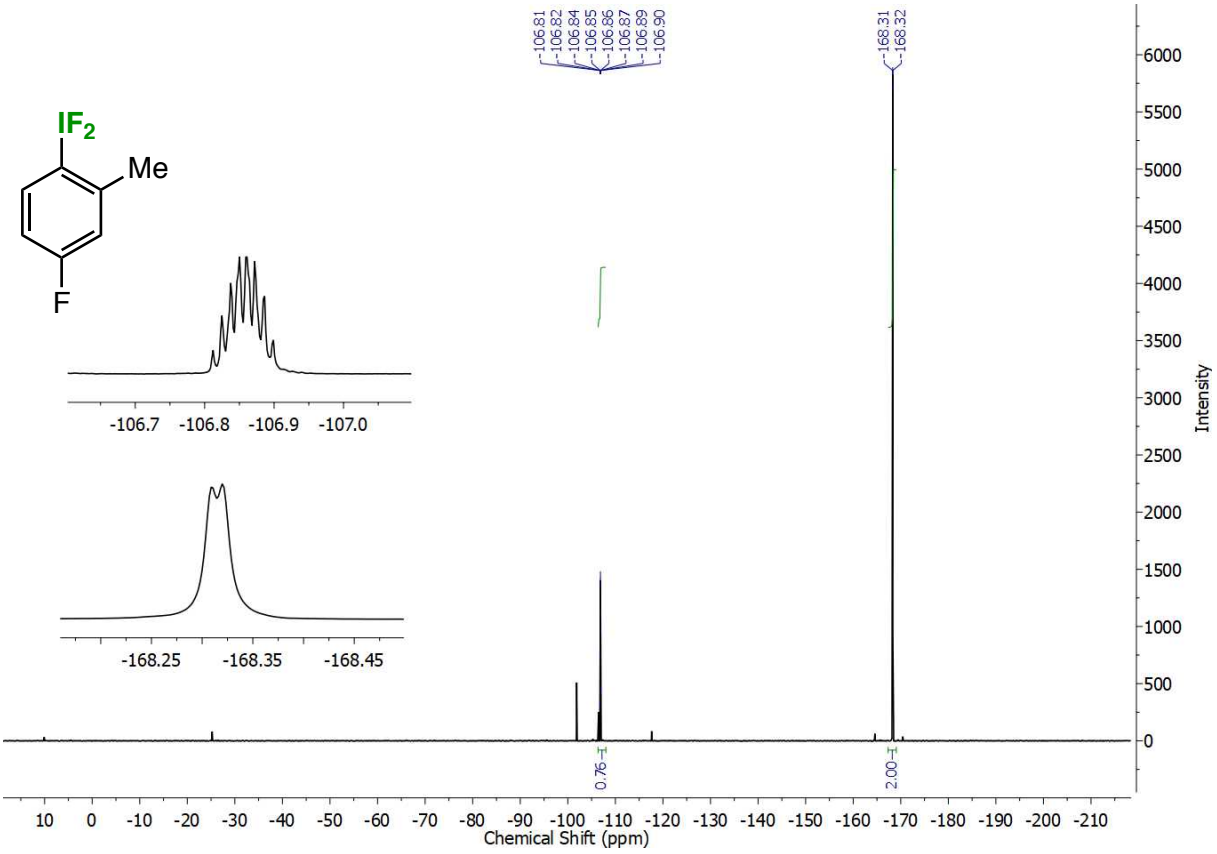

Figure S 52. ^{19}F NMR spectrum of (4-fluoro-2-methylphenyl)difluoro-λ^3-iodane (compound **18**).

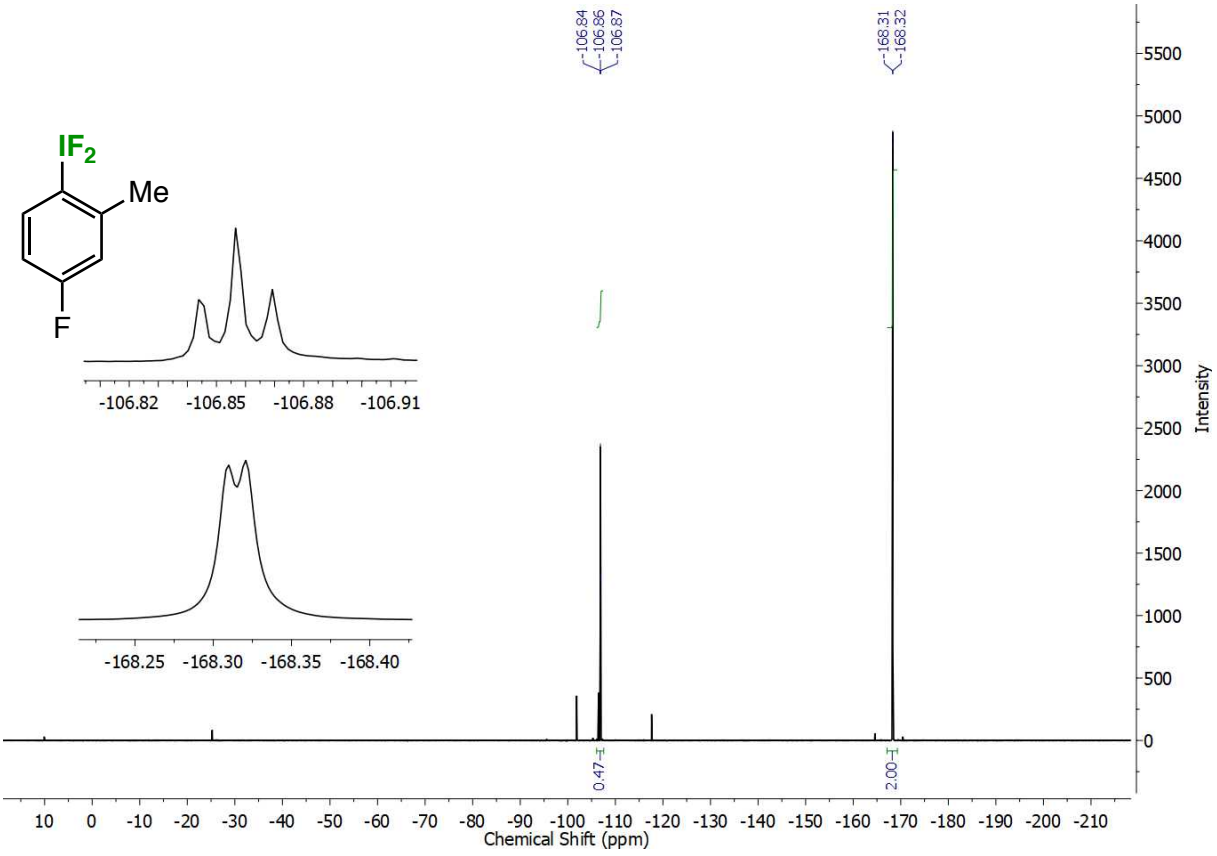

Figure S 53. $^{19}F\{^{1}H\}$ NMR spectrum of (4-fluoro-2-methylphenyl)difluoro-λ^3-iodane (compound **18**).

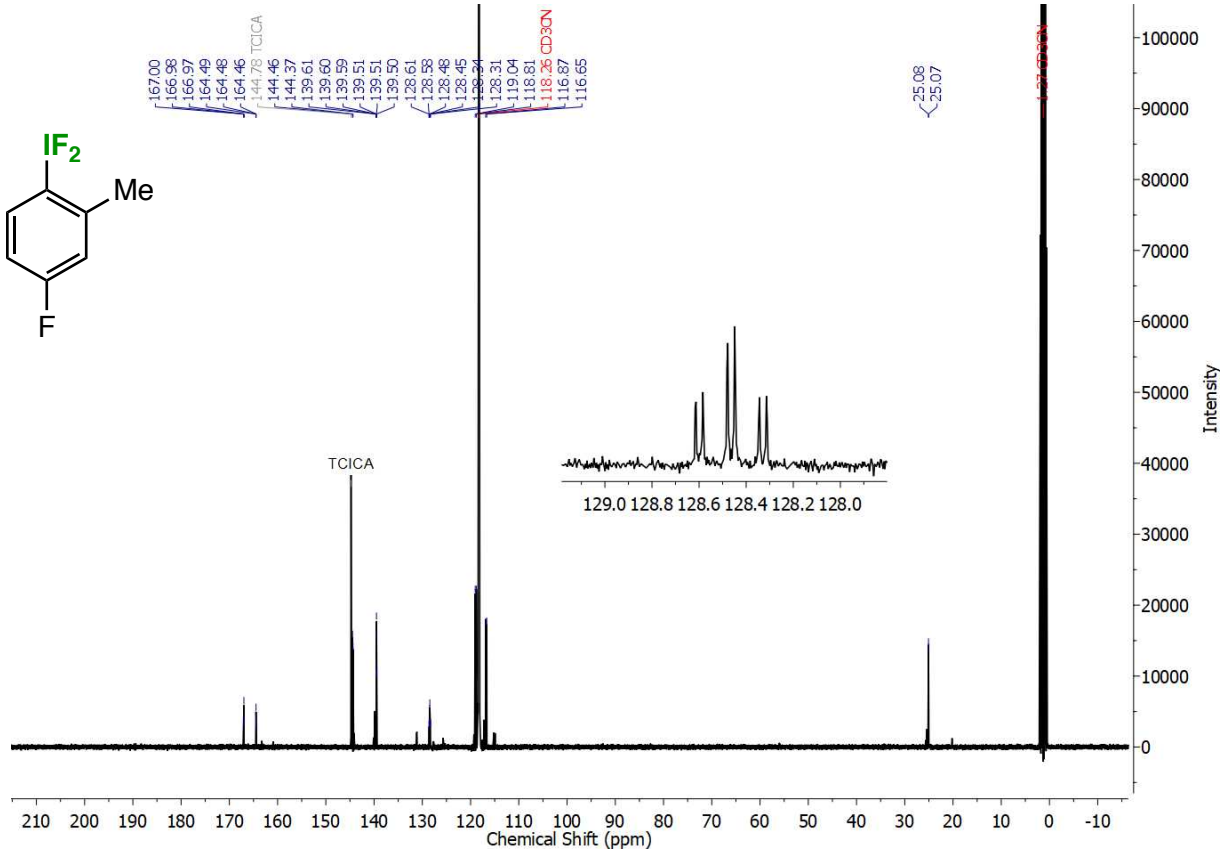

Figure S 54. $^{13}C\{^{1}H\}$ NMR spectrum of (4-fluoro-2-methylphenyl)difluoro-λ^3-iodane (compound **18**).

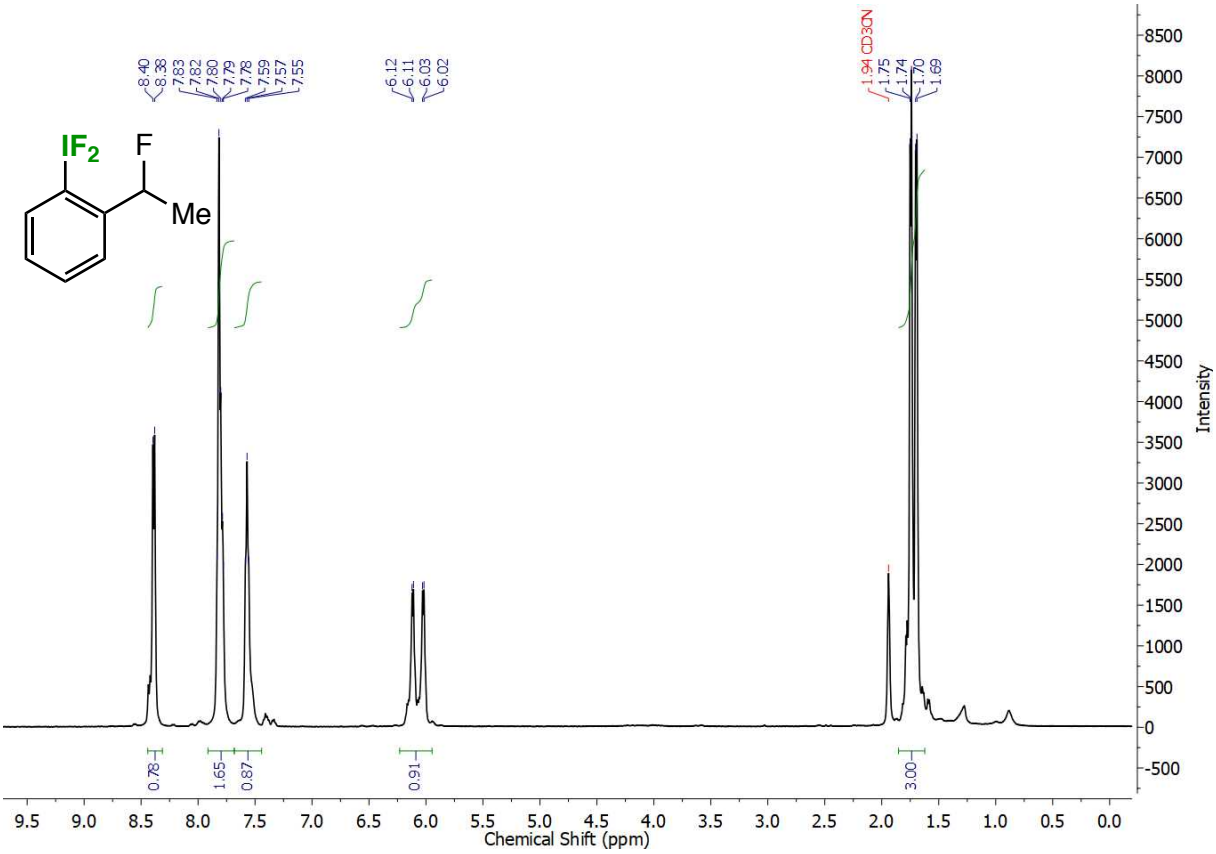

Figure S 55. ^{1}H NMR spectrum of difluoro(2-(1-fluoroethyl)phenyl)-λ^{3}-iodane (compound **19**).

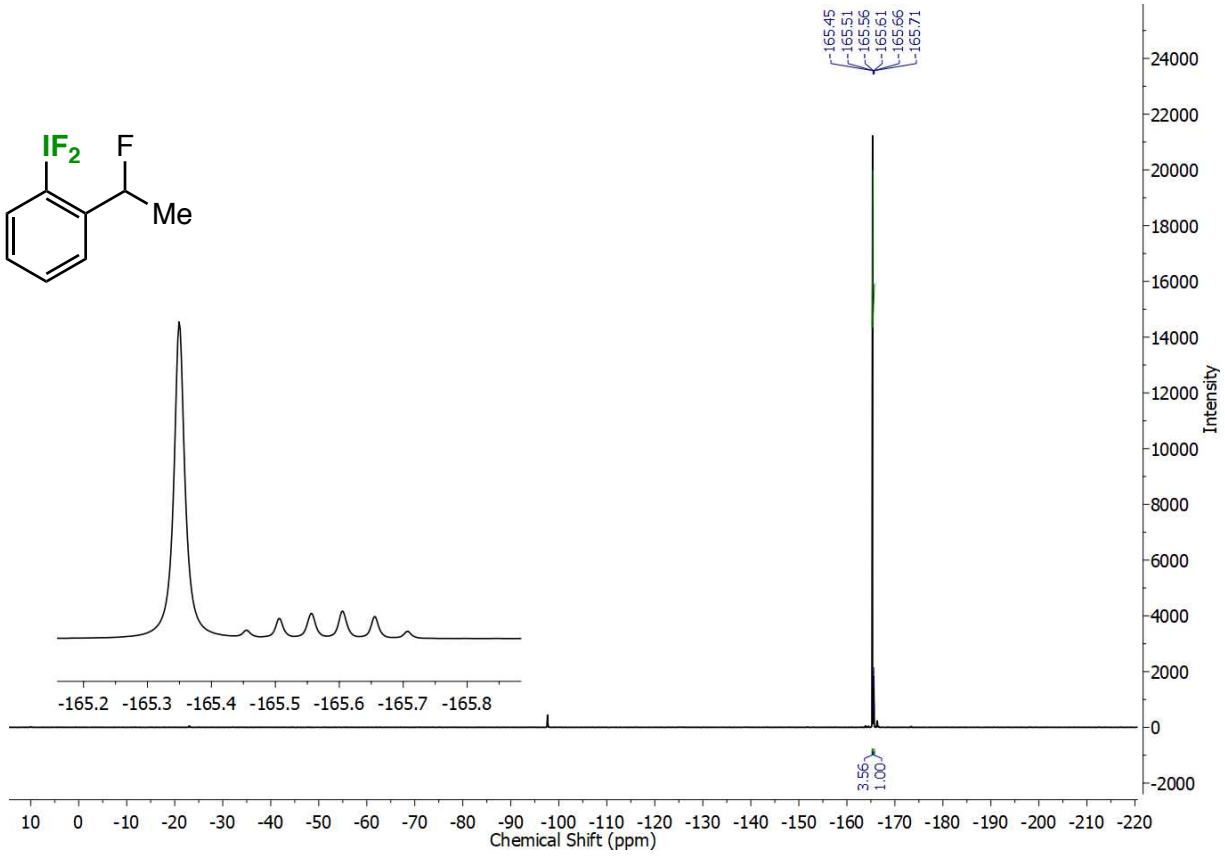

Figure S 56. ^{19}F NMR spectrum of difluoro(2-(1-fluoroethyl)phenyl)-λ^3-iodane (compound **19**).

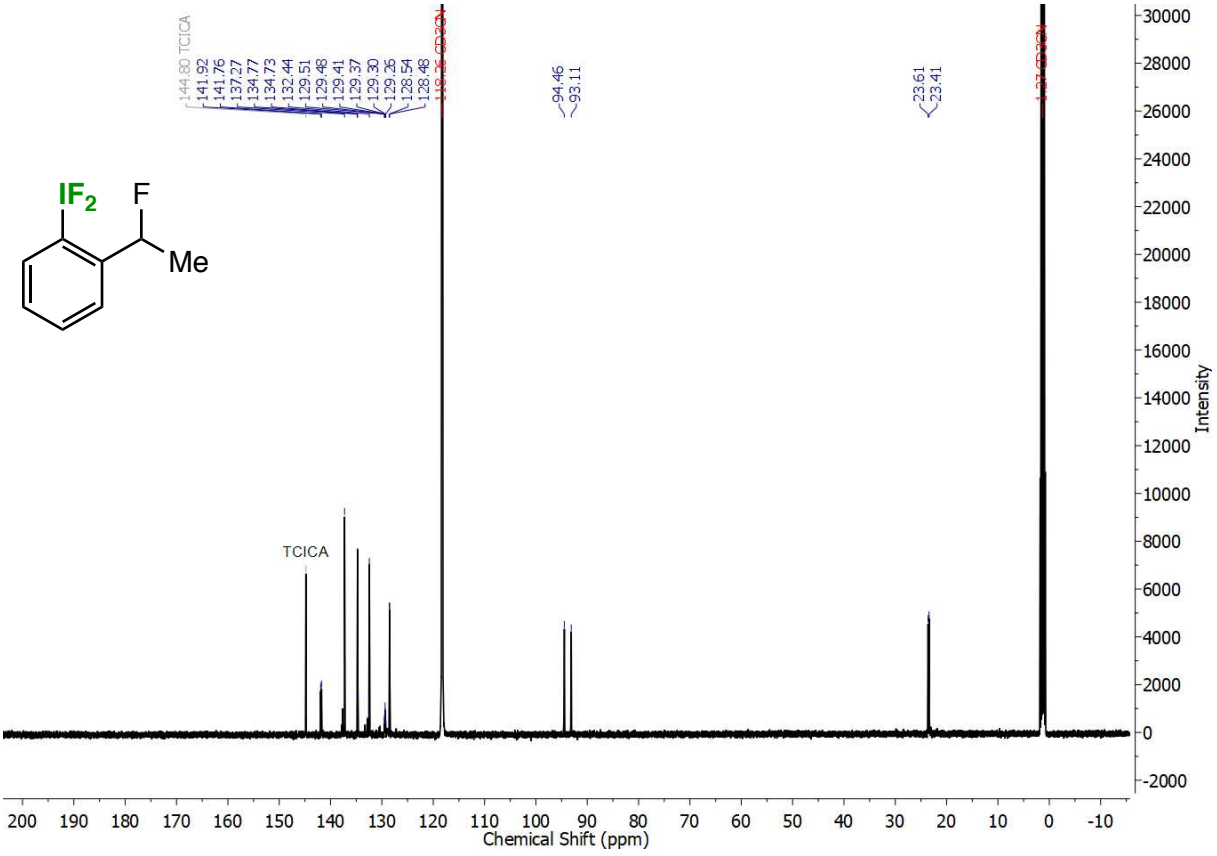

Figure S 57. $^{13}C\{^{1}H\}$ NMR spectrum of difluoro(2-(1-fluoroethyl)phenyl)-λ^3-iodane (compound **19**).

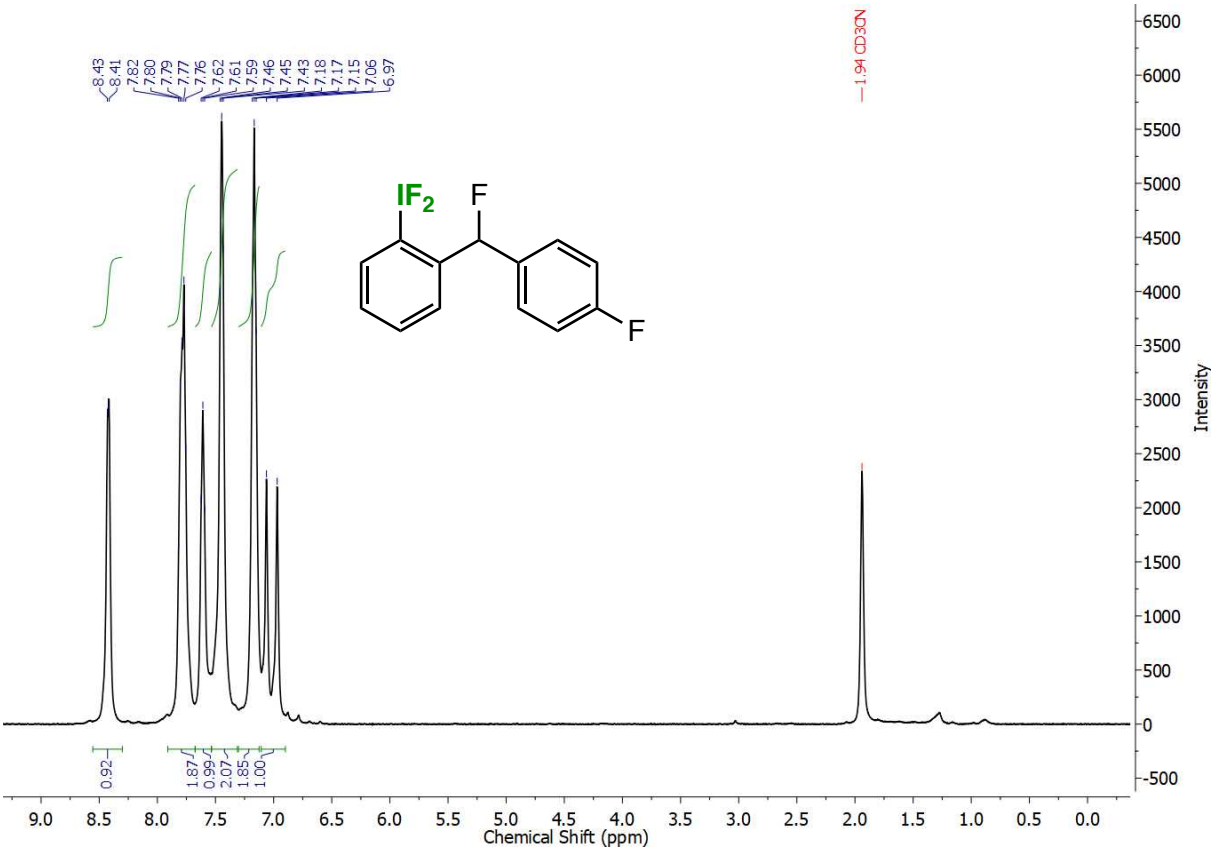

Figure S 58. ^{1}H NMR spectrum of difluoro(2-(fluoro(4-fluorophenyl)methyl)phenyl)-λ^3-iodane (compound **20**).

Figure S 59. ^{19}F NMR spectrum of difluoro(2-(fluoro(4-fluorophenyl)methyl)phenyl)-λ^3-iodane (compound **20**).

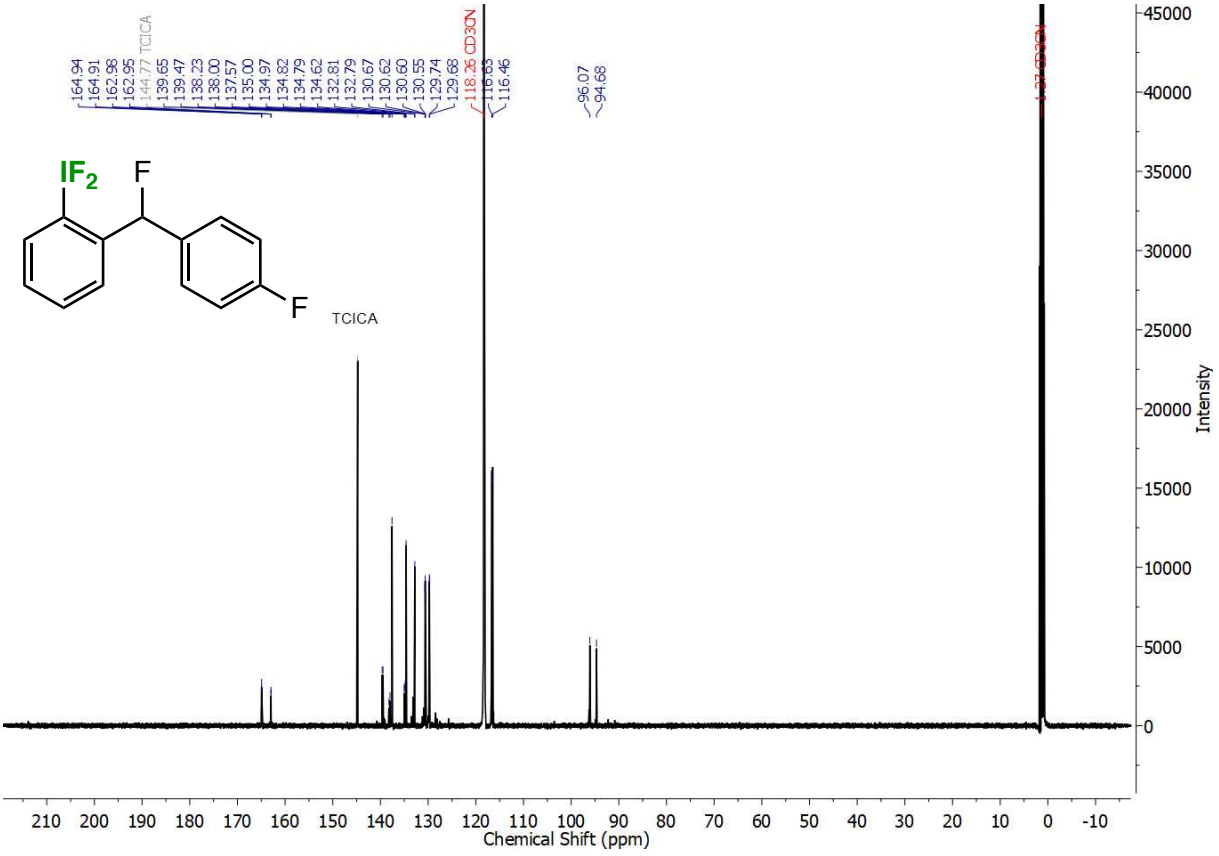

Figure S 60. $^{13}C\{^{1}H\}$ NMR spectrum of difluoro(2-(fluoro(4-fluorophenyl)methyl)phenyl)-λ^3-iodane (compound **20**).

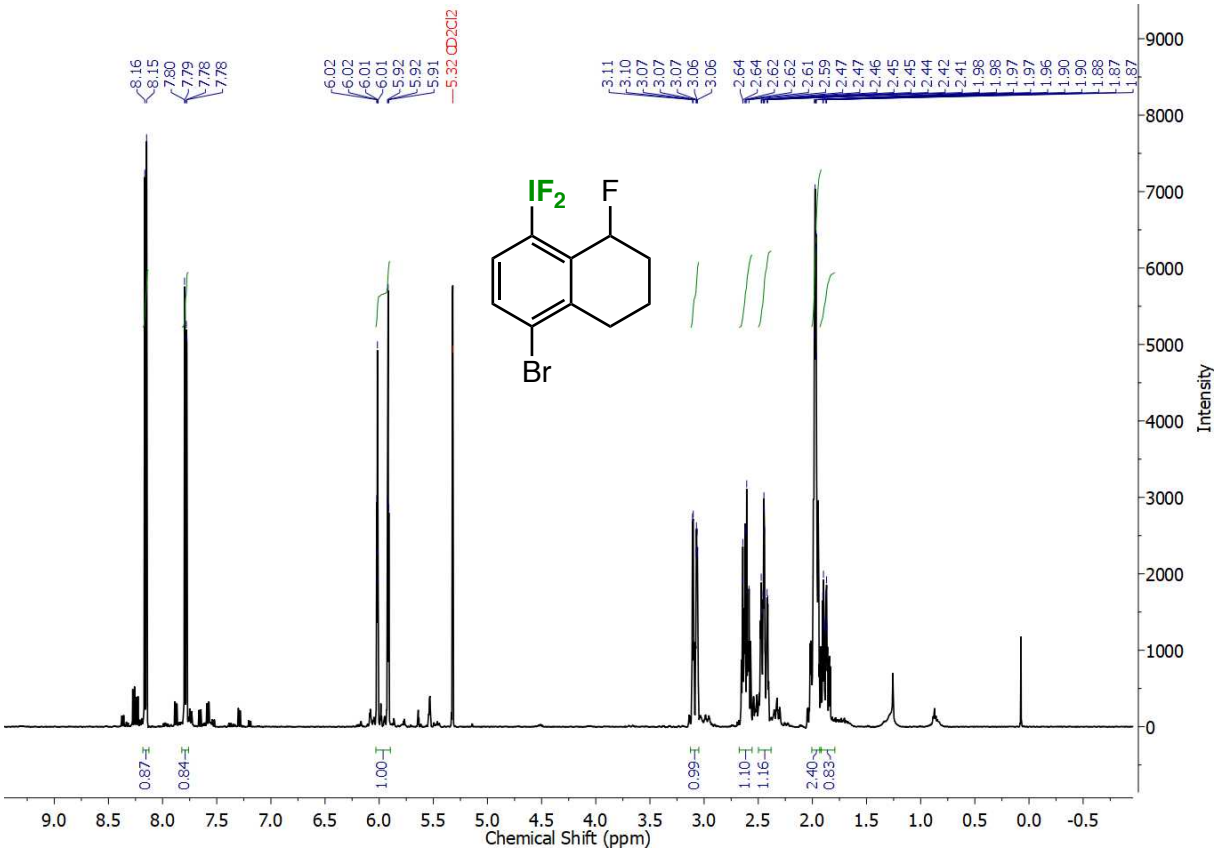

Figure S 61. ^{1}H NMR spectrum of (4-bromo-8-fluoro-5,6,7,8-tetrahydronaphthalen-1-yl)difluoro-λ^{3}-iodane (compound **21**).

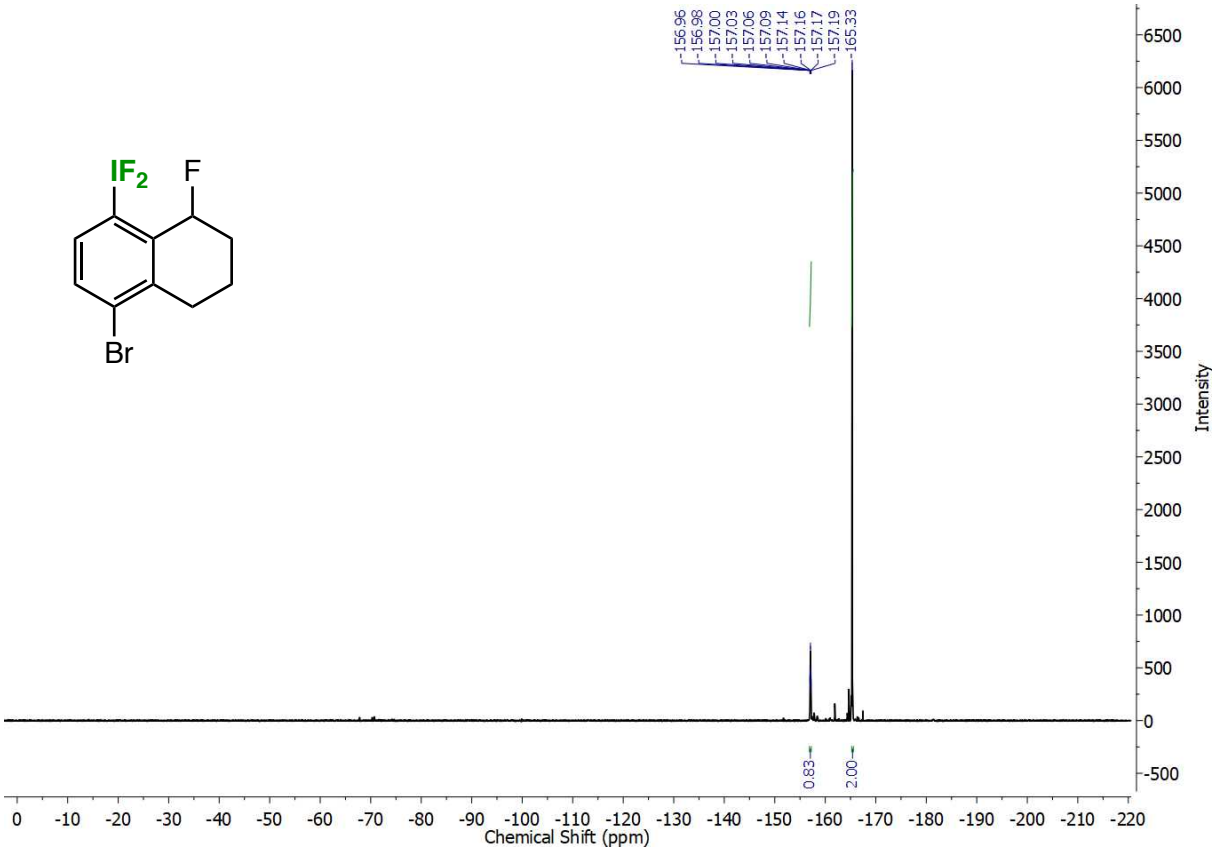

Figure S 62. ^{19}F NMR spectrum of (4-bromo-8-fluoro-5,6,7,8-tetrahydronaphthalen-1-yl)difluoro-λ^{3}-iodane (compound **21**).

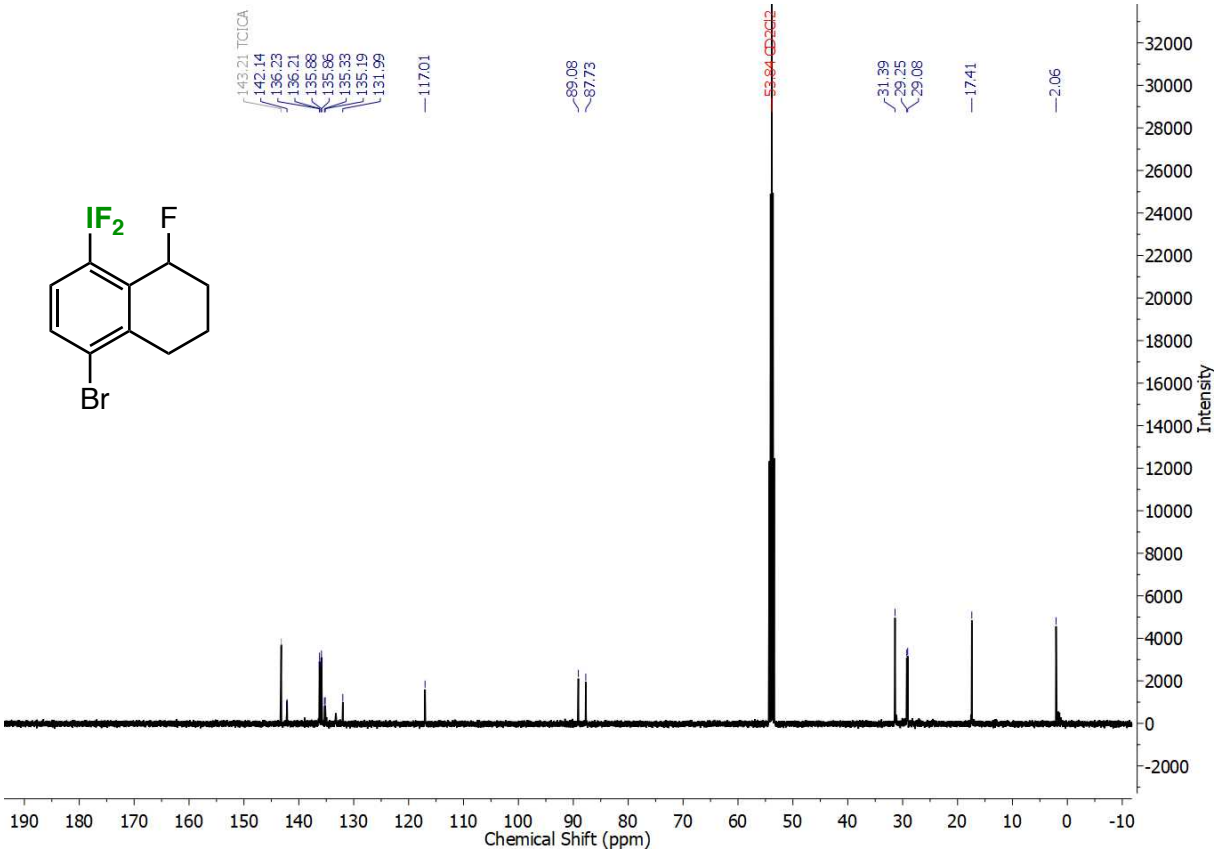

Figure S 63. $^{13}C\{^{1}H\}$ NMR spectrum of (4-bromo-8-fluoro-5,6,7,8-tetrahydronaphthalen-1-yl)difluoro-λ^{3}-iodane (compound **21**).

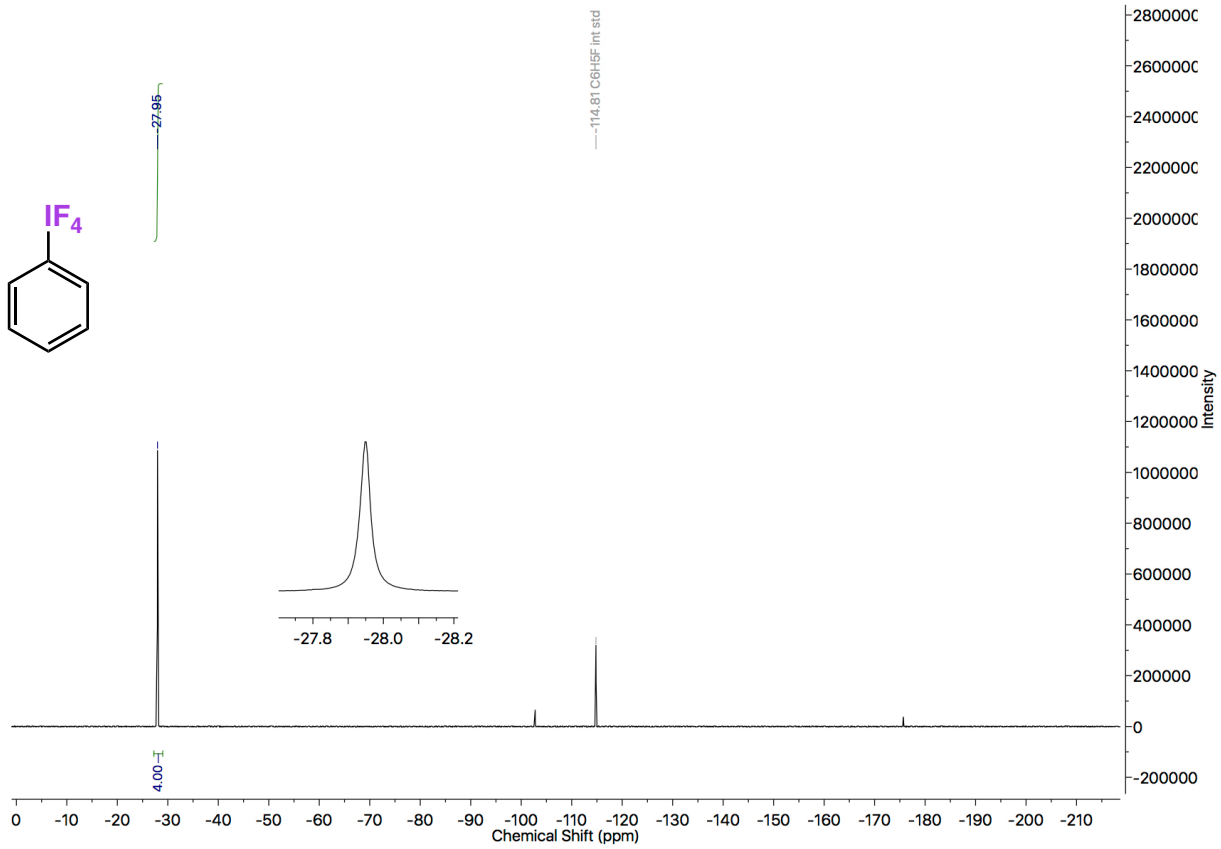

Figure S 64. ^{19}F NMR spectrum of tetrafluoro(phenyl)-λ^5-iodane (compound **25**).

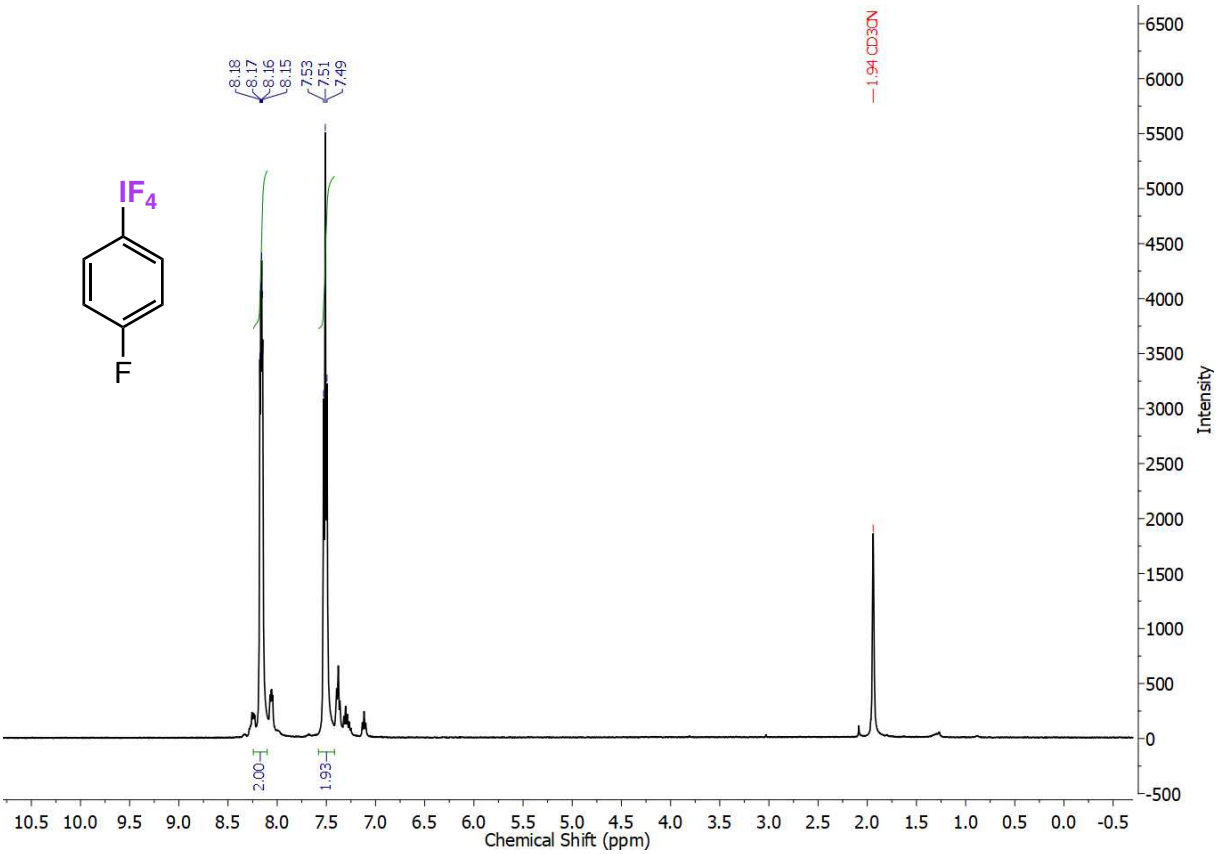

Figure S 65. ^{1}H NMR spectrum of tetrafluoro(4-fluorophenyl)-λ^{5}-iodane (compound **26**).

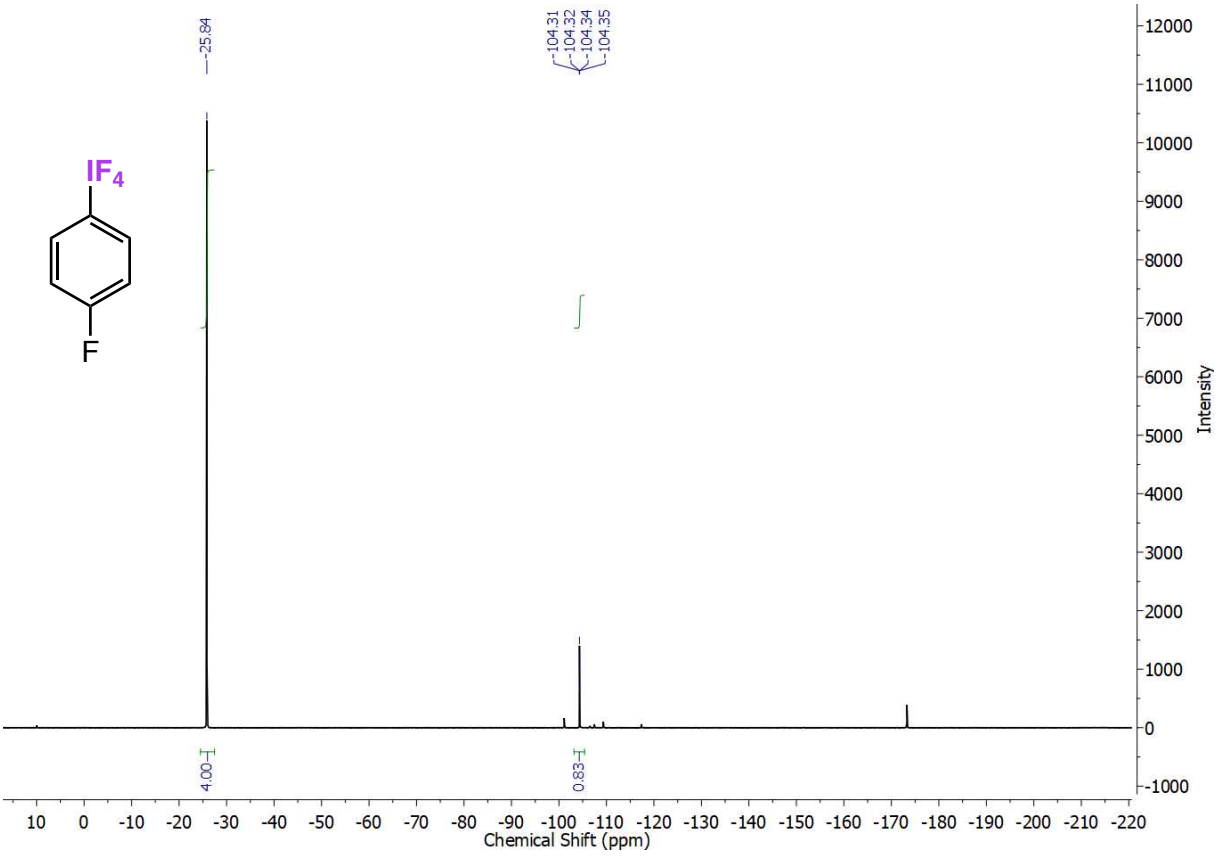

Figure S 66. ^{19}F NMR spectrum of tetrafluoro(4-fluorophenyl)-λ^5-iodane (compound **26**).

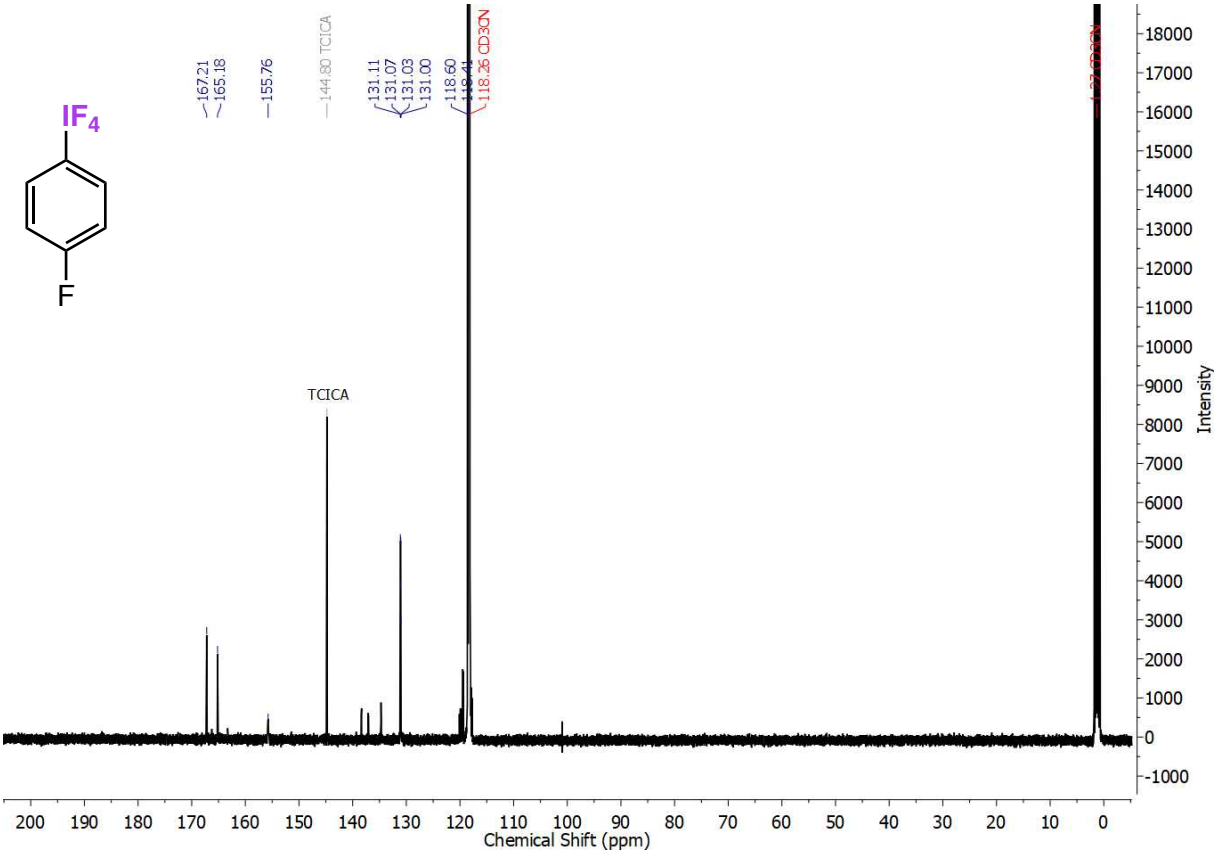

Figure S 67. $^{13}C\{^{1}H\}$ NMR spectrum of tetrafluoro(4-fluorophenyl)-λ^5-iodane (compound **26**).

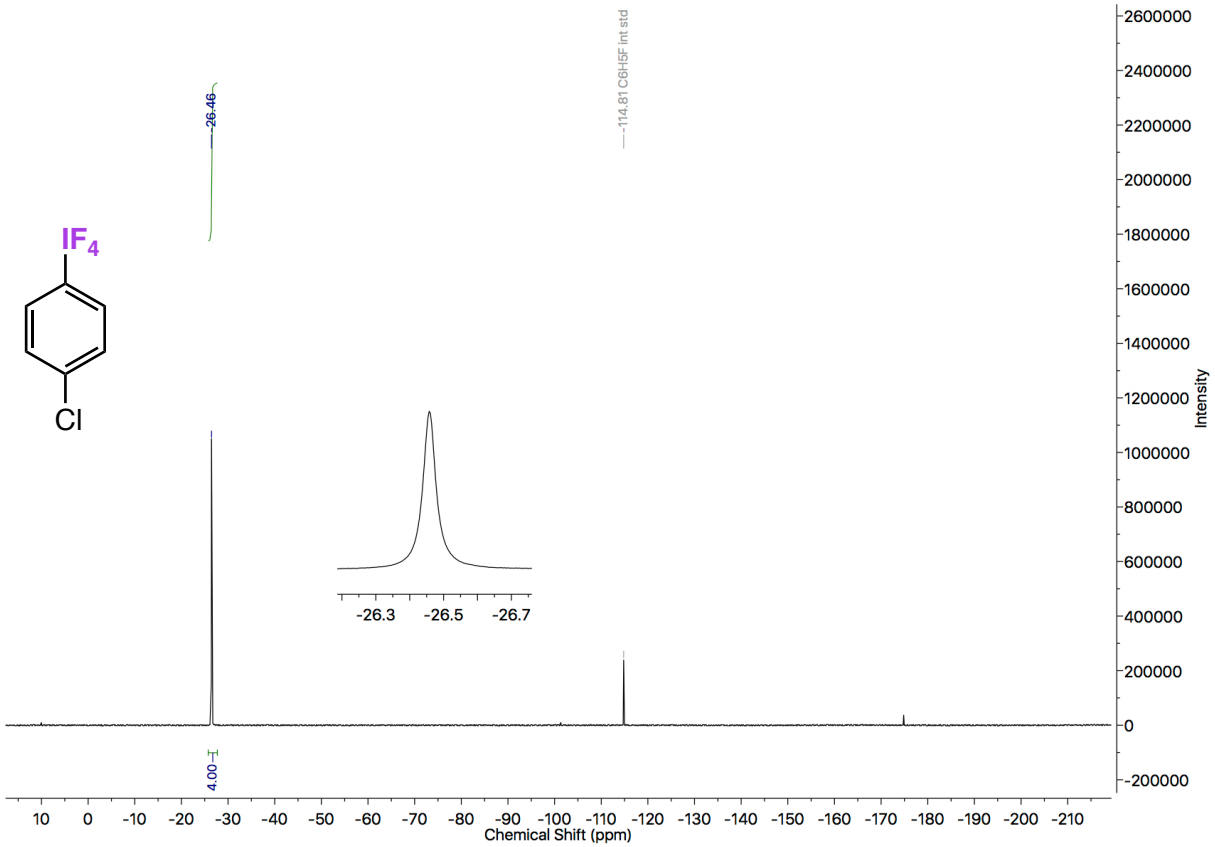

Figure S 68. ^{19}F NMR spectrum of tetrafluoro(4-chlorophenyl)-λ^5-iodane (compound **27**).

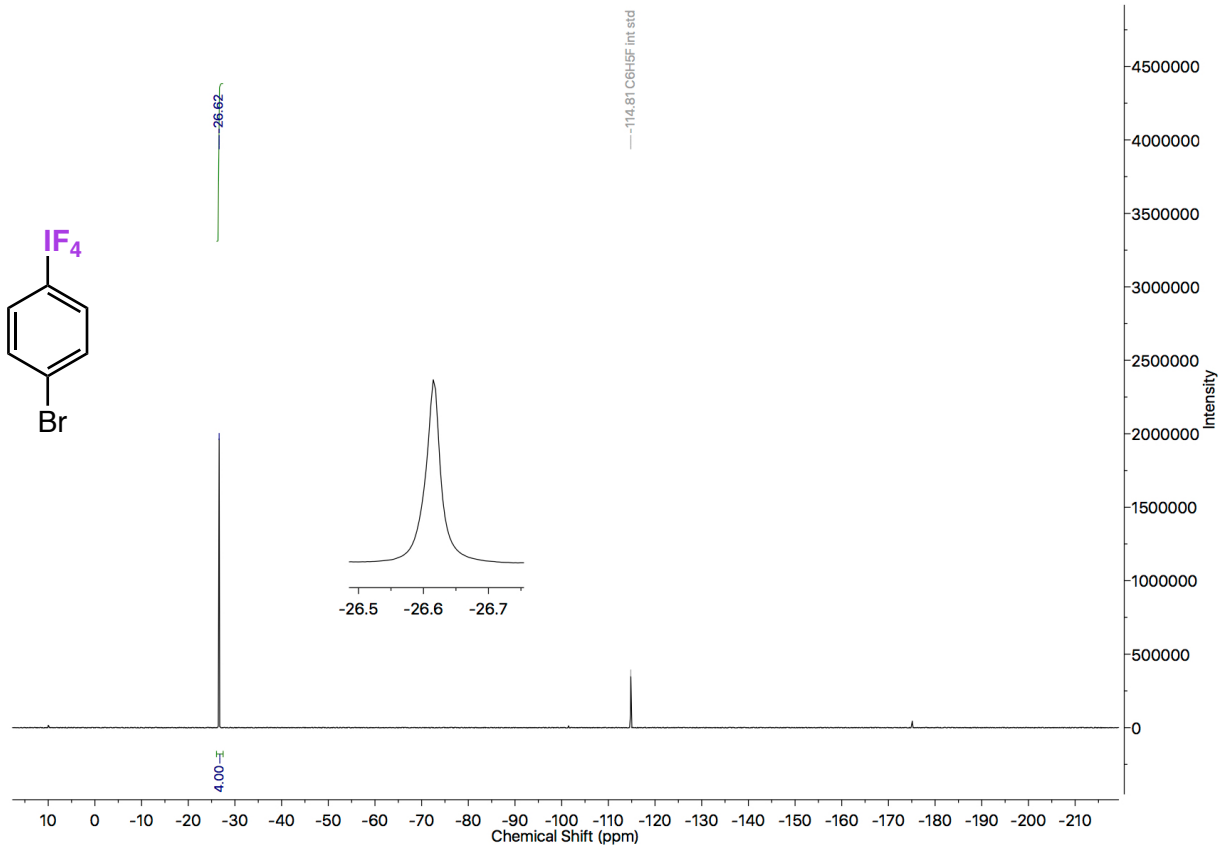

Figure S 69. ^{19}F NMR spectrum of tetrafluoro(4-bromophenyl)-λ^5-iodane (compound **28**).

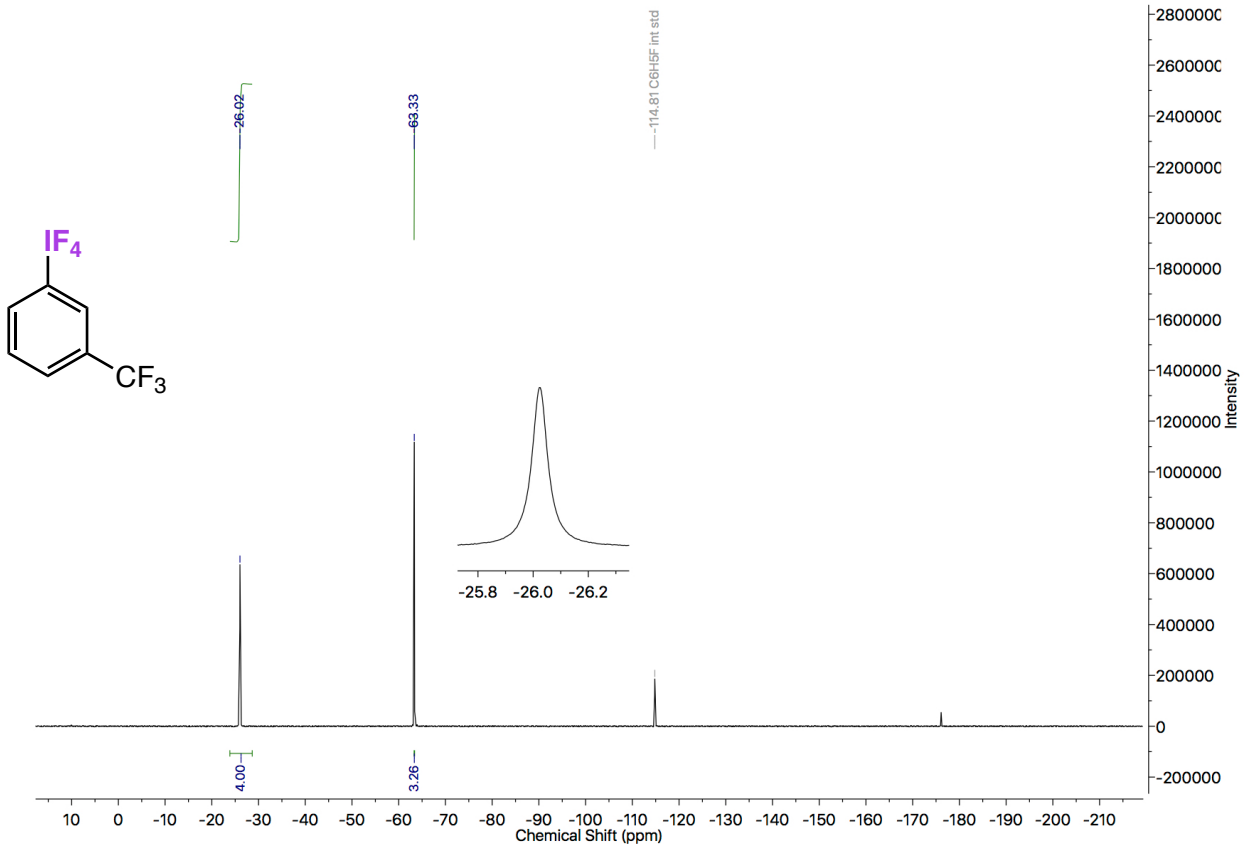

Figure S 70. ^{19}F NMR spectrum of tetrafluoro(3-(trifluoromethyl)phenyl)-λ^5-iodane (compound **29**).

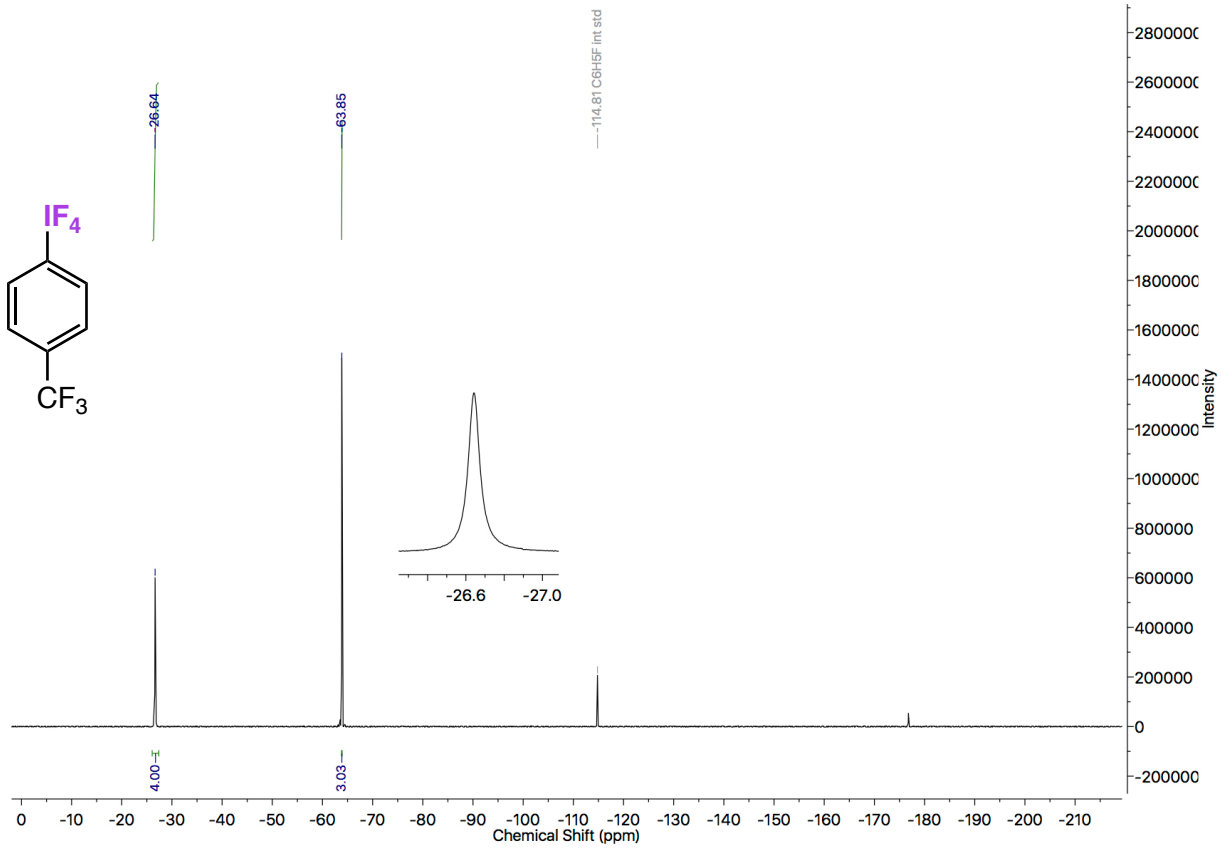

Figure S 71. ^{19}F NMR spectrum of tetrafluoro(4-(trifluoromethyl)phenyl)-λ^5-iodane (compound **30**).

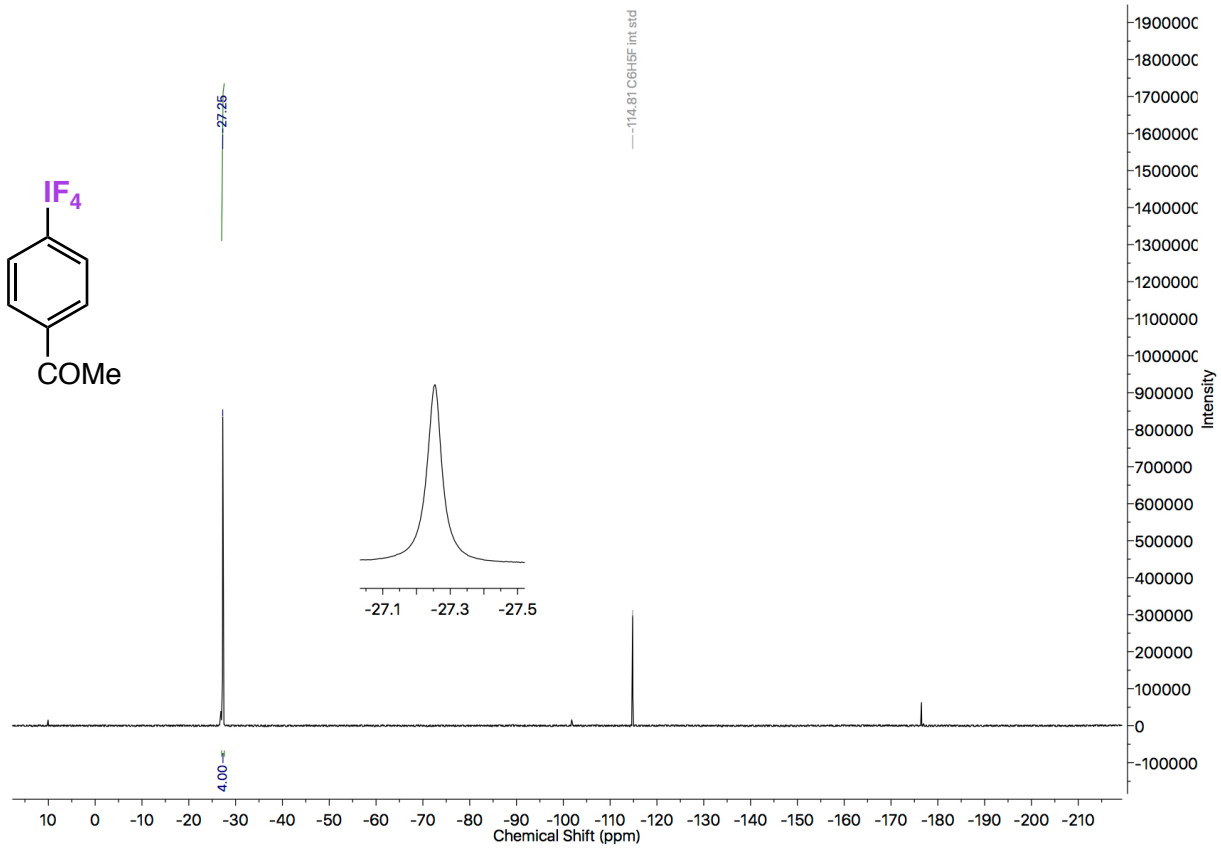

Figure S 72. ^{19}F NMR spectrum of 1-(4-(tetrafluoro-λ^5-iodaneyl)phenyl)ethan-1-one (compound **31**).

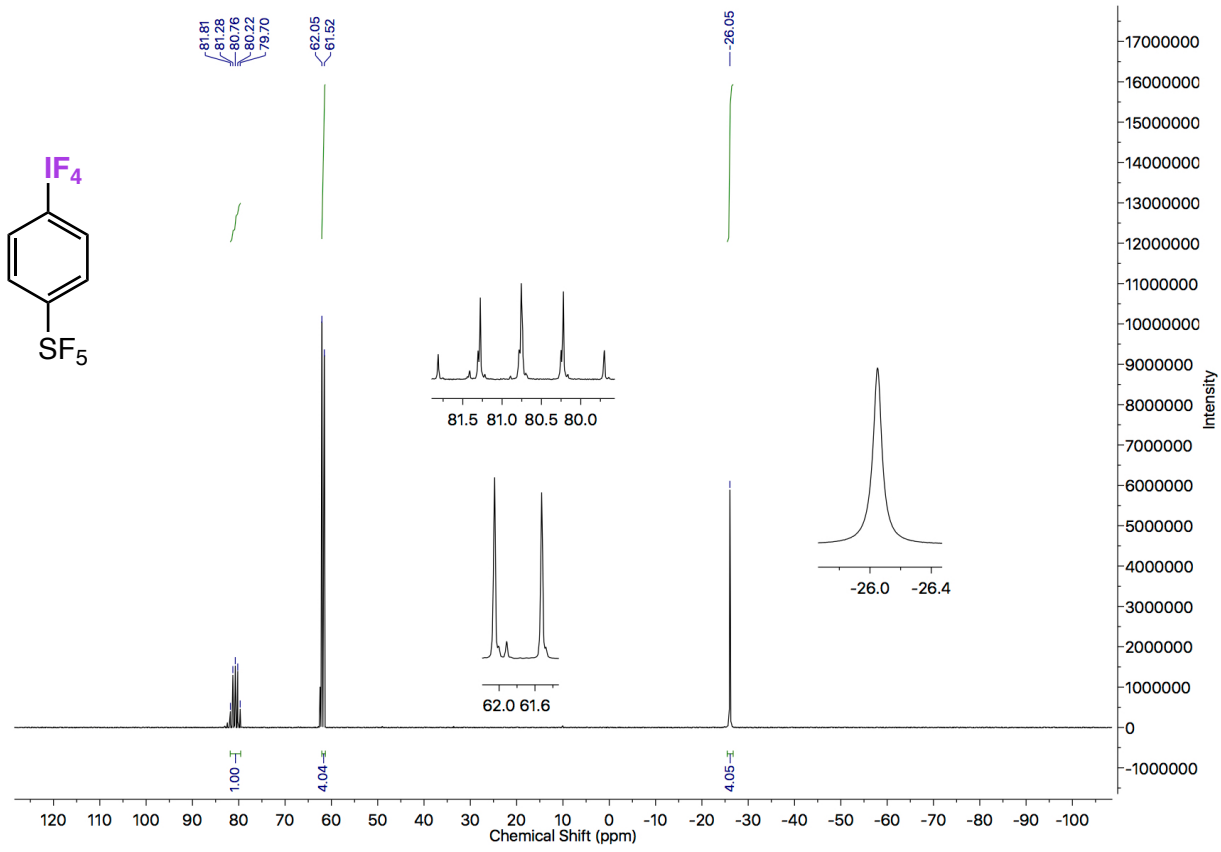

Figure S 73. ^{19}F NMR spectrum of pentafluoro(4-(tetrafluoro-λ^5-iodaneyl)phenyl)-λ^6-sulfane (compound **32**).

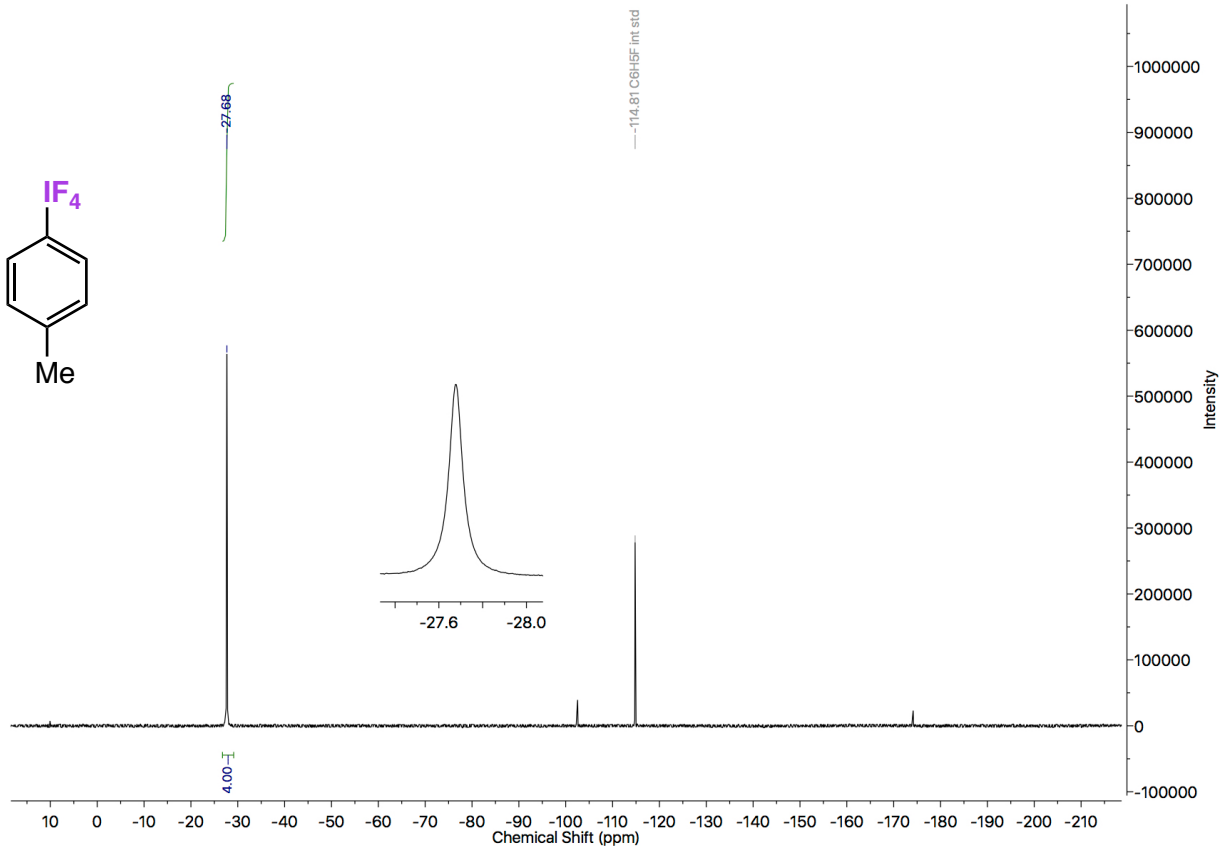

Figure S 74. ^{19}F NMR spectrum of tetrafluoro(4-tolyl)-λ^5-iodane (compound **33**).

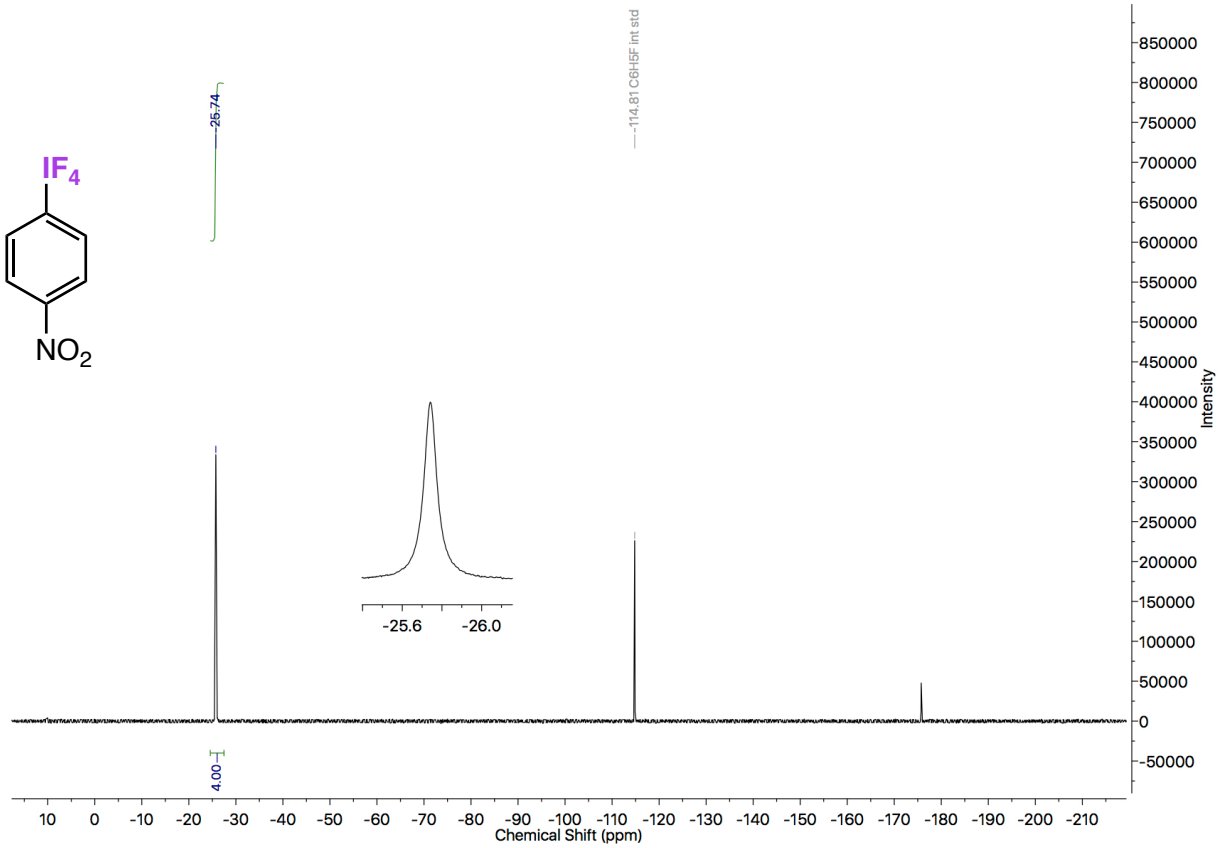

Figure S 75. ^{19}F NMR spectrum of tetrafluoro(4-nitrophenyl)-λ^5-iodane (compound **34**).

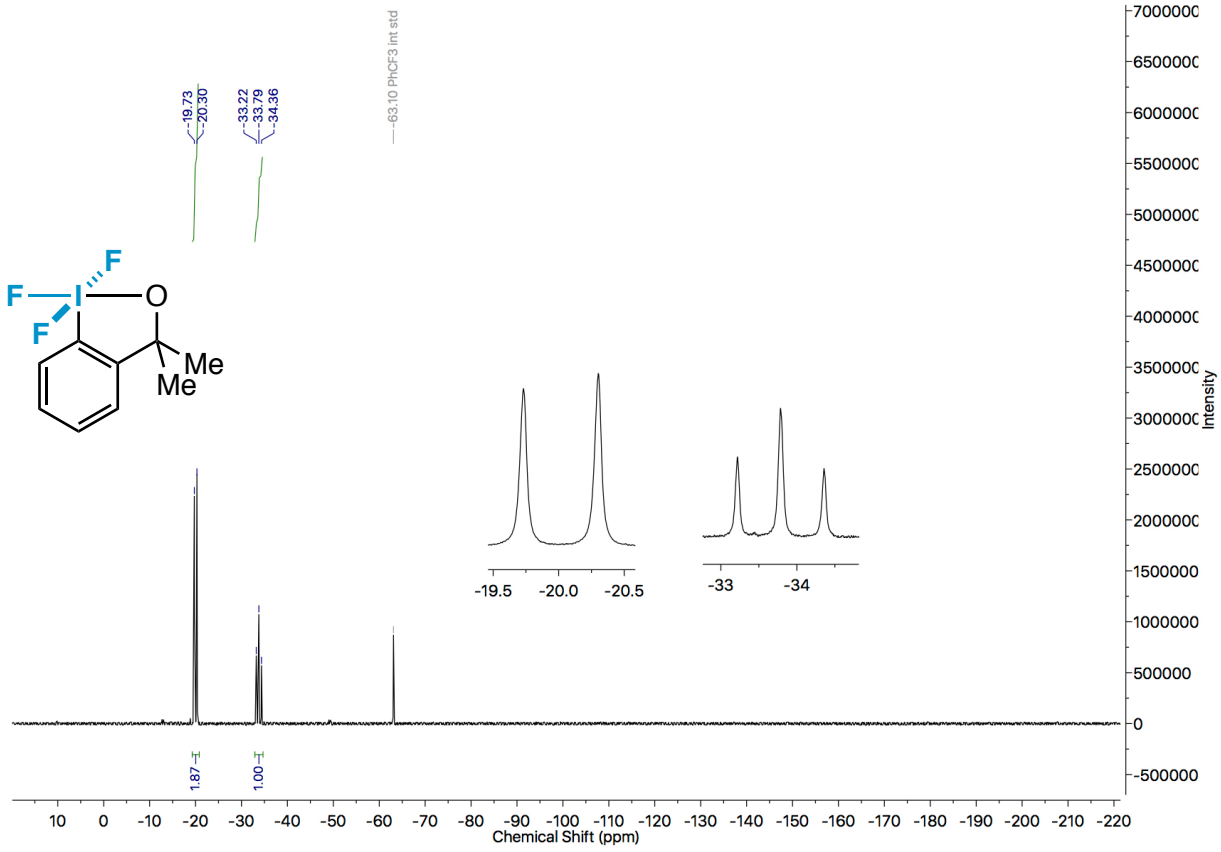

Figure S 76. ^{19}F NMR spectrum of 1,1,1-trifluoro-3,3-dimethyl-1,3-dihydro-1λ^5-benzo[*d*][1,2]iodaoxole (compound **37**).

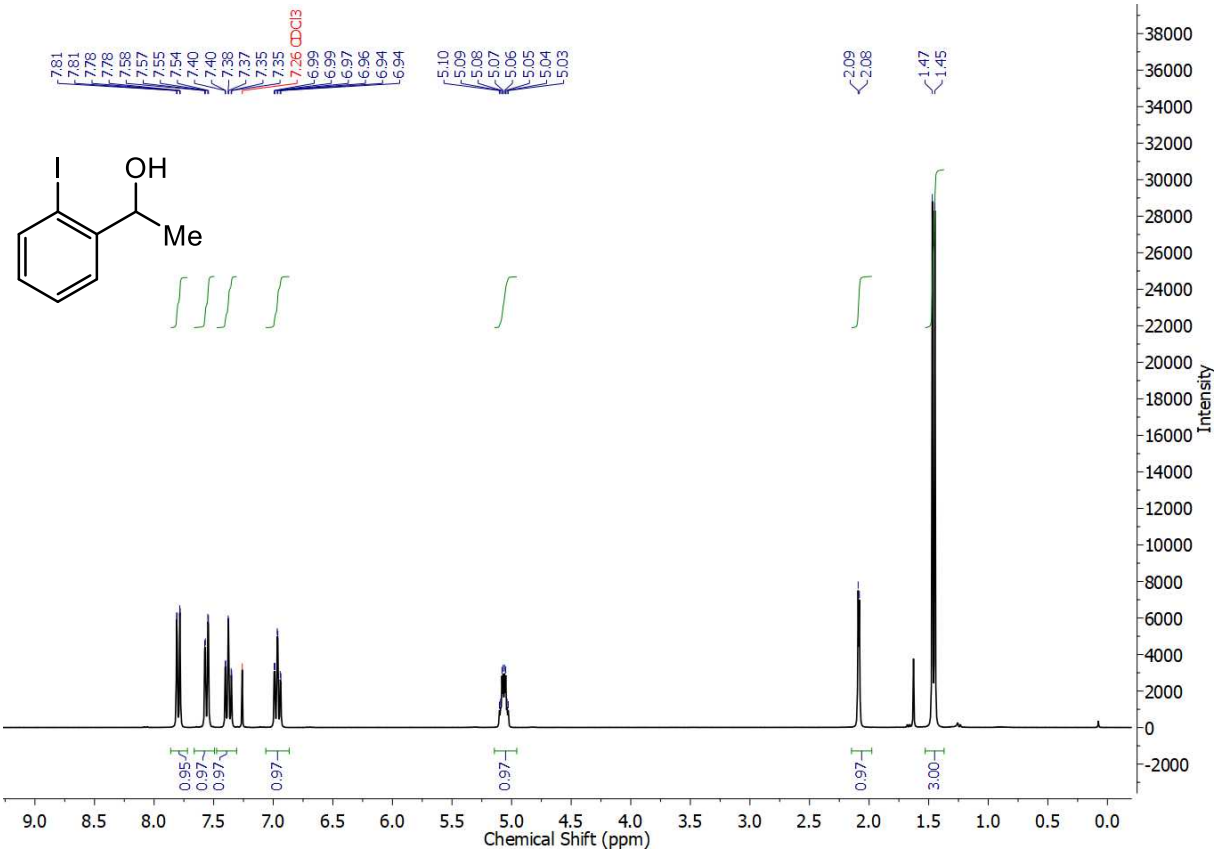

Figure S 77. ^{1}H NMR spectrum of 1-(2-iodophenyl)ethan-1-ol.

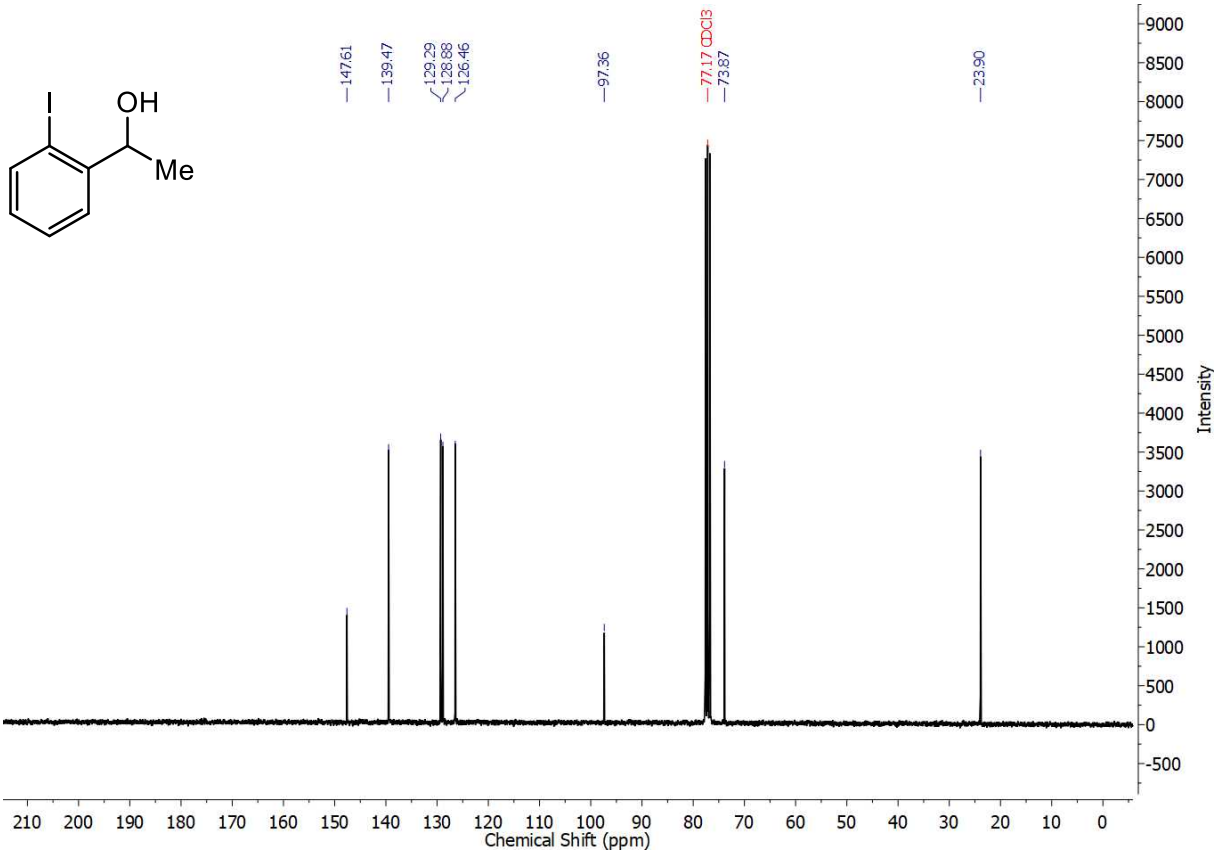

Figure S 78. $^{13}C\{^{1}H\}$ NMR spectrum of 1-(2-iodophenyl)ethan-1-ol.

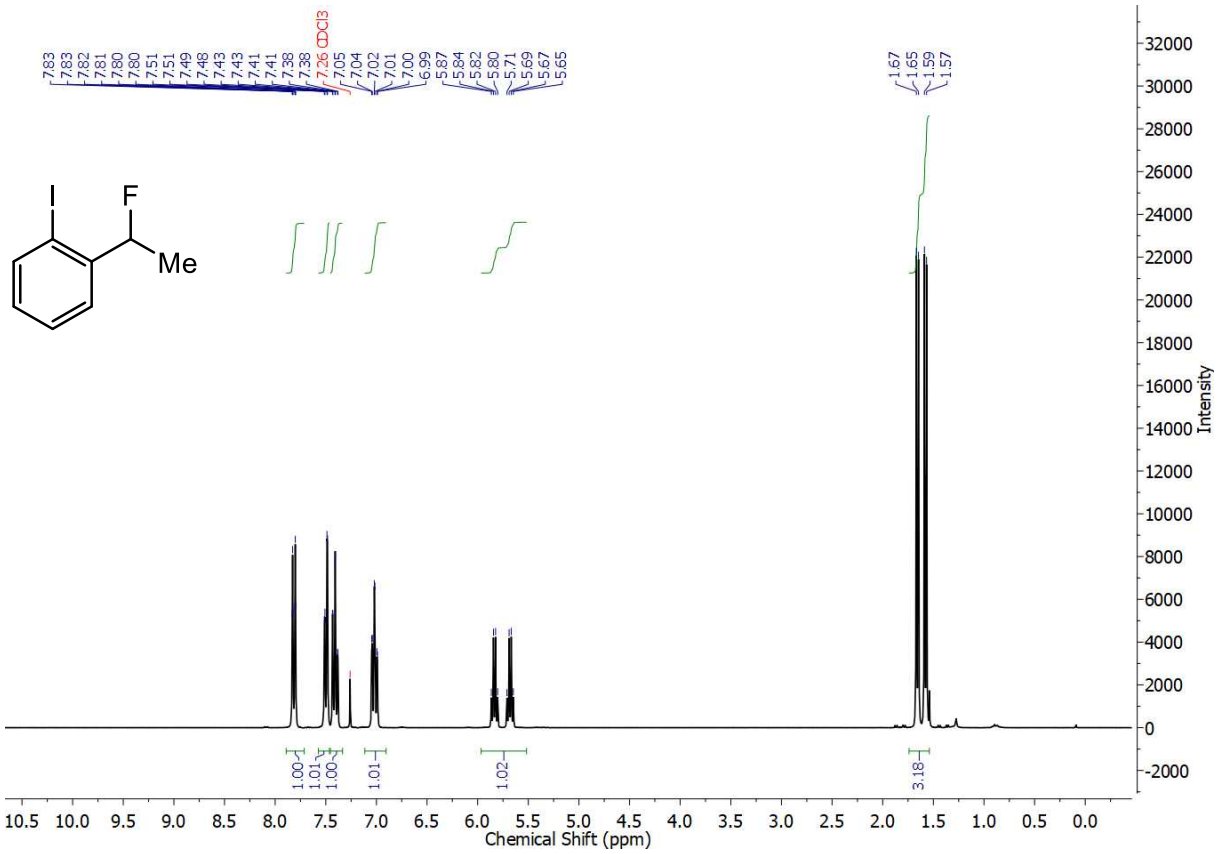

Figure S 79. ^{1}H NMR spectrum of 1-(1-fluoroethyl)-2-iodobenzene.

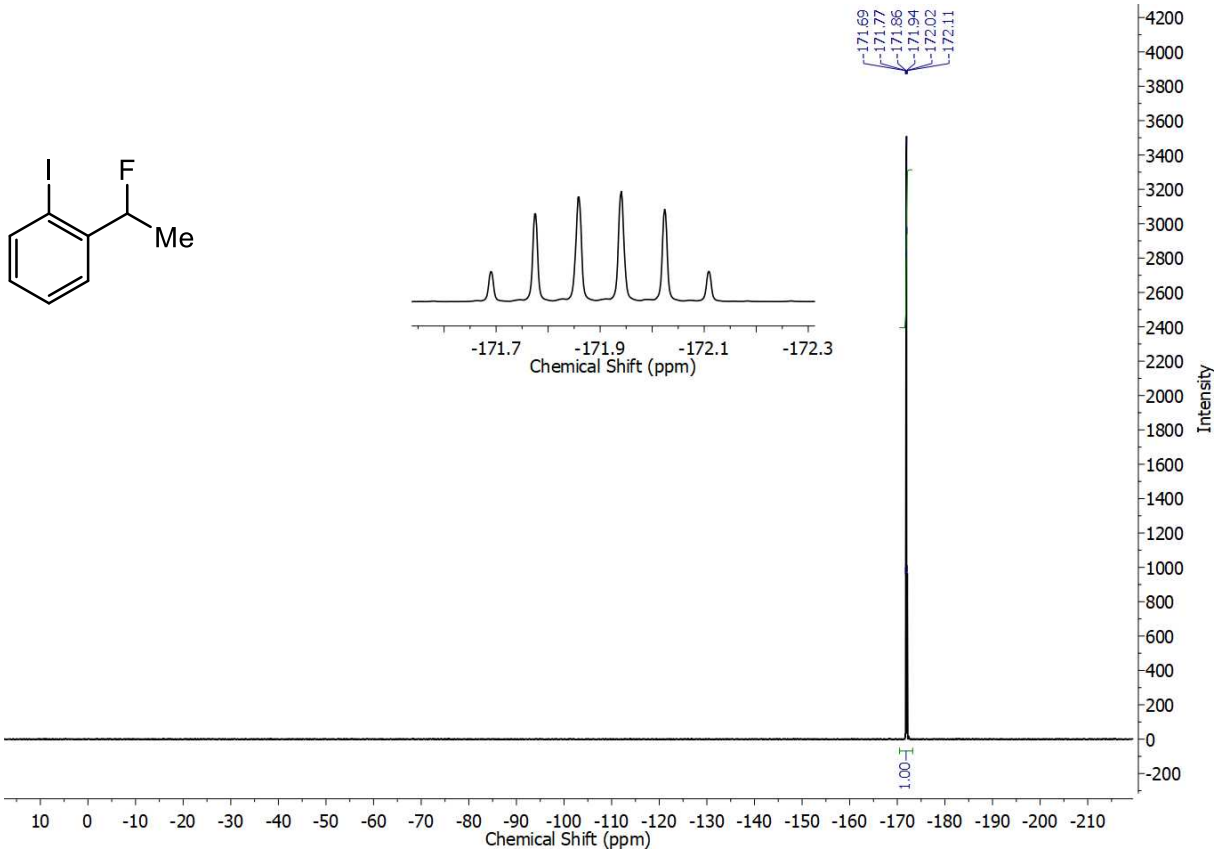

Figure S 80. ^{19}F NMR spectrum of 1-(1-fluoroethyl)-2-iodobenzene.

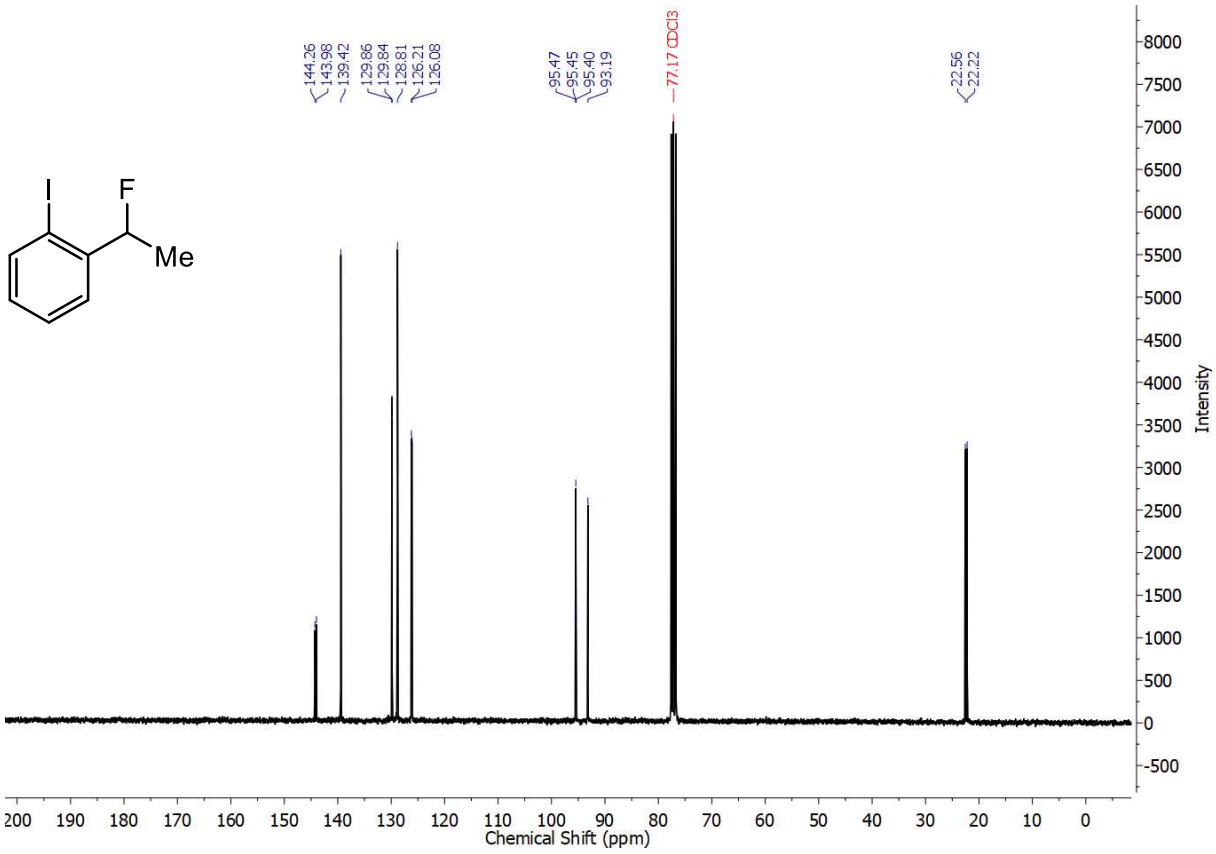

Figure S 81. $^{13}C\{^{1}H\}$ NMR spectrum of 1-(1-fluoroethyl)-2-iodobenzene.

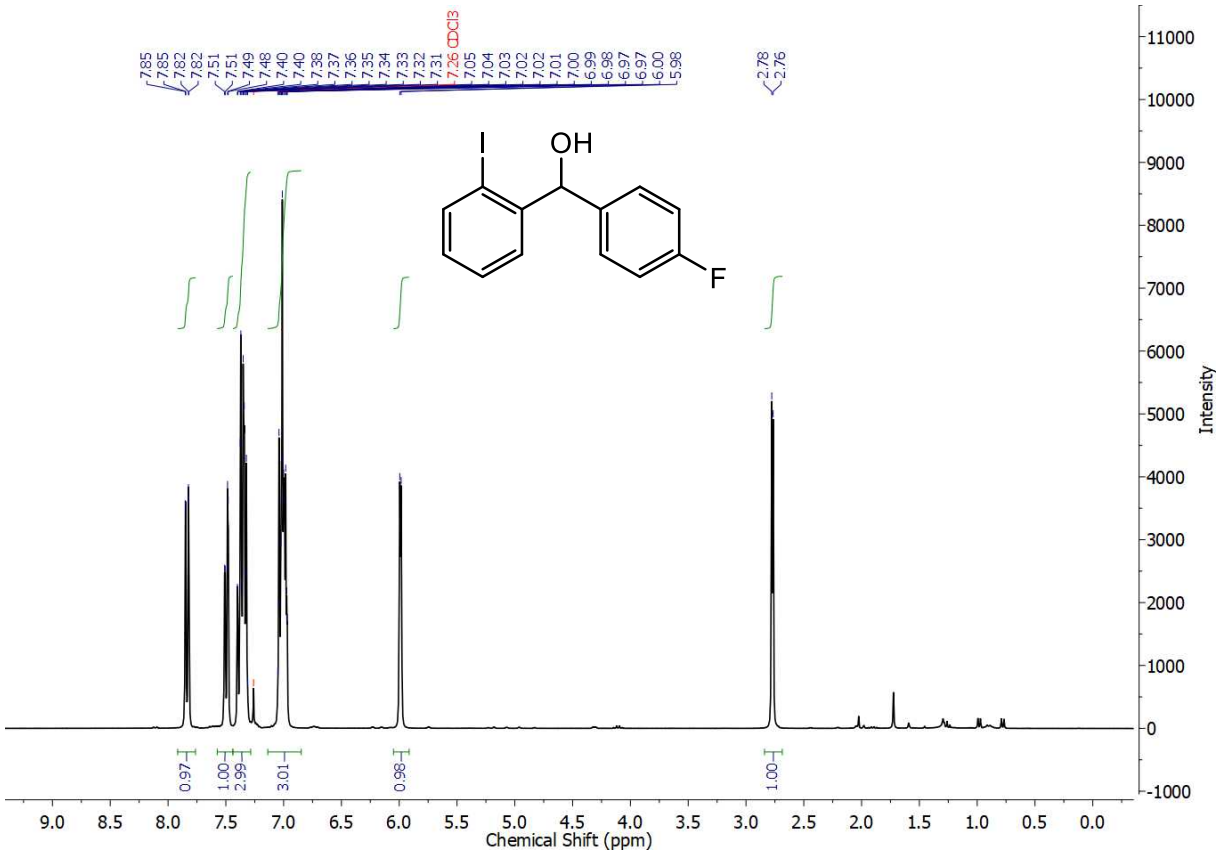

Figure S 82. ^{1}H NMR spectrum of (4-fluorophenyl)(2-iodophenyl)methanol.

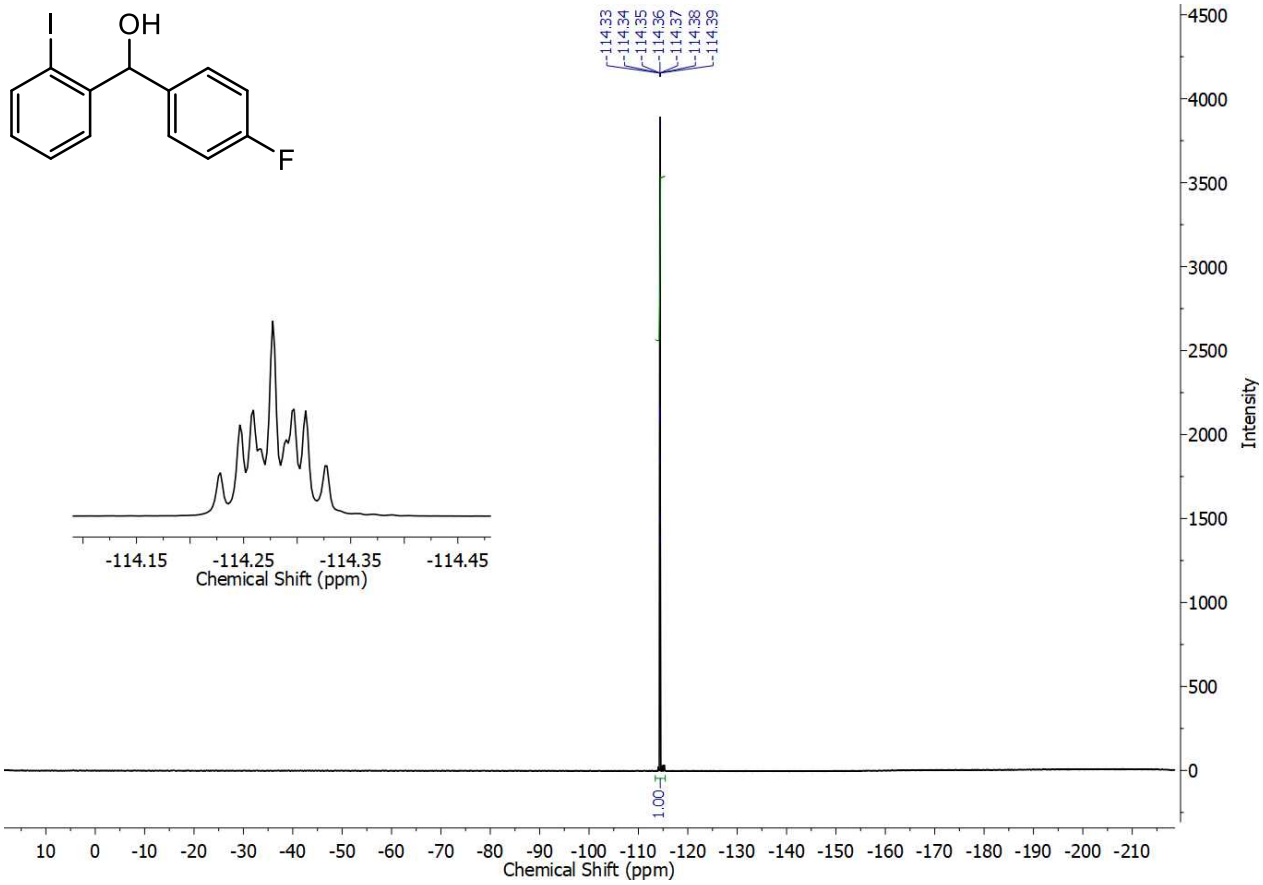

Figure S 83. ^{19}F NMR spectrum of (4-fluorophenyl)(2-iodophenyl)methanol.

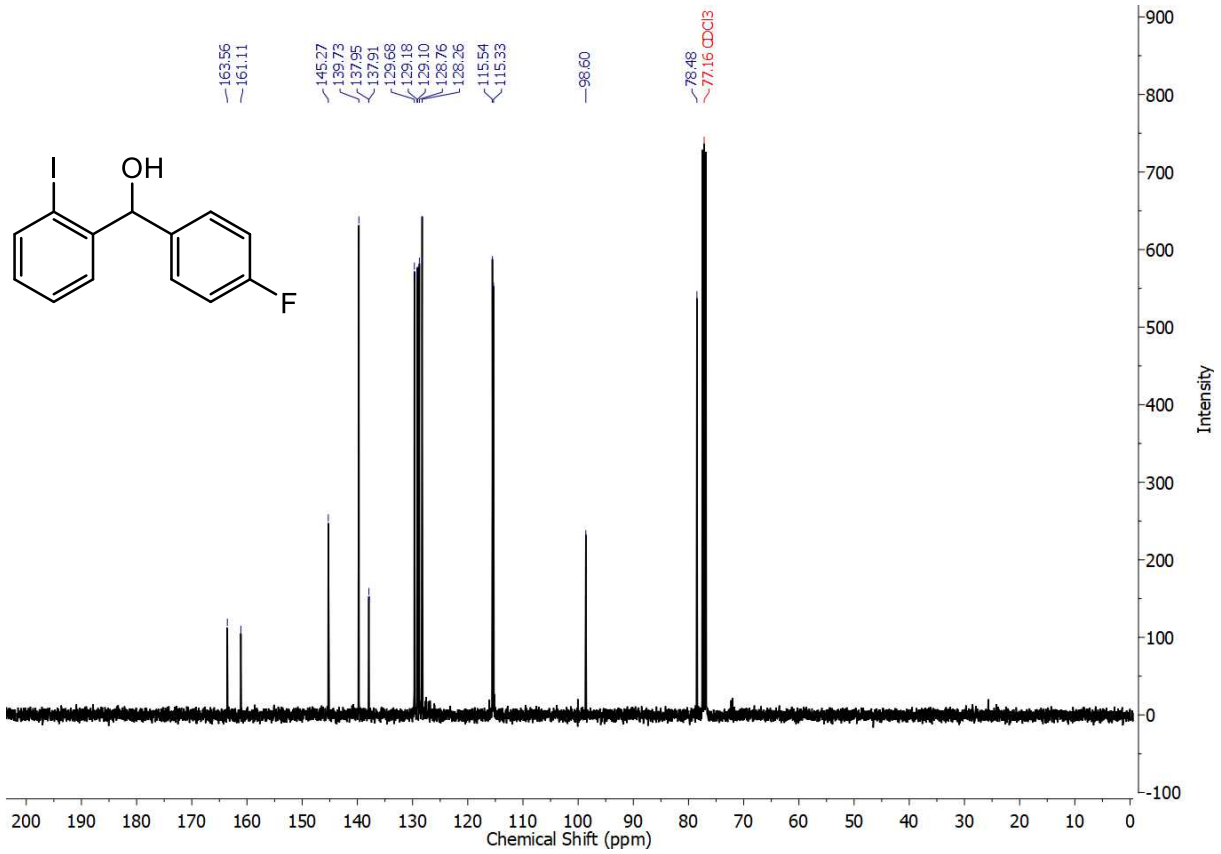

Figure S 84. $^{13}C\{^{1}H\}$ NMR spectrum of (4-fluorophenyl)(2-iodophenyl)methanol.

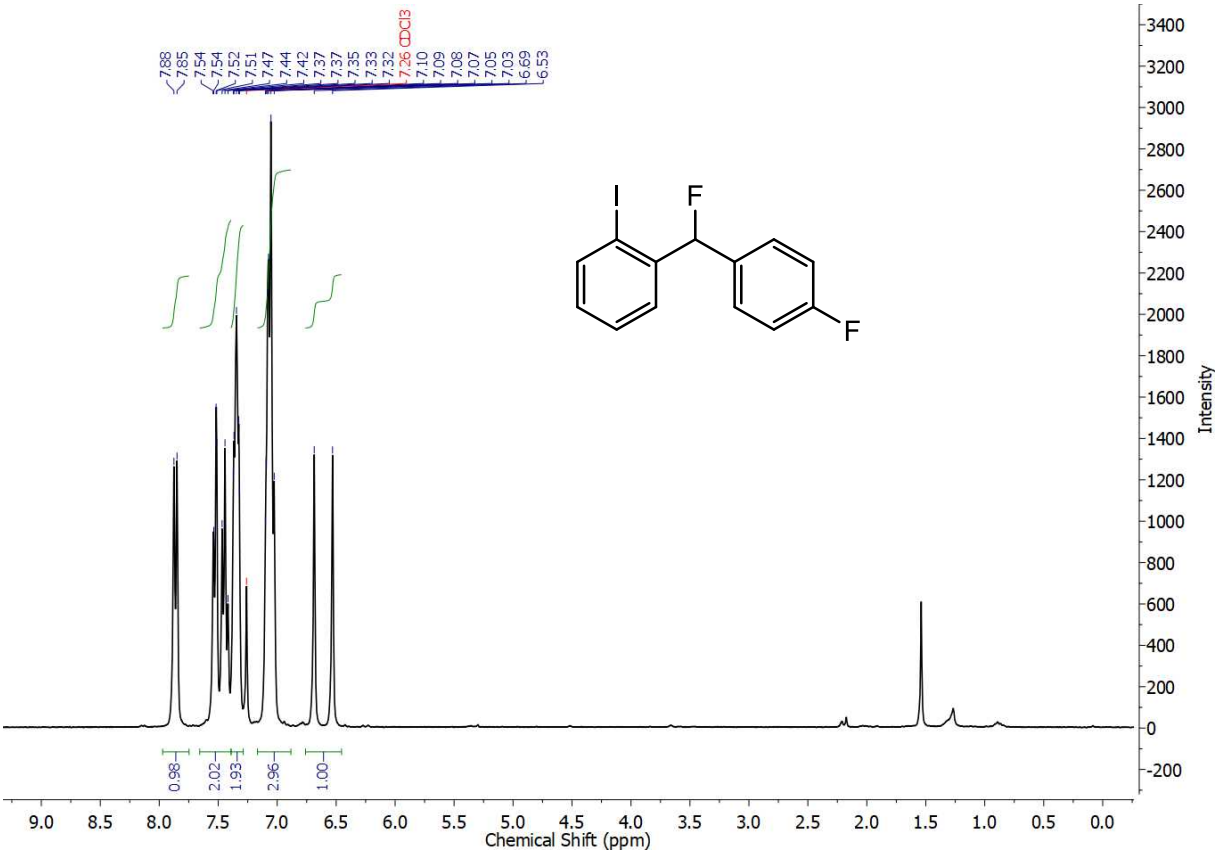

Figure S 85. ^{1}H NMR spectrum of 1-(fluoro(4-fluorophenyl)methyl)-2-iodobenzene.

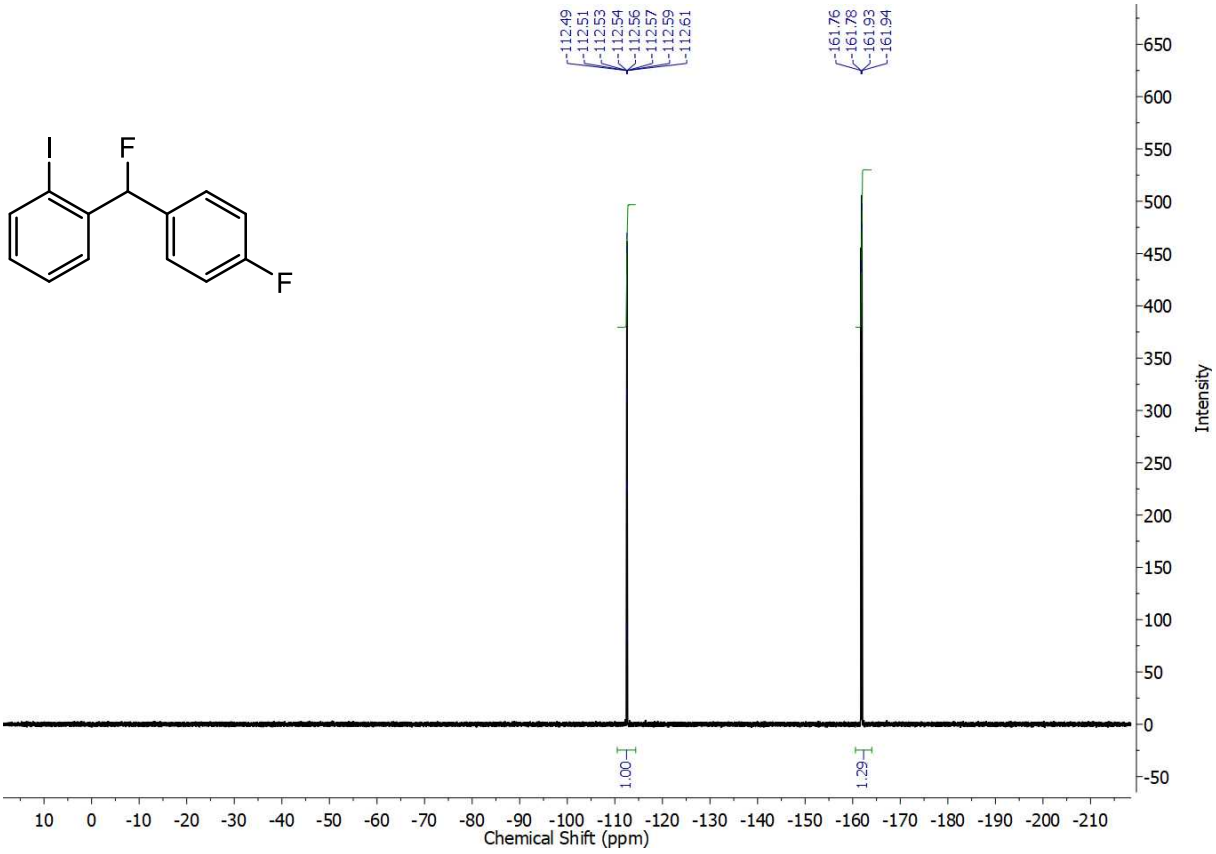

Figure S 86. ^{19}F NMR spectrum of 1-(fluoro(4-fluorophenyl)methyl)-2-iodobenzene.

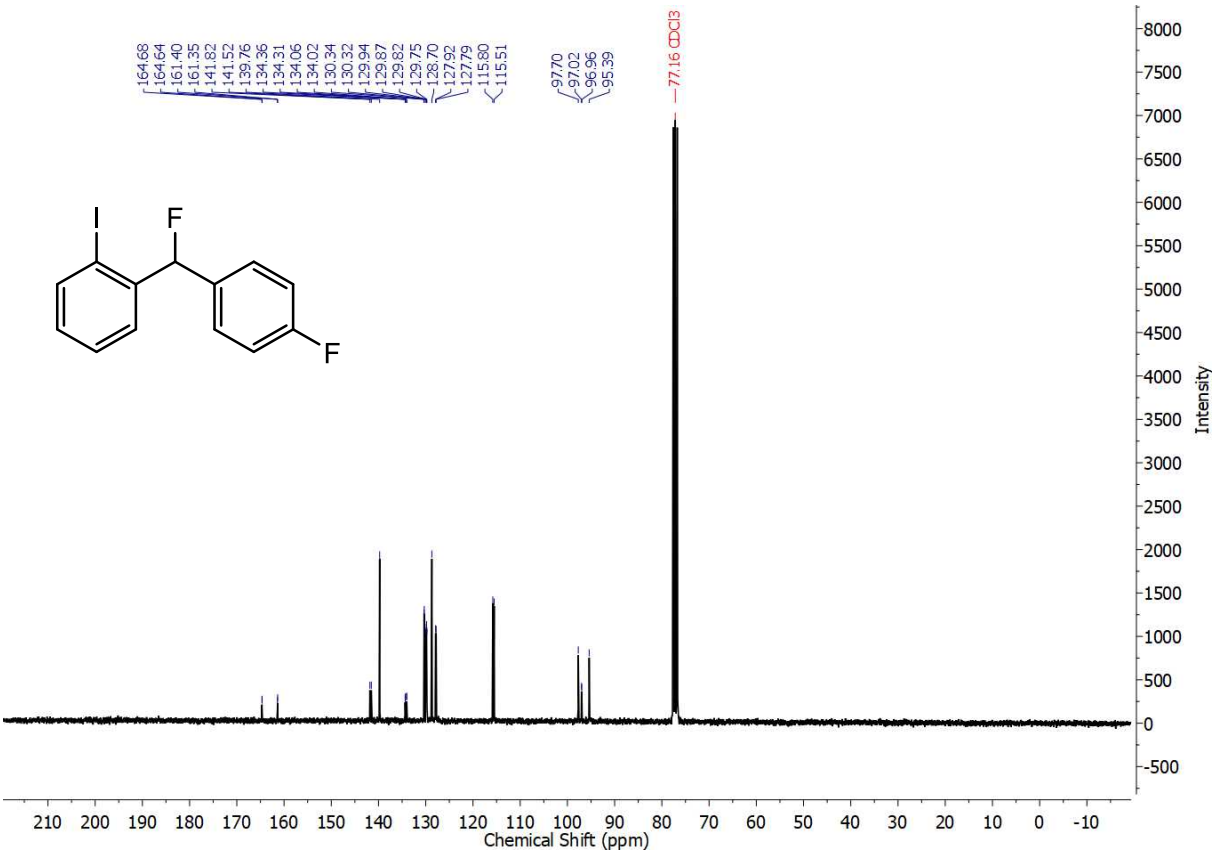

Figure S 87. $^{13}C\{^{1}H\}$ NMR spectrum of 1-(fluoro(4-fluorophenyl)methyl)-2-iodobenzene.

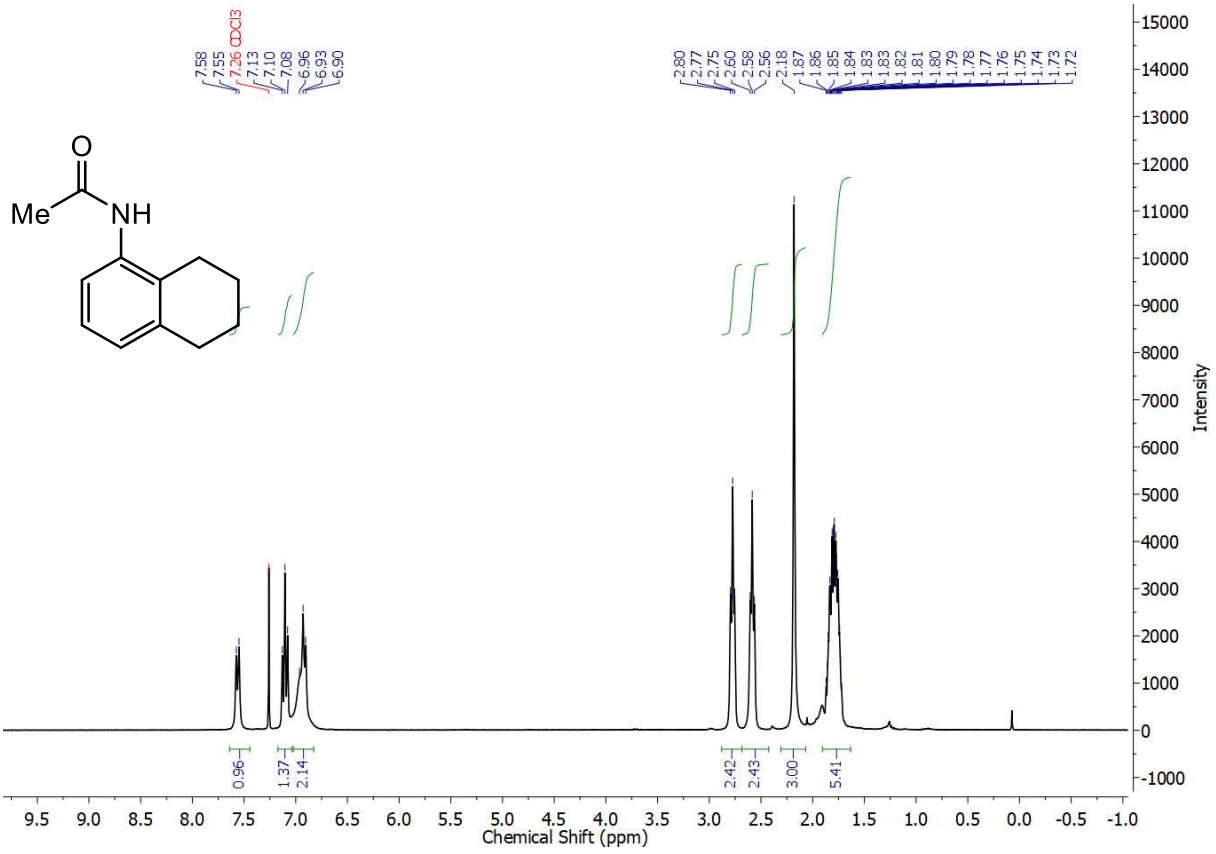

Figure S 88. ^{1}H NMR spectrum of N-(5,6,7,8-tetrahydronaphthalen-1-yl)acetamide.

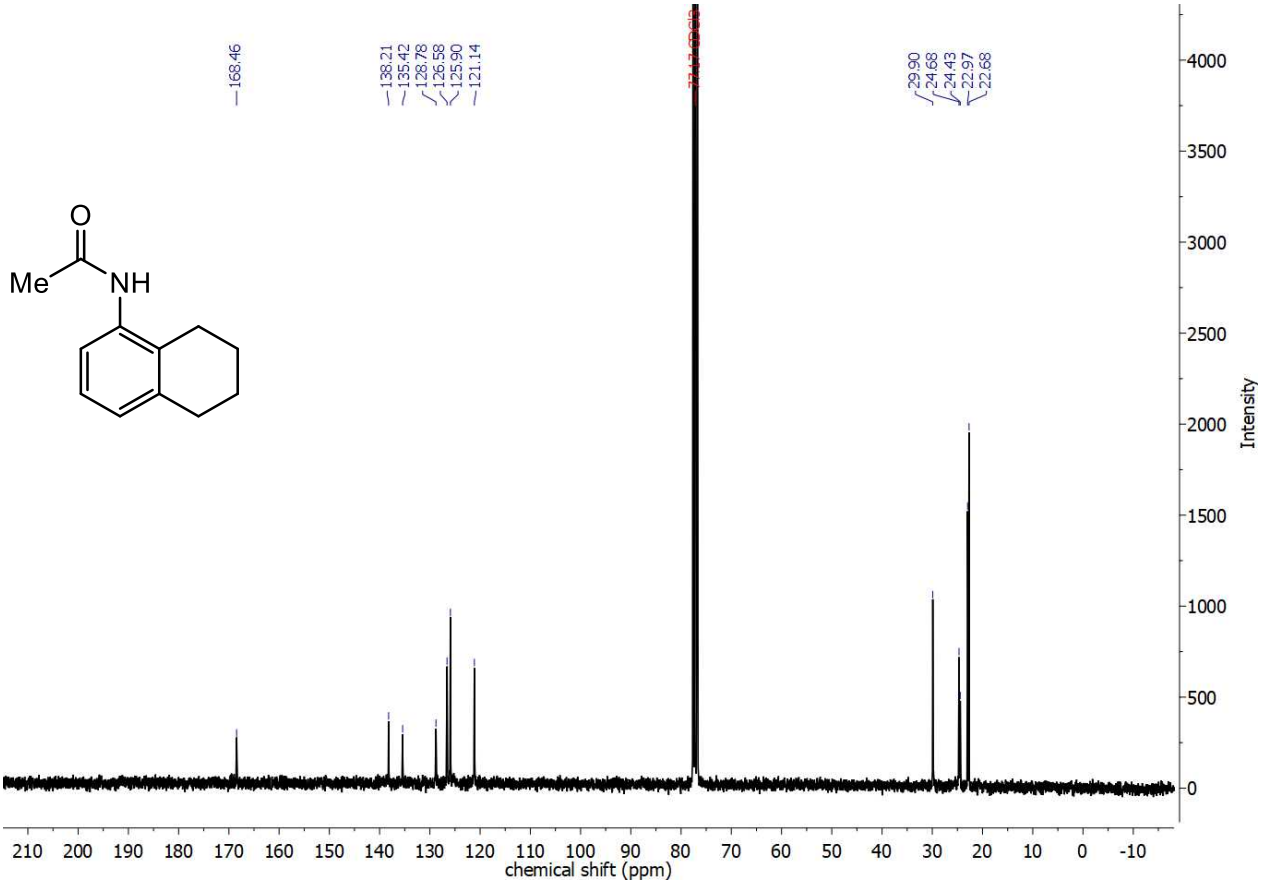

Figure S 89. $^{13}C\{^{1}H\}$ NMR spectrum of N-(5,6,7,8-tetrahydronaphthalen-1-yl)acetamide.

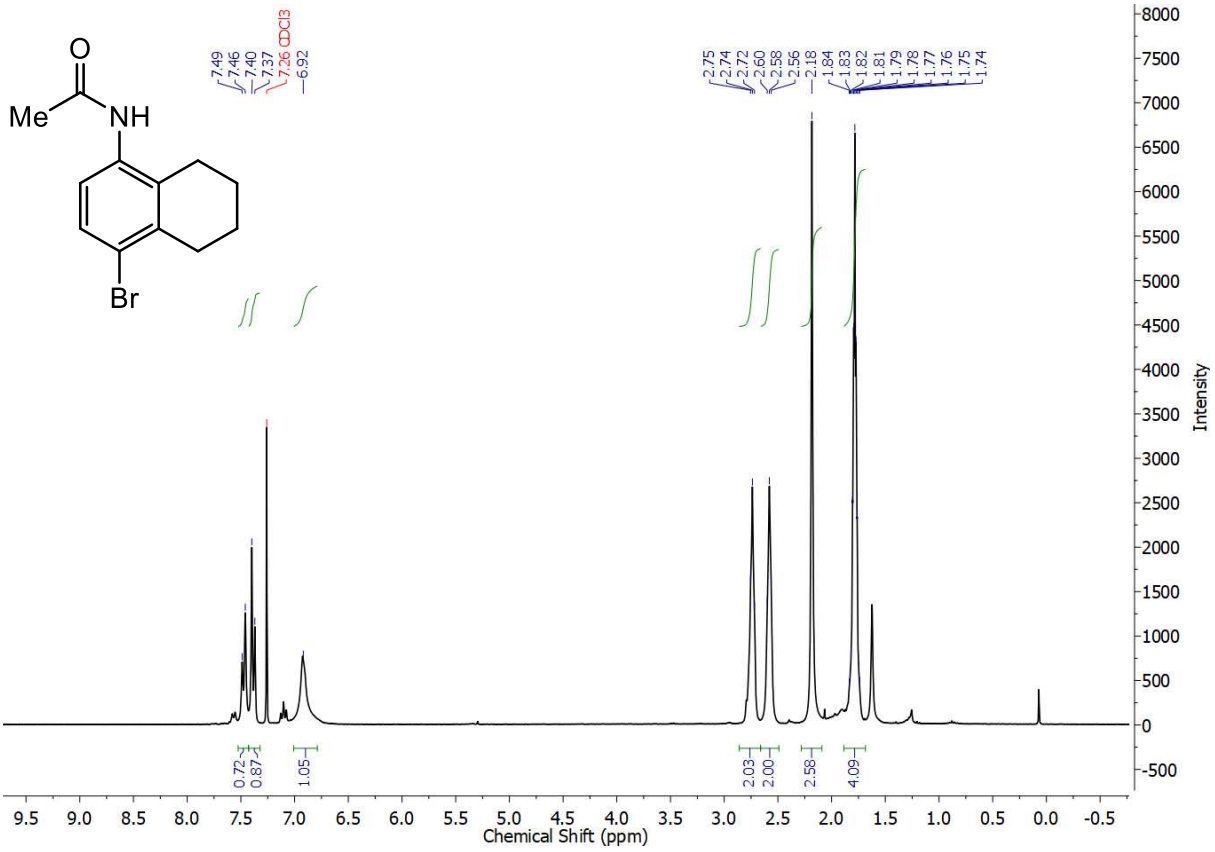

Figure S 90. ^{1}H NMR spectrum of N-(4-bromo-5,6,7,8-tetrahydronaphthalen-1-yl)acetamide.

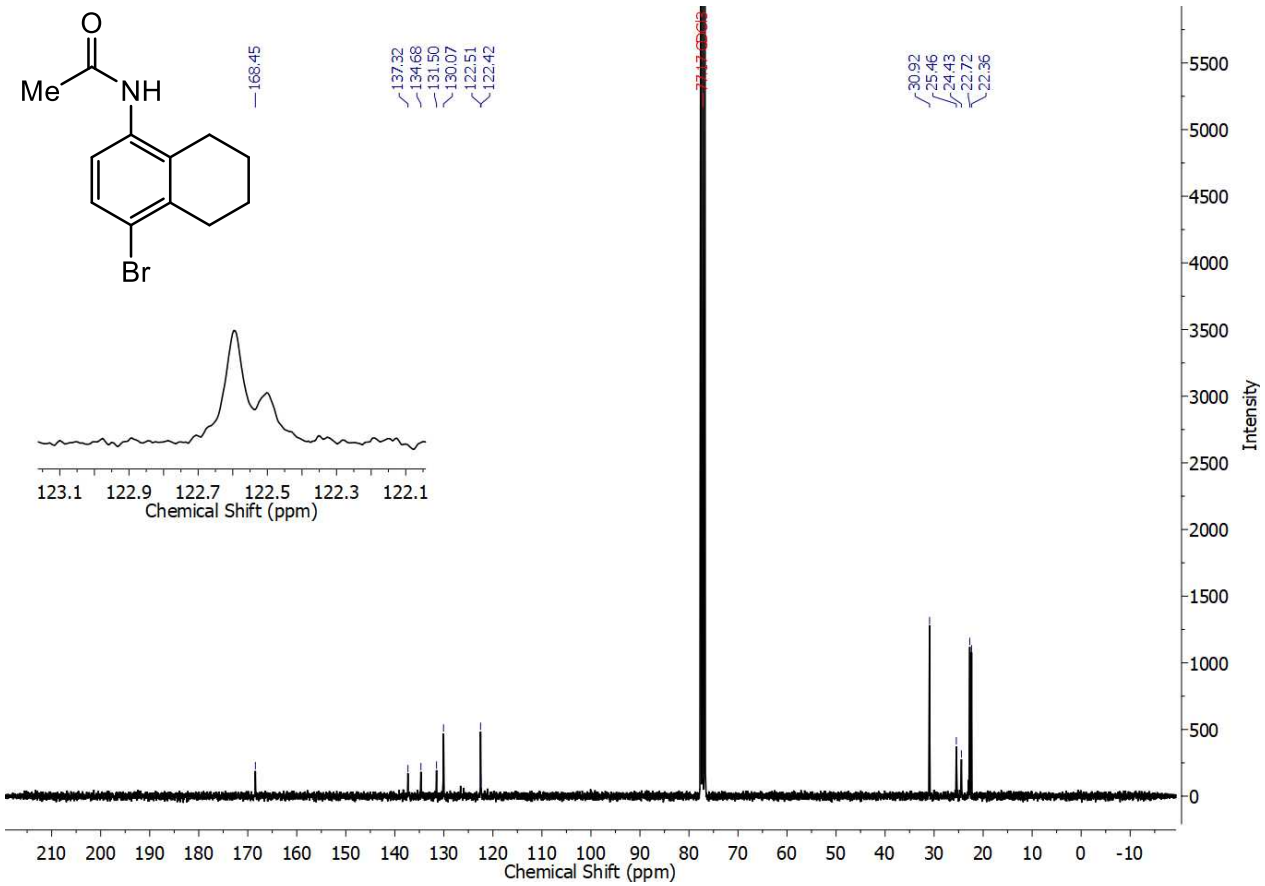

Figure S 91. $^{13}C\{^{1}H\}$ NMR spectrum of N-(4-bromo-5,6,7,8-tetrahydronaphthalen-1-yl)acetamide.

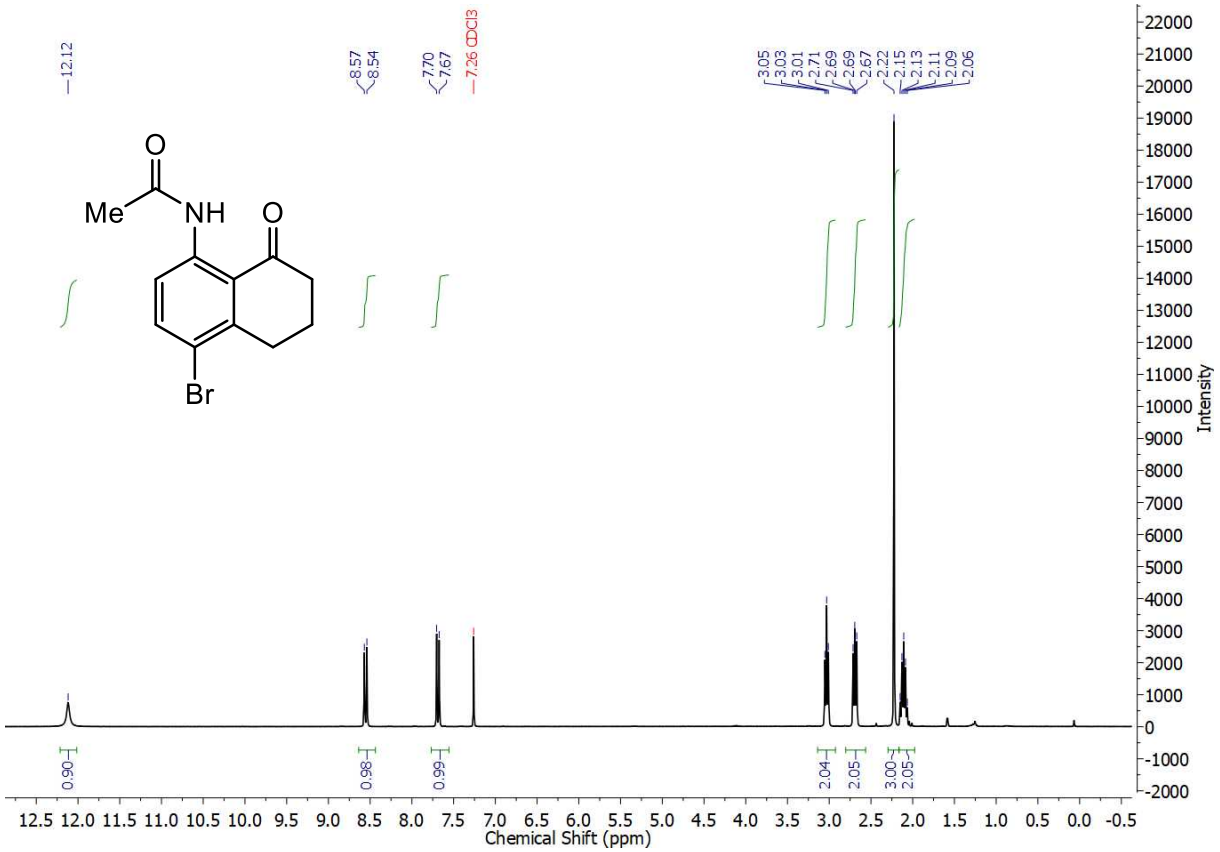

Figure S 92. ^{1}H NMR spectrum of N-(4-bromo-8-oxo-5,6,7,8-tetrahydronaphthalen-1-yl)acetamide.

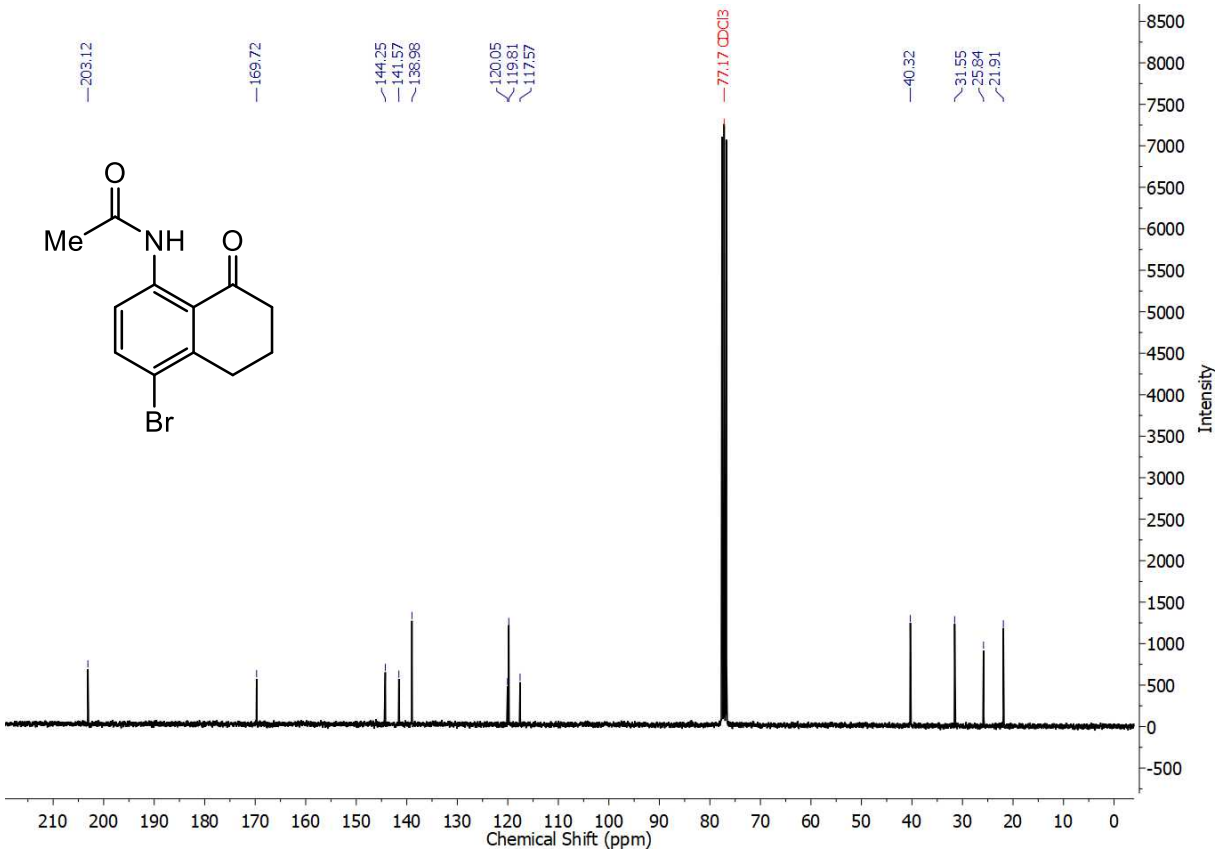

Figure S 93. $^{13}C\{^{1}H\}$ NMR spectrum of N-(4-bromo-8-oxo-5,6,7,8-tetrahydronaphthalen-1-yl)acetamide.

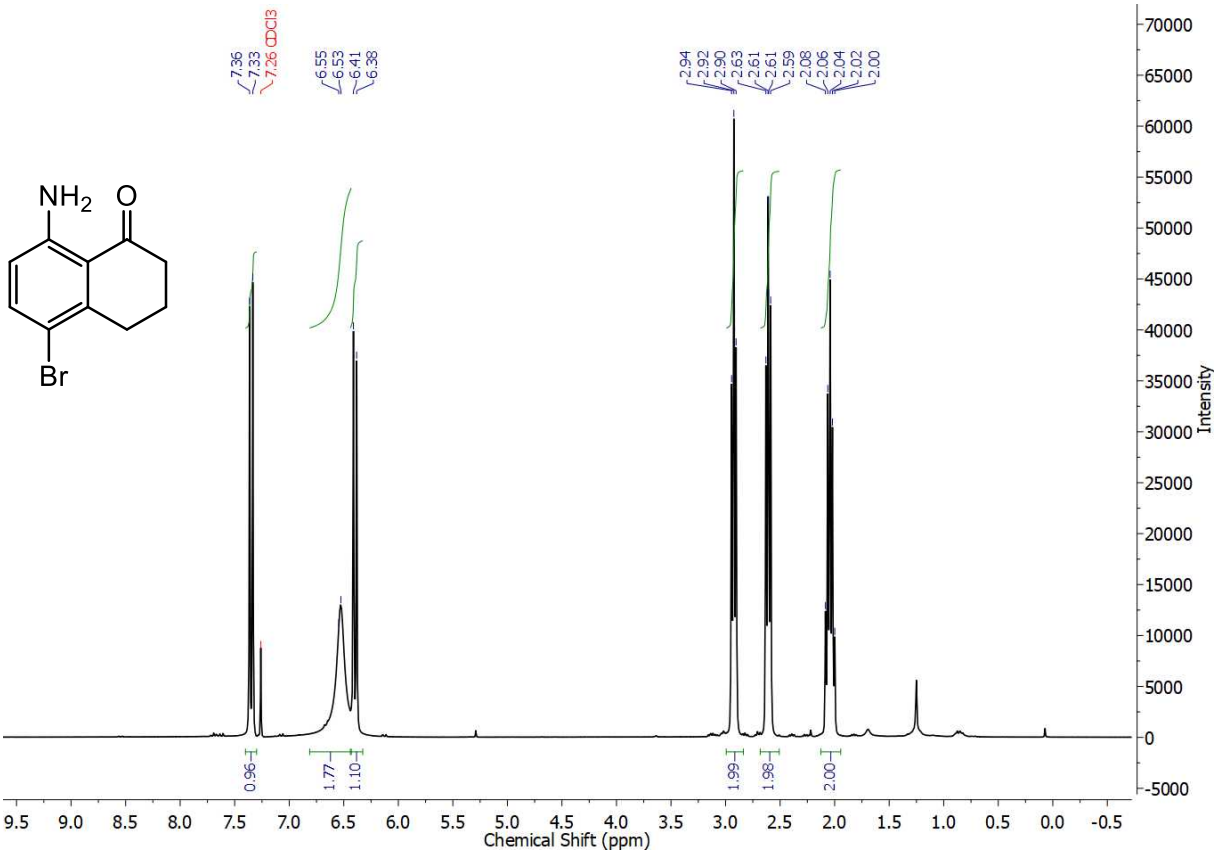

Figure S 94. ^{1}H NMR spectrum of 8-amino-5-bromo-3,4-dihydronaphthalen-1(2H)-one.

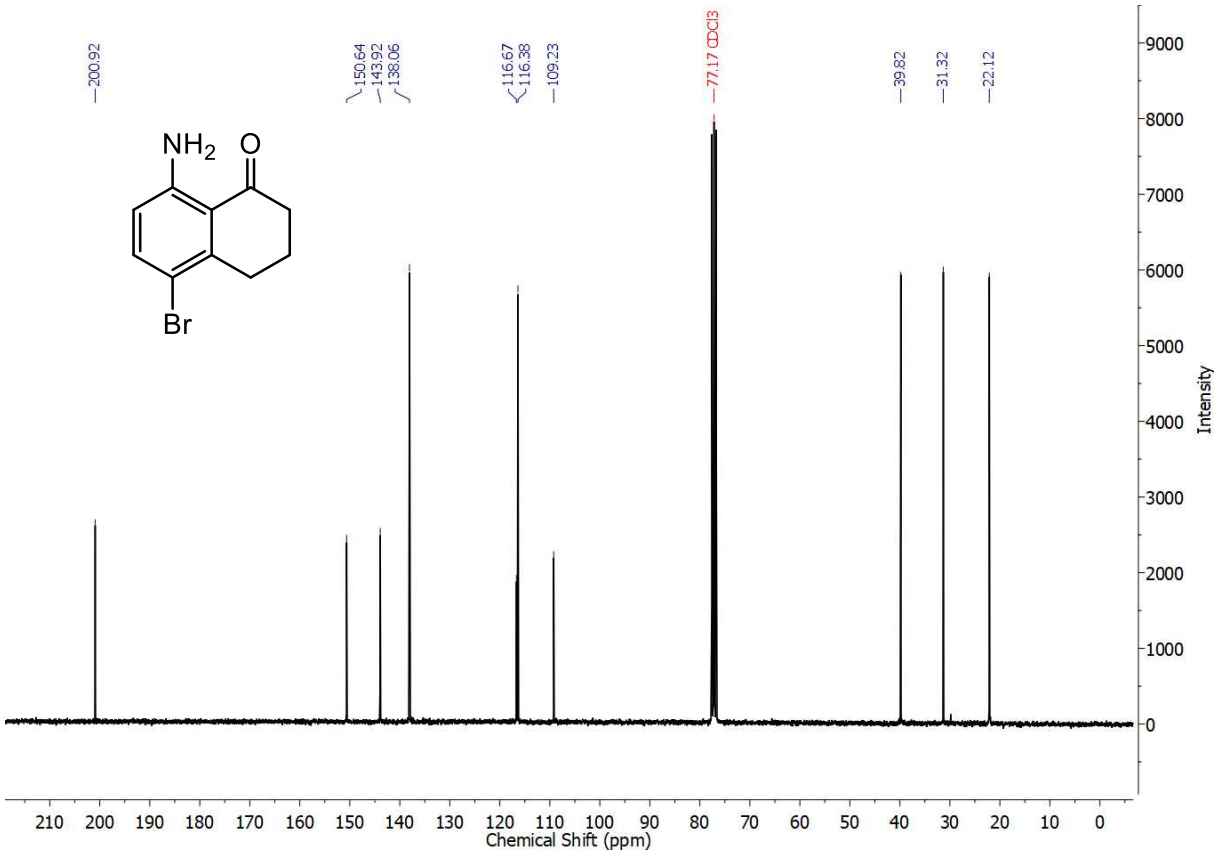

Figure S 95. $^{13}C\{^{1}H\}$ NMR spectrum of 8-amino-5-bromo-3,4-dihydronaphthalen-1(2H)-one.

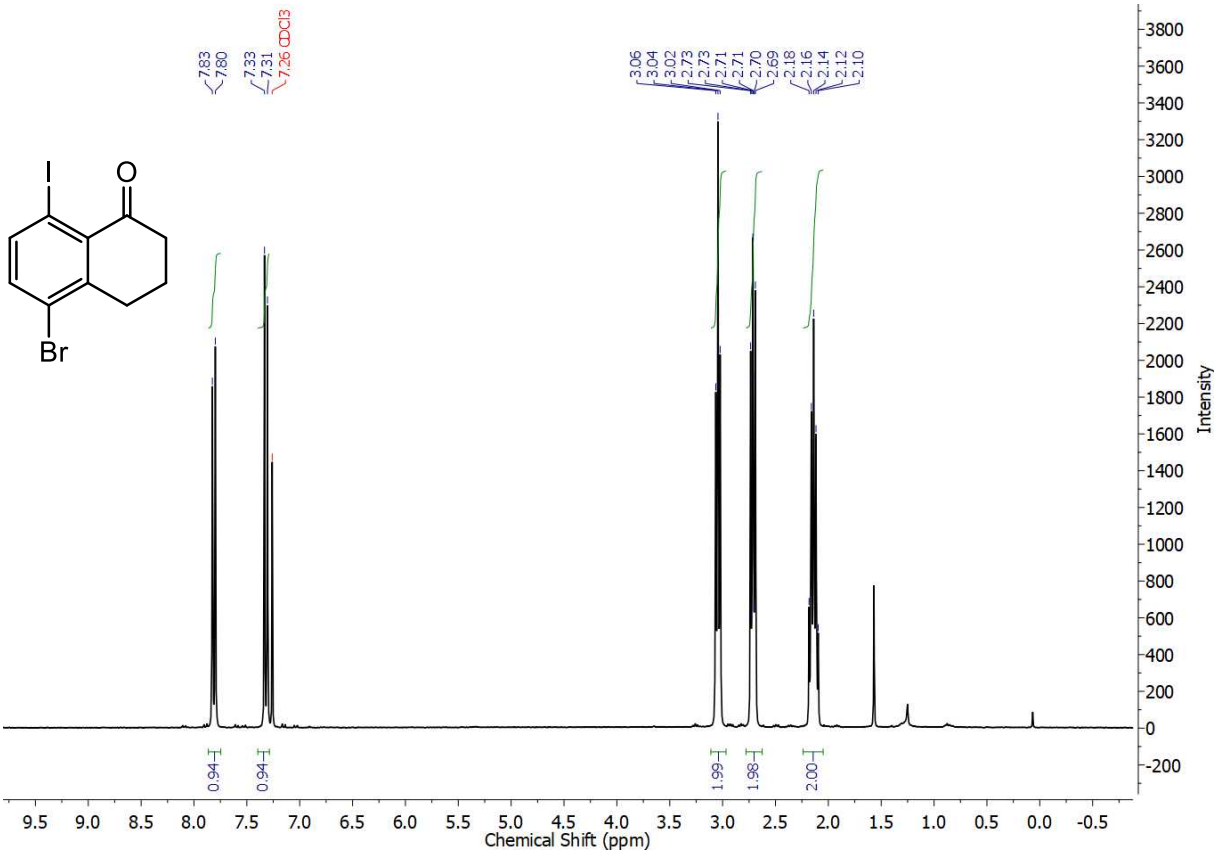

Figure S 96. ^{1}H NMR spectrum of 5-bromo-8-iodo-3,4-dihydronaphthalen-1(2H)-one.

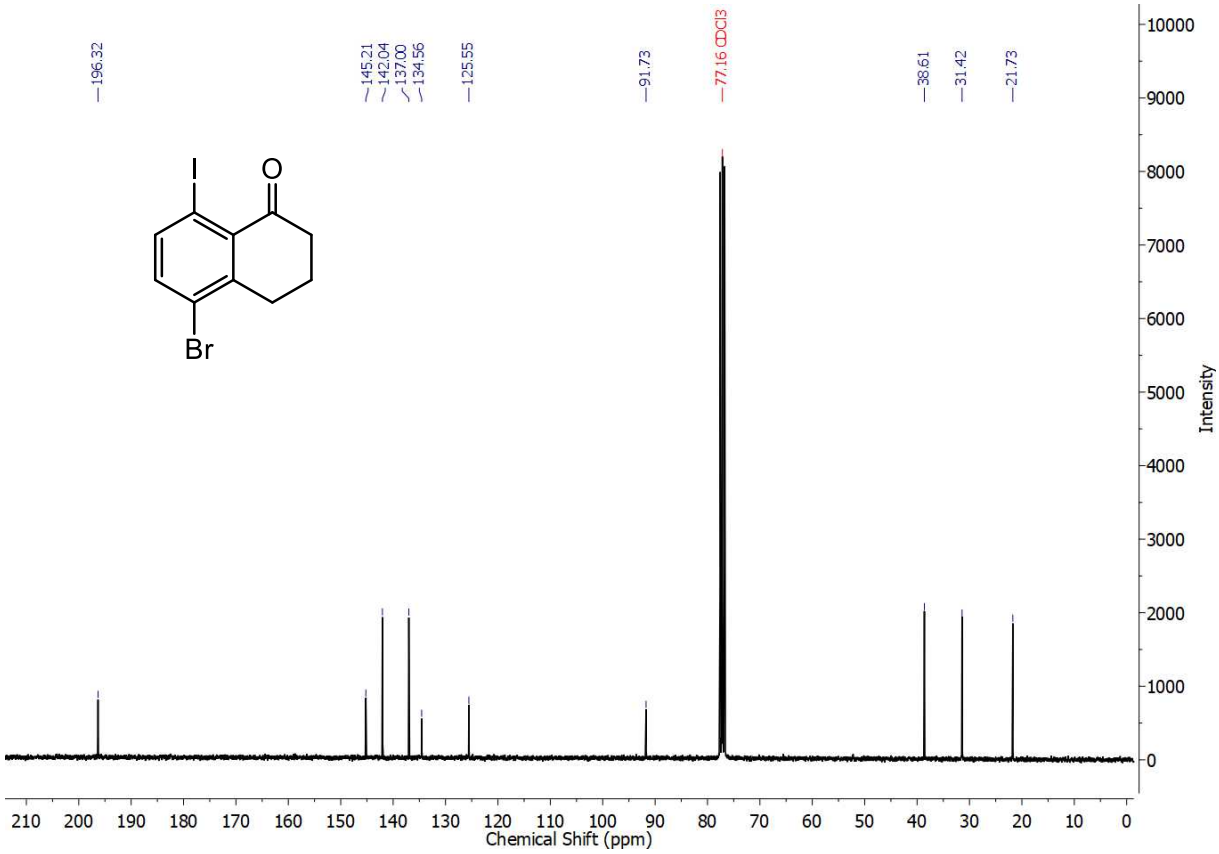

Figure S 97. $^{13}C\{^{1}H\}$ NMR spectrum of 5-bromo-8-iodo-3,4-dihydronaphthalen-1(2H)-one.

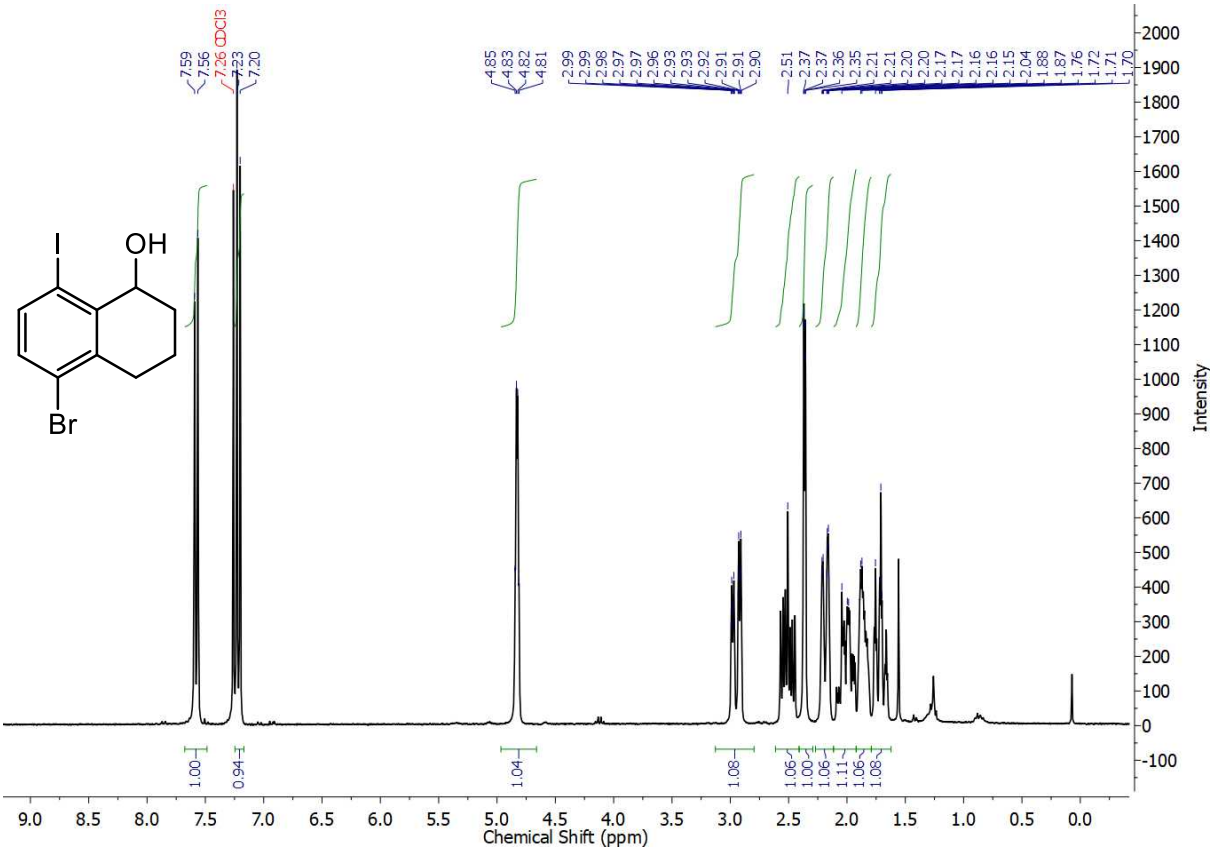

Figure S 98. ^{1}H NMR spectrum of 5-bromo-8-iodo-1,2,3,4-tetrahydronaphthalen-1-ol.

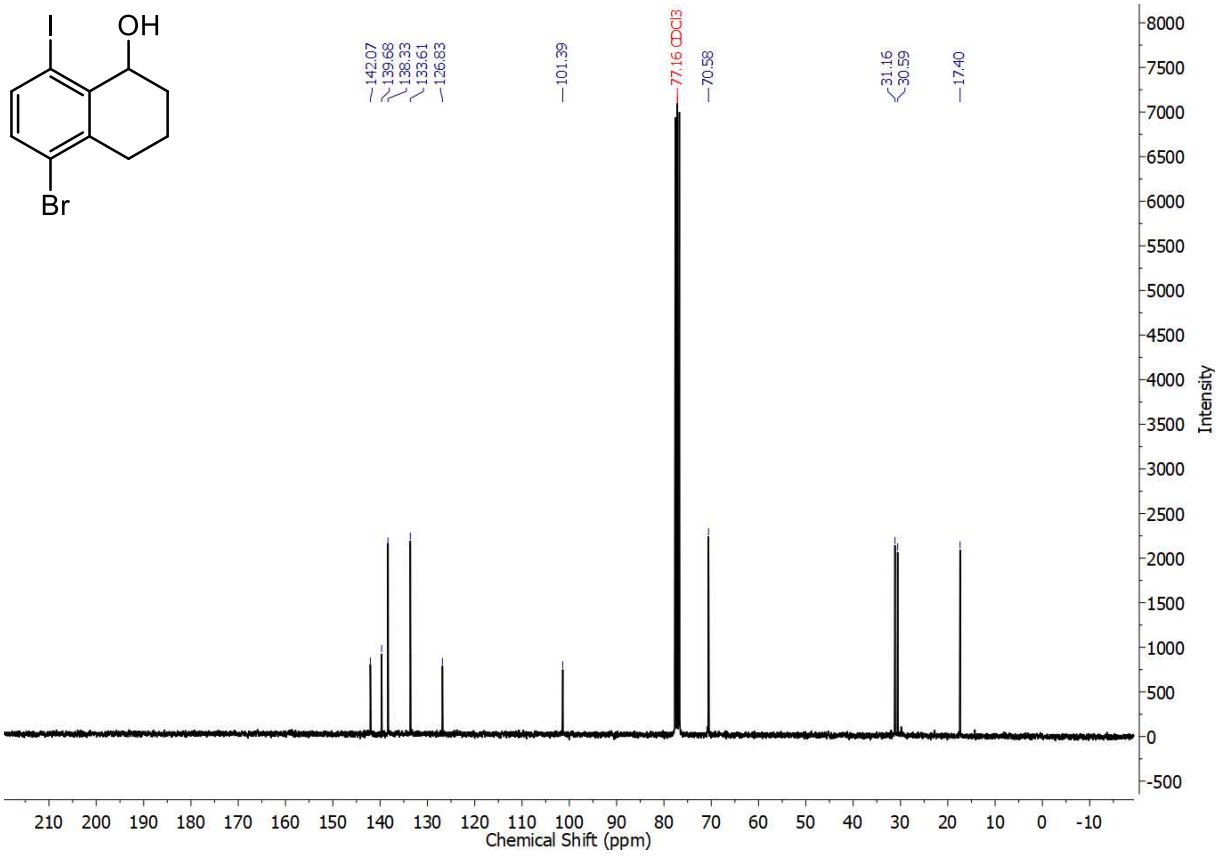

Figure S 99. $^{13}C\{^{1}H\}$ NMR spectrum of 5-bromo-8-iodo-1,2,3,4-tetrahydronaphthalen-1-ol.

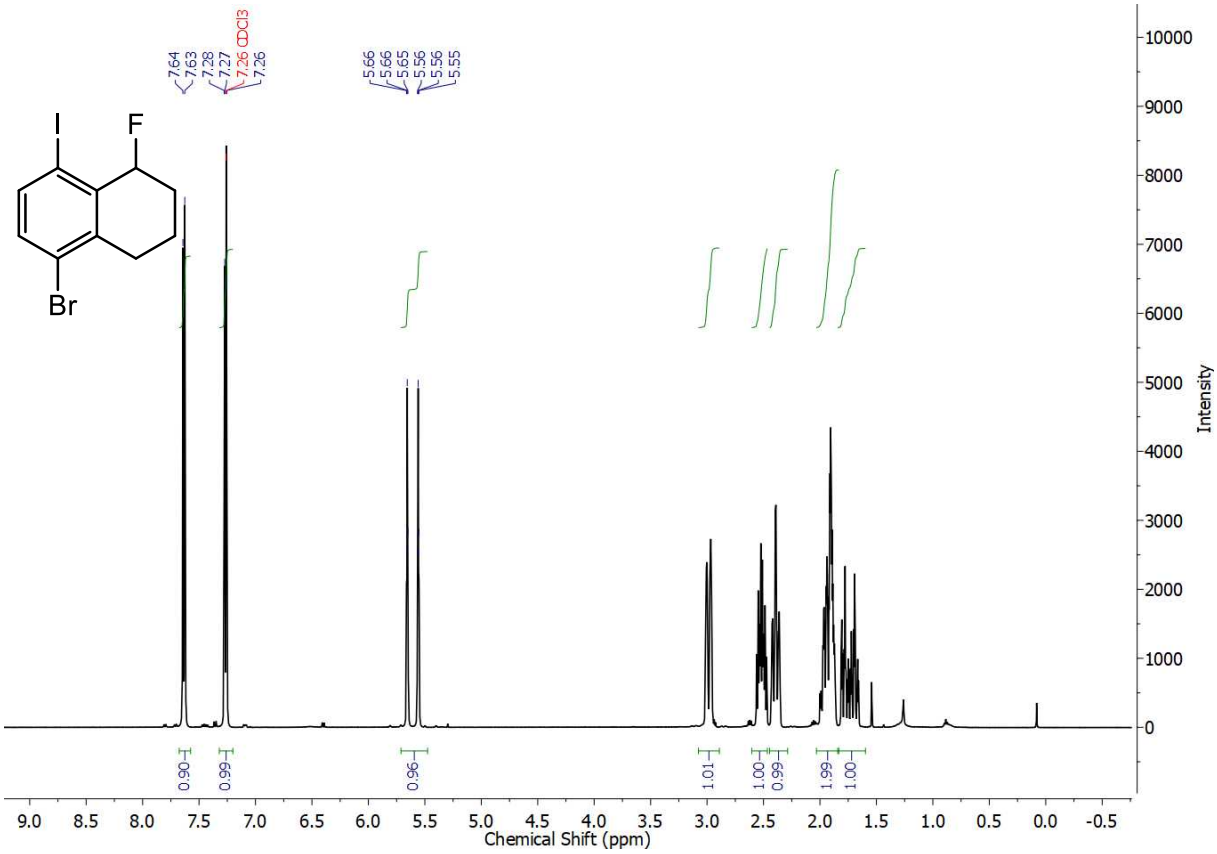

Figure S 100. ^{1}H NMR spectrum of 5-bromo-1-fluoro-8-iodo-1,2,3,4-tetrahydronaphthalene.

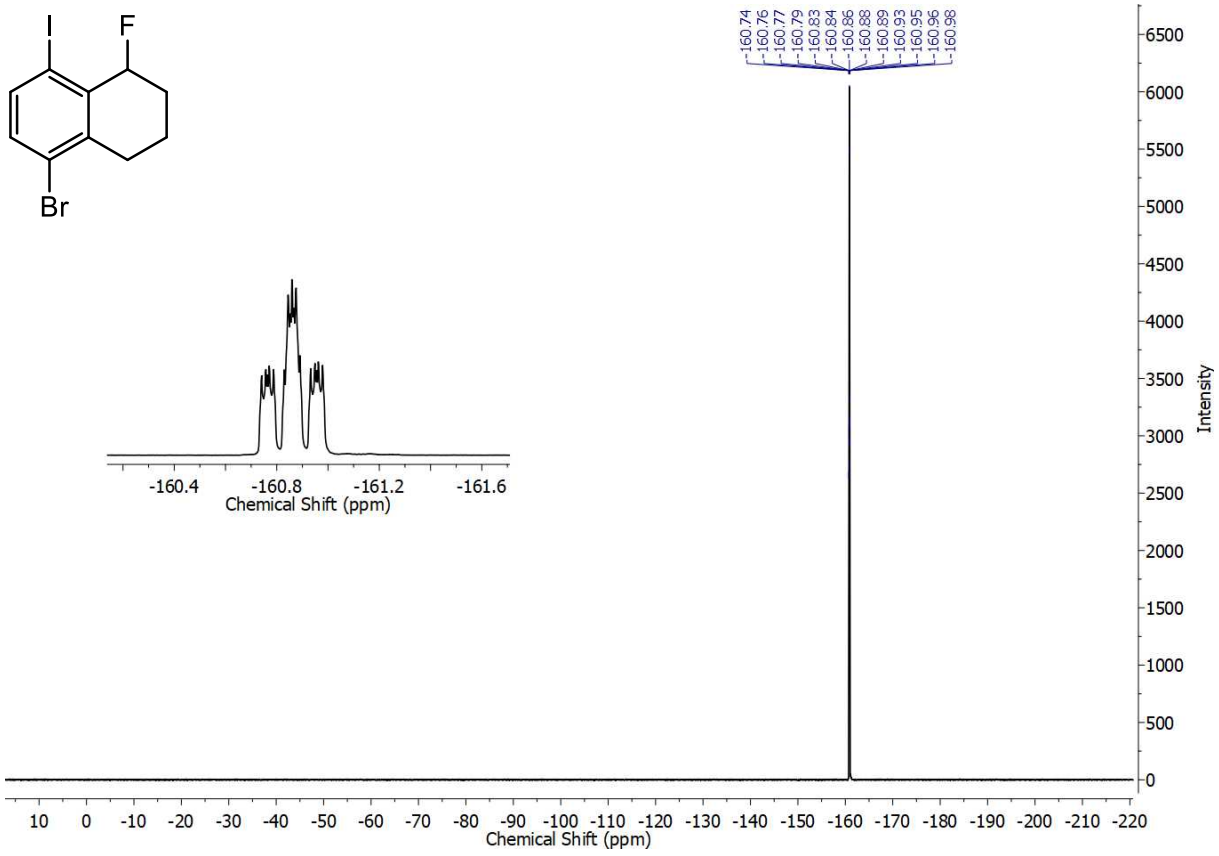

Figure S 101. ^{19}F NMR spectrum of 5-bromo-1-fluoro-8-iodo-1,2,3,4-tetrahydronaphthalene.

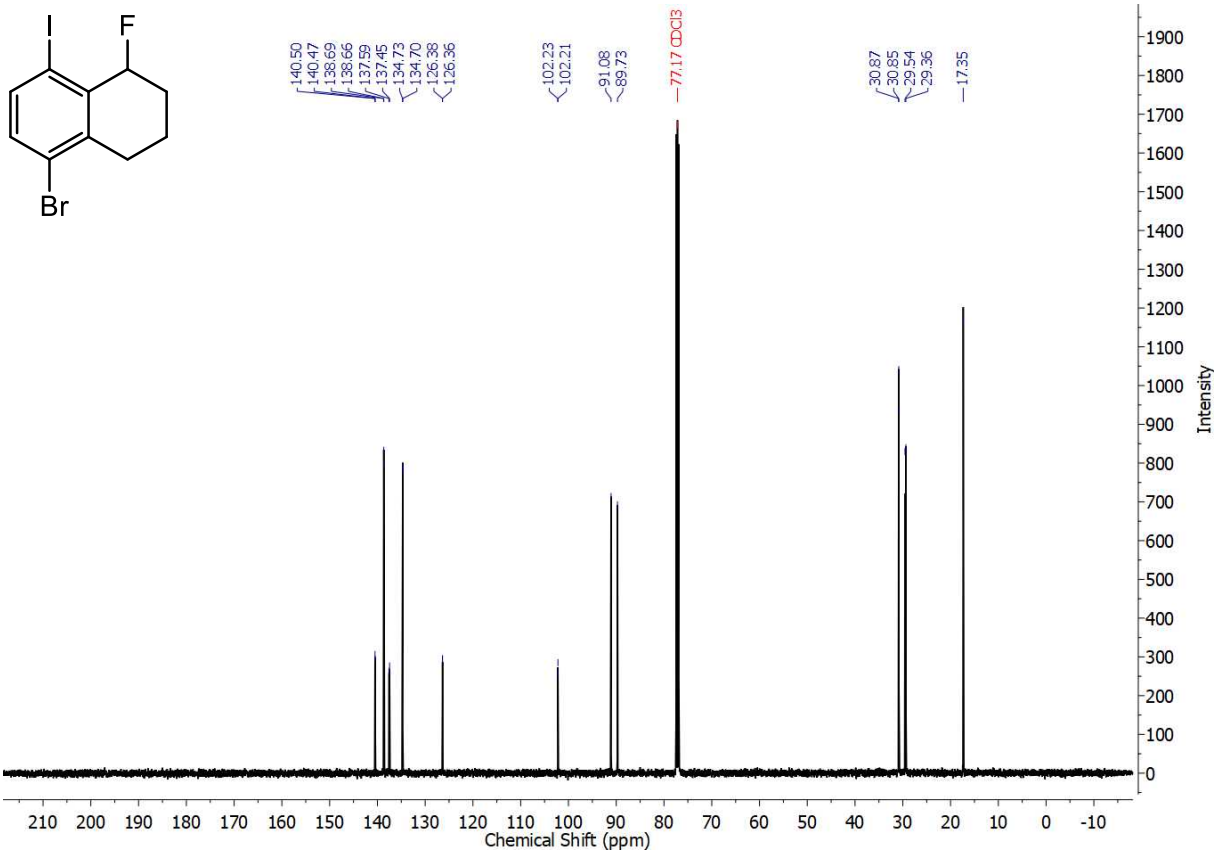

Figure S 102. $^{13}C\{^{1}H\}$ NMR spectrum of 5-bromo-1-fluoro-8-iodo-1,2,3,4-tetrahydronaphthalene.

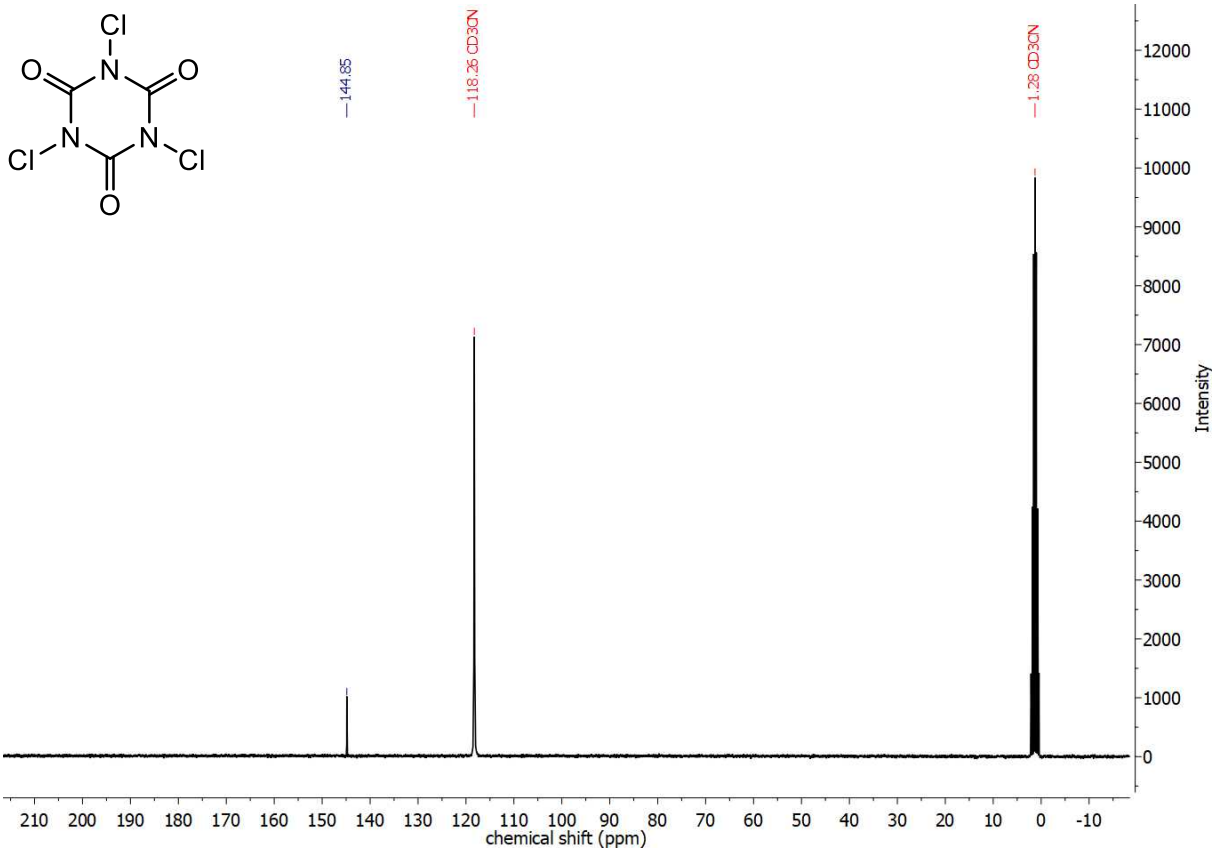

Figure S 103. $^{13}C\{^{1}H\}$ NMR spectrum of trichloroisocyanuric acid (TCICA).

VT-NMR Overlay of ^{1}H NMR Spectra for 21

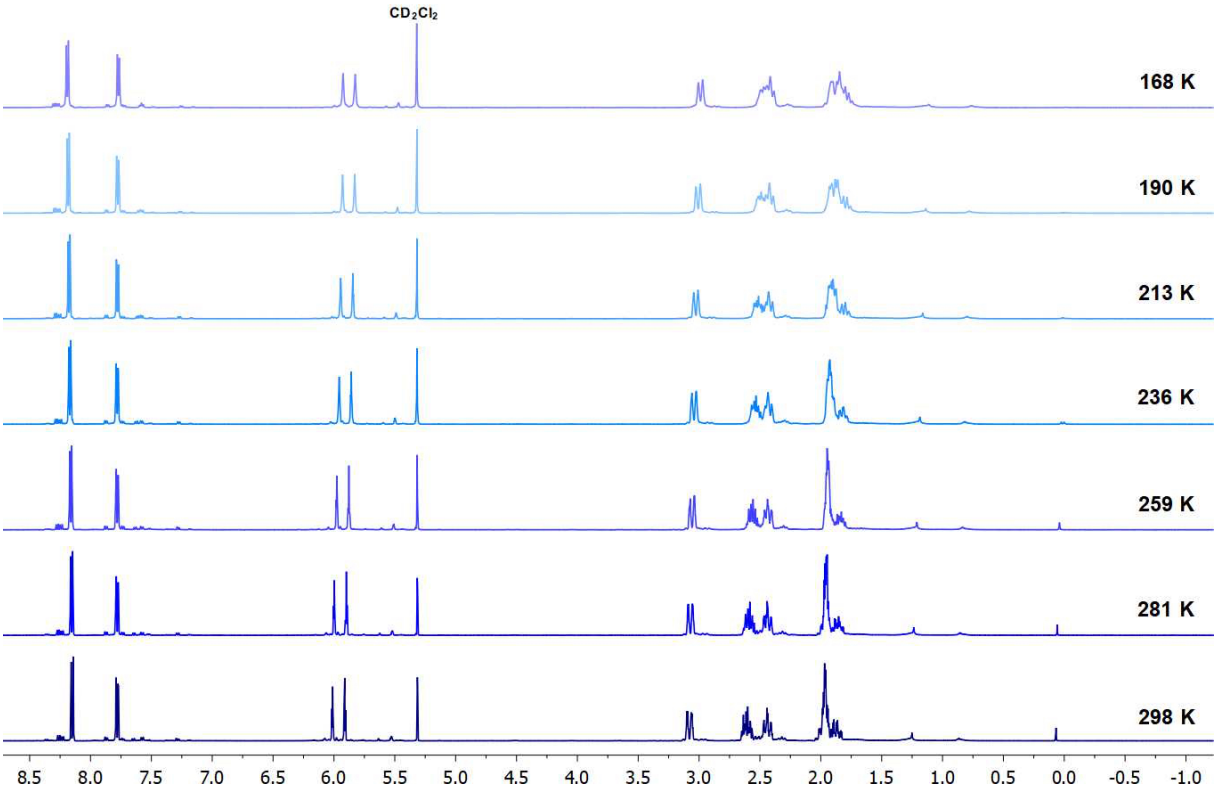

Figure S 104. Overlay of ^{1}H NMR spectra of compound **21** in CD_2Cl_2 at various temperatures.

Controlled Hydrolysis Experimental Data

Experimental Procedure for Hydrolysis Experiments

1. The aryl-IF_2 compounds were formed under standard reaction conditions (0.375 mmol of aryl iodide) using a mixture of CD_3CN (40%) and CH_3CN as a solvent.
2. Internal standard, either fluorobenzene or trifluoromethylbenzene (30 μL), were added to the reaction mixture.
3. The reaction mixture was filtered into a separate microwave vial under an argon atmosphere.
4. Three NMR samples were prepared, each containing 0.5 mL of filtered reaction mixture. The NMR tubes were previously capped with a rubber septum and put under an argon atmosphere.
5. A ^{19}F NMR spectrum was measured before the addition of water.
6. 0.1 mL of water was added to the NMR tube and a ^{19}F NMR spectrum was measured every 30 s. The starting time of the first measurement after the water addition was denoted separately.

***Note*:** For all the measurements, the experimental parameters were kept constant:

Number of scans: 4; Number of dummy scans: 0; Relaxation delay: 5.00 s; time difference between two measurements: 30.00 s

Data Analysis for Hydrolysis Experiments

The hydrolytic decay of the aryl-IF_2 compound was monitored looking the relative integral of the IF_2 signal with respect to an internal standard. Therefore, the integral of the IF_2 signal was set to 1.00 and relative integral of the standard signal was determined (denoted as relative integral). Within the plots, the relative integral is denoted as the concentration of the aryl-IF_2 compound, since the concentration is directly correlated to the relative integral. For simplicity, all integrals were normalized, which allowed to compare the different runs and experiments.

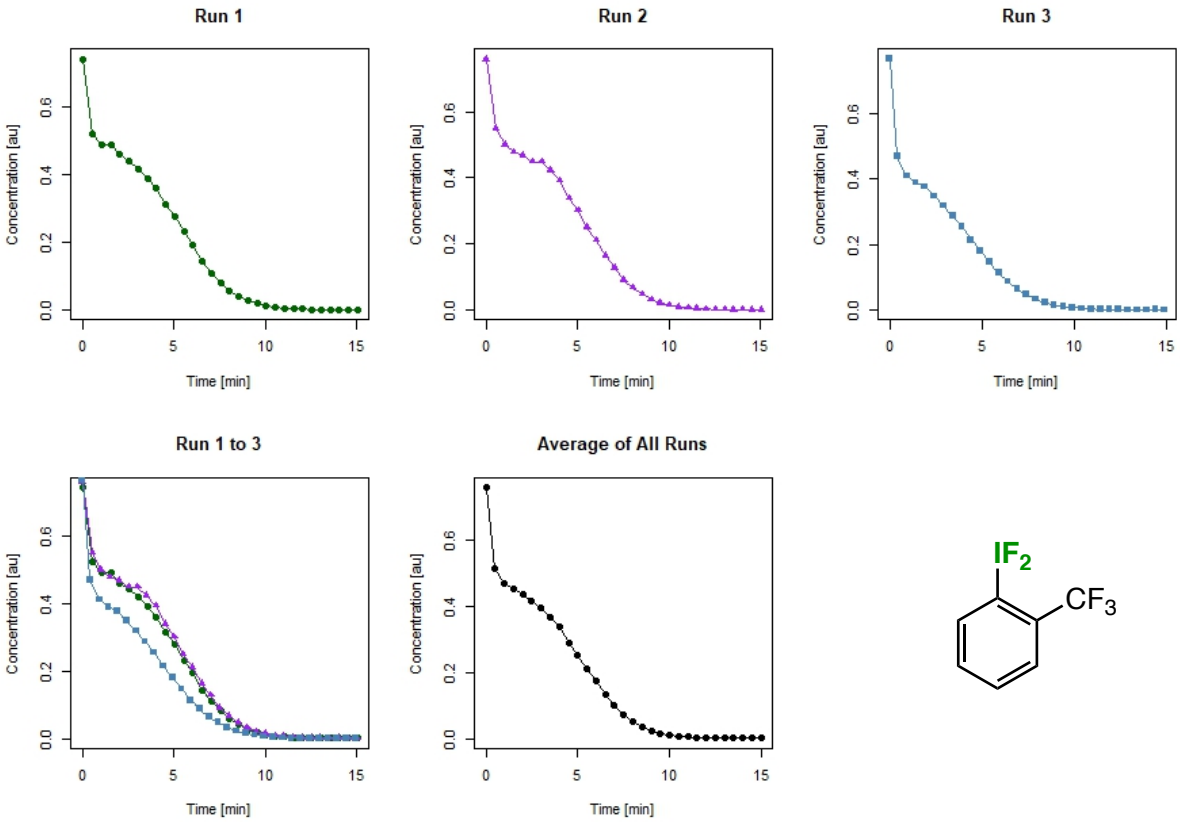

Run 1		Run2		Run 3	
Time [min]	**Relative Integral**	**Time [min]**	**Relative Integral**	**Time [min]**	**Relative Integral**
0.00	0.31	0.00	0.29	0.00	0.30
0.55	0.44	0.53	0.40	0.43	0.49
1.05	0.47	1.03	0.44	0.93	0.56
1.55	0.47	1.53	0.46	1.43	0.59
2.05	0.50	2.03	0.47	1.93	0.61
2.55	0.52	2.53	0.49	2.43	0.66
3.05	0.55	3.03	0.49	2.93	0.72
3.55	0.59	3.53	0.52	3.43	0.80
4.05	0.64	4.03	0.56	3.93	0.90
4.55	0.73	4.53	0.65	4.43	1.07
5.05	0.83	5.03	0.73	4.93	1.27
5.55	0.99	5.53	0.88	5.43	1.56
6.05	1.19	6.03	1.04	5.93	2.02
6.55	1.59	6.53	1.34	6.43	2.63
7.05	2.08	7.03	1.71	6.93	3.56
7.55	2.82	7.53	2.41	7.43	4.81
8.05	4.01	8.03	3.24	7.93	6.80
8.55	5.54	8.53	4.58	8.43	9.92
9.05	8.15	9.03	6.75	8.93	14.6
9.55	12.1	9.53	10.2	9.43	22.0
10.05	18.9	10.03	14.0	9.93	33.4
10.55	26.2	10.53	21.8	10.43	45.4
11.05	41.6	11.03	30.6	10.93	74.2
11.55	49.4	11.53	39.5	11.43	101
12.05	58.3	12.03	59.4	11.93	119
12.55	89.3	12.53	86.6	12.43	177
13.05	134	13.03	88.9	12.93	321
13.55	120	13.53	230	13.43	233
14.05	143	14.03	95.2	13.93	329
14.55	225	14.53	136	14.43	206
15.05	138	15.03	122	14.93	256

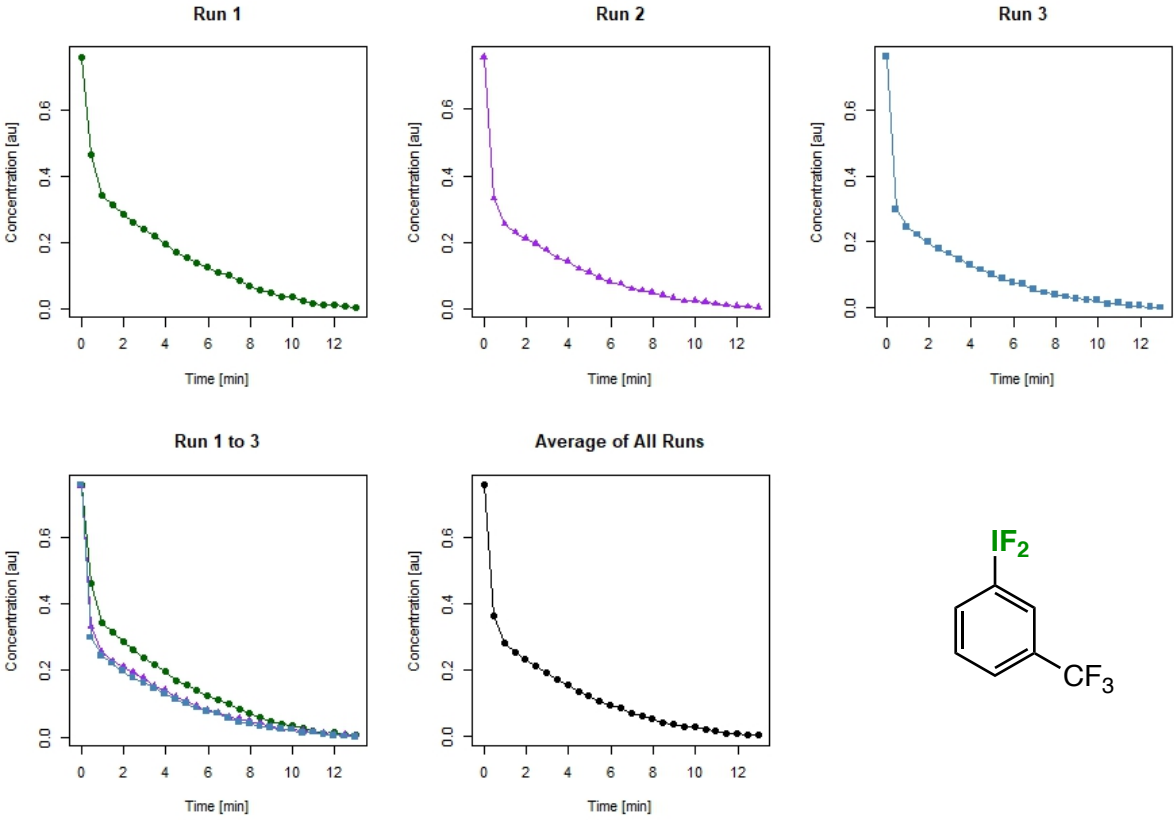

Run 1		Run2		Run 3	
Time [min]	Relative Integral	Time [min]	Relative Integral	Time [min]	Relative Integral
0.00	1.32	0.00	1.19	0.00	1.33
0.48	2.16	0.48	2.71	0.46	3.37
0.98	2.91	0.98	3.53	0.96	4.11
1.48	3.18	1.48	3.92	1.46	4.54
1.98	3.48	1.98	4.25	1.96	5.06
2.48	3.83	2.48	4.61	2.46	5.66
2.98	4.16	2.98	5.09	2.96	6.13
3.48	4.56	3.48	5.88	3.46	6.82
3.98	5.06	3.98	6.35	3.96	7.76
4.48	5.87	4.48	7.47	4.46	8.74
4.98	6.44	4.98	8.21	4.96	9.91
5.48	7.12	5.48	9.64	5.46	11.5
5.98	8.00	5.98	11.3	5.96	12.9
6.48	8.90	6.48	11.9	6.46	14.0
6.98	9.91	6.98	14.7	6.96	18.1
7.48	11.7	7.48	15.8	7.46	22.3
7.98	14.0	7.98	18.5	7.96	24.9
8.48	17.3	8.48	22.1	8.46	30.1
8.98	21.0	8.98	27.0	8.96	35.4
9.48	25.5	9.48	38.3	9.46	41.4
9.98	27.3	9.98	37.3	9.96	44.0
10.48	36.9	10.48	45.1	10.46	80.3
10.98	56.6	10.98	58.0	10.96	69.3
11.48	78.4	11.48	82.1	11.46	136
11.98	70.2	11.98	105	11.96	170
12.48	127	12.48	120	12.46	370
12.98	204	12.98	200	12.96	700

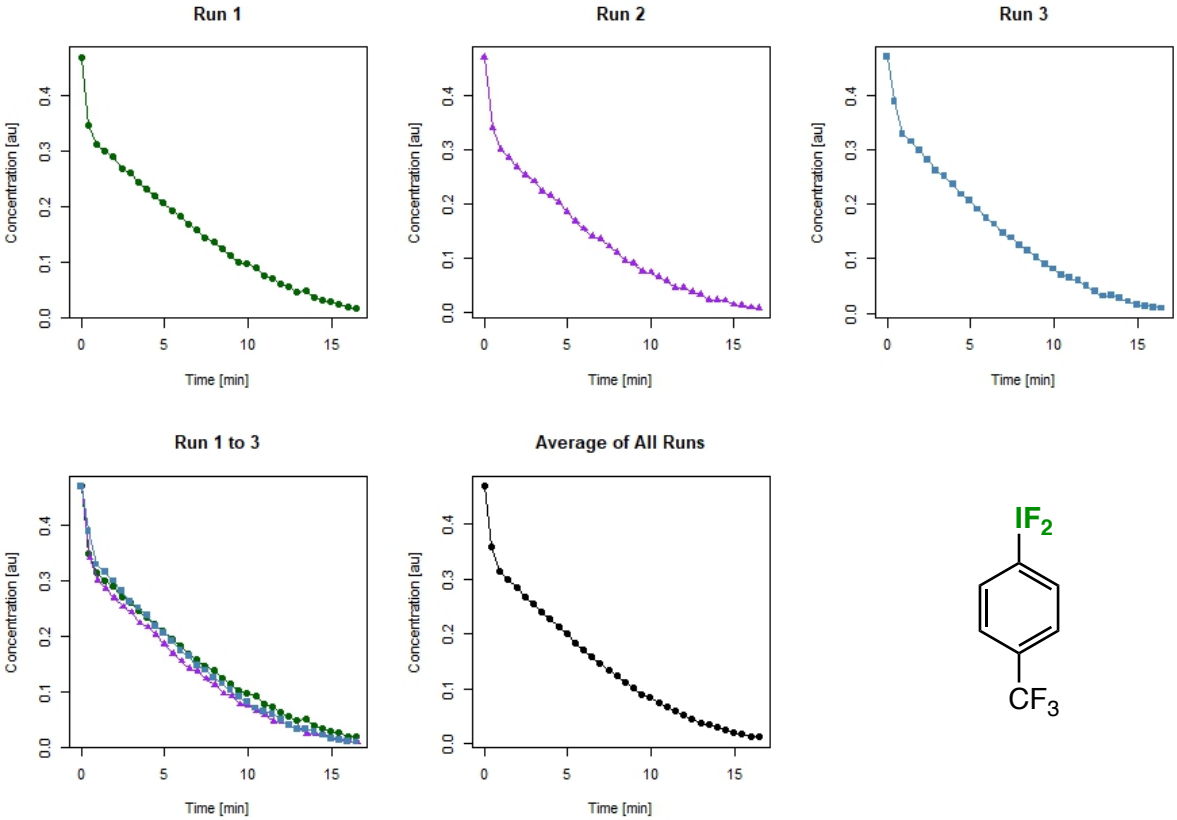

Run 1		Run2		Run 3	
Time [min]	Relative Integral	Time [min]	Relative Integral	Time [min]	Relative Integral
0.00	2.13	0.00	2.37	0.00	3.27
0.42	2.88	0.50	3.27	0.43	3.95
0.92	3.19	1.00	3.71	0.93	4.67
1.42	3.33	1.50	3.90	1.43	4.88
1.92	3.44	2.00	4.15	1.93	5.13
2.42	3.71	2.50	4.41	2.43	5.47
2.92	3.83	3.00	4.60	2.93	5.87
3.42	4.08	3.50	5.00	3.43	6.12
3.92	4.29	4.00	5.16	3.93	6.47
4.42	4.52	4.50	5.50	4.43	7.05
4.92	4.80	5.00	6.09	4.93	7.45
5.42	5.15	5.50	6.62	5.43	8.05
5.92	5.48	6.00	7.22	5.93	8.81
6.42	5.94	6.50	7.88	6.43	9.40
6.92	6.32	7.00	8.20	6.93	10.5
7.42	6.92	7.50	9.16	7.43	11.1
7.92	7.27	8.00	10.2	7.93	12.3
8.42	8.06	8.50	11.6	8.43	13.5
8.92	8.85	9.00	12.2	8.93	15.1
9.42	9.90	9.50	14.6	9.43	16.6
9.92	10.3	10.00	15.2	9.93	19.3
10.42	11.0	10.50	17.7	10.43	22.2
10.92	12.7	11.00	19.2	10.93	24.2
11.42	14.0	11.50	23.5	11.43	26.3
11.92	15.6	12.00	23.5	11.93	31.0
12.42	18.2	12.50	28.6	12.43	38.7
12.92	20.7	13.00	33.0	12.93	49.0
13.42	20.5	13.50	46.0	13.43	47.7
13.92	27.0	14.00	48.2	13.93	56-4
14.42	29.2	14.50	49.8	14.43	72.4
14.92	34.4	15.00	73.1	14.93	102
15.42	38.9	15.50	77.1	15.43	116
15.92	51.1	16.00	110	15.93	147
16.42	56.6	16.50	130	16.43	173

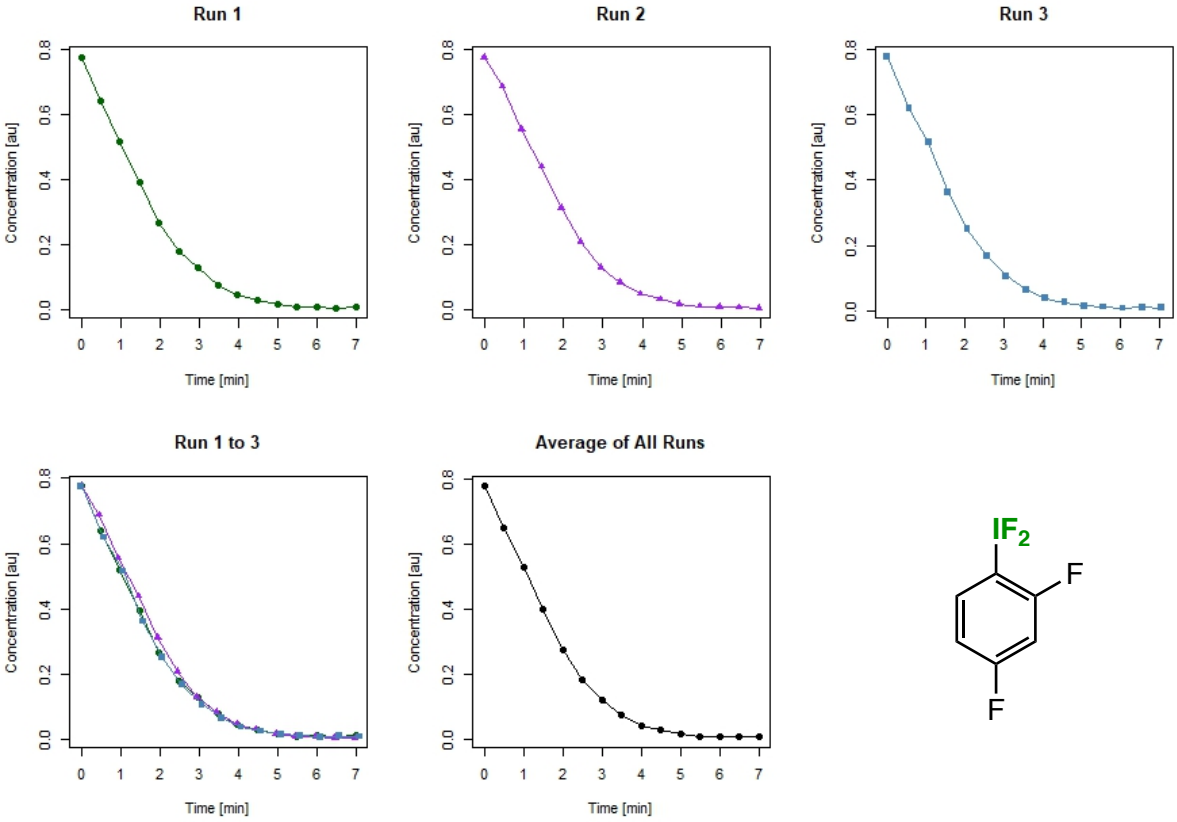

Run 1		Run2		Run 3	
Time [min]	**Relative Integral**	**Time [min]**	**Relative Integral**	**Time [min]**	**Relative Integral**
0.00	1.29	0.00	1.30	0.00	1.34
0.48	1.56	0.45	1.47	0.57	1.68
0.98	1.93	0.95	1.82	1.07	2.02
1.48	2.54	1.45	2.30	1.57	2.88
1.98	3.75	1.95	3.24	2.07	4.16
2.48	5.59	2.45	4.86	2.57	6.21
2.98	7.73	2.95	7.88	3.07	9.80
3.48	12.9	3.45	12.1	3.57	16.1
3.98	21.5	3.95	21.4	4.07	27.6
4.48	34.4	4.45	32.8	4.57	42.1
4.98	58.9	4.95	64.2	5.07	72.0
5.48	105	5.45	114	5.57	91.7
5.98	89.9	5.95	129	6.07	138
6.48	162	6.45	213	6.57	105
6.98	98.0	6.95	365	7.07	127

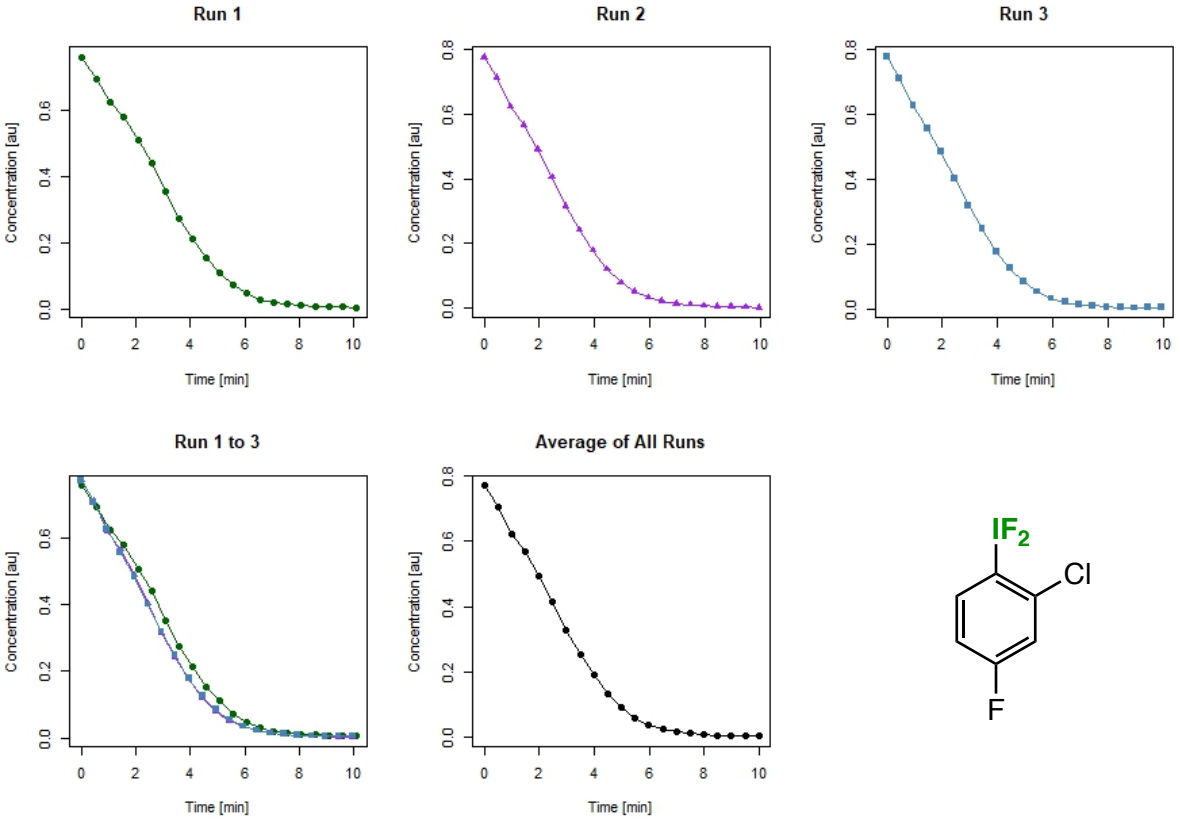

Run 1		Run2		Run 3	
Time [min]	Relative Integral	Time [min]	Relative Integral	Time [min]	Relative Integral
0.00	1.16	0.00	1.22	0.00	1.18
0.58	1.27	0.45	1.33	0.45	1.29
1.08	1.41	0.95	1.52	0.95	1.46
1.58	1.52	1.45	1.67	1.45	1.64
2.08	1.73	1.95	1.93	1.95	1.89
2.58	1.99	2.45	2.34	2.45	2.28
3.08	2.49	2.95	3.01	2.95	2.86
3.58	3.20	3.45	3.91	3.45	3.69
4.08	4.11	3.95	5.30	3.95	5.12
4.58	5.70	4.45	7.79	4.45	7.24
5.08	7.91	4.95	12.0	4.95	10.7
5.58	12.2	5.45	18.3	5.45	16.5
6.08	18.0	5.95	28.2	5.95	26.4
6.58	28.7	6.45	43.7	6.45	40.3
7.08	43.3	6.95	65.8	6.95	62.9
7.58	53.8	7.45	82.8	7.45	80.0
8.08	81.4	7.95	117	7.95	109
8.58	102	8.45	175	8.45	147
9.08	129	8.95	204	8.95	175
9.58	119	9.45	297	9.45	137
10.08	193	9.95	798	9.95	136

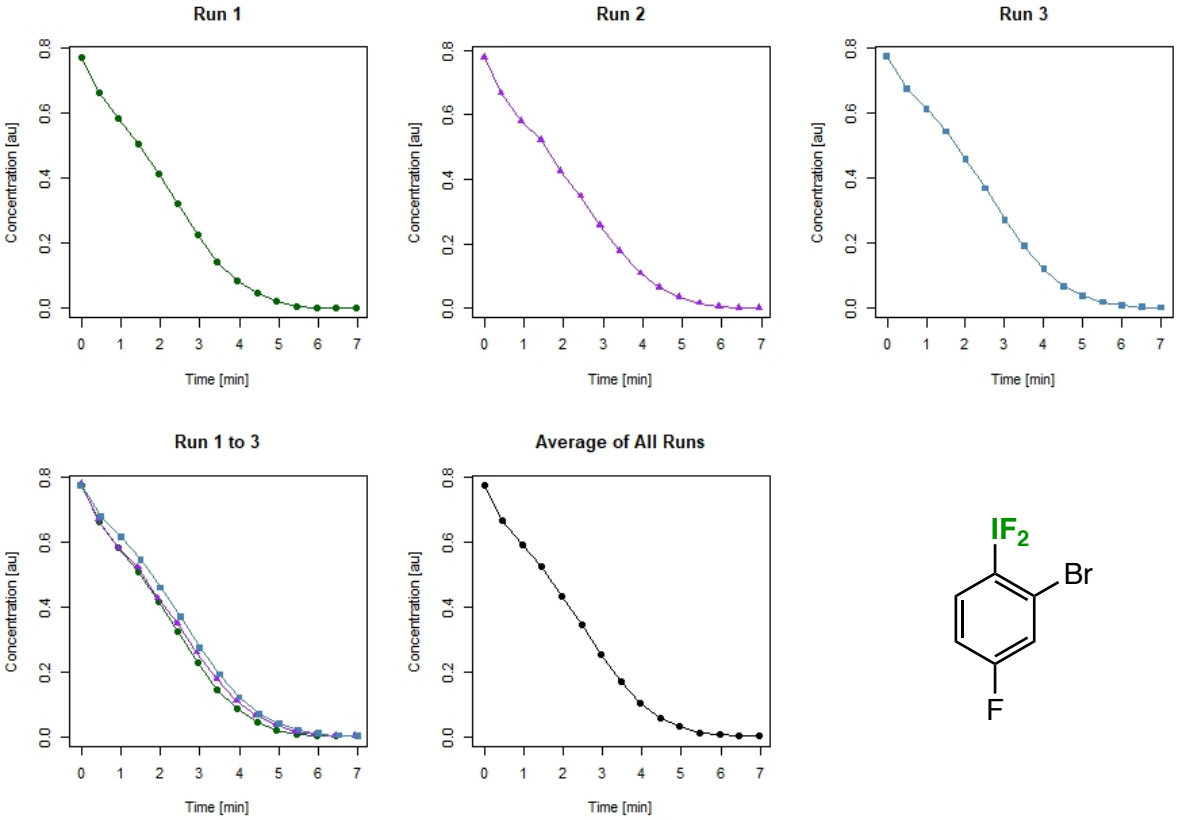

Run 1		Run2		Run 3	
Time [min]	**Relative Integral**	**Time [min]**	**Relative Integral**	**Time [min]**	**Relative Integral**
0.00	1.27	0.00	1.26	0.00	1.23
0.45	1.48	0.43	1.47	0.52	1.41
0.95	1.68	0.93	1.69	1.02	1.55
1.45	1.94	1.43	1.88	1.52	1.75
1.95	2.37	1.93	2.30	2.02	2.08
2.45	3.04	2.43	2.82	2.52	2.58
2.95	4.32	2.93	3.80	3.02	3.50
3.45	6.89	3.43	5.52	3.52	5.00
3.95	11.5	3.93	9.05	4.02	7.98
4.45	21.5	4.43	15.2	4.52	14.1
4.95	47.4	4.93	27.6	5.02	25.2
5.45	205	5.43	61.1	5.52	51.3
5.95	641	5.93	135	6.02	113
6.45	3736	6.43	487	6.52	351
6.95	1159	6.93	532	7.02	567

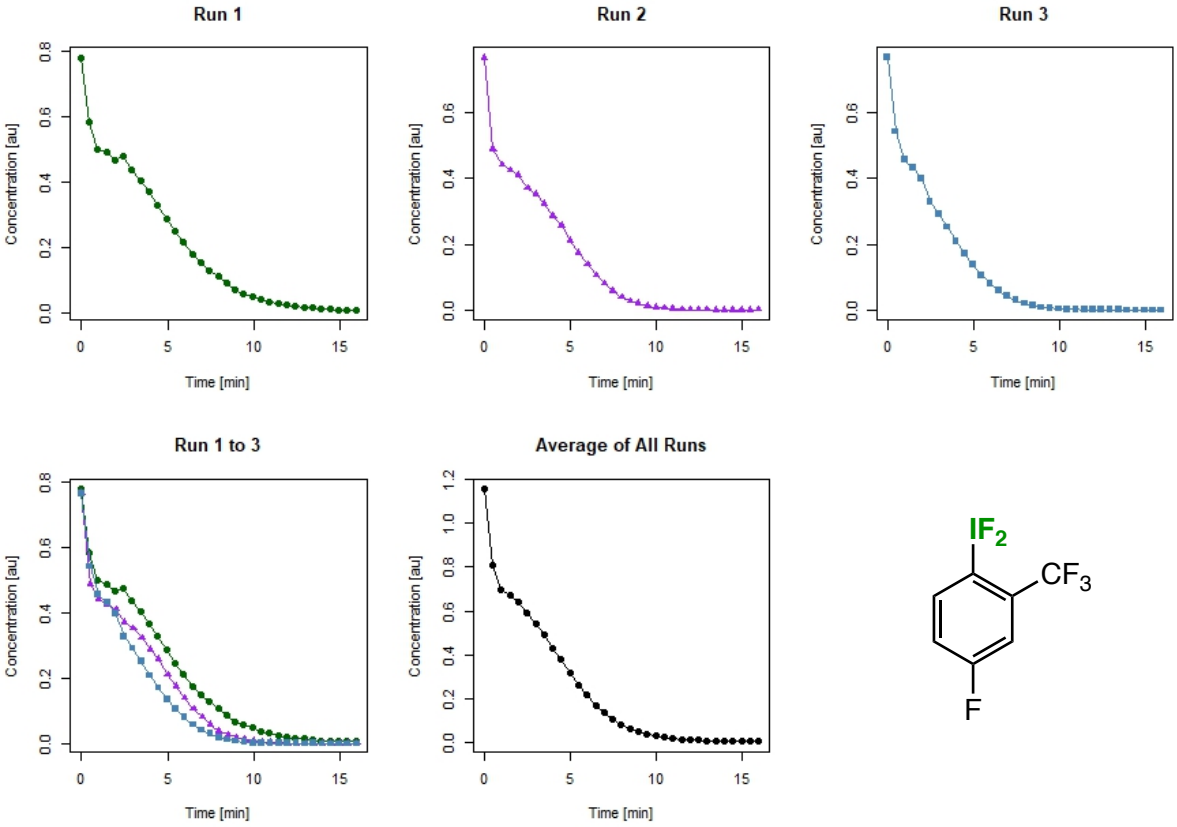

Run 1		Run2		Run 3	
Time [min]	Relative Integral	Time [min]	Relative Integral	Time [min]	Relative Integral
0.00	0.27	0.00	0.30	0.00	0.34
0.43	0.36	0.50	0.47	0.48	0.48
0.93	0.42	1.00	0.52	0.98	0.57
1.43	0.43	1.50	0.54	1.48	0.60
1.93	0.45	2.00	0.56	1.98	0.65
2.43	0.44	2.50	0.62	2.48	0.79
2.93	0.48	3.00	0.65	2.98	0.89
3.43	0.52	3.50	0.71	3.48	1.03
3.93	0.57	4.00	0.80	3.98	1.24
4.43	0.64	4.50	0.89	4.48	1.51
4.93	0.73	5.00	1.09	4.98	1.89
5.43	0.85	5.50	1.31	5.48	2.43
5.93	0.98	6.00	1.64	5.98	3.20
6.43	1.18	6.50	2.15	6.48	4.38
6.93	1.38	7.00	2.79	6.98	6.08
7.43	1.63	7.50	3.85	7.48	8.43
7.93	1.91	8.00	5.82	7.98	12.2
8.43	2.35	8.50	8.00	8.48	18.5
8.93	3.09	9.00	11.1	8.98	28.8
9.43	3.57	9.50	16.4	9.48	36.0
9.93	4.19	10.00	23.1	9.98	57.7
10.43	5.29	10.50	32.4	10.48	74.3
10.93	6.41	11.00	50.0	10.98	89.4
11.43	7.74	11.50	61.4	11.48	140
11.93	9.37	12.00	92.5	11.98	131
12.43	11.7	12.50	96.4	12.48	143
12.93	13.2	13.00	89.0	12.98	210
13.43	15.4	13.50	141	13.48	136
13.93	19.2	14.00	115	13.98	274
14.43	20.4	14.50	154	14.48	316
14.93	24.7	15.00	112	14.98	327
15.43	25.4	15.50	243	15.48	362
15.93	28.0	16.00	89.2	15.98	366

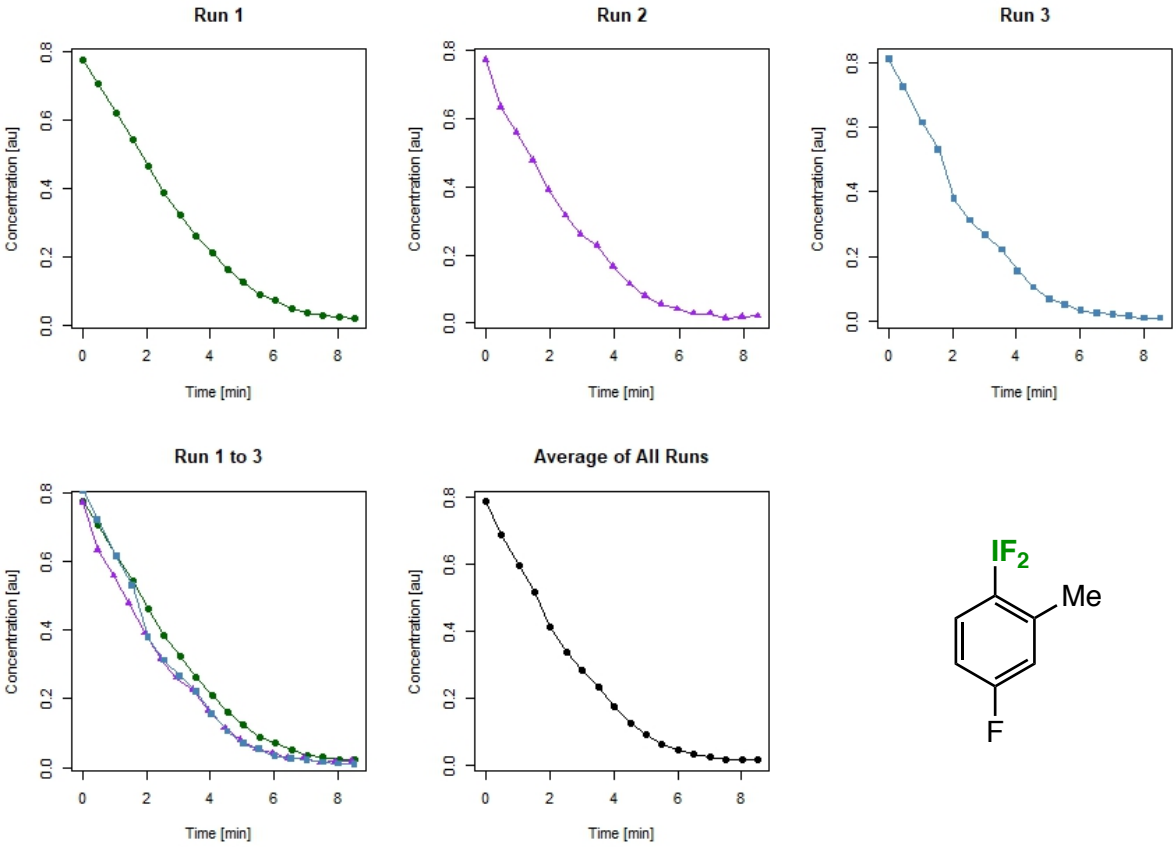

Run 1		Run2		Run 3	
Time [min]	**Relative Integral**	**Time [min]**	**Relative Integral**	**Time [min]**	**Relative Integral**
0.00	1.73	0.00	1.72	0.00	1.77
0.45	1.90	0.45	2.10	0.45	1.98
1.05	2.17	0.95	2.38	1.05	2.33
1.55	2.47	1.45	2.78	1.55	2.70
2.05	2.89	1.95	3.40	2.05	3.78
2.55	3.47	2.45	4.21	2.55	4.59
3.05	4.15	2.95	5.11	3.05	5.39
3.55	5.12	3.45	5.88	3.55	6.47
4.05	6.36	3.95	8.02	4.05	9.19
4.55	8.28	4.45	11.6	4.55	13.7
5.05	10.7	4.95	16.6	5.05	20.7
5.55	15.0	5.45	24.5	5.55	27.4
6.05	18.6	5.95	32.3	6.05	44.2
6.55	27.0	6.45	48.9	6.55	56.6
7.05	37.7	6.95	48.3	7.05	68.7
7.55	45.3	7.45	98.7	7.55	98.0
8.05	55.4	7.95	75.0	8.05	143
8.55	64.6	8.45	68.0	8.55	145

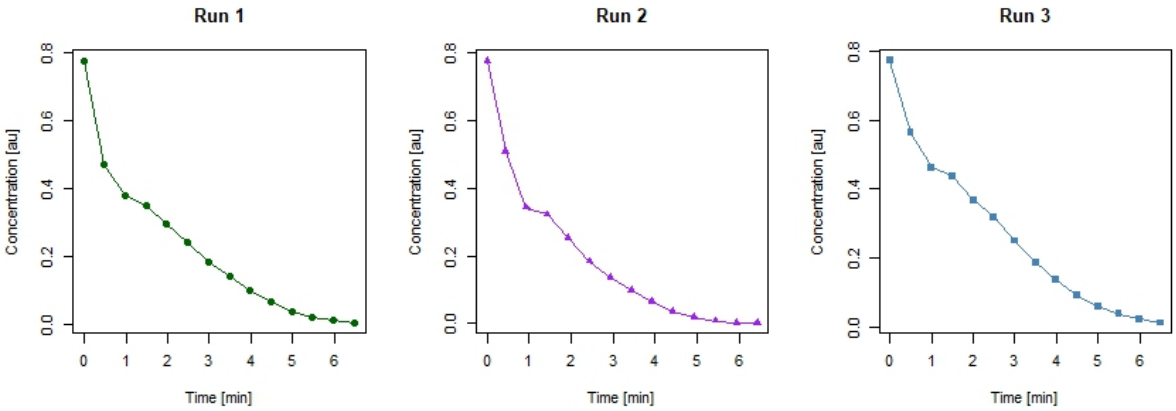

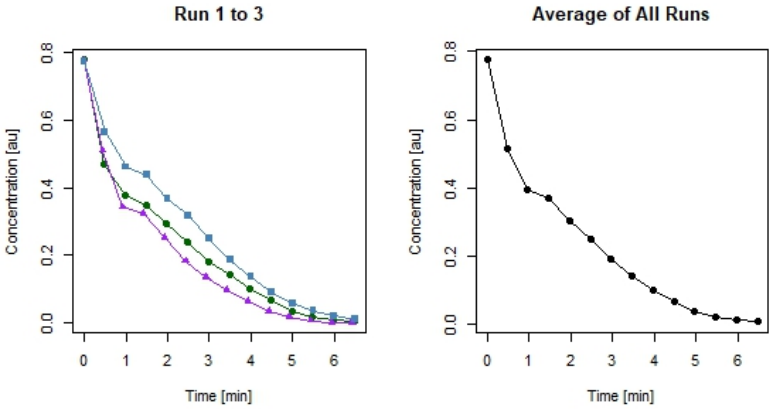

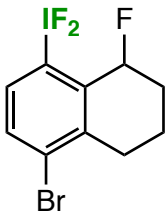

Run 1		Run2		Run 3	
Time [min]	**Relative Integral**	**Time [min]**	**Relative Integral**	**Time [min]**	**Relative Integral**
0.00	1.48	0.00	1.52	0.00	1.32
0.48	2.44	0.43	2.32	0.50	1.81
0.98	3.03	0.93	3.45	1.00	2.21
1.48	3.29	1.43	3.66	1.50	2.33
1.98	3.90	1.93	4.67	2.00	2.78
2.48	4.76	2.43	6.45	2.50	3.21
2.98	6.30	2.93	8.66	3.00	4.09
3.48	8.08	3.43	12.1	3.50	5.47
3.98	11.3	3.93	18.5	4.00	7.48
4.48	17.2	4.43	33.0	4.50	11.3
4.98	32.4	4.93	61.0	5.00	17.4
5.48	58.0	5.43	152	5.50	28.2
5.98	108	5.93	708	6.00	48.0
6.48	304	6.43	480	6.50	92.5

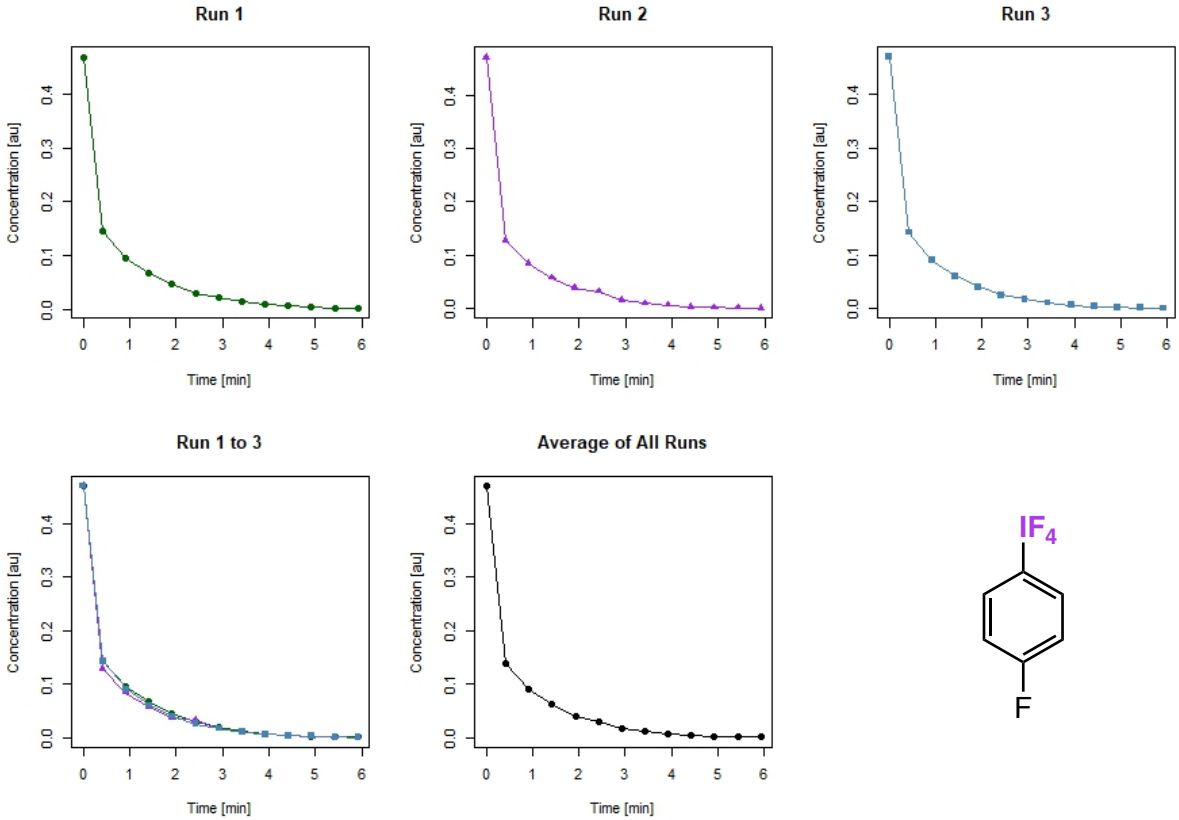

Run 1		Run2		Run 3	
Time [min]	**Relative Integral**	**Time [min]**	**Relative Integral**	**Time [min]**	**Relative Integral**
0.00	0.42	0.00	0.47	0.00	0.63
0.42	1.36	0.42	1.72	0.43	2.07
0.92	2.06	0.92	2.62	0.93	3.29
1.42	2.93	1.42	3.83	1.43	4.89
1.92	4.33	1.92	5.71	1.93	7.36
2.42	6.55	2.42	6.78	2.43	11.5
2.92	9.56	2.92	13.2	2.93	16.9
3.42	15.4	3.42	21.4	3.43	27.3
3.92	24.1	3.92	32.0	3.93	41.9
4.42	34.7	4.42	52.1	4.43	70.7
4.92	52.8	4.92	78.4	4.93	95.0
5.42	84.8	5.42	111	5.43	187
5.92	146	5.92	223	5.93	296

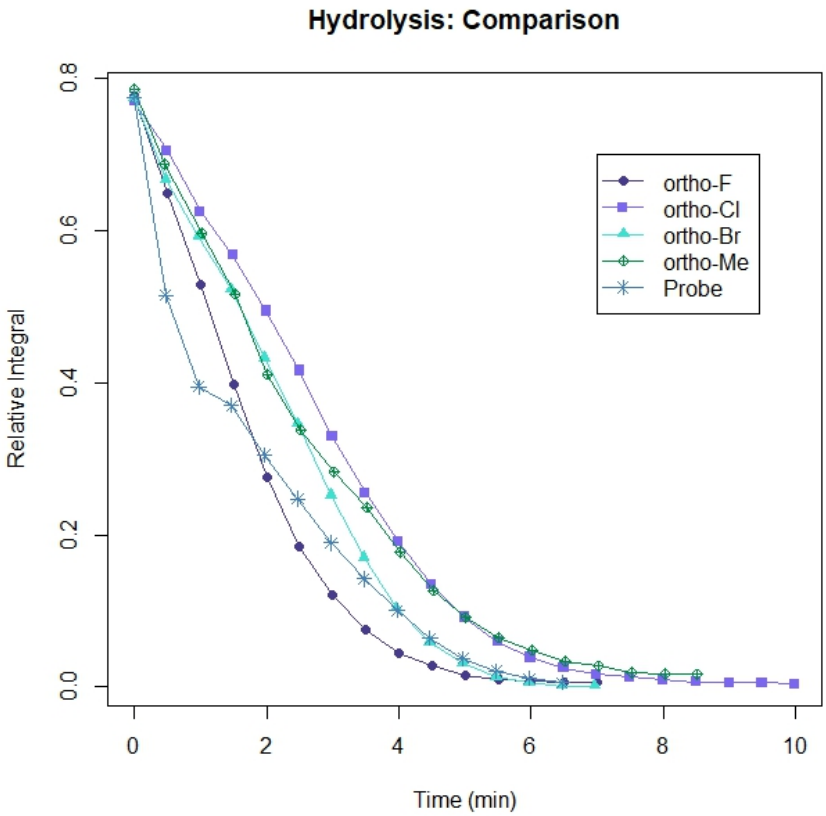

Figure S 105. Overlay of hydrolysis data comparing a variety of *ortho*-substituents, as well as probe molecule **21**.

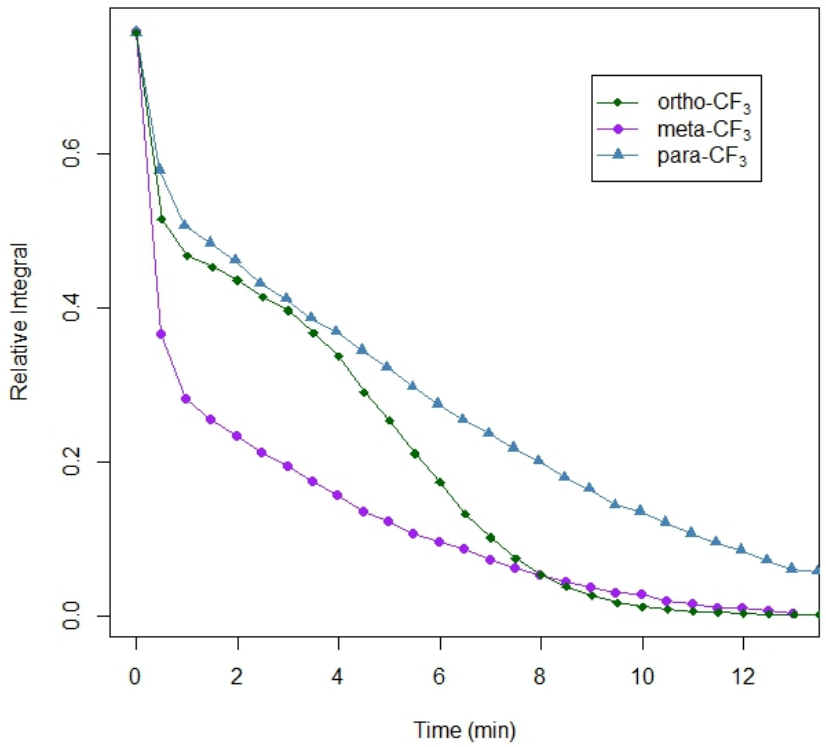

Figure S 106. Overlay of hydrolysis data comparing *ortho*-, *meta*-, and *para*-trifluoromethyl substituted isomers.

Computational Data

Table S 10. Coordinates for calculated structure of compound **2**.

Compound 2 Re atomic coordinates (Angstroms) and total energy (Hartree)

C	-2.45308564	2.42808429	-0.26126747
C	-2.58121925	1.05458712	-0.09186804
C	-1.45995599	0.22308103	0.00756419
C	-0.19976895	0.82504744	-0.07507097
C	-0.05601404	2.20315990	-0.21327767
C	-1.18858654	3.00573838	-0.30800526
H	-3.34720486	3.04777906	-0.33776606
H	-3.57079152	0.60589750	-0.01460360
H	0.93990417	2.64315945	-0.21564040
H	-1.07249387	4.08435939	-0.42043685
I	1.64719281	-0.23135318	-0.04635436
F	2.32283879	1.32566742	1.05062156
F	0.77632416	-1.60634625	-1.21270632
C	-1.73722783	-1.25209651	0.24310225
F	-0.78273270	-1.84936142	0.96684023
F	-1.89789800	-1.92551611	-0.89511096
F	-2.88469710	-1.39389770	0.93904059

E(RwB97XD) = -1063.88312776 au

Table S 11. Coordinates for calculated structure of compound **21**.

Compound 21 Re atomic coordinates (Angstroms) and total energy (Hartree)

C	-0.52146700	2.01315100	-0.00454200
C	0.40897000	3.16293500	-0.32042500
C	1.70131900	3.02320100	0.46867200
C	2.43727900	1.75963000	0.04105900
H	-1.38887200	2.02214600	-0.67543000
H	0.61289800	3.16253500	-1.40473600
H	-0.11654500	4.09912100	-0.08570100
H	2.35239900	3.89685900	0.32559600
H	1.45654300	2.96876700	1.54142500
H	2.89161300	1.90570600	-0.95572400
H	3.27423600	1.55477400	0.72356200
C	1.33229700	-1.90586800	-0.06110300
C	-0.05232000	-1.79397700	-0.05957200
C	-0.61136100	-0.52525400	-0.08405700
C	0.14711400	0.64993300	-0.06121400
C	1.55180300	0.53406600	-0.02400300
C	2.10958900	-0.75400300	-0.05855700
H	1.80366300	-2.88786500	-0.06427300
H	-0.67758000	-2.68456600	-0.02289700
F	-1.00921900	2.17803700	1.30342000
Br	3.99700700	-0.98486100	-0.09621400
I	-2.73571800	-0.50283200	-0.08635400
F	-2.65052200	0.75644500	-1.67478900
F	-2.57691400	-1.81227400	1.43191400

E(RwB97XD) = -3555.74338716 au

Table S 12. Coordinates for calculated structure of compound **21-*iso***.

Compound 21-iso local minimum atomic coordinates (Angstroms) and total energy (Hartree)

C	0.43417500	1.93546700	0.12722700
C	-0.46644500	3.06374700	0.57970400
C	-1.76671700	3.03438100	-0.21034200
C	-2.52927300	1.74746200	0.08310600
H	1.31061500	1.85250200	0.78511900
H	-0.66405900	2.94488700	1.65857900
H	0.07357600	4.01133500	0.44548900
H	-2.39721300	3.90155900	0.03136300
H	-1.52780100	3.09339900	-1.28414800
H	-2.99270300	1.80379200	1.08457900
H	-3.36278400	1.62660800	-0.62388000
C	-1.48330400	-1.93519000	-0.06847600
C	-0.09392300	-1.83581400	-0.08486400
C	0.50821600	-0.58346800	-0.02915900
C	-0.26179500	0.58912400	0.04905000
C	-1.66444200	0.50690500	0.03672300
C	-2.24266200	-0.77531600	-0.00479500
H	-1.97033100	-2.90943500	-0.09660900
H	0.50597200	-2.74732700	-0.12701000
F	0.91839600	2.23773700	-1.15797100
Br	-4.13411200	-0.97538400	0.04120600
I	2.65068900	-0.57939200	-0.24223700
F	4.59781200	-0.46391500	0.28627800
F	2.55370000	0.09119500	1.61100700

E(RwB97XD) = -3555.70250332 au

Table S 13. Coordinates for calculated structure of compound **22**.

Compound 22 Re atomic coordinates (Angstroms) and total energy (Hartree)

C	-2.14949900	1.78796600	-0.01087100
C	-2.05746700	0.39867600	-0.01384500
C	-0.81470000	-0.23809100	-0.01133900
C	0.31298200	0.56574600	-0.00137700
C	0.26664600	1.95490500	0.00341600
C	-0.98849400	2.55909100	-0.00175900
H	-3.12806600	2.26637100	-0.01846700
H	1.18928600	2.53329900	0.00907700
H	-1.05795800	3.64756200	-0.00053100
I	2.22278600	-0.38455800	0.00039900
F	3.01928500	1.46880800	0.00490700
F	1.22339500	-2.13648500	-0.00429400
C	-3.29708200	-0.45946200	-0.00004600
F	-4.41004900	0.25949900	-0.21383500
F	-3.44586600	-1.08378300	1.18033900
F	-3.24499200	-1.41414800	-0.94236500
H	-0.72120700	-1.32364800	-0.01905900

E(RwB97XD) = -1063.89879005 au

Table S 14. Coordinates for calculated structure of compound **23**.

Compound 23 Re atomic coordinates (Angstroms) and total energy (Hartree)

C	2.335359	0.024911	0.000019
C	1.639226	1.230154	0.000040
C	0.244471	1.234364	0.000032
C	-0.403461	0.008408	0.000005
C	0.259478	-1.213288	-0.000014
C	1.650234	-1.191595	-0.000006
H	-0.302054	-2.146243	-0.000032
H	2.202271	-2.132237	-0.000015
I	-2.535643	-0.004386	-0.000003
F	-2.425623	-2.017839	0.000028
F	-2.450619	2.009917	-0.000030
H	-0.326483	2.161543	0.000051
6	3.842113	0.004303	-0.000002
F	4.322368	-0.637531	-1.078825
F	4.322392	-0.638084	1.078481
F	4.368105	1.238055	0.000306
H	2.181229	2.175167	0.000066

E(RwB97XD) = -1063.89881725 au

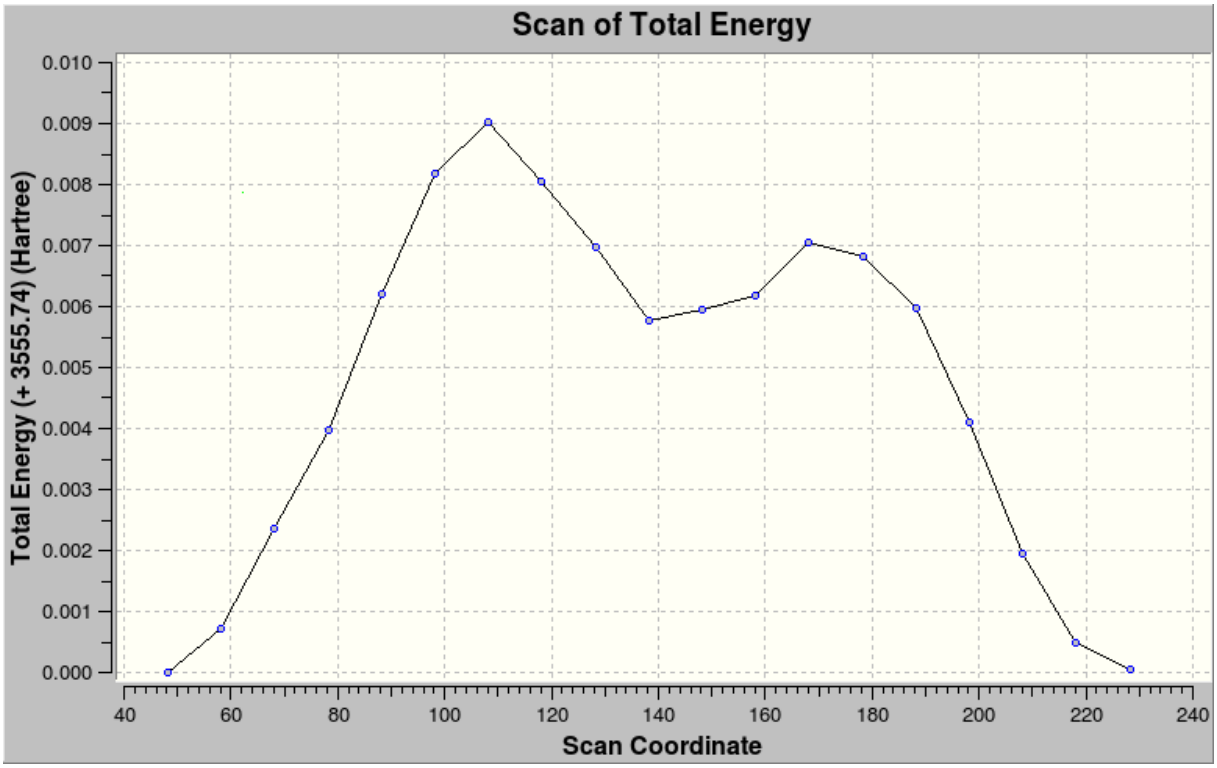

Figure S 107. Rotational scan for compound **21**. Compound **21** was optimized at the wB97xD/cc-pvdz level of theory (cc-pvdz-PP for the iodine atom), and then the IF_2 group was rotated 180° about the C-I bond in 12° increments.

Table S 15. Coordinates for highest-energy calculated structure of compound **21** in Figure S 107.

Compound 21 atomic coordinates (Angstroms) and total energy (Hartree) at maximum point of potential curve (see: Figure S 107) for rotation about C-I bond

C	-0.53315523	1.95794117	-0.35556356
C	0.40483503	3.00301751	-0.92299284
C	1.66796176	3.06598829	-0.07804499
C	2.42403628	1.74742107	-0.17891451
H	-1.38299308	1.80604478	-1.03964619
H	0.64552343	2.74004972	-1.96725193
H	-0.12709149	3.96448228	-0.93847868
H	2.31948020	3.89145337	-0.39671952
H	1.38144659	3.25910484	0.96765185
H	2.94963220	1.68691618	-1.14876409
H	3.21018277	1.69409225	0.58833166
C	1.34641383	-1.90902299	0.16159121
C	-0.03942756	-1.80905422	0.14503632
C	-0.61691788	-0.55122575	0.04612122
C	0.13789144	0.61922819	-0.10447884
C	1.54287616	0.52342063	-0.05546204
C	2.11246096	-0.75384275	0.07228243
H	1.82687525	-2.88298443	0.24642046
H	-0.64976208	-2.70832238	0.21599999
F	-1.05903217	2.43378364	0.84317381
Br	4.00210816	-0.96187253	0.10185641
I	-2.72736861	-0.52251480	0.00019069
F	-2.51825398	-1.27053788	-1.86395312
F	-2.68697960	0.23061637	1.85632697

E(RwB97XD) = -3555.73436000 au

Single-crystal X-ray Structural Data

General

Single crystalline samples were measured on a Rigaku Oxford Diffraction XtaLAB Synergy-S Dualflex kappa diffractometer equipped with a Dectris Pilatus 300 HPAD detector and using microfocus sealed tube Cu-*K*α radiation with mirror optics (λ = 1.54178 Å, **21**&**26**) and a Bruker APEX-II fixed-chi diffractometer with sealed tube, graphite-monochromated Mo-*K*α radiation (λ = 0.71073 Å, **37**). All measurements were carried out at 100K using an Oxford Cryosystems Cryostream 800 or Bruker Kryoflex sample cryostat. Samples **21**&**26** were retrieved, prepared and mounted on Kapton micromounts (MiTeGen) under a nitrogen atmosphere at low temperatures (253 to 273K) using a *μ*CHILL microscopy stage to prevent crystal damage.[11]

Data collected on the Bruker instrument were integrated using SAINT from the Bruker Apex-II program. Data collected on the Rigaku instrument were integrated using CrysAlisPro and corrected for absorption effects using a combination of empirical (ABSPACK) and numerical corrections.[12] The structures were solved using SHELXS[13] or SHELXT[14] and refined by full-matrix least-squares analysis (SHELXL)[13,15] using the program package OLEX2.[16] Non-hydrogen atoms were refined anisotropically and hydrogen atoms were constrained to ideal geometries and refined with fixed isotropic displacement parameters (in terms of a riding model). CCDC 1913138-1913140 contain the supplementary crystallographic data for this paper, including structure factors and refinement instructions. These data can be obtained free of charge from The Cambridge Crystallographic Data Centre, 12 Union Road, Cambridge CB2 1EZ, UK (fax: +44(1223)-336-033; e-mail: deposit@ccdc.cam.ac.uk), or *via* https://www.ccdc.cam.ac.uk/structures.

[11] M. Solar and N. Trapp, *J. Appl. Cryst.*, 2018, **51**, 541.
[12] *CrysAlisPro and ABSPACK*. Rigaku Oxford Diffraction, 2016.
[13] G. M. Sheldrick, *Acta Cryst*., 2008, **A64**, 112.
[14] G. M. Sheldrick, *Acta Cryst*., 2015, **A71**, 3.
[15] G. M. Sheldrick, *Acta Cryst*., 2015, **C71**, 3.
[16] O. V. Dolomanov, L. J. Bourhis, R. J. Gildea, J. A. K. Howard, and H. Puschmann, *J. Appl. Cryst*., 2009, **42**, 339.

Crystal structure data

	21	**26**	**37**
CCDC No.	1913138	1913139	1913140
Empirical formula	$C_{10}H_9BrF_3I$	$C_6H_4F_5I$	$C_9H_{10}F_3IO$
Formula weight	392.98	297.99	318.07
Temperature/K	100.0(1)	100.0(1)	100.0(2)
Crystal system	monoclinic	monoclinic	monoclinic
Space group	*C*2/*c*	$P2_1/n$	$P2_1/c$
a/Å	23.483(2)	8.90830(10)	15.2690(11)
b/Å	8.4119(3)	6.03640(10)	10.8007(9)
c/Å	15.9818(15)	14.1452(2)	13.7770(11)
β/°	134.610(17)	91.6270(10)	116.7259(14)
Volume/Å^3	2247.4(6)	760.338(19)	2029.3(3)
Z	8	4	8
ρ_{calc} g/cm^3	2.323	2.603	2.082
μ/mm^{-1}	26.661	33.528	3.164
F(000)	1472.0	552.0	1216.0
Crystal size/mm^3	0.129 × 0.108 × 0.014	0.168 × 0.127 × 0.061	0.078 × 0.031 × 0.025
Crystal description	clear colourless plate	clear colourless block	clear colourless plate
Radiation	Cu*K*α (λ = 1.54184)	Cu*K*α (λ = 1.54184)	Mo*K*α (λ = 0.71073)
2Θ range for data collection/°	10.584 to 156.888	11.592 to 156.632	2.986 to 61.238
Index ranges	-28 ≤ h ≤ 29 -10 ≤ k ≤ 10 -18 ≤ l ≤ 20	-11 ≤ h ≤ 11 -7 ≤ k ≤ 5 -17 ≤ l ≤ 17	-21 ≤ h ≤ 21 -15 ≤ k ≤ 15 -19 ≤ l ≤ 19
Reflections collected	11254	7652	33393
Independent reflections	2383 R_{int} = 0.0334 R_{sigma} = 0.0188	1608 R_{int} = 0.0380 R_{sigma} = 0.0196	6167 R_{int} = 0.1044 R_{sigma} = 0.0783
Data/restraints/parameters	2383/86/173	1608/0/109	6167/0/258
Goodness-of-fit on F^2	1.109	1.141	0.989
Final *R* indexes [$I \geq 2\sigma(I)$]	R_1 = 0.0310 wR_2 = 0.0841	R_1 = 0.0276 wR_2 = 0.0784	R_1 = 0.0464 wR_2 = 0.0842
Final *R* indexes [all data]	R_1 = 0.0322 wR_2 = 0.0848	R_1 = 0.0278 wR_2 = 0.0787	R_1 = 0.0676 wR_2 = 0.0909
Largest diff. peak/hole /eÅ^{-3}	0.98/-1.49	0.81/-1.57	2.83/-2.30

Notes on crystal structures

(4-Bromo-8-fluoro-5,6,7,8-tetrahydronaphthalen-1-yl)difluoro-λ^3-iodane (21)

Clear colourless platelet crystals of **21** were obtained by slow solvent evaporation of a mixture of DCM and n-hexane under inert atmosphere in a PFA vessel. The structure contains one molecule per asymmetric unit and exhibits a special kind of disorder, in which both possible enantiomers co-crystallize on the same position. Atoms outside the fluorinated hexyl subunit almost exactly overlap, with slightly expanded anisotropic displacement parameters observed for the fluorine atoms connected to iodine (Figure S108).

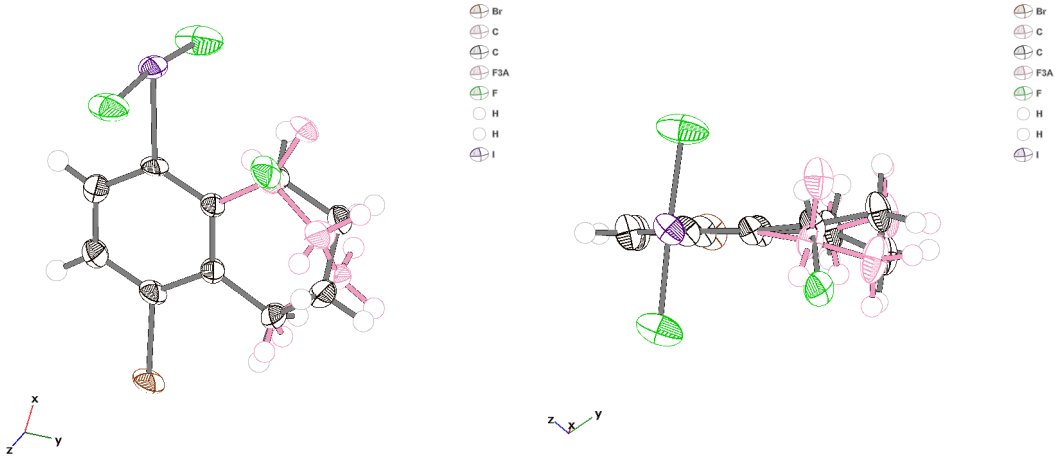

Figure S 108. Asymmetric unit of the crystal structure of **21**, ellipsoids depicted at 50% probability, minor part of disorder drawn in magenta.

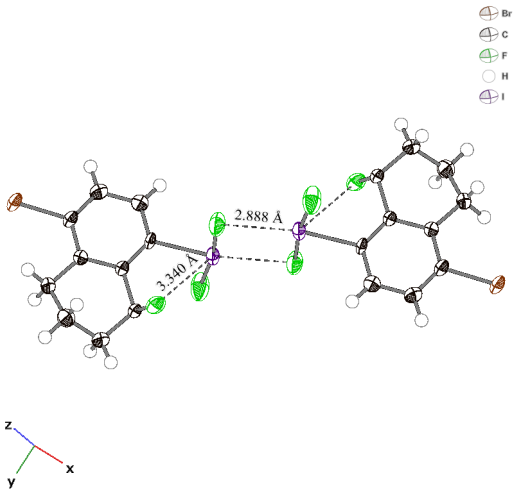

Figure S 109. Closest C-I…F contacts in the crystal structure of **21**, ellipsoids depicted at 50% probability.

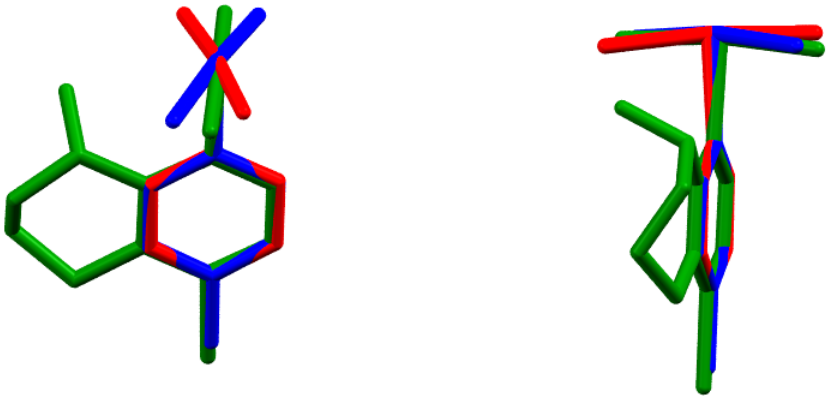

Figure S 110. Comparison of the geometry of **21** with both symmetry-independent moieties observed in the known crystal structure of 1-(Difluoroiodo)-4-methylbenzene, recorded at 100K (red/blue, coordinates as deposited under CCDC 1555065).[17]

Table S 16. Selected geometrical parameters from the crystal structure of **21** compared to previously reported compounds. For multiple occurrences (partly due to multiple symmetrically independent moieties within the same structures), averaged values are printed in italics. C_{ortho} refers to the unsubstituted side for compound **21** and to the torsion angles < 90° for all other compounds.

	21	1-(Difluoroiodo)-4-methylbenzene[17]	all known compounds[17,18,19,20,21,22]
d(C-I)/Å (range/Å)	2.097(7)	*2.088* 2.083-2.093	*2.089* 2.051-2.115
d(I-F)/Å (range/Å)	*1.998* 1.998(3)-1.998(4)	*2.013* 1.993-2.036	*2.003* 1.96-2.032
F-I-F/° (range/°)	171.9(2)	*172.0* 170.8-173.3	*168.2* 158.6-174.4
C-I-F/° (range/°)	*86.0* 85.5(2)-86.5(2)	*86.2* 85.08-87.62	*84.0* 79.2-88.3
C_{ortho}-C_{ipso}-I-F/° (range/°)	*82.9* 82.4(3)-83.4(3)	*70.0* 60.9-79.3	*70.0* 60.9-79.3
shortest C-I…F-I/Å	2.888(3)	2.905	2.742
shortest I-F…F-I/Å	2.891(3)	2.793	2.766

[17] J. C. Sarie, C. Thiehoff, R. J. Mudd, C. G. Daniliuc, G. Kehr, and R. Gilmour, *J. Org. Chem.*, 2017, **82**, 11792.
[18] CCDC 1555065,[17] 273254,[19] 139385,[20] 938893,[21] 760658,[22] 760659, [22] 760660. [22]
[19] C. Ye, B. Twamley, and J. M. Shreeve, *Org. Lett.*, 2005, **7**, 3961.
[20] F. Bailly, P. Barthen, W. Breuer, H.-J. Frohn, M. Giesen, J. Helber, G. Henkel, and A. Priwitzer, *Z. Anorg. Allg. Chem.*, 2000, **626**, 1406.
[21] U. Flörke, *CSD Private Communication*, 2013.
[22] H.-J.Frohn, M. E. Hirschberg, U. Westphal, U. Flörke, R. Boese, and D. Bläser, *Z. Anorg. Allg. Chem.*, 2009, **635**, 2249.

Tetrafluoro(4-fluorophenyl)-λ^5-iodane (26)

Clear colourless block-shaped crystals of **26** were obtained by cooling a concentrated solution in n-hexane in a PFA vessel to ca. -20 °C in a glove box freezer. The structure contains one molecule per asymmetric unit (Figure S111).

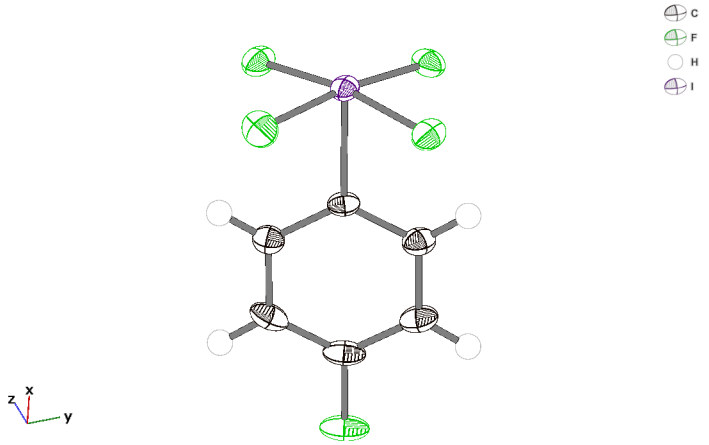

Figure S 111. Asymmetric unit of the crystal structure of **26**, ellipsoids depicted at 50% probability.

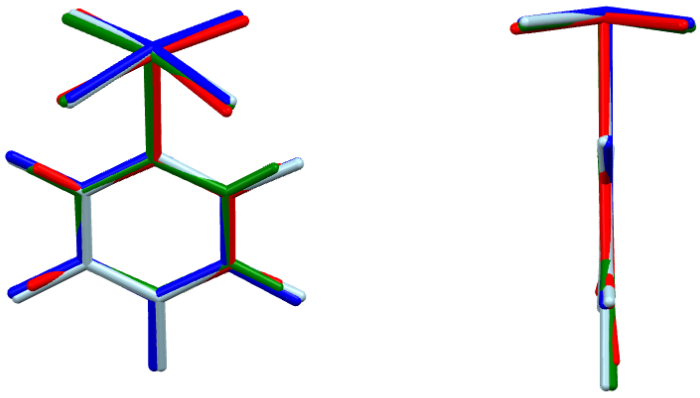

Figure S 112. Overlay of the geometries of **26** (green) and two known tetrafluoro-iodane crystal structures, CCDC 216480 (red, RT)[25] and CSD 59004/FIZ Karlsruhe (two symmetry-independent moieties depicted blue/light blue, 150K).[24]

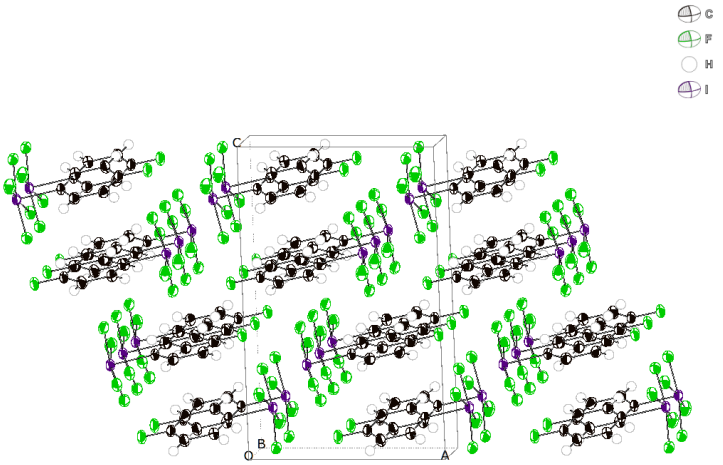

Figure S 113. Packing motif of **26**, ellipsoids depicted at 50% probability.

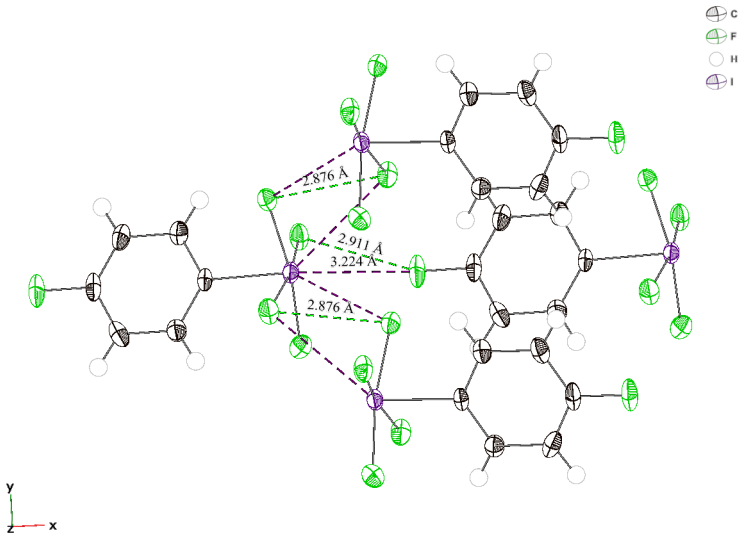

Figure S 114. Intermolecular I…F (purple broken lines) and F…F contacts (green broken lines) within the sum of van-der-Waals radii in the crystal structure of **26**, ellipsoids depicted at 50% probability.

Table S 17. Selected geometrical parameters from the crystal structure of **26** compared to previously reported compounds. For multiple occurrences (partly due to multiple symmetrically independent moieties within the same structures), averaged values are printed in italics. In the structure of pentafluorophenyl-tetrakis(fluoro)iodine,[23,24] one of two symmetry-independent moieties is located on a crystallographic 2-fold axis through the C-I bond.

	26	Phenyl-tetrafluoro-iodine[23,25]	Pentafluorophenyl-tetrakis(fluoro)iodine[23,24]
d(C-I)/Å (range/Å)	2.078(4)	2.082	*2.085* 2.082-2.088
d(I-F)/Å (range/Å)	*1.939* 1.915(1)-1.960(1)	*1.935* 1.922-1.951	*1.917* 1.906-1.928
trans F-I-F/° (range/°)	*170.1* 169.9(1)-170.4(1)	*170.5* 170.0-171.0	*168.5* 167.8-169.3
cis F-I-F/° (range/°)	*89.6* 87.6(1)-90.7(1)	*89.6* 87.1-91.2	*89.4* 87.3-91.3
C-I-F/° (range/°)	*85.1* 83.9(1)-86.7(1)	*85.4* 84.4-85.9	*84.3* 83.1-84.9
$\lvert C_{ortho}\text{-}C_{ipso}\text{-I-F}\rvert$/° (range/°)	*44.7* 42.0(1)-47.8(1)	*44.8* 41.8-48.8	*45.6* 44.4-46.8
shortest C-I…F-I/Å	2.999(1)	3.072	3.046
shortest I-F…F-I/Å	2.876(2)	3.035	2.744

1,1,1-Trifluoro-3,3-dimethyl-1,3-dihydro-1λ^5-benzo[*d*][1,2]iodaoxole (37)

Clear colourless platelet crystals of **37** were obtained by sublimation. The structure contains two symmetry-independent molecules per asymmetric unit with slightly differing rotation angles about the C-I axes (O-I-C1-C2 torsion angles 172.9° *vs.* 174.7°).

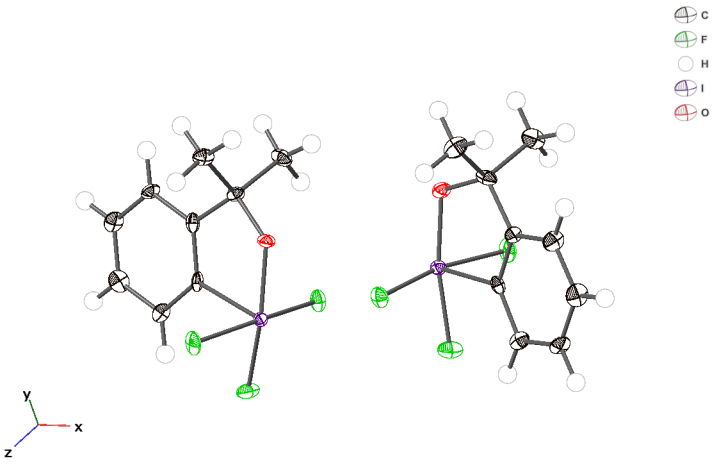

Figure S 115. Asymmetric unit of the crystal structure of **37**, ellipsoids depicted at 50% probability.

[23] CCDC 216480,[25] CSD 59004 (FIZ Karlsruhe).[24]
[24] H.-J. Frohn, S. Görg, G. Henkel, and M. Läge, *Z. Anorg. Allg. Chem.*, 1995, **621**, 1251.
[25] S. Hoyer and K. Seppelt, *J. Fluorine Chem.*, 2004, **125**, 989.

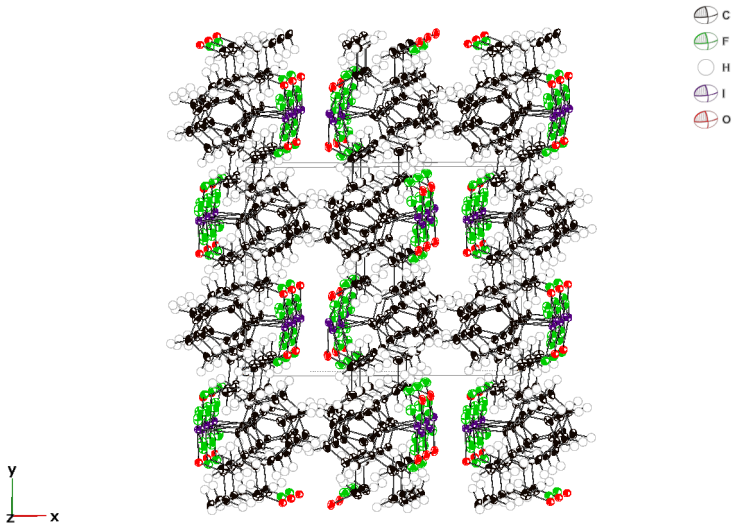

Figure S 116. Packing motif of **37**, ellipsoids depicted at 50% probability.

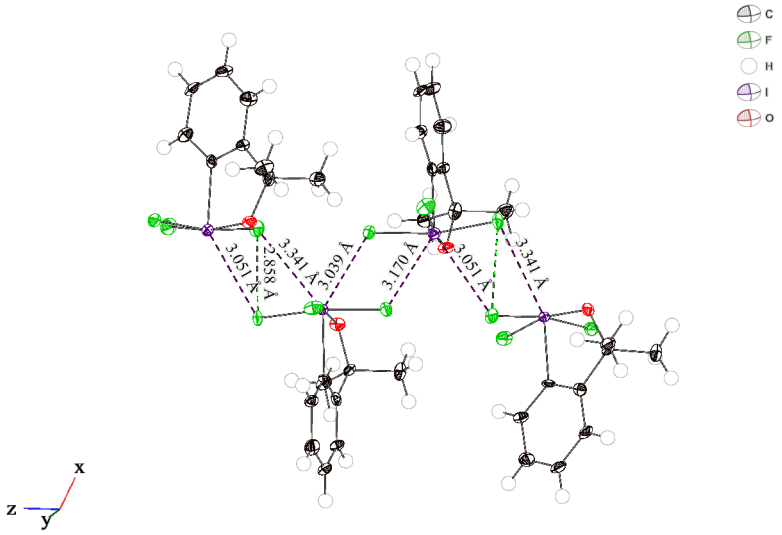

Figure S 117. Intermolecular I…F (purple broken lines) and F…F contacts (green broken lines, all equivalent) within the sum of van-der-Waals radii in the crystal structure of **37**, ellipsoids depicted at 50% probability.

Table S 18. Selected geometrical parameters for both moieties in the crystal structure of **37**. C_{ortho} refers to the substituted side of the molecule.

	moiety A	**moiety B**	***av.***
d(C-I)/Å	2.076(7)	2.068(7)	*2.072*
d(I-O)/Å	1.925(5)	1.922(4)	*1.924*
d(I-F_{trans})/Å	1.974(4)	1.984(4)	*1.979*
d(I-F_{cis})/Å	1.956(4), 1.972(4)	1.961(4), 1.963(4)	*1.963*
d(C-O)/Å	1.454(7)	1.465(8)	*1.460*
trans O-I-F/°	167.2(2)	168.6(2)	*167.9*
trans F-I-F/°	169.0(2)	167.9(2)	*168.5*
cis O-I-F/°	90.6(2), 95.8(2)	90.2(2), 95.0(2)	*92.9*
cis F-I-F/°	83.9(2), 88.0(2)	84.8(2), 88.0(2)	*86.2*
C-I-O/°	82.7(2)	82.2(2)	*82.5*
C-I-F range/°	84.5(3)-87.5(3)	84.9(3)-87.2(2)	*85.8*
O-C-C_{ortho}/°	107.8(5)	108.0(5)	*107.9*
|C_{ortho}-C_{ipso}-I-F_{trans}|/°	172.4(6)	171.3(6)	*171.9*
|C_{ortho}-C_{ipso}-I-F_{cis}|/°	88.4(6), 99.2(6)	86.3(6), 100.4(6)	*87.4, 99.8*
shortest C-I…F-I/Å		3.038(4)	
shortest I-F…F-I/Å		2.858(6)	